

# **Developing an *in vitro* co-culture Model to Investigate the Role of TRAIL in Lung Inflammation**

---

Thesis Submitted for the Degree of

**Doctor of Philosophy**

at the

University of Leicester

By

Munisha Devi BSc (Hons), MSc (University of Birmingham)

MRC Toxicology Unit

September 2015

# Developing an *in vitro* co-culture Model to Investigate the Role of TRAIL in Lung Inflammation

**By Munisha Devi**

MRC Toxicology Unit, University of Leicester, Hodgkin Building, Lancaster Rd, Leicester, LE1 9HN

Lung inflammatory conditions such as asthma and Chronic Obstructive Pulmonary Disease (COPD) are on the rise and there is a need for improved treatments. Current therapies such as corticosteroids simply alleviate symptoms which can lead to further complications. Apoptosis has an important role in the clearance of infiltrating immune cells, thus the balance between pro-inflammatory and pro-apoptotic signals dictates the severity of the inflammation.

TRAIL, a ligand of the TNF superfamily, can signal to both apoptosis and NF $\kappa$ B activation and therefore could be of therapeutic benefit. However, its role in lung inflammation is yet to be fully understood. The aim of this thesis was to develop an *in vitro* model of lung inflammation to elucidate the potential role of the TRAIL/TRAIL-R1/R2 signalling axis in this setting. To implement the model, activated CD4<sup>+</sup> and CD8<sup>+</sup> T cells, important drivers of inflammation in asthma and COPD, were co-cultured with lung epithelial cells.

Before developing a co-culture model, basal TRAIL/TRAIL-R1/R2 signalling was established in both cell types. NHBE cells were characterised for the first time for their basal TRAIL signalling and were found to be dependent on TRAIL-R2 for efficient TRAIL signalling. Several lines of evidence advocated the iHBEC cell line to be the most representative cell line of primary lung epithelial cells (NHBE cells). For example, downstream of a complete and active TRAIL Death Inducing Signalling Complex (DISC) in both iHBEC and NHBE cells, caspase 3 was insufficiently active to induce apoptosis and instead NF $\kappa$ B was found to be active as shown by phosphorylation of I $\kappa$ B and the translocation of p65 to the nucleus. ILZ TRAIL, a highly oligomerised form of TRAIL, was synthesised as it signals more efficiently *via* TRAIL-R2. Crucially, ILZ TRAIL proved to be an invaluable tool for distinguishing between TRAIL-R1/TRAIL-R2 signalling in this project.

The co-culture of activated T cells and lung epithelial cells provided a novel *in vitro* model of lung inflammation, as demonstrated by the secretion of pro-inflammatory cytokines. The inclusion of exogenous TRAIL/ILZ TRAIL in this model revealed a potential pro-inflammatory role for TRAIL/TRAIL-R1/2 signalling in this setting that was not evident when lung epithelial cells were cultured alone. These data suggest that TRAIL/ILZ TRAIL signalling is context dependent. Further evaluation of the role of TRAIL in lung inflammation could provide potential new insights in the pathogenesis of inflammatory conditions such as asthma or COPD.

## **Acknowledgements**

I would like to thank my supervisors Prof. Marion MacFarlane and Prof. Stuart Farrow for the opportunity to undertake this PhD and for their continued support during the course of it. I would also like to thank GSK and the MRC for the funding of this PhD project.

There are a few people whom without, elements of this project would not have been possible. Firstly, I would like to thank Sheila Porteous, for providing me with as much healthy volunteer blood as I requested, even at the most ridiculous hour. Secondly I would like to thank Jenny Edwards, for the help with immunocytochemistry and for generally being such a lovely person. I would like to acknowledge David Read, for the expert assistance when using the microscopes and Dr Claudia Langlais for the assistance with size exclusion chromatography experiments. Lastly, a sincere thank you to Dr William Coward, whom I am indebted to for the excellent advice and constant encouragement.

I am very thankful to the members of lab 416, both past and present, with all of whom I have shared many useful and productive scientific conversations. I am equally as thankful for all of the laughs, tea breaks and chats I have shared with them. I would also like to thank Dr Xiao-Ming Sun and Dr Andy Craxton who have always been very entertaining as my lab bay buddies.

I would like to say a massive thank you to all of the PhD students in the Unit; I will miss the close group of friends we have become.

A special thank you to my family; Mum, Dad, Meera, Karam and Rishi, for always reminding me what is important in life and helping me to reach my goals. Last but definitely not least, a thank you to Josh, for the unwavering belief in me and for making me the happiest person on the planet – you are the best.

# Table of Contents

ABSTRACT .....	ERROR! BOOKMARK NOT DEFINED.
ACKNOWLEDGEMENTS.....	II
TABLE OF CONTENTS .....	1
LIST OF FIGURES .....	5
LIST OF TABLES .....	9
ABBREVIATIONS .....	10
<b>1 INTRODUCTION .....</b>	<b>14</b>
1.1 LUNG INFLAMMATION .....	15
1.1.1 <i>Causes, Symptoms and Clinical Features</i> .....	15
1.1.2 <i>The Immune Response</i> .....	18
1.1.3 <i>Current Therapies</i> .....	22
1.1.3.1 Corticosteroids and Bronchodilators.....	22
1.1.3.2 Phosphodiesterase Inhibitors.....	23
1.1.3.3 Monoclonal Antibody Treatment.....	23
1.2 APOPTOSIS .....	23
1.2.1 <i>Hallmarks of Apoptosis</i> .....	24
1.2.2 <i>Caspases</i> .....	26
1.2.3 <i>The Intrinsic Pathway</i> .....	29
1.2.4 <i>The Extrinsic Pathway</i> .....	32
1.2.5 <i>The Bcl-2 family</i> .....	33
1.2.6 <i>Inhibitor of Apoptosis Proteins</i> .....	35
1.3 TRAIL AND APOPTOSIS .....	37
1.4 TRAIL, TNF AND NFkB ACTIVATION .....	38
1.5 TRAIL AND TNF IN LUNG INFLAMMATION .....	42
1.6 AIMS .....	44
<b>2 MATERIALS AND METHODS.....</b>	<b>45</b>
2.1 MATERIALS .....	46
2.2 METHODS .....	47
2.2.1 <i>Cell lines and culture conditions</i> .....	47
2.2.2 <i>Primary cells and culture conditions</i> .....	48
2.2.3 <i>Induction of apoptosis</i> .....	49
2.2.4 <i>Measurement of cell death</i> .....	50

2.2.5	<i>Receptor crosslinking</i> .....	51
2.2.6	<i>Surface expression analysis</i> .....	51
2.2.7	<i>Protein concentration</i> .....	52
2.2.8	<i>Western Blotting</i> .....	52
2.2.9	<i>Immunoblotting</i> .....	52
2.2.10	<i>Coomassie blue staining</i> .....	54
2.2.11	<i>Confocal microscopy</i> .....	54
2.2.12	<i>Phase contrast and digital image contrast videography</i> .....	55
2.2.13	<i>Generation of ILZ TRAIL expression construct</i> .....	55
2.2.14	<i>Generation and purification of recombinant TRAIL and ILZ TRAIL</i> .....	55
2.2.15	<i>TRAIL and ILZ TRAIL crosslinking</i> .....	56
2.2.16	<i>Biotinylation of TRAIL and ILZ TRAIL</i> .....	56
2.2.17	<i>TRAIL and ILZ TRAIL DISC isolation</i> .....	56
2.2.18	<i>Size-exclusion chromatography</i> .....	57
2.2.19	<i>Enzyme linked immunosorbent assay</i> .....	57
2.2.20	<i>Protein profiler arrays</i> .....	57
2.2.21	<i>Statistical analysis</i> .....	58

**3 RESULTS: CHARACTERISATION OF TRAIL-R1/R2-DEPENDENT CELL DEATH IN LUNG EPITHELIAL AND T CELL LINES – GENERATION OF ILZ TRAIL.....59**

3.1	INTRODUCTION.....	60
3.2	RESULTS.....	62
3.2.1	<i>Characterisation of the lung epithelial cell line, BEAS-2B and the leukemic T lymphocyte cell line, Jurkat E6.1</i> .....	62
3.2.1.1	BEAS-2B and Jurkat E6.1 cells display concentration-dependent sensitivity to TRAIL-induced apoptosis 62	
3.2.1.2	Treatment of BEAS-2B and Jurkat E6.1 cells with cross-linked agonistic antibody to TRAIL-R2 results in increased cell death compared with TRAIL-R2 agonistic antibody alone .....	65
3.2.2	<i>Generation and validation of ILZ TRAIL</i> .....	67
3.2.2.1	Synthesis and purification of ILZ TRAIL.....	67
3.2.2.2	Validation of the oligomerised conformation of ILZ TRAIL.....	69
3.2.2.3	ILZ TRAIL induces increased cell death in BEAS-2B and Jurkat E6.1 cells compared to TRAIL.....	72
3.2.3	<i>Optimisation of ILZ TRAIL DISC isolations</i> .....	75
3.2.3.1	Strep-tagged ILZ TRAIL DISC can be isolated in Jurkat E6.1 cells, but not without non-specific interactions 75	
3.2.3.2	Biotinylation of ILZ TRAIL allows for specific isolation of the ILZ TRAIL DISC in Jurkat E6.1 cells ..	79
3.3	DISCUSSION .....	82

<b>4</b>	<b>CHARACTERISATION OF TRAIL/TRAIL-R SIGNALLING IN LUNG EPITHELIAL CELLS .....</b>	<b>85</b>
4.1	INTRODUCTION.....	86
4.2	RESULTS.....	88
4.2.1	<i>Characterisation of TRAIL/TRAIL-R signalling in lung epithelial cell lines, A549, BEAS-2B, 16HBE and iHBEC .....</i>	<i>88</i>
4.2.1.1	TRAIL, TRAIL-R and CD95 surface expression profile of A549, BEAS-2B, 16HBE and iHBEC cells..	88
4.2.1.2	A549 and BEAS-2B but not 16HBE or iHBEC cells display a concentration-dependent sensitivity to TRAIL	90
4.2.1.3	bTRAIL induces TRAIL DISC formation in A549, BEAS-2B and iHBEC but not 16HBE cells.....	94
4.2.1.4	The SMAC mimetic LBW242 sensitises A549, but not iHBEC cells to TRAIL-induced apoptosis....	97
4.2.1.5	iHBEC cells treated with TRAIL or ILZ TRAIL do not undergo apoptosis but do display a time- and concentration-dependent cleavage of caspase 8 and caspase 3 and phosphorylation of I $\kappa$ B $\alpha$ .....	100
4.2.1.6	TRAIL or ILZ TRAIL treatment of iHBEC cells induces p65 translocation to the nucleus in a time-dependent manner.....	104
4.2.2	<i>Characterisation of NHBE cells .....</i>	<i>107</i>
4.2.2.1	NHBE cells treated with TRAIL do not undergo apoptosis but do display a concentration-dependent cleavage of caspase 8 and caspase 3 .....	107
4.2.2.2	iHBEC and NHBE cells express E-cadherin on their cell surface when cultured to confluency ...	109
4.2.2.3	NHBE cells form a DISC upon TRAIL treatment but are not sensitised to TRAIL-induced apoptosis when pre-treated with the SMAC mimetic, LBW242 .....	111
4.2.2.4	NHBE cells treated with TRAIL or ILZ TRAIL do not undergo apoptosis but do display a time- and concentration-dependent cleavage of caspase 8 and caspase 3 and phosphorylation of I $\kappa$ B $\alpha$ .....	114
4.2.2.5	TRAIL or ILZ TRAIL treatment of NHBE cells induces p65 translocation to the nucleus in a time-dependent manner.....	117
4.2.2.6	Profile of the key pro- and anti-apoptotic proteins involved in regulating the mitochondrial amplification loop.....	120
4.3	DISCUSSION .....	122
<b>5</b>	<b>CHARACTERISATION OF TRAIL/TRAIL-R SIGNALLING IN PRIMARY T CELLS AND DEVELOPMENT OF A CO-CULTURE OF LUNG EPITHELIAL CELLS AND ACTIVATED T CELLS .....</b>	<b>126</b>
5.1	INTRODUCTION.....	127
5.2	RESULTS.....	129
5.2.1	<i>Characterisation of TRAIL/TRAIL-R Signalling in Primary T cells.....</i>	<i>129</i>
5.2.1.1	Isolation of T cells by positive selection .....	129
5.2.1.2	Surface expression profile of naïve and 19 h activated CD4 <sup>+</sup> and CD8 <sup>+</sup> T cells .....	131
5.2.1.3	Naïve and 19 h activated CD4 <sup>+</sup> T cells are not sensitive to TRAIL or ILZ TRAIL treatment.....	133
5.2.1.4	Cell surface expression profile of 6 day activated CD4 <sup>+</sup> and CD8 <sup>+</sup> T cells.....	135
5.2.1.5	CD4 <sup>+</sup> and CD8 <sup>+</sup> T cells activated for 6 days are not sensitive to TRAIL or ILZ TRAIL treatment...	137
5.2.2	<i>Implementation of a co-culture of lung epithelial cells and primary T cells .....</i>	<i>140</i>

5.2.2.1	Work flow for the establishment of the conditioned media and cell-to-cell co-culture models of lung epithelial cells and primary T cells.....	140
5.2.2.2	Cell surface expression profile of iHBEC cells co-cultured with activated CD4 <sup>+</sup> T cells .....	143
5.2.2.3	Cell surface expression profile of iHBEC cells co-cultured with activated CD8 <sup>+</sup> T cells .....	145
5.2.2.4	iHBEC cells co-cultured with activated CD4 <sup>+</sup> or CD8 <sup>+</sup> T cells do not die by apoptosis but do display cleavage of caspase 8 and caspase 3.....	147
5.2.2.5	Profiling of cytokines released from CD4 <sup>+</sup> , CD8 <sup>+</sup> T cells and iHBEC cells cultured alone or following ILZ TRAIL treatment .....	149
5.2.2.6	Profiling the cytokines released by iHBEC cells co-cultured with conditioned media from CD4 <sup>+</sup> or CD8 <sup>+</sup> T cells or iHBEC cells co-cultured cell-to-cell with CD4 <sup>+</sup> or CD8 <sup>+</sup> T cells, both in the absence or presence of ILZ TRAIL	152
5.2.2.7	Cell surface expression profile of NHBE cells co-cultured with activated CD4 <sup>+</sup> T cells.....	156
5.2.2.8	The addition of TRAIL or ILZ TRAIL to NHBE cells co-cultured with activated CD4 <sup>+</sup> T cells resulted in apoptosis of NHBE cells .....	158
5.2.2.9	Profiling cytokines released by CD4 <sup>+</sup> , CD8 <sup>+</sup> T cells and NHBE cells cultured alone or following ILZ TRAIL treatment .....	160
5.2.2.10	Profiling cytokines released by NHBE cells co-cultured with conditioned media from CD4 <sup>+</sup> or CD8 <sup>+</sup> T cells of NHBE cells co-cultured cell-to-cell with CD4 <sup>+</sup> or CD8 <sup>+</sup> T cells, both in the absence or presence of ILZ TRAIL	162
5.2.2.11	Cell surface expression profile of differentiated NHBE cells .....	166
5.3	DISCUSSION .....	168
<b>6</b>	<b>FINAL DISCUSSION.....</b>	<b>176</b>
6.1	OVERVIEW.....	177
6.2	CONCLUSIONS .....	186
6.3	FUTURE WORK.....	188
<b>7</b>	<b>REFERENCES .....</b>	<b>189</b>

## List of Figures

Figure 1.1 Cells of the immune response.....	21
Figure 1.2 The hallmarks of apoptosis .....	25
Figure 1.3 The initiator and executioner caspases.....	28
Figure 1.4 The Intrinsic and extrinsic arms of apoptosis .....	31
Figure 1.5 The direct and indirect models showing the regulation of the activation of the effector proteins Bax and Bak by the Bcl-2 family of proteins .....	34
Figure 1.6 The structure of the key IAPs.....	36
Figure 1.7 Downstream signalling parallels between TRAIL and TNF .....	41
Figure 3.1 BEAS-2B and Jurkat E6.1 cells display concentration-dependent sensitivity to TRAIL-induced apoptosis .....	64
Figure 3.2 Treatment of BEAS-2B and Jurkat E6.1 cells with cross-linked agonistic antibody to TRAIL-R2 results in increased cell death compared with TRAIL-R2 agonistic antibody alone.....	66
Figure 3.3 Synthesis and purification of ILZ TRAIL.....	68
Figure 3.4 Validation of the oligomerised conformation of ILZ TRAIL.....	71
Figure 3.5 ILZ TRAIL induces increased cell death in BEAS-2B and Jurkat E6.1 cells compared to TRAIL .....	74
Figure 3.6 Strep-tagged ILZ TRAIL DISC can be isolated in Jurkat E6.1 cells, but not without non-specific interactions .....	78
Figure 3.7 Biotinylation of ILZ TRAIL allows specific isolation of the ILZ TRAIL DISC in Jurkat E6.1 cells .....	81

Figure 4.1 TRAIL, TRAIL-R and CD95 surface expression profile of A549, BEAS-2B, 16HBE and iHBEC cells.....	89
Figure 4.2 A549 and BEAS-2B but not 16HBE and iHBEC cells display a concentration-dependent sensitivity to TRAIL.....	93
Figure 4.3 bTRAIL induces TRAIL DISC formation in A549, BEAS-2B and iHBEC but not 16HBE cells.....	96
Figure 4.4 The SMAC mimetic LBW242 sensitises A549, but not iHBEC cells to TRAIL-induced apoptosis .....	99
Figure 4.5 iHBEC cells treated with TRAIL or ILZ TRAIL do not undergo apoptosis but do display a time- and concentration-dependent cleavage of caspase 8 and caspase 3 and phosphorylation of I $\kappa$ B $\alpha$ .....	103
Figure 4.6 TRAIL or ILZ TRAIL treatment of iHBEC cells induces p65 translocation to the nucleus in a time-dependent manner .....	105
Figure 4.7 NHBE cells treated with TRAIL do not undergo apoptosis but do display a concentration-dependent cleavage of caspase 8 and caspase 3 .....	108
Figure 4.8 iHBEC and NHBE cells express E-cadherin on their cell surface when cultured to confluency .....	110
Figure 4.9 NHBE cells form a DISC upon TRAIL treatment but are not sensitised to TRAIL-induced apoptosis when pre-treated with the SMAC mimetic, LBW242..	113
Figure 4.10 NHBE cells treated with TRAIL or ILZ TRAIL do not undergo apoptosis but do display a time- and concentration-dependent cleavage of caspase 8 and caspase 3 and phosphorylation of I $\kappa$ B $\alpha$ .....	116
Figure 4.11 TRAIL or ILZ TRAIL treatment of NHBE cells induces p65 translocation to the nucleus in a time-dependent manner .....	118
Figure 4.12 Profile of the key pro- and anti-apoptotic proteins involved in regulating the mitochondrial amplification loop .....	121

Figure 5.1 T cells isolation method by positive selection .....	130
Figure 5.2 Surface expression profile of naïve and 19 h activated CD4 <sup>+</sup> and CD8 <sup>+</sup> T cells .....	132
Figure 5.3 Naïve and 19 h activated CD4 <sup>+</sup> T cells are not sensitive to TRAIL or ILZ TRAIL treatment .....	134
Figure 5.4 Cell surface expression profile of 6 day activated CD4 <sup>+</sup> and CD8 <sup>+</sup> T cells .....	136
Figure 5.5 CD4 <sup>+</sup> and CD8 <sup>+</sup> T cells activated for 6 days are not sensitive to TRAIL or ILZ TRAIL treatment .....	139
Figure 5.6 Work flow for the establishment of the conditioned media and cell-to-cell co-culture models of lung epithelial cells and primary T cells .....	142
Figure 5.7 Cell surface expression profile of iHBEC cells co-cultured with activated CD4 <sup>+</sup> T cells .....	144
Figure 5.8 Cell surface expression profile of iHBEC cells co-cultured with activated CD8 <sup>+</sup> T cells .....	146
Figure 5.9 iHBEC cells co-cultured with activated CD4 <sup>+</sup> or CD8 <sup>+</sup> T cells do not die by apoptosis but do display cleavage of caspase 8 and caspase 3.....	148
Figure 5.10 Profiling cytokines released of CD4 <sup>+</sup> , CD8 <sup>+</sup> T cells and iHBEC cells cultured alone or following ILZ TRAIL treatment .....	151
Figure 5.11 Profiling of cytokines released by iHBEC cells co-cultured with conditioned media from CD4 <sup>+</sup> or CD8 <sup>+</sup> T cells or iHBEC cells co-cultured cell-to-cell with CD4 <sup>+</sup> or CD8 <sup>+</sup> T cells, both in the absence or presence of ILZ TRAIL .....	154
Figure 5.12 Cell surface expression profile of NHBE cells co-cultured with activated CD4 <sup>+</sup> T cells .....	157

Figure 5.13 The addition of TRAIL or ILZ TRAIL to NHBE cells co-cultured with activated CD4 <sup>+</sup> T cells results in apoptosis of NHBE cells .....	159
Figure 5.14 Profiling cytokines released by CD4 <sup>+</sup> , CD8 <sup>+</sup> T cells and NHBE cells cultured alone or following ILZ TRAIL treatment .....	161
Figure 5.15 Profiling cytokines released by NHBE cells co-cultured with conditioned media from CD4 <sup>+</sup> or CD8 <sup>+</sup> T cells of NHBE cells co-cultured cell-to-cell with CD4 <sup>+</sup> or CD8 <sup>+</sup> T cells, both in the absence and presence of ILZ TRAIL.....	164
Figure 5.16 Cell surface expression profile of differentiated NHBE cells .....	167
Figure 6. 1 Dissecting basal levels of TRAIL/TRAIL-R signalling in iHBEC and NHBE cells .....	181
Figure 6.2 Key changes in cell surface expression of death receptors and ligands in naive and activated T cells and in iHBEC and NHBE cells co-cultured .....	183

## List of Tables

Table 1 Primary antibodies used for immunoblotting .....	53
Table 2 Secondary antibodies used for immunoblotting .....	53

## Abbreviations

AICD	Activation-induced cell death
ALI	Air-liquid interface
APAF-1	Apoptosis Protease Activating Factor-1
APC	Antigen Presenting Cell
Bak	Bcl-2 homologous Antagonist/Killer
Bax	Bcl-2–Associated X protein
Bcl-2	B-cell lymphoma 2
Bcl-X <sub>L</sub>	Basal Cell Lymphoma-extra large
BDNF	Brain-Derived Neurotrophic Factor
BEGM	Bronchial Epithelial Cell Growth Medium
BH	Bcl-2 Homology
bILZ TRAIL	Biotinylated ILZ TRAIL
Biotin	D-Biotinoyl- $\epsilon$ -amidocaproic acid-N- hydroxysuccinimide ester
BIR	Baculovirus IAP Repeat
BPE	Bovine Pituitary Extract
BS <sup>3</sup>	Bis(sulfosuccinimidyl)suberate
BSA	Bovine serum albumin
bTRAIL	Soluble biotinylated TRAIL
C2C	Cell-to-Cell
CARD	Caspase Activation and Recruitment Domain
CD	Cluster of differentiation
cFLIP	Cellular FLICE (FADD-like IL-1 $\beta$ -converting enzyme)-inhibitory protein
CH11	Anti-CD95 antibody
clAP1	Cellular Inhibitor of Apoptosis Protein-1
clAP2	Cellular Inhibitor of Apoptosis Protein-2
CM	Conditioned Media
COPD	Chronic Obstructive Pulmonary Disease
CTL	Cytotoxic T
DISC	Death Inducing Signalling Complex

DKK1	Dickkopf WNT signalling pathway inhibitor 1
DMEM	Dulbecco's Modified Essential Medium
DMSO	Dimethyl Sulphoxide
ECL	Enhanced Chemiluminescence
EDTA	Ethylenediaminetetraacetic Acid
EMMPRIN	Extracellular Matrix Metalloproteinase Inducer
ENA-78	Epithelial-derived Neutrophil-Activating protein 78
ETR1	Mapatumumab
ETR2	Lexatumumab
FACS	Fluorescence Activated Cell Sorter
FADD	Fas-associated Death Domain protein
FGF-19	Fibroblast Growth Factor 19
FITC	Fluorescein isothiocyanate
FSC	Forward Scatter Channel
GDF-15	Growth Differentiation Factor 15
GM-CSF	Granulocyte Macrophage Colony-Stimulating Factor
GRO- $\alpha$	Melanoma Growth stimulating activity alpha
hEGF	Human Epidermal Growth Factor
HRP	Horseradish Peroxidase
IAP	Inhibitor of Apoptosis Protein
ICC	Immunocytochemistry
IFN- $\gamma$	Interferon Gamma
IgE	Immunoglobulin E
IGFBP-2	Insulin-like growth factor binding protein 2
IL	Interleukin
ILZ TRAIL	Isoleucine Zipper TNF-related Apoptosis-Inducing Ligand
IPTG	Isopropyl $\beta$ -D-1-thiogalactopyranoside
KSFM	Keratinocyte Serum Free Medium
LZ	Leucine Zipper motifs
LZ TRAIL	Leucine Zipper TRAIL
MIF	Macrophage Migration Inhibitory Factor
MIP-3 $\alpha$	Macrophage Inflammatory Protein-3 alpha

MMP	Mitochondrial Membrane Potential
MMP-9	Matrix Metalloproteinase 9
MOMP	Mitochondrial Outer Membrane Permeabilisation
NFκB	Nuclear Factor kappa-light-chain-enhancer of activated B cells
NHBE	Normal Human Bronchial Epithelial cells
OPG	Osteoprotegerin
PAGE	Polyacrylamide Gel Electrophoresis
PBS	Phosphate Buffered Saline
PDGF-AA	Platelet-Derived Growth Factor AA
PE	Phycoerythrin
PenStrep	Penicillin Streptomycin
PFA	Paraformaldehyde
PI	Propidium Iodide
PLAD	Pre-Ligand-binding Assembly Domain
PS	Phosphatidylserine
PUMA	P53-Upregulated Modulator of Apoptosis
r-IL-2	Recombinant interleukin-2
RING	Really Interesting New Gene
RIP	Receptor Interacting Protein
RPMI	Roswell Park Memorial Institute
SDS	Sodium Dodecyl Sulphate
SEM	Standard Error of Mean
SHBG	Sex hormone binding globulin
ST2	Suppression of tumourigenicity 2
STS	Staurosporine
tBid	Truncated Bid
TCR	T Cell Receptor
TEMED	Tetramethylethylenediamine
Th	T helper
Tm	T memory
TMRE	Tetramethylrhodamine, ethyl ester, perchlorate
TRADD	TNFRSF1A-Associated Via Death Domain

TRAIL	TNF-related Apoptosis-Inducing Ligand
TRAIL-R1	TRAIL Receptor 1 (DR4)
TRAIL-R2	TRAIL Receptor 2 (DR5)
TRAIL-R3	TRAIL Receptor 3 (DcR1)
TRAIL-R4	TRAIL Receptor 4 (DcR2)
Treg	T regulatory
uPAR	Urokinase receptor
US	Unstimulated
UT	Untreated
VEGF	Vascular Endothelial Growth Factor A
Vitamin D BP	Vitamin D Binding Protein
XIAP	X-linked Inhibitor of Apoptosis Protein
XL	Crosslinking antibody
zVAD.fmk	Carbobenzoxy-Val-Ala-Asp-(O-methyl)-fluoromethylketone

# 1 Introduction

## **1.1 Lung Inflammation**

Chronic lung inflammatory conditions are becoming more common, with the World Health Organisation estimating more than 235 million people worldwide suffering from asthma alone (<http://www.who.int/mediacentre/factsheets/fs307/en/> 2012). In particular, asthma and chronic obstructive pulmonary disease (COPD) are becoming a greater problem, especially in the western world. These chronic lung inflammatory conditions arise due to the lack of resolution of acute inflammation. Acute inflammation occurs within minutes to hours of exposure to a stimulus and is characterised by neutrophil infiltration. However, when acute inflammation persists and is not cleared, chronic inflammation ensues.

Chronic lung inflammation is characterised by the infiltration of mononuclear immune cells such as lymphocytes and macrophages attempting, but failing to eliminate pathogens and/or foreign bodies that may or may not be present. Persistence of this immune microenvironment in the lung leads to tissue damage. There are many types of lung inflammatory conditions, such as asthma, COPD, emphysema, asbestosis and pulmonary idiopathic fibrosis. What makes asthma and COPD similar to one another but different to other lung conditions is that they both affect the airways of the lung. In addition, the current treatments for these two conditions ease the symptoms but do not resolve the underlying inflammation. Thus, clearance of the immune cells or inhibition of their effects on lung tissue are areas of particular interest to researchers in this field. In particular, regulation of apoptosis of immune cells is an important area of research for the resolution of asthma and COPD.

### **1.1.1 Causes, Symptoms and Clinical Features**

Currently, in terms of clinical features, there is some controversy over whether asthma and COPD are one and the same disease. Kraft (2006) has proposed they are variations of the same condition and this called the 'Dutch hypothesis', whereas Barnes (2006) suggested that COPD and asthma are separate and different diseases which is referred to as the 'British hypothesis'. This classification has not yet been resolved due to the overlap documented between the two conditions. The

Dutch hypothesis is based on the observation that it can be difficult diagnosing asthma or COPD since there are overlaps in their phenotypes in some patients. For instance, although classically asthma responds well to bronchodilators and corticosteroids and COPD does not, there are occasions where a patient's response falls between the two types of response. Advocates of the British hypothesis would argue that the patient most likely has both conditions concurrently. In a clinical sense there is further research and analysis required of the two conditions to evaluate whether asthma and COPD are one and the same condition. Elucidation of the underlying causes of both conditions may shed light on this matter.

There are a number of postulated causes of asthma; however there has not been a definitive explanation for its occurrence. Atopy, a medical term used to describe one's potential to be hyperallergic, is thought to be one of these causes. Atopic patients usually present with high circulating levels of specific immunoglobulin E (IgE) to known allergens or elevated total IgE levels. Allergens such as house dust mites or irritants such as tobacco are the most widely known causes of asthma. In addition, genetics and viral infections have been implicated (Levy et al., 2006). More specifically, it has been shown that elevated total IgE levels has an inheritable genetic component as does another phenotype of asthma – airway hyperresponsiveness. However, the two phenotypes are not necessarily genetically linked as shown by a population study (Palmer et al., 2000). In addition, there have been discoveries of genetic susceptibility to asthma by positional gene cloning – a technique that uses Mendelian inheritance in a population of patients to identify genetic mutations associated with the pathophysiology of a disease. Multiple genes have been identified for increased susceptibility to asthma including *SPINK5*, *GRPA* and *DPP10* (Allen et al., 2003; Laitinen et al., 2004; Walley et al., 2001). Although the function of these genes is unclear they have been grouped together in a later study based on their expression in terminally differentiated lung epithelium, suggesting that they play a role in managing damage caused to the tissue (Cookson, 2004). Despite the identification of areas of genetic susceptibility there is still a great deal more research required to uncover the genetic contribution to the development of asthma.

Asthma mainly affects the upper airways and common symptoms described by asthmatics include; shortness of breath, wheezing, chest tightness, coughing and hyperventilation (Löwhagen, 2012). These symptoms are caused by three main clinical features of asthma, all regarding the upper airways; hyperresponsiveness, inflammation and remodelling all ultimately causing bronchial constriction. Airway hyperresponsiveness is characterised by increased sensitivity to constrictor agonists such as histamine therefore causing bronchospasm (O'Byrne and Inman, 2003) whereas, airway remodelling as the name suggests, refers to structural changes in the lung. Common examples of this are smooth muscle cell layer thickening and collagen deposition under the epithelial cell layer causing basement membrane thickening (Benayoun et al., 2003). These changes facilitate mucus hyperproduction and contribute to the airways narrowing (Bergeron et al., 2010).

More is known about the causes of COPD compared with asthma, particularly the association of COPD with tobacco. The World Health Organisation estimates that smokers account for 73% of COPD mortalities in high-income populations (Lopez et al., 2006). Similar to asthma, but in a more specific manner, genetic factors have been implicated in the prevalence of COPD. Alpha1 antitrypsin deficiency has been the most documented genetic risk factor associated with COPD with 1-3 % of COPD patients known to be affected (Stoller et al., 2006). However, there have been other genes implicated, for example, Celedón et al., (2004) implicated polymorphisms of transforming growth factor-beta 1, Keatings et al., (2000) proposed polymorphisms of TNF and Cheng et al., (2004) implicated polymorphisms of epoxide hydrolase and glutathione-S-transferase. All of the polymorphisms found in these genes either promoted COPD or caused predisposition to a poor prognosis for the disease. Furthermore, a wide range of other factors have also been documented to cause or increase the risk of COPD, such as air pollutants, ageing, bacterial or viral infections and even asthma (Mannino and Buist, 2007). The most common clinical symptoms are breathlessness, a chronic cough, excessive production of sputum, wheezing and tightness of the chest (Rabe et al., 2007).

In contrast to asthma, COPD affects the small airways and is characterised by two clinical features, airway obstruction and emphysema. Airway obstruction in COPD

is similar to asthma but occurs in the small rather than the large airways. Additionally, COPD airway obstruction worsens over time and is irreversible whereas in asthma, airway obstruction is variable and is reversible (Hogg et al., 2013). Emphysema is a term used to describe the limitation of the small airways and is caused by the destruction of the alveolar walls which decreases gas exchange and therefore air flow (Leopold and Gough, 1957; McDonough et al., 2011).

It is clear that although there are similarities between asthma and COPD, particularly regarding airway constriction, the localisation of each condition within the airways is different and therefore the clinical features and symptoms are not alike. These differences will partially be caused by the differences in mechanism of inflammation i.e. the inflammatory cell types involved in each condition.

### **1.1.2 The Immune Response**

Chronic lung inflammation in its most fundamental form is caused by the persistence of the adaptive inflammatory response and for both asthma and COPD the main drivers of inflammation are T cells, a type of white blood cell (leukocyte). As shown in Figure 1.1, T cells are a type of lymphocyte that mature in the thymus and are distinct from B cells (matured in the bone marrow). The primary difference between these lymphocytes is that B cells attack cells infected with pathogens indirectly by the production of antibodies whereas T cells attack infected cells directly. Additionally, T cells are characterised by the presence of the T cell receptor (TCR).

The T cell family consists of a complicated and varied subset of cells (Figure 1.1). In general, the two main and most widely studied populations are the 'cluster of differentiation' 4 ( $CD4^+$ ) and  $CD8^+$  subsets. These cells are classified as such due to the surface presence of their respective CD marker.

$CD4^+$  T cells can be further categorised into the most studied subsets; T helper 1 (Th1), Th2, Th17, T regulatory (Treg) and T memory (Tm) cells. Th1 cells are commonly known to assist in the clearance of bacterial infections. In contrast, Th2 cells are known to facilitate clearance of extracellular parasites.  $CD8^+$  T cells are

also known as cytotoxic T lymphocyte (CTL) cells and are involved in the clearance of virally infected cells. Both CD4<sup>+</sup> and CD8<sup>+</sup> T cells are referred to as naïve until they are activated. Activation is a necessary step for the immune function of these cells. Activation involves antigen-presenting cells (APC) such as dendritic cells, presenting processed antigens from invading pathogens to T cells *via* the TCR. Both CD3 and CD28 co-stimulatory molecules on the naïve T cell are required to engage with the APC in order for the T cell to become activated. This is a two-step process and is regulated in this way to avoid auto-reactions.

In asthma, CD4<sup>+</sup> T cells are known to be the predominant T cell infiltrating into the lungs. More specifically asthma is a Th2 cell driven condition (Meyer et al., 2008) whereas for COPD, Th1 cells have been shown to be main CD4<sup>+</sup> T cell infiltrates (Larché, 2007). However, in COPD, CD8<sup>+</sup> T cells have been described to be present in greater numbers than CD4<sup>+</sup> T cells (Saetta et al., 1998).

In addition to T cells, other leukocytes have been implicated in the persistent inflammation that causes COPD and asthma. Granulocytes have been detected in both conditions with eosinophils being recruited by T cells in asthma and neutrophils in COPD (Green et al., 2002; Keatings et al., 1996).

All of the described immune cells secrete cytokines as part of their immune function. Cytokines are soluble mediators of inflammation. These 5 – 20 kDa proteins allow for immune cells to communicate to one another and with other cell types, in this context, epithelial cells. Cytokines can be categorised into chemokines, interferons, lymphokines and interleukins. Chemokines attract other immune cells and interferons are involved in anti-viral functions. Lymphokines are released by lymphocytes, and interleukins, although originally described as mediators that targeted leukocytes, now comprise mediators with varying functions, with the vast majority of interleukins produced by Th cells.

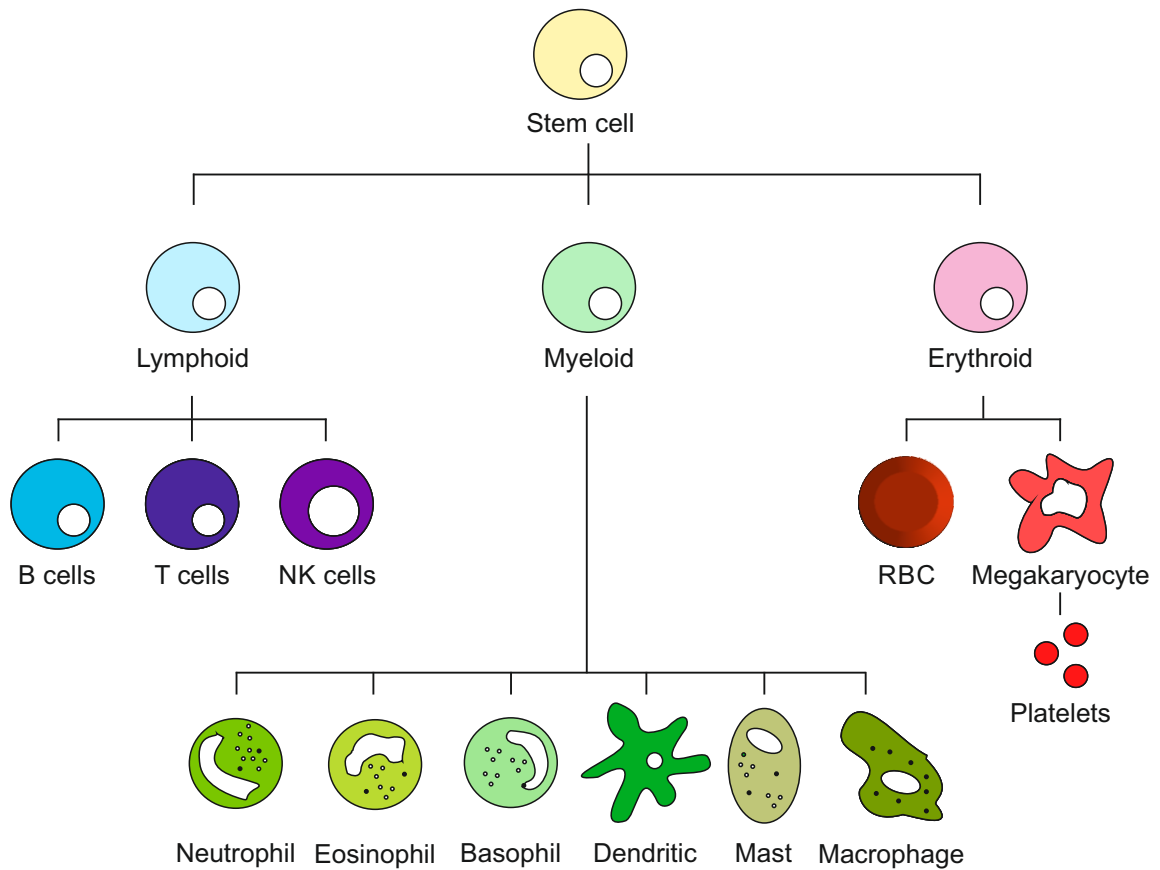
There are an array of cytokines released by immune cells and airway epithelial cells in both asthma and COPD. For example, IL-17 is detected at high levels in asthmatic patients, implicating Th17 cells to be active (Bhakta and Woodruff, 2011). In COPD,

TNF and IL-8 were the first cytokines to be identified as elevated in the sputum of patients (Barnes, 2009; Keatings et al., 1996).

In asthma and COPD, along with cytokines, adhesion molecules and lipid mediators are also known to be released. In asthma, approximately 100 mediators have been reported to contribute to the immune response (Barnes et al., 1998), emphasising how complex the inflammatory milieu is in these conditions, with multiple cells interacting with multiple mediators.

Epithelial cells have also been shown to play a role in exacerbating the inflammation seen in asthma and COPD. Epithelial cells themselves become activated and therefore release inflammatory mediators (described above). The release of these mediators is usually due to an upregulation in transcription of the genes that encode them, resulting in an increase in their translation and secretion. In asthmatic patients, the transcription factor shown to control the increase in transcription of these genes is nuclear factor kappa B (NFκB) (Barnes and Karin, 1997; Hart and Davidson, 1999). NFκB signalling is described in section 1.4.

## Lymphoid, Myeloid and Erythroid Cells



## T Cells

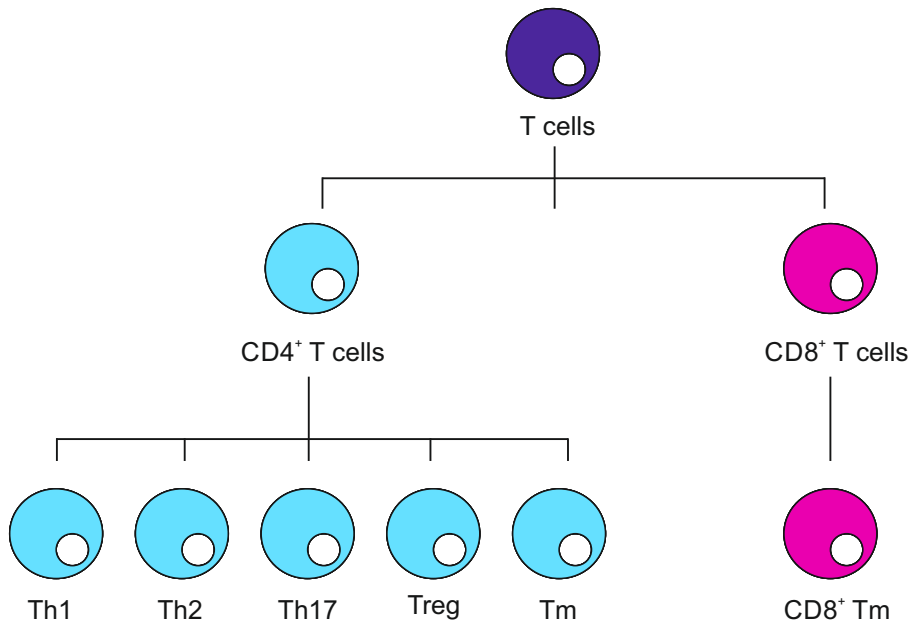


**Figure 1.1 Cells of the immune response** Schematics showing the development of different subsets of lymphoid, myeloid and erythroid cells as well as the CD4<sup>+</sup> and CD8<sup>+</sup> subsets of T cells.

### **1.1.3 Current Therapies**

The current rationale behind developing therapies for lung inflammatory conditions is to attempt to dampen down the immune system by targeting cytokine and lipid mediators. However, the vast majority of treatment options fall under the category of 'symptom relievers'.

#### **1.1.3.1 Corticosteroids and Bronchodilators**

Currently corticosteroids or glucocorticosteroids are the most common and effective treatment option for patients with asthma. They are used for the treatment of mild to moderate asthma and function to suppress the immune response. Mediators of inflammation such as cytokines and lipids are targeted, leading to a reduction in immune cells, particularly mast cells, T cells and eosinophils (Barnes and Adcock, 2003). Corticosteroids downregulate the transcription of pro-inflammatory mediators by binding to glucocorticoid receptors in epithelial cells; the receptors translocate to the nucleus to bind to glucocorticoid response elements. Here deacetylation of histone proteins is promoted causing a downregulation of the transcription of NFκB-mediated genes (Barnes and Adcock, 2003). However, corticosteroids are rarely used as a monotherapy for asthma, they are usually combined with bronchodilators.

Bronchodilators relieve the symptom of breathlessness in both asthma and COPD. Bronchodilators fall under one of two categories; long acting or short acting and within the long acting category there are either beta-2 agonists or muscarinic agonists. Short acting bronchodilators such as salbutamol relieve symptoms rapidly. Long acting beta-2 agonists cause smooth muscle to relax therefore widening the airways whereas muscarinic agonists inhibit cholinergic nerves from releasing acetylcholine, a chemical that signals to smooth muscle to contract. However, corticosteroid and bronchodilator therapies do cause both systemic and local side effects such as palpitations, headaches, coughing and increased risk of osteoporosis or glaucoma to name but a few (Holgate and Polosa, 2008; Roland et al., 2004).

### **1.1.3.2 Phosphodiesterase Inhibitors**

Phosphodiesterase enzymes are therapeutically targeted since they are involved in the upregulation of the activity of the smooth muscle in the lung airways. Inhibitors of phosphodiesterases are used in the treatment of COPD and act as bronchodilators. However, there are gastrointestinal side effects associated with their use (Franciosi et al., 2013; Stokes, 2014).

### **1.1.3.3 Monoclonal Antibody Treatment**

Currently, the most targeted and least toxic treatments for asthma and COPD are monoclonal antibodies. By using antibodies with high affinities for target proteins, potential side effects are reduced. Cytokines such as TNF, IL-9 and IL-5 are the most targeted proteins for such therapies (Holgate et al., 2011; Oh et al., 2013). However, the most successful monoclonal antibody for asthma to date has been omalizumab which targets IgE molecules known to be released by eosinophils (Rodrigo et al., 2011). Importantly, not all patients will benefit from this therapy as it appears to be most beneficial to patients with severe asthma (Bousquet et al., 2004).

The common theme for all of the current therapies for asthma and COPD is that they alleviate rather than resolve the underlying inflammation. Therefore there is a need for improved therapies. Apoptosis is evidently important for clearing infiltrating inflammatory cells (Savill, 1997). Further understanding of the link between apoptosis and the pathogenesis of lung inflammatory conditions in asthma could lead to the development of therapeutics that resolve the underlying inflammation.

## **1.2 Apoptosis**

Apoptosis was first described as a novel mechanism of cell death by Karl Vogt in 1842 but the term apoptosis was not used until 1972 by Kerr et al., at which point apoptosis had already been implicated in cancer, development and immunity. Today, the term “apoptosis” brings up in excess of 295 000 research articles on PubMed, with more than 18 000 of these articles being published in 2015 alone.

This highlights the importance given to this mode of programmed cell death in health and disease by scientific researchers around the world.

Apoptosis is vital for the homeostasis of multicellular organisms, allowing for the disposal of senescent, damaged or excess cells in a way that does not affect surrounding cells and therefore healthy tissue. This process is highly controlled and regulated leading to the identification of very specific and distinct hallmarks of apoptosis.

### **1.2.1 Hallmarks of Apoptosis**

Apoptosis causes defined morphological changes in a cell making it easily distinguishable from necrosis, an unsystematic form of cell death that results in an inflammatory response (Figure 1.2). One of the earliest morphological changes to occur in an apoptotic cell is the condensation of the nucleus, which is followed by the fragmentation of the nucleus. DNA fragmentation also occurs, an event that is so highly ordered that cleaved fragments of DNA are present in specific sizes that allow detection of a very reproducible pattern referred to as a “DNA ladder” by agarose gel electrophoresis (Wyllie et al., 1980).

Apoptotic cells expose a phospholipid usually present on the inner leaflet of the cell membrane to the outer leaflet of the membrane. This phospholipid is called phosphatidylserine (PS) and its exposure is thought to be a signal for recruiting nearby immune cells (Fadok et al., 1992). Detachment of the extracellular matrix allows apoptotic cells to withdraw from surrounding cells. Breakdown of the cytoskeleton leads to “blebbing” of the membrane, whereby the membrane pinches off allowing formation of apoptotic bodies. These apoptotic bodies are the product of the cell disassembling itself in a controlled manner (Figure 1.2). Apoptotic bodies are characterised by the presence of pinched off membranes encasing what was once intracellular content (Cotter et al., 1992). In this way, surrounding cells are not exposed to intracellular milieu, which may otherwise initiate an inflammatory response. In order to remove cellular debris and prevent inflammation, phagocytes are recruited to engulf the apoptotic bodies.

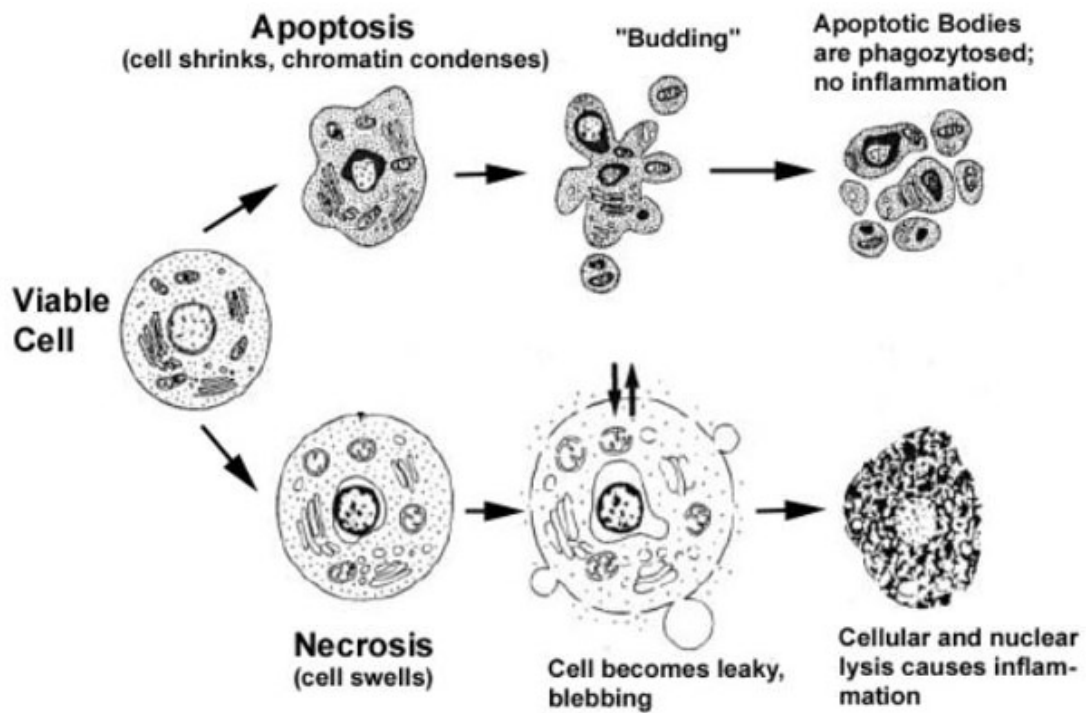


**Figure 1.2 The hallmarks of apoptosis** Cells undergoing apoptosis display a distinct morphology. Nuclear condensation and membrane blebbing or ‘budding’ occur leading to the formation of apoptotic bodies to be engulfed by phagocytes. In contrast necrosis is a much less controlled pathway resulting in the swelling of cell and subsequent leakage of intracellular contents. Image taken from Cruchten and Van Den Broeck (2002).

### 1.2.2 Caspases

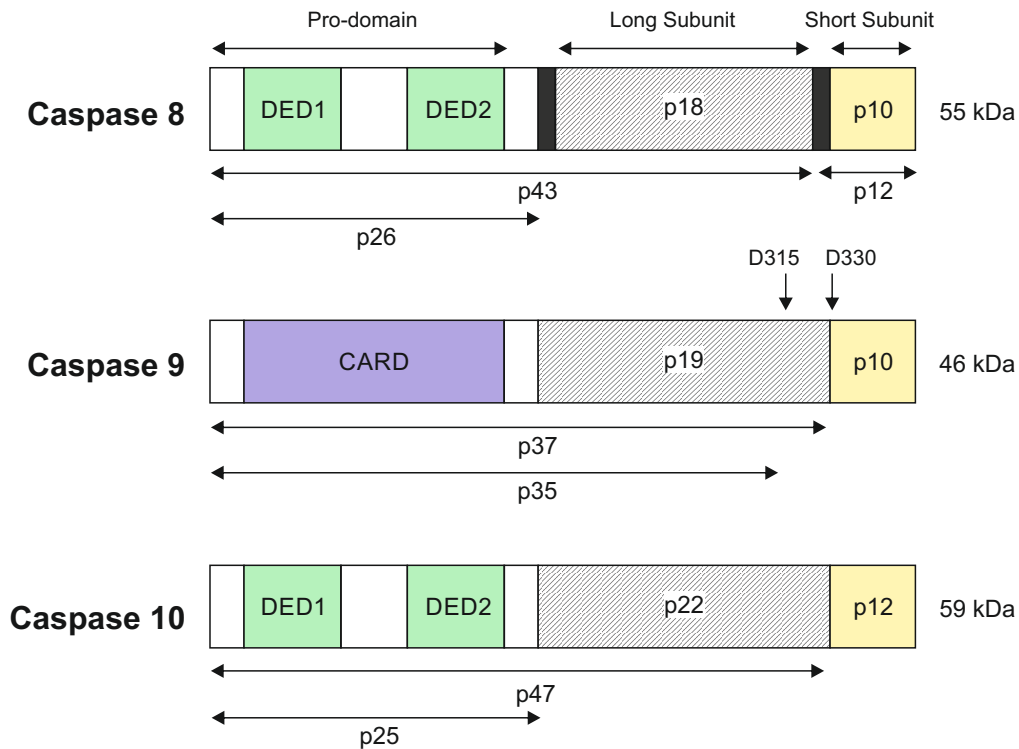
Cysteine dependent aspartate-specific proteases, or caspases as they are widely referred to, are a distinct family of proteases that have a very important role to play in the process of apoptosis. There are currently 11 members known to be expressed in humans and their highly conserved active site containing the five amino acid motif 'QACXG' distinguishes them from other proteases (Alnemri et al., 1996; Cohen, 1997; Fuentes-Prior and Salvesen, 2004; Shi, 2002). Caspases specifically recognise their substrates at a particular tetrapeptide sequence, where cleavage always occurs after the highly conserved aspartate residue in the sequence (Stennicke et al., 2000; Thornberry et al., 1997). This specificity is central to apoptosis as the cleaved substrates of caspases are known to cause many of the distinct morphological changes observed in apoptosis (Fischer et al., 2003). Seven of the 11 caspases are known to be involved in apoptosis and are classified into two categories; the initiator and the effector caspases. Initiator or 'apical' caspases are unique because they are able to cleave and activate themselves as well as activating downstream effector caspases, which in turn cleave cellular substrates. This two-step process means that a small pool of active initiator caspases, can lead to the activation of a much larger pool of caspases thereby transducing the apoptotic signal throughout the cell very quickly.

Structurally, the initiator caspases, caspases 8, 9 and 10, are characterised by their long N-terminal pro-domains, whereas the effector caspases, caspases 3 and 7, possess much shorter pro-domains (Figure 1.3). However, both types of zymogen contain a large and a small catalytic subunit. The activation process between initiator and effector caspases is dissimilar. Initiator caspases exist naturally in monomeric forms while the effector caspases exist as dimers. In order for initiator caspases to become active, they require homo-dimerisation to occur *via* an adaptor protein in a signalling platform, for example in either the DISC or apoptosome (see sections 1.2.3 and 1.2.4). Interaction with adaptor proteins in these signalling platforms occurs *via* the N-terminal Death Effector Domain (DED) of caspase 8 and 10 or *via* the Caspase Activation and Recruitment Domain (CARD) domain of caspase 9, respectively. The most widely accepted model of initiator caspase

activation is the induced-proximity model which proposes that dimerisation, without cleavage, is sufficient to activate these initiator caspases (Boatright et al., 2003; Salvesen and Dixit, 1999). Our laboratory has shown that although this is true, in the context of CD95 signalling – another death receptor, the CD95 Death Inducing Signalling Complex (DISC) formation, the dimerised non-cleaved caspase 8 has limited activity as an enzyme and therefore requires a second proteolytic cleavage step to become fully active (Dickens et al., 2012; Hughes et al., 2009).

As the effector or executioner caspases exist as dimers in their latent form they only require cleavage by initiator caspases to become catalytically active. Caspase 3, the archetypal executioner caspase, is cleaved at the interdomain linker which leads to autocatalytic cleavage resulting in the fully mature active cleavage fragments p19 and p17 (Boatright and Salvesen, 2003).

## Initiator Caspases



## Executioner Caspases

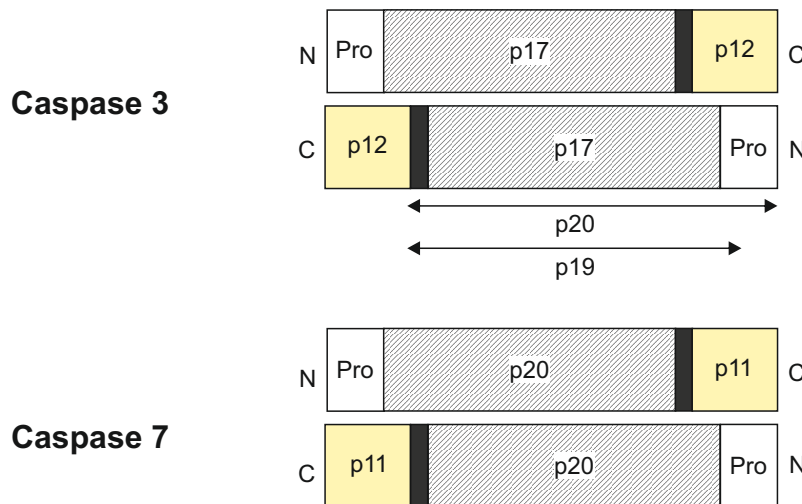


**Figure 1.3 The initiator and executioner caspases** The initiator caspases, caspases 8, 9 and 10 are monomers that from the N-terminal consist of a pro-domain, a long subunit (striped) and a small subunit (yellow) and in some cases a linker (black) separates each domain. Within the pro-domain lie the critical domain required for caspase function, the DED (green) in caspase 8 and 10 and the CARD (purple) in caspase 9. Notably, procaspase 9 cleavage at D330 by caspase 3 gives rise to the p37 cleavage fragment whereas cleavage at D315 occurs due to autocatalytic activity of procaspase 9 itself. The executioner caspases, caspases 3 and 7 are dimers that also consist of short and long subunits but have short pro-domains (Pro).

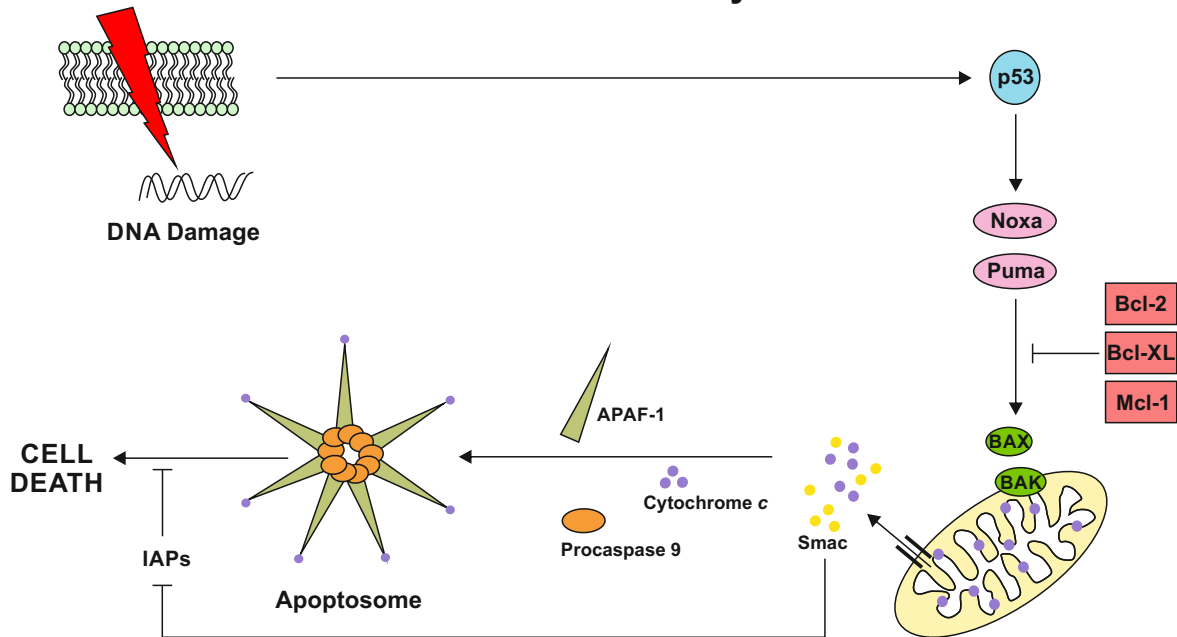
### 1.2.3 The Intrinsic Pathway

Apoptosis can occur *via* three different routes; these are activation of the granzyme B pathway, the intrinsic pathway or the extrinsic pathway. The granzyme B pathway is physiologically relevant in cytotoxic T cells that release serine proteases known as granzymes into target pathogen-infected cells to induce caspase 3 activation and therefore apoptosis (Pardo et al., 2009). However, the primary and widely occurring pathways of apoptosis are the intrinsic and extrinsic pathways.

The intrinsic pathway, as its name suggests, occurs due to a signal arising from within the cell. As shown in Figure 1.4, DNA damage is the most common intrinsic cell death signal but stress signals such as growth factor deprivation and cytokine withdrawal can also initiate this pathway. In the case of DNA damage, the tumour suppressor protein, p53 typically initiates a series of events that leads to the permeabilisation of the outer mitochondrial membrane (MOMP) (Chipuk et al., 2006; Tait and Green, 2010). This permeabilisation step is widely considered to be a pivotal point in the cell's decision to undergo apoptosis due to the release of proteins involved in transducing the apoptotic signal that otherwise would remain in the inner mitochondrial space. Thus, the steps leading to MOMP are highly regulated by a family of proteins called the B-cell lymphoma 2 (Bcl-2) family (Chao and Korsmeyer, 1998). Two members of this family, Noxa and p53-upregulated modulator of apoptosis (PUMA) are upregulated by p53 to activate other pro-apoptotic Bcl-2 family members, Bak and Bax (Nakano and Vousden, 2001; Oda et al., 2000). These two key proteins of the intrinsic apoptotic pathway associate at the mitochondria into oligomers, which leads to MOMP and therefore the formation of pores in the mitochondria. In an energy-dependent manner, cytoplasmic cytochrome *c*, is then able to initiate the formation of the holoenzyme scaffold complex named the Apoptosome. In its full form, the Apoptosome consists of a seven-spoked wheel, each spoke containing the adaptor protein, apoptosis protease activating factor -1 (APAF-1), cytochrome *c* and procaspase 9 (Acehan et al., 2002; Cain et al., 2002; Riedl and Salvesen, 2007). As described previously, procaspase 9 is able to bind to APAF-1 *via* its CARD, leading to dimerisation and subsequent autocatalytic cleavage generating active caspase 9. Along with the

release of cytochrome *c*, MOMP allows for the release of Smac/Diablo and Omi/HtrA2, proteins that are involved in promoting apoptosis by relieving inhibitory factors such as the inhibitor of apoptosis (IAP) family of proteins (G. Wu et al., 2000) (see section 1.2.6).

## The Intrinsic Pathway



## The Extrinsic Pathway

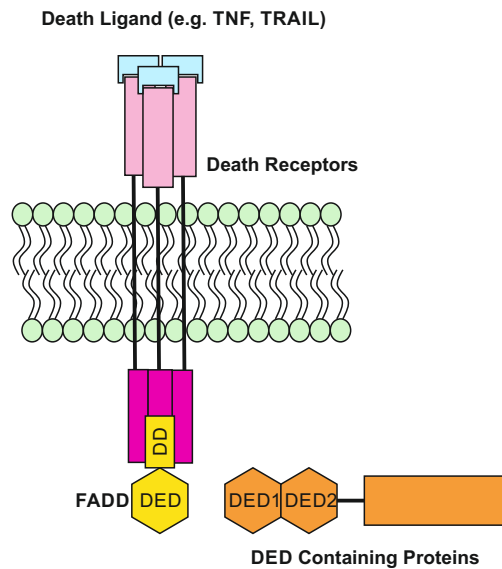


**Figure 1.4 Intrinsic and extrinsic cell apoptosis** The intrinsic arm of apoptosis can be initiated by the activation of p53 following DNA damage or cellular stress. This leads to the upregulation of pro-apoptotic Bcl-2 proteins, NOXA and PUMA. Downstream activation of BAX and BAK causes permeabilisation of the mitochondrial membrane releasing cytochrome c to associate with APAF-1 and procaspase 9 to form the Apoptosome which ultimately leads to cell death. Ligation of death ligands to their cognate receptors causes the activation of the extrinsic pathway. Binding of the adaptor protein FADD to the intracellular DD of trimeric receptors allows for the recruitment of DED-containing caspases. This now assembled signalling platform is called the Death-Inducing Signalling Complex (DISC).

#### 1.2.4 The Extrinsic Pathway

The extrinsic arm of apoptosis signalling is initiated by extracellular signals – cytokines, also known as ligands, which bind to their cognate receptors (Figure 1.4). These death ligands are all structurally similar and fall under the same umbrella classification, the tumour necrosis factor (TNF) superfamily. Contained within this family are TNF, CD95L and TNF-related apoptosis inducing ligand (TRAIL) (Aggarwal, 2003). Each of these ligands bind specifically to their respective transmembrane receptors and this specificity is conferred by the cysteine rich extracellular domains of the receptors (Locksley et al., 2001). Another defining characteristic of these receptors is the presence of intracellular death domains (DD) that allow for the homotypic binding of DD contained within key adaptor molecules (Park et al., 2007). However, binding of DDs to adaptor proteins can only occur following trimerisation of ligand and receptor complexes in the membrane, mediated by the pre-ligand-binding assembly domain (PLAD) contained in the cysteine rich extracellular domains of the death receptors (Siegel et al., 2000).

DDs are critical for transducing the apoptotic signal and are present in many of the TNF receptor superfamily and all of the death receptors, namely TNFR1, CD95, DR3 and TRAIL-R1/R2 as well as in the adaptor proteins FADD, TNFRSF1A-Associated Via Death Domain (TRADD) and RIP (Ashkenazi, 2002). Adapter proteins contain a characteristic C-terminal death effector domain (DED) in addition to the DD. The DED allows for the binding of initiator caspases *via* homotypic DED interactions, giving rise to the formation of a scaffold complex: the death-inducing signalling complex (DISC) analogous to the aforementioned Apoptosome. The initiator caspases as described previously are caspases 8 and 10. Dimerisation of these caspases can occur upon complete formation of the DISC, allowing for further activation by autocatalytic cleavage and subsequent propagation of the signalling cascade to cell death by cleavage of effector caspases such as caspase 3 or 7 (Gonzalvez and Ashkenazi, 2010; Kischkel et al., 2000).

In some cells, the signalling cascade initiated by the extrinsic pathway is insufficient to fully activate the effector caspases; therefore amplification of the apoptotic signal is required. In addition to cleaving caspase 3, active caspase 8 goes on to cleave

the Bcl-2 protein, Bid. The truncated form of Bid, tBid translocates to the mitochondria and leads to MOMP and therefore cytochrome c release and Apoptosome formation *via* activation of Bak and Bax (H. Li et al., 1998; Luo et al., 1998). This phenomenon is referred to as 'crosstalk' since the extrinsic pathway engages the intrinsic pathway in order to augment the apoptotic signal. Cells that require crosstalk are called type II cells with respect to extrinsic pathway activation, whereas cells that do not require this so called 'amplification loop' are referred to as type I cells (Rudner et al., 2005).

### **1.2.5 The Bcl-2 family**

The Bcl-2 family of proteins consists of over 20 members which regulate the activation of the intrinsic apoptotic signal. They are characterised by the presence of single or multiple Bcl-2 homology (BH) domains (Muchmore et al., 1996; Sattler et al., 1997). This family of proteins can be classified into pro-apoptotic proteins such as Bak, Bax, Bid and Bim and anti-apoptotic proteins such as Bcl-2, Bcl-XL and Mcl-1. The pro-apoptotic Bcl-2 members can also be sub classified into BH3 only proteins which only contain BH domain 3. Members of this subfamily include Noxa, PUMA and Bid. Bax and Bak are referred to as effector Bcl-2 proteins since their activation leads to the permeabilisation of mitochondria. Currently there is evidence to support two models for the regulation of the activation of Bax and Bak, the direct and the indirect model, as shown in Figure 1.5 (Letai et al., 2002; Willis et al., 2007). The vital role in the Bcl-2 family lies with the effector proteins; without Bax and Bak activation, dimerisation and subsequent multimerisation, there would not be MOMP, which is a requirement for the release of cytochrome c for the formation of the Apoptosome. In addition, Smac, a protein that regulates inhibitor of apoptosis proteins would otherwise not be released from the mitochondria.

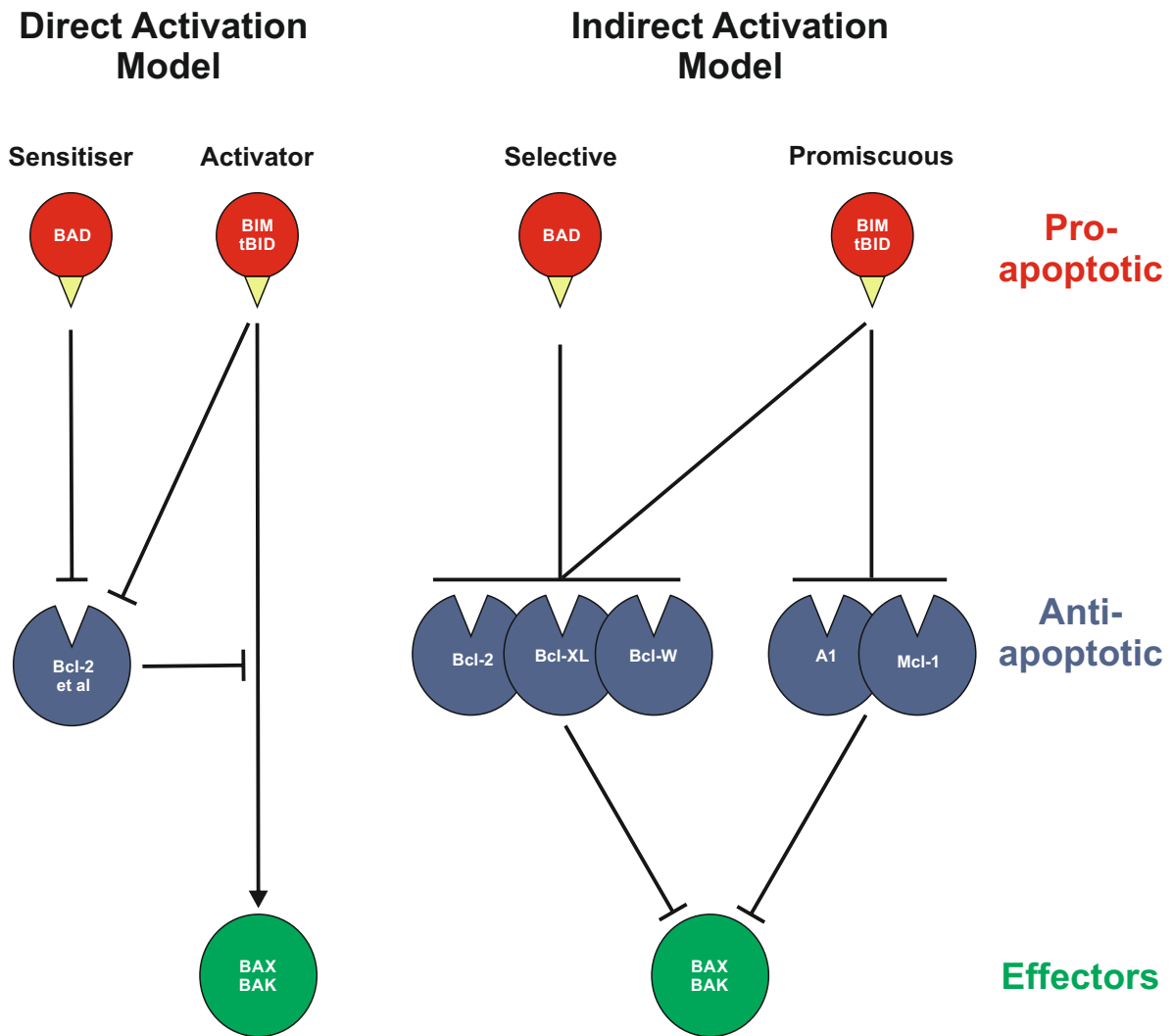


**Figure 1.5 The direct and indirect models showing the regulation of the activation of the effector proteins BAX and BAK by the Bcl-2 family of proteins** Two models of activating BAX and BAK have been proposed, the direct or the indirect model. In the direct activation model, pro-apoptotic BH3 only proteins shown in red can activate BAX or BAK (shown in green) directly whereas 'sensitiser' BH3 only proteins such as BAD bind and sequester the anti-apoptotic Bcl-2 family of proteins (shown in blue). In the indirect activation model, 'selective' and 'promiscuous' pro-apoptotic BH3 only proteins do not bind to BAX or BAK directly, instead they bind and sequester the anti-apoptotic Bcl-2 proteins that keep BAX and BAK in check. Adapted from Adams and Cory (2007).

### 1.2.6 Inhibitor of Apoptosis Proteins

There is another group of proteins, the inhibitor of apoptosis proteins (IAP) that regulate the activation and extent to which apoptosis occurs in a cell. In a similar manner to the Bcl-2 family of proteins, this family is characterised structurally by the presence of one to three baculovirus IAP repeat (BIR) domains. In addition to the BIR domain, some IAPs contain a really interesting new gene (RING) domain. The RING domain has the capability to act as a ligase to add ubiquitin to proteins by recruiting E2 ubiquitin-conjugated enzymes. In contrast, the BIR domain is known to inhibit caspases (Figure 1.6).

XIAP is the most widely researched IAP of the eight mammalian members and is also the IAP documented with the most anti-apoptotic function. XIAP contains BIR3 which inhibits caspase 9 and BIR2 which inhibits caspases 3 and 7. BIR2 inhibits caspase 9 by directly binding to the monomeric form and stabilising it, therefore preventing homodimerisation and thus activation of caspase 9 (Shiozaki et al., 2003; Srinivasula et al., 2001). In contrast BIR3 acts to inhibit caspase 3 in a competitive manner, which allows for relief of this inhibition by a protein known as Smac or Diablo. As previously described, Smac is released by the mitochondria during apoptosis and, by inhibiting XIAP, can allow for the full maturation of caspase 3 to its most active cleavage fragments (Scott et al., 2005; Srinivasula et al., 2001). Agents that mimic the function of Smac, referred to as Smac mimetics (SM) were initially developed to allow for relief of XIAP inhibition of caspase 3 and 7 processing. However, it has been recently discovered that SM can directly cause cell death by the degradation of cIAP1 and cIAP2 (Darding et al., 2011).

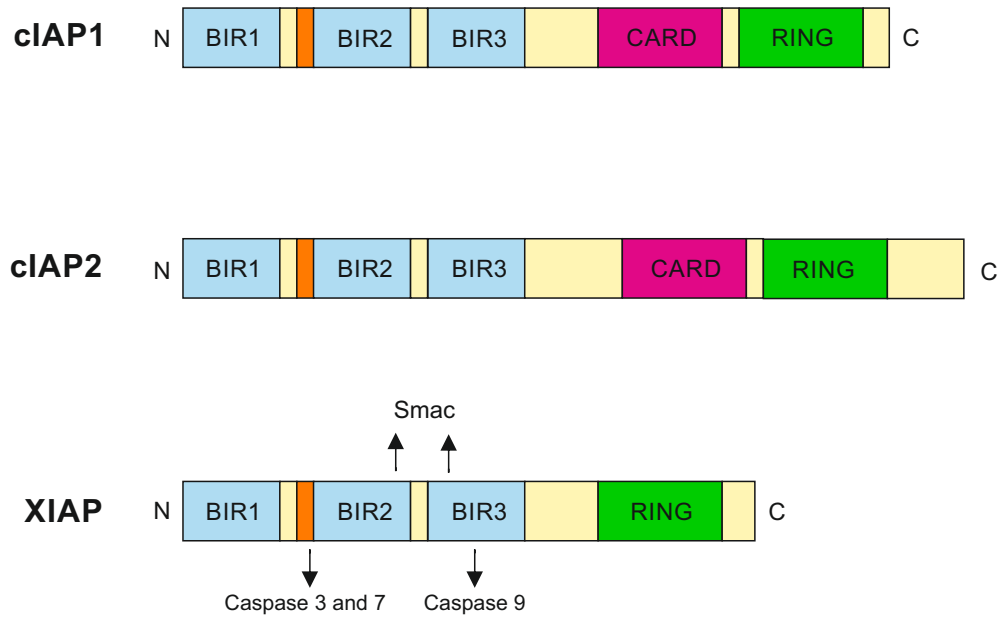


**Figure 1.6 The structure of the key IAPs** The IAPs consist of multiple N-terminal BIR domains (blue) and a C-terminal RING domain (green). cIAP1 and cIAP2 also contain CARD domains (pink). XIAP binds directly to Smac via BIR2 and BIR3 and binds to caspase 3 and 7 via BIR2 to inhibit their processing. Binding via BIR3 to caspase 9 inhibits its processing. Adapted from Ribe et al (2008).

### 1.3 TRAIL and apoptosis

As described previously, TRAIL is a member of the TNF superfamily and signals to apoptosis through the extrinsic pathway. Since its discovery in 1995 (Wiley et al.,) it has been shown to be expressed as a type II transmembrane protein which can be cleaved, giving rise to a soluble form of the ligand (Walczak and Haas, 2008). Both soluble and membrane-bound forms of TRAIL are capable of binding their cognate receptors.

Of the five mammalian TRAIL receptors, three are type I transmembrane proteins; TRAIL-R1, TRAIL-R2, and TRAIL-R4. TRAIL-R3 is associated with the membrane *via* a glycosyl-phosphatidylinositol anchor. The TRAIL-Rs discovered in 1997, TRAIL-R1 (Pan et al., 1997) and TRAIL-R2 (MacFarlane et al., 1997; W. G. Wu et al., 2000) were found to contain the key fully functional intracellular DD. Hence they are able to transduce the apoptotic signal upon ligation by TRAIL. In addition, both receptors are known to be post-translationally modified; TRAIL-R1 is palmitoylated and TRAIL-R2 is glycosylated (Rossin et al., 2009; Wagner et al., 2007).

However, TRAIL-R3 and TRAIL-R4 also discovered and cloned in 1997 were found to not possess and fully functional DD (MacFarlane et al., 1997; Marsters et al., 1997). In fact, TRAIL-R3 was found to lack a DD entirely whilst TRAIL-R4 possesses a truncated and therefore non-functional DD. Thus, these receptors are incapable of transducing an apoptotic signal in the cell. In fact, there is evidence for their role as decoy receptors, limiting the apoptotic signal (TRAIL) presented to a cell. The mechanism for this action is quite different for each receptor. Whilst TRAIL-R3 has been shown to directly compete with other receptors for the ligation of TRAIL, TRAIL-R4 binds to the already-formed TRAIL-R2 DISC, thus reducing the activity of the DISC (Clancy et al., 2005; Mérimo et al., 2006).

The fifth receptor osteoprotegerin (OPG), cloned in 1998, was found to be intracellular and exhibit a lower affinity for TRAIL compared with the other cognate receptors (Truneh et al., 2000). As suggested by its name, OPG is found to be abundant in osteoclast cells where it exhibits a key role for regulating cell death (Kong et al., 1999).

Binding of TRAIL to either TRAIL-R1 or TRAIL-R2 causes trimerisation of these receptors and the initiation of DISC formation with FADD as the adaptor protein, allowing for procaspase 8 binding (Chinnaiyan et al., 1995). Relative components of the catalytically active DISC dictate the strength of the apoptotic signal transduced downstream. Cellular FLICE (FADD-like IL-1 $\beta$ -converting enzyme)-inhibitory protein (cFLIP) is a protein known to regulate the activity of the DISC. This protein has three expressed splice variants; cFLIP<sub>short</sub>, cFLIP<sub>long</sub> and cFLIP<sub>raji</sub> (Golks et al., 2005). All three isoforms contain two DED which are similar in structure to the N-terminal domain of procaspase 8. cFLIP<sub>long</sub> also has the p12 and p10 subunits found in procaspase 8; however, unlike procaspase 8, cFLIP<sub>long</sub> is catalytically inactive (Tschopp et al., 1998). cFLIP<sub>short</sub> recruitment to the DISC causes inhibition of caspase activation (Krueger et al., 2001). Interestingly, high cFLIP<sub>long</sub> levels in the DISC cause inactivation of caspase 8 whereas low or endogenous levels of cFLIP<sub>long</sub> aid DISC-mediated activation of caspase 8 and therefore the transduction of the apoptotic signal (Chang et al., 2002; Fricker et al., 2010; Hughes et al., 2009).

As described previously, once the TRAIL DISC has formed, in type I cells, active caspase 8 is able to directly cleave procaspase 3 to generate active caspase 3 fragments p19/p17, which in turn cleave a large repertoire of substrates to cause cell death (Fischer et al., 2003). In contrast, in type II cells, activation of the intrinsic arm of apoptosis, through the cleavage of Bid, is required for sufficient activation of caspase 3.

#### **1.4 TRAIL, TNF and NF $\kappa$ B activation**

Although apoptosis is the primary pathway activated by TRAIL, it is important to acknowledge that TRAIL can also induce signalling to pathways other than apoptosis, namely activation of NF $\kappa$ B. NF $\kappa$ B is a pro-inflammatory transcription factor that binds to  $\kappa$ B sites present on various promoters when dimerised. The dimer can be comprised of a mixture of the following five NF $\kappa$ B subunits, RelA (p65), RelB, cRel, p105 or p100 (Pahl, 1999). These subunits are sequestered by inhibitors of  $\kappa$ B (I $\kappa$ B $\alpha$ ) in the cytoplasm in their inactive states.

TNF, the founding member of the TNF superfamily is able to function as a death inducing ligand but is primarily known to activate NF $\kappa$ B as its principal signalling cascade upon ligation to one its cognate receptors, TNF-R1 (Figure 1.7). Receptor-interacting protein (RIP) binds to the TNF/TNF-R1 complex by homotypic DD interactions. The adapter molecule TNF receptor-1-associated death domain protein (TRADD) is able to bind to RIP leading to the recruitment of TRAF2 and NF $\kappa$ B essential modulator/IKK $\gamma$  (NEMO) (Hsu et al., 1996). TNF complex I, as it is referred is to, is then complete and able to recruit I $\kappa$ B kinase  $\alpha$  (IKK $\alpha$ ) and IKK $\beta$ . NEMO, IKK $\alpha$  and IKK $\beta$  are collectively called the IKK complex. This complex phosphorylates I $\kappa$ B $\alpha$  in order for it to be ubiquitinated and subsequently degraded. Thus NF $\kappa$ B subunits are released and are free to translocate to the nucleus to function as transcription factors for various pro-inflammatory cytokines and chemokines (Mercurio et al., 1997; Zandi et al., 1997).

Unlike TNF, TRAIL-induced NF $\kappa$ B signalling is a secondary signalling cascade and requires the initial formation of the DISC (Figure 1.7). Upon endocytosis of the TRAIL DISC, a secondary complex is able to assemble named TRAIL complex II. It is important to note that complex II forms without the ligand and receptor interaction present in the DISC (Varfolomeev et al., 2005). However, FADD and caspase 8 have been reported to be essential for this complex (Grunert et al., 2012; Varfolomeev et al., 2005). Both RIP and TRADD adapter molecules have been shown to be required in TRAIL complex II for the downstream signalling that leads to the assembly of the IKK complex (Harper et al., 2001; Lin et al., 2000). It is not entirely clear whether TRAF2 is critical for the nucleation of the IKK complex since embryonic fibroblasts from TRAF-2-deficient mice are still able to signal to TRAIL-mediated NF $\kappa$ B activation (Lin et al., 2000). However, TRAF2 has been shown to be recruited into TRAIL complex II (Hsu et al., 1996). The downstream events following IKK complex formation are much the same as for TNF-induced NF $\kappa$ B activation; I $\kappa$ B is phosphorylated and therefore degraded, allowing NF $\kappa$ B to translocate to the nucleus. Nevertheless, it has been reported that the potency of the TRAIL-induced NF $\kappa$ B activation signal is much less than that for TNF-induced NF $\kappa$ B activation signal is much less than TNF-induced NF $\kappa$ B (Sheridan et al., 1997). This may provide an explanation for the lack of understanding and knowledge of the

downstream targets of NFκB when activated by TRAIL. It has been documented that rather than inducing a pro-inflammatory signal, TRAIL-induced NFκB activation upregulates anti-apoptotic proteins such as cFLIP, XIAP, cIAP1, cIAP2 and Bcl-XL in order to inhibit the TRAIL apoptotic signal (Gonzalvez and Ashkenazi, 2010; Ravi et al., 2001). This provides evidence for the idea that apoptosis and NFκB activation do not occur in parallel or simultaneously. To further emphasise this point it has been shown by our laboratory that inhibiting the apoptotic activity of the TRAIL DISC at the level of apical caspases causes TRAIL to shunt its signalling to NFκB activation (Harper et al., 2001). Thus indicating the requirement for one or many anti-apoptotic factors at the DISC in order to switch the apoptotic signal to NFκB activation in an *in vivo* setting. In line with this idea, cFLIP<sub>long</sub> has been reported to not only inhibit the cleavage of caspase 8 at the DISC but also promote NFκB activation (Song et al., 2007). It has to be noted that this study was carried out in a lung cancer setting where native signalling can be altered. In contrast to this, the Leverkus laboratory has shown that cFLIP<sub>long</sub> recruitment into the TRAIL DISC causes inhibition of NFκB activation in keratinocytes (Wachter et al., 2004). Despite the controversy over the role of cFLIP<sub>long</sub> in TRAIL-induced NFκB activation, it is evident that parallels can be drawn between the signalling cascades initiated by TRAIL and TNF. That is to say, they are both capable of transducing an apoptotic signal and an NFκB activation signal, albeit with opposing preferences/intensities.

Interestingly, there is also an important parallel to be made between signalling through TRAIL-R2 and TNF-R2. TNF-R2 signals to NFκB activation preferentially through presentation of a membrane-bound form of TNF, and TRAIL-R2 primarily signals to apoptosis through presentation of a membrane-bound form of its cognate ligand (Natoni et al., 2007; Wajant et al., 2001).

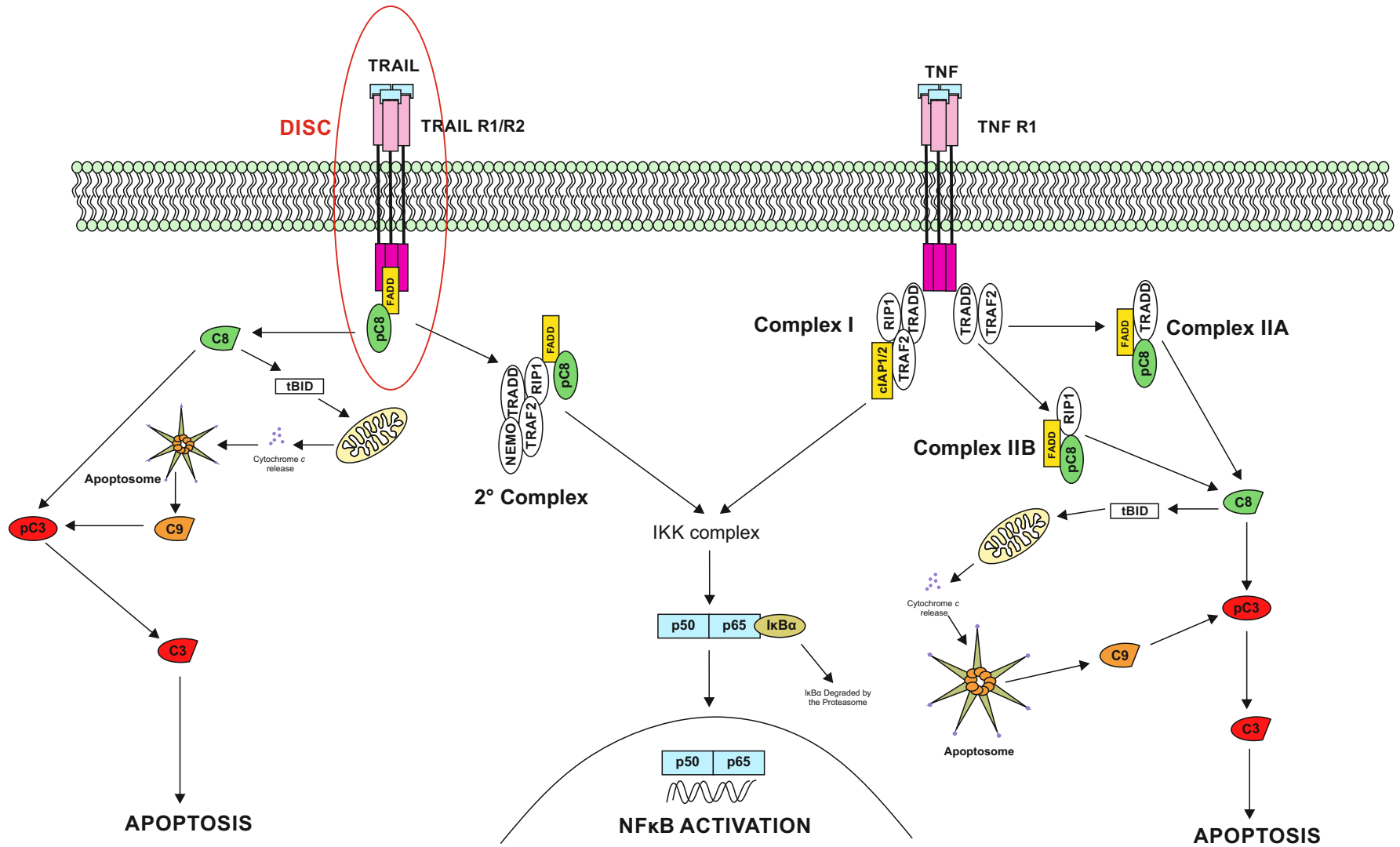


**Figure 1.7 Downstream signalling parallels between TRAIL and TNF** Ligation of TRAIL to its cognate death receptors, TRAIL-R1 or TRAIL-R2 primarily leads to the assembly of the DISC and subsequent apoptosis, however a secondary complex can form that instead signals to NFκB activation. The secondary complex consists of procaspase 8 and FADD (internalised following DISC formation), with RIP1 being recruited, as well as TRADD, TRAF2 and NEMO. This complex is then able to signal to the formation of the IKK complex which leads to the phosphorylation of IκB and therefore the activation of NFκB. TNF ligation to TNF-R1 leads to the activation of NFκB primarily, although, in some circumstances, apoptosis can be induced in a similar way to TRAIL.

## 1.5 TRAIL and TNF in lung inflammation

In the context of the lung, TNF $\alpha$  or TNF is well-documented to be pro-inflammatory in the acute phase of inflammation but anti-inflammatory in the resolution phase (Lawrence et al., 2001). In addition, TNF has been implicated in disease settings where chronic inflammation predominates; for example, both mRNA and protein levels of the cytokine are elevated in the lungs of asthmatics (Bradding et al., 1994; Ying et al., 1991). TNF has been documented to act as a chemoattractant to recruit neutrophils and eosinophils in airway lung inflammation (Lukacs et al., 1995). Moreover, Scheurich et al., (1987) have demonstrated that TNF treatment of T cells facilitates the immune functions of these cells. Importantly, the benefits of targeting TNF by antibody-based therapies *in vivo* has been demonstrated by Howarth et al., (2005) and Berry et al., (2006) who reported an improvement in lung function and overall quality of life for asthmatic patients. However, the safety of TNF-based therapies in lung inflammatory conditions is in question. Reports of an increased risk of pneumonia in COPD patients have caused concern which harks back to the aforementioned need for safe and improved drug therapies for these conditions (Berry et al., 2007; Bongartz et al., 2006).

In general, TRAIL research in the context of lung inflammation has been contradictory, with reports demonstrating both pro- and anti-inflammatory roles. Weckmann et al., (2007) implicated a pro-inflammatory role for TRAIL using ovalbumin-induced allergic asthma in TRAIL-deficient mice. More specifically, TRAIL was found to drive T helper (Th) 2 responses therefore contributing to inflammation. In the same study, the sputum of asthmatics was found to contain increased TRAIL levels compared to non-asthmatic patients. This corroborates with reports of TRAIL being heavily expressed on the lung epithelium of asthmatic patients when compared to healthy volunteers (Robertson et al., 2002). In contrast, although not in lung tissue, TRAIL has been implicated in the resolution phase, but not acute phase, of granulomatous experimental autoimmune thyroiditis. Mouse thyroglobulin-induced splenocytes were treated with a neutralising antibody to TRAIL in both acute and resolution phases of inflammation and TRAIL was found to increase thyroid fibrosis in the resolution phase of inflammation (Fang et

al., 2008). In the same vein, TRAIL was found to assist in macrophage-mediated clearance of *Streptococcus pneumoniae* infected mice. In addition, compared to TRAIL-deficient mice, alveoli from wild type mice were found to release TRAIL adding to the argument that TRAIL has a pro-resolving role in bacterial infections of the lung (Steinwede et al., 2012).

As indicated previously, there are parallels to be drawn between TRAIL and TNF signalling, both in terms of the intracellular signalling pathways that are activated by these cytokines (predominantly apoptosis, NFκB activation) and at the disease level. However, the transcriptional targets downstream of NFκB activation induced by TRAIL and TNF maybe different as indicated by the reported differences in potency of the activation of this transcription factor (Sheridan et al., 1997).

Significantly, CD4<sup>+</sup> and CD8<sup>+</sup> T cells express low levels of TNF-R2 and following activation, T cells become sensitised to TNF-induced apoptosis (Faustman and Davis, 2010). However, the only scenario where T cells are seen to be sensitive to TRAIL-mediated cell death is when CD8<sup>+</sup> T cells are re-stimulated when they have been stimulated initially without the help of CD4<sup>+</sup> T cells (Janssen et al., 2005). Additionally, a mouse model of lipopolysaccharide-induced acute lung injury in TRAIL-deficient mice has been used to show that TRAIL may have potential therapeutic benefit as a pro-resolving mediator (McGrath et al., 2011). Conversely, the same group later showed that TRAIL may be detrimental in an idiopathic pulmonary fibrosis model in TRAIL-deficient mice using a bleomycin to induce pulmonary inflammation (McGrath et al., 2012).

As alluded to above, TRAIL-deficient mice have been utilised a great deal to explore the role of TRAIL in multiple lung inflammatory conditions. This approach is useful for identifying phenotypic effects of TRAIL. However, there are limitations to this approach also. For instance, it is difficult to elucidate the cellular and molecular mechanisms causing the phenotypic effects observed. Revealing the cellular and molecular causes could explain the differences in TRAIL's role in inflammation seen in the aforementioned studies.

## 1.6 Aims

The interplay between activated T cells and the lung epithelium in an inflammatory setting, with regards to TRAIL and TRAIL-R signalling has not previously been examined. Moreover, since TRAIL has the capacity to induce both apoptotic and NFκB signalling arms it is likely that the potential cross-talk between these pathways in the context of lung inflammation is complex. The question of this thesis is to investigate whether TRAIL has a differential signalling role in the key cells of lung inflammation – lung epithelial cells and T cells when co-cultured together compared to when cultured individually. To address this, an *in vitro* model of lung inflammation is required. Implementation of a co-culture model of activated T cells and lung epithelial cells will be used to establish initially basal cellular signalling *via* the TRAIL/TRAIL-R1/R2 axis as well as the impact of soluble TRAIL versus membrane bound TRAIL on lung epithelial cells co-cultured with activated T cells.

- A panel of lung epithelial cell lines will be profiled for basal TRAIL/TRAIL-R1/R2 signalling in order to assess which cell line is most representative of basal TRAIL/TRAIL-R signalling in primary lung epithelial cells.
- Based on the TRAIL-R1 and TRAIL-R2 levels present in these cells, it will be determined whether the generation of a highly oligomerised form of TRAIL, Isoleucine zipper (ILZ) TRAIL is required to more efficiently target TRAIL-R2 on the surface of cells compared to WT soluble TRAIL for downstream signalling to either NFκB activation or apoptosis.
- Primary naïve and activated CD4<sup>+</sup> and CD8<sup>+</sup> T cells will be assessed for their basal TRAIL/TRAIL-R1/R2 signalling prior to implementing the co-culture.
- Subsequently, a co-culture consisting of the most appropriate lung epithelial cell line and activated T cells will be implemented and changes in the levels and/or the balance of apoptosis and inflammation will be investigated. The inclusion of exogenous TRAIL/ILZ TRAIL in the *in vitro* co-culture model will address the question of the potential role of TRAIL in lung inflammation.

## **2 Materials and Methods**

## 2.1 Materials

Unless otherwise stated, all materials were obtained from ThermoFisher Scientific Ltd (Loughborough, UK). BSA, ammonium persulfate,  $\beta$ -mercaptoethanol, bromophenol blue, DMSO, paraformaldehyde, glycerol, glycine, HEPES, imidazole, Kodak biomax XAR Film, magnesium chloride, ponceau S, PI, goat sera, SDS, TEMED, triton X-100, tween 20 and NuncImmuno™ MicroWell™ 96-well plates were all obtained from Sigma-Aldrich (Poole, UK). Acrylamide and ProtoBlue™ Safe Colloidal Coomassie G-250 were obtained from Geneflow (Staffordshire, UK). Protein assay reagent and precision plus protein standard were both obtained from Bio-Rad (Hertfordshire, UK). ECL was obtained from GE Healthcare (Buckinghamshire, UK). Nitrocellulose membrane (Hybond C) was obtained from Amersham (Buckinghamshire, UK). E. coli (BL21-DE3) competent cells, IPTG, S.O.C media, kanamycin-sulphate, TMRE, RPMI 1640, DMEM, KSFM, advanced RPMI, sodium pyruvate, Dyna-M280 streptavidin beads, goat anti-mouse Alexa-Fluor 488® antibody, were obtained from Invitrogen (Paisley, UK). PE-conjugated TRAIL-R1 and -R2, CD95L PE-Mouse IgG1,  $\kappa$  isotope control were obtained from eBioscience (San Diego, USA). TRIS, complete™ protease Inhibitor with/without EDTA and biotin were obtained from Roche (Sussex, UK). Ni-NTA agarose beads were obtained from Qiagen (Sussex, UK). The pan-caspase inhibitor zVAD.fmk was obtained from MP Biomedicals (Illkirch, France). The e-cadherin antibody for confocal microscopy was purchased from BD (San Jose, USA). All human ELISA kits (IL-6, IL-8), CD28 and CD3 $\epsilon$  antibodies and Protein Profiler Array™ Human XL Cytokine Array Kit, were purchased from R&D Systems (Minneapolis, Minnesota). The cocktail antibody anti-human CD8-FITC, CD4-PE was obtained from AbD Serotec (Kidlington, UK). ETR1 and ETR2 were obtained from Human Genome Sciences (Rockville, USA) and DRAQ7 from Abcam (Cambridge, UK). Phalloidin CruzFluor™ was obtained from Santa Cruz Biotechnology, Inc. (Dallas, USA). BEGM and corresponding supplements were purchased from Lonza. Recombinant TRAIL and ILZ TRAIL were made in-house (Harper and Macfarlane, 2008; MacFarlane et al., 1997; Macfarlane et al., 2005b). FITC conjugated annexin V was made in house.

## 2.2 Methods

### 2.2.1 Cell lines and culture conditions

The carcinomatous lung epithelial cell line, A549 was purchased from ATCC # CCL-185 and cultured in Dulbecco's Modified Eagle's Medium (DMEM) (+ L-glutamine) supplemented with 10 % fetal calf serum (FCS). Cells were seeded at  $0.25 - 0.5 \times 10^6$ /ml and passaged every 3 – 4 days.

The non-carcinomatous lung bronchial epithelial cell line, BEAS-2B was purchased from ATCC # CRL-9609 and cultured in DMEM (+ L-glutamine) supplemented with 10 % FCS. Cells were seeded at  $0.25 - 0.5 \times 10^6$ /ml and passaged every 3 – 4 days.

The normal lung bronchial epithelial cell line, 16HBE was a kind gift from Prof. Stuart Farrow (GlaxoSmithKline) and was cultured in Minimum Essential Media supplemented with 10 % FCS and 2 mM Glutamax. Cells were seeded at  $0.25 - 0.5 \times 10^6$ /ml and passaged every 3 – 4 days.

The non-carcinomatous lung bronchial epithelial cell line, iHBEC, was a kind gift from Prof. Jerry Shay (University of Texas Southwestern Medical Center) and was cultured in Keratinocyte Serum Free Medium (KSFM) supplemented with 25 µg/ml bovine pituitary extract (BPE) and 0.2 ng/ml human epidermal growth factor (hEGF) and passaged every 3 – 4 days. Cells were seeded at  $0.076 \times 10^6$ /ml and grown in supplemented KSFM until 80 % confluent and subsequently maintained at 100 % confluency in non-supplemented KSFM. Cells were cultured with a half-medium change every two days.

The leukaemic T lymphocyte Jurkat E6.1 cell line was purchased from the European collection of animal cell cultures # 88042803 (Wiltshire, UK) and cultured in RPMI-1640 supplemented with 10 % FCS and 2 mM Glutamax. Cells were seeded at  $0.25 - 0.5 \times 10^6$ /ml and passaged every 3 – 4 days.

The adenocarcinoma cervical epithelial cell line, HeLa was purchased from the European Collection of Cell Cultures (Salisbury, UK) and was cultured in DMEM

supplemented with 10 % FCS. Cells were seeded at  $0.25 - 0.5 \times 10^6/\text{ml}$  and passaged every 3 – 4 days.

All cell lines were incubated at 37 °C, 5 % CO<sub>2</sub> in a humidified atmosphere.

### **2.2.2 Primary cells and culture conditions**

Normal bronchial epithelial (NHBE) cells were purchased from Lonza (Basel, Switzerland): # CC-2540 from two healthy donors; donor 1 (40 year old male) and donor 2 (13 year old male). Cells were passaged for a maximum of five times and were cultured according to manufacturer's instructions. In brief, cells were cultured in Bronchial Epithelial Cell Growth Medium (BEGM) and supplemented with BPE, hydrocortisone, hEGF, epinephrine, transferrin, insulin, retinoic acid, triiodothyronine and gentamicin and amphotericin-1000 (concentrations not specified by Lonza). Cells were seeded at  $0.1 \times 10^6/\text{ml}$  and were grown to 100 % confluency before use. Cells were cultured with a full media change every two days.

NHBE cells for culturing using the air-liquid interface (ALI) method were purchased from Lonza: # CC-2540S from a healthy donor (49 year old female) and were differentiated according to the Lonza B-ALI™ method. In brief, cells were expanded in a 75 cm<sup>3</sup> flask for 48 h in B-ALI™ growth medium. Subsequently, cells were trypsinised and plated into collagen-coated (in-house) transwell inserts in 24-well plates at a density of 50 000 cells per well in B-ALI™ differentiation medium. Both media contained the following supplements (concentrations not specified); BPE, insulin, hydrocortisone, GA-1000, retinoic acid, transferrin, triiodothyronine, epinephrine and hEGF. Medium (500 µl) was added to the basal chamber and cells left to recover for 24 h. Medium from the apical chamber was removed and fresh medium (100 µl) added along with replacement of basal chamber medium. After 48 h the medium from the apical chamber was removed and not replaced. B-ALI™ inducer was added to differentiation medium, 10 µl for every 5 ml and 500 µl of this was added to the basal chamber. Cells were cultured with a full media change every two to three days. The cells were maintained in this manner for 30 – 50 days before use.

Primary CD4<sup>+</sup> and CD8<sup>+</sup> T cells were isolated from human peripheral blood from healthy donors fresh on the day of each use with local ethical consent. A positive selection method was employed using Dynabead CD4<sup>+</sup> and CD8<sup>+</sup> positive isolation kits according to the ThermoFisher Scientific's instructions. Cells were subsequently maintained in advanced RPMI supplemented with 10 % FCS, 2 nM Glutamax, 10 U penicillin and 100 µg/ml streptomycin (PenStrep), 2.5 µg/ml fungizone and 10 ng/ml recombinant interleukin-2 (rIL-2).

To determine the percentage of either CD4<sup>+</sup> or CD8<sup>+</sup> T cells, the anti-human CD8-FITC, CD4-PE dual antibody cocktail was diluted 1:10 in ice cold PBS with  $0.2 \times 10^6$  cells, incubated in the dark for 20 min at room temperature (RT) and washed once using ice cold PBS and resuspended in a final volume of 300 µl ice cold PBS. DRAQ7 (AbCam) was added in order to determine the viability of the freshly isolated T cells. Cells were analysed by flow cytometry using the BD FACSCanto™II (BD FACSDiva software).

Where mentioned, activation of T cells refers to cells being incubated for either 19 h or 6 days on 1 ng/ml CD3 and 10 ng/ml CD28 antibody coated plates (in-house, overnight at 4 °C). Upon activation, T cells express CD69 on their cell surface, therefore activation status of T cells was determined using CD69-FITC antibody, diluted 1:10 in ice cold PBS added to  $0.2 \times 10^6$  cells, incubated in the dark for 20 min at RT and washed once using ice cold PBS and resuspended in a final volume of 300 µl ice cold PBS. DRAQ7 was added in order to determine the viability of the activated cells. Cells were analysed by flow cytometry using the method described above.

### **2.2.3 Induction of apoptosis**

Cells were seeded 24 h prior to treatments, excepting iHBEC and NHBE cells which were treated once 100 % confluency was reached. Cells were treated with various apoptotic stimuli, including TRAIL, ILZ TRAIL, anti-CD95 antibody (CH11), etoposide or staurosporine (STS). At the point of harvesting, a proportion of cells were taken for western blot analysis of caspase cleavage (section 2.2.8 & 2.2.9) in addition to flow cytometry analysis of cell death.

#### 2.2.4 Measurement of cell death

During apoptosis, phosphatidylserine (PS) becomes exposed on the outer leaflet of the membrane, annexin V binds with high affinity to PS. Annexin conjugated with Fluorescein isothiocyanate (FITC) was used for fluorescent labelling allowing for detection of cells that have PS externalisation. Propidium Iodide (PI) was used in conjunction with annexin V-FITC, to identify necrotic or cells in late stage apoptosis since PI intercalates with DNA but is also membrane impermeable. Therefore late stage apoptotic cells, whose membrane integrity has been compromised, can be measured. Annexin V-FITC and PI staining were carried out as previously described (Macfarlane et al., 2002). In brief, annexin buffer (10 mM Hepes (pH 7.4), 150 mM NaCl, 5 mM KCl, 1mM MgCl<sub>2</sub>, 1.8 mM CaCl<sub>2</sub>) was added to samples, containing approximately  $0.2 \times 10^6$  cells. Cells were incubated in the dark for 8 min with 1.5  $\mu$ l annexin V-FITC. PI (50  $\mu$ g/ml) was then added and incubation on ice for 2 min was followed by PS<sup>+</sup>/PI<sup>+</sup> analysis. Cells were analysed by flow cytometry as previously described.

Mitochondrial outer membrane permeabilisation (MOMP) can occur either when intrinsic apoptosis is activated or when extrinsic signalling activates the BH3 only protein, Bid. MOMP causes loss of mitochondrial membrane potential (MMP) which can be detected using tetramethylrhodamine ethyl ester perchlorate (TMRE). TMRE is a fluorescent dye that is sequestered in the mitochondria of healthy cells by MMP, whereas in apoptotic cells TMRE is diffuse within the cytoplasm. Flow cytometry was employed to detect the fluorescence intensity change to measure percentage of apoptotic cells, as previously described (Sun et al., 1999). In brief, 1.5  $\mu$ l TMRE was added to control and treated samples containing approximately  $0.2 \times 10^6$  cells in pre-warmed media, for 10 min at 37 °C. Subsequent flow cytometry analysis of samples followed using the method described above.

### **2.2.5 Receptor crosslinking**

Agonistic antibodies specific to either TRAIL-R1, Mapatumumab (ETR1) or TRAIL-R2, Lexatumumab (ETR2) were used in conjunction with F(ab)<sub>2</sub> fragment (goat anti-human IgG Fc $\gamma$ ) specific crosslinking antibody. ETR1/2 were diluted with the aforementioned crosslinking antibody (XL) at a ratio of 1:3 in PBS and then incubated at RT for 30 min prior to use. The final concentration used in cells was 0.5  $\mu$ g/ml.

### **2.2.6 Surface expression analysis**

Surface expression of TRAIL-R1 and TRAIL-R2 was determined as previously described (Macfarlane et al., 2002). In brief, for each receptor and controls, approximately  $0.5 \times 10^6$  cells were pelleted at 200 g for 3 min at 4 °C, washed in ice cold PBS and resuspended in 10 % goat sera. PE-conjugated TRAIL-R1 or TRAIL-R2 antibodies or IgG isotype control antibody was added 1:10 to relevant aliquots of cells and incubated on ice for 1 h in the dark. Cells were then washed three times in ice cold PBS and resuspended in 500  $\mu$ l PBS. Cells were analysed by flow cytometry as previously described, with the FL-2 channel (fluorescence on a log scale) measuring antibody binding. Both TRAIL (with FITC conjugated antibody) and CD95L (with PE conjugated antibody) surface expression were determined in the same manner.

Similarly, CD95 surface expression was determined using 1:10 CH11 incubation with cells in 10 % goat sera for 1h on ice in the dark. Cells were then washed in ice cold PBS, incubated with the corresponding FITC-conjugated secondary antibody for 1 h on ice in the dark. Cells were then washed three times in ice cold PBS and resuspended in 500  $\mu$ l PBS. Cells were analysed by flow cytometry as previously described, with the FL-1 channel (fluorescence on a log scale) measuring antibody binding. Analysis of all surface expression data was carried out using FlowJo software version 7.6.4.

### **2.2.7 Protein concentration**

Bio-Rad Protein Assay (Bradford, 1976) was used to determine the protein concentration of cell lysates. Bovine serum albumin (BSA) (1-8 µg/ml) was used to generate a standard curve in duplicate and test samples analysed by transferring 1 µl of appropriately diluted sample into 999 µl of diluted dye reagent. Absorbance was measured on a spectrophotometer (Beckman Coulter) at λ595 nm and compared against the standard curve.

### **2.2.8 Western Blotting**

Control cells and cells treated with apoptotic stimuli (approximately  $1 \times 10^6$ ) immediately post treatment were pelleted at 200 g for 3 min at 4 °C, washed twice in ice cold PBS and resuspended in 100 µl SDS-PAGE sample buffer (62 mM TRIS, 0.05 % bromophenol blue, 15 % glycerol, 2 % SDS, 5 % β-mercaptoethanol), sonicated and analysed by western blotting.

### **2.2.9 Immunoblotting**

Proteins were separated according to size by SDS-PAGE, transferred onto a nitrocellulose membrane and immunoblotted as previously described (Harper et al., 2001). In brief, a Bio-Rad MiniPROTEAN 3 cell kit in a TRIS/Glycine buffer system was used for running denatured proteins on SDS-PAGE. The gel was transferred onto a nitrocellulose membrane and incubated with the appropriate primary antibody (see Table 1) using standard protocols. The corresponding secondary antibody was then incubated with the membrane using standard protocols (see Table 2). Enzymatic activity was visualised on X-ray film using the enhanced chemiluminescence (ECL) detection system as outlined in the manufacturer's protocol. Films were developed on a Compact X4 Xograph imaging system and scanned using Photoshop Elements version 7.

**Table 1 Primary antibodies used for immunoblotting**

<b>Antibody</b>	<b>Source</b>	<b>Host</b>	<b>Dilution</b>
Bcl-2	Dako	Mouse	1:2000
Bcl-XL	BD (610212)	Rabbit	1:2000
Bim	Cell Signalling (C34C5)	Rabbit	1:500
Bid	Santa Cruz (SC-11423)	Rabbit	1:2000
Bax	Millipore (ABC11)	Rabbit	1:1000
Bak	AbD Serotec (1782)	Rabbit	1:1000
Caspase-8	In-house	Rabbit	1:2000
Caspase-3	In-house	Rabbit	1:2000
Caspase-9	MBL (MO54-3)	Mouse	1:1000
TRAIL-R1	ProSci (1139)	Rabbit	1:1000
TRAIL-R2	ProSci (2019)	Mouse	1:1000
TRAIL-R2	Cell Signalling (3696)	Rabbit	1:1000
FADD	BD (610400)	Mouse	1:250
cFLIP	Enzo Life Sciences (ALX804428C050)	Mouse	1:250
PARP	Alexis (804210)	Mouse	1:2500
MCL-1	Santa Cruz (SC-819)	Rabbit	1:500
XIAP	BD (610763)	Mouse	1:2000
GAPDH	Abcam (2118)	Mouse	1:5000
$\alpha$ -tubulin	Calbiochem (CP06)	Mouse	1:1000
clAP1	R&D Systems (AF8181)	Goat	1:2000
clAP2	R&D Systems (AF8171)	Goat	1:2000
Streptavidin HRP	Cell Signalling (3999)	Mouse	1:2000
His-6X	Abcam (18184)	Mouse	1:2000
I $\kappa$ B $\alpha$	Cell Signalling	Mouse	1:1000
phosphoI $\kappa$ B $\alpha$	Cell Signalling (2859)	Rabbit	1:750
E-cadherin	Cell Signalling (31955)	Rabbit	1:1000

**Table 2 Secondary antibodies used for immunoblotting**

<b>Antibody</b>	<b>Source</b>	<b>Host</b>	<b>Dilution</b>
Anti-Rabbit	Dako	Goat	1:2000
Anti-Mouse	Sigma	Goat	1:2000
Anti-Goat	Dako	Rabbit	1:2000

### **2.2.10 Coomassie blue staining**

ProtoBlue™ Safe Colloidal Coomassie G-250 stain was used to stain gels overnight at RT. Multiple distilled water washes were performed to reduce background staining, and improve protein band visualisation.

### **2.2.11 Confocal microscopy**

TRAIL has the potential to signal to pro-survival pathways such as activation of NFκB. Activation of this pathway involves translocation of p65 to the nucleus. Immunocytochemistry (ICC) was performed on treated and control cells to determine the cellular localisation of p65 and therefore the activation of this pathway. NHBE and iHBEC cells were seeded at  $0.2 \times 10^6$  and  $0.4 \times 10^6$  respectively, on collagen coated (in-house) coverslips and cultured to confluency (described previously). Cells were treated with either 1 µg/ml TRAIL or ILZ TRAIL for 0 – 5 h incubated at 37 °C. Cells were washed once with PBS to stop the stimuli and fixed using 4 % paraformaldehyde (PFA) for 10 min at room temperature (RT). PFA was removed and 0.5 % triton X-100 in PBS was used to permeabilise the cells for 10 min at RT. Coverslips were incubated overnight in the p65 antibody (1:200) in 1 % BSA at 4 °C and were subsequently washed in PBS, and incubated with 1:1000 anti-rabbit secondary antibody conjugated with Alexa-Fluor 488®, 1:5000 phalloidin in 1 % BSA in PBS for 1 h at RT in the dark. The cells were washed once in PBS, incubated with Hoechst 33342 for 2 min at RT and mounted onto slides using Fluoromount (Sigma) to analyse the fluorescence using confocal microscopy (Zeiss LSM510 on a Zeiss AxioObserver Z1 motorized microscope).

The presence of tight junctions in epithelial cells can be confirmed with the localisation of E-cadherin at the cell surface. NHBE and iHBEC cells were seeded as above and stained using 1:1000 anti-rabbit E-cadherin overnight at 4 °C. Subsequently, the secondary antibody, phalloidin and Hoechst staining was performed as above. Once mounted on slides, fluorescence emissions were analysed as described above.

### **2.2.12 Phase contrast and digital image contrast videography**

The Zeiss Axiovert 200M microscope with AxioCam HR colour camera was used to take videography of NHBE grown by ALI with the help of David Read (Microscopist, MRC Toxicology Unit). The 40x objective used was the Zeiss LD Acroplan 40x/0.6 Korr Ph2 (phase contrast). The 100x objective used was Zeiss EC Plan-NeoFluar 100x/1.3 oil (digital image contrast).

### **2.2.13 Generation of ILZ TRAIL expression construct**

Isoleucine zippered (ILZ) TRAIL with N-terminal STREP tag was sub cloned from pcDNA3.1 expression construct, previously generated by Nick Harper, into empty vector pET28 using Hind III and Xho I restriction enzymes to generate an N-terminal His<sub>6</sub>, STREP, ILZ TRAIL construct.

### **2.2.14 Generation and purification of recombinant TRAIL and ILZ TRAIL**

Recombinant His<sub>6</sub>-tagged TRAIL and similarly ILZ TRAIL were generated and purified as previously described (MacFarlane et al., 1997; Harper & Macfarlane, 2008). In brief, pET28a-TRAIL expression vector was transformed into competent cells by heat shock at 42 °C for 45 s, 200 µl S.O.C medium added and cells shaken at 37 °C for 45 min. Transformed bacteria were plated out onto LB-Agar kanamycin selection plates and incubated overnight at 37 °C. LB media (4 ml) (8 ml for ILZ TRAIL batch) was inoculated with a single colony from the selection plate and cultured overnight with shaking at 37 °C. The overnight culture was added to 400 ml LB medium (800 ml for ILZ TRAIL batch) and cultured with shaking at 37 °C until OD ( $\lambda$ 600 nm) was 0.6-0.8. The culture was then induced with 1 mM IPTG and incubated at 37 °C with shaking for 3 h. The culture was then pelleted at 2000 g for 15 min at 4 °C. The pellet was then washed once in ice cold PBS, pelleted, snap frozen and stored at -80 °C until purification was required. Nickel affinity beads were used to purify both recombinant proteins, TRAIL and ILZ TRAIL.

### **2.2.15 TRAIL and ILZ TRAIL crosslinking**

Bis(sulfosuccinimidyl)suberate (BS<sup>3</sup>) is a crosslinking agent that allows for stable linking of proteins *via* amine residues. The spacer arm of BS<sup>3</sup> is 11.4 Å which is an appropriate length to allow for stable linkage of molecules in a complex. BS<sup>3</sup> (2 or 5 mM) was added to 5 µg TRAIL or ILZ TRAIL and incubated at 4 °C for 2 h. A quenching buffer consisting of Tris was added to a final concentration of 20 mM. Samples were subsequently prepared for analysis by SDS-PAGE.

### **2.2.16 Biotinylation of TRAIL and ILZ TRAIL**

Recombinant TRAIL was biotinylated (bTRAIL), as was recombinant ILZ TRAIL (bILZ TRAIL) using D-Biotinoyl-ε-Amidocaproic Acid-N-Hydroxysuccinimide ester (biotin) according to the manufacturer's instructions and as previously described (Harper & Macfarlane, 2008). In brief, nickel-purified His<sub>6</sub>-tagged TRAIL or ILZ TRAIL were washed and resuspended in PBS and labelled with 40 mg/ml and 12 mg/ml biotin respectively, on an end-to-end shaker for 1 h at 4 °C. Beads were then washed in lysis buffer (see below) and eluted with 150 mM EDTA. Biotinylated TRAIL and ILZ TRAIL were then aliquoted and stored at -80 °C.

### **2.2.17 TRAIL and ILZ TRAIL DISC isolation**

TRAIL or ILZ TRAIL death-inducing signalling complexes (DISC) were isolated from cells using the method as previously described (Harper and Macfarlane, 2008; Sprick et al., 2000). In brief, approximately 60 x 10<sup>6</sup> cells per treatment condition were treated with 1 µg/ml bTRAIL or 1 µg/ml bILZ TRAIL for the required amount of time at 37 °C; with or without a 1 h bTRAIL or bILZ TRAIL pre-chill incubation at 4 °C, as appropriate. Cells were then washed three times in ice cold PBS. DISC lysis buffer (30 mM Tris-HCl (pH 7.5), 150 mM NaCl, 10 % glycerol, 1 % triton X-100, supplemented with Complete™ protease inhibitor) was added to the cells and incubated on ice for 20 min. Cell lysates were pelleted at 17 700 g for 30 min. Streptavidin Dyna-M280 beads (50 µl) were added to each treatment condition and incubated with rotation overnight at 4 °C. bTRAIL complexes were eluted from the

beads by addition of SDS sample buffer and heating to 99 °C for 5 min. Subsequent analysis for DISC proteins by immunoblotting was performed.

### **2.2.18 Size-exclusion chromatography**

All size-exclusion of TRAIL and ILZ TRAIL experiments were conducted with the help of Dr Claudia Langlais (MRC Toxicology Unit). The Superdex™ 200 PC 3.2/30 gel filtration column was used in conjunction with the SMART® system (GE Healthcare). The running buffer was composed of 20 mM HEPES-KOH, 150 mM NaCl, 5 % sucrose, 0.1 % CHAPS and 5 mM dithiothreitol, pH 7.0. (pH and NaCl concentrations were subject to variation where stated). Samples were applied to the SMART® system and eluted in 50 µl fractions at a rate of 40 µl/min. The elution fractions were analysed by SDS-PAGE separation and subsequently either Western blot or coomassie staining. All columns were calibrated using protein standards from both high and low molecular weight kits (GE Healthcare).

### **2.2.19 Enzyme linked immunosorbent assay**

Interleukin-8 (IL-8), Interleukin-6 (IL-6), secretion into media of treated and control cells was determined by enzyme linked immunosorbent assay (ELISA) according to manufacturer's instructions. In brief, capture antibodies were coated on 96-well plates overnight at RT followed by blocking at RT for 1 h prior to conditioned media samples (in duplicate) and purified recombinant cytokine (for standard curve determination) addition for 2 h at RT. Conditioned media were diluted as appropriate to fall within linear range of the standard curve. The relevant detection antibody was added and incubated for 2 h at RT following addition of Streptavidin-HRP for 20 min at RT in the dark. Final addition of tetramethylbenzidine substrate solution allowed for colour development relative to protein amount. Optical Density was determined at λ450 nm with readings at λ570 nm subtracted from these values to account for any plate imperfections.

### **2.2.20 Protein profiler arrays**

The Protein Profiler Array™ Human XL Cytokine Array Kit was used to determine cytokine and chemokine signature changes in conditioned media of co-culture

samples (Chapter 5) according to the manufacturer's instructions. In brief, arrays were blocked in array buffer for 1 h at RT, prior to the addition of the conditioned media. Conditioned media (500  $\mu$ l) were thawed and brought to RT and diluted in array buffer to a final volume of 1.5 ml. Diluted samples were incubated with the arrays overnight at 4 °C. The following day, samples were aspirated and arrays washed three times for 10 min in wash buffer. A cocktail of detection antibodies were added to each array and incubated for 1 h at RT. Following three washes, the arrays were incubated with streptavidin-HRP for 30 min at RT. A final three washes followed, with subsequent addition of ChemiReagent. The enzymatic activity of the ECL in the ChemiReagent was visualised on FujiFilm™ LAS4000 Imager. The spots were quantified by densitometry using ImageJ™ and the Protein Array Analyser Plug-in. The arrays were normalised according to the positive and negative control spots. Each array was compared to the appropriate control array to determine degree of protein change.

### **2.2.21 Statistical analysis**

Data are presented as mean  $\pm$  standard error of mean (SEM) throughout. Where statistical analysis was appropriate one-way analysis of variance (ANOVA) was calculated using GraphPad PRISM®. The statistical significance classifications are as follows; \* where  $p < 0.05$ , \*\* where  $p < 0.01$  and \*\*\* where  $p < 0.001$ .

### **3 Results: Characterisation of TRAIL-R1/R2-dependent Cell Death in Lung Epithelial and T Cell Lines – Generation of ILZ TRAIL**

### 3.1 Introduction

The overall aim of this Chapter was to elucidate whether TRAIL-R1 signalling was significantly different to TRAIL-R2 signalling and therefore whether another tool was required to be developed for use further on in the project for elucidating the TRAIL/TRAIL-R signalling axis in different cell types.

In this Chapter, TRAIL-induced signalling to apoptosis in the lung epithelial cell line, BEAS-2B and the T cell line, Jurkat E6.1 was investigated with two aims; firstly, to uncover which death receptor is more active in driving apoptosis in these cells and secondly, to identify the preferred conformation of TRAIL, i.e. does soluble or membrane-bound ligand induce a stronger signal to apoptosis.

TRAIL-induced apoptosis occurs through ligation of TRAIL to the death receptors, TRAIL-R1 or TRAIL-R2. As described in Chapter 1, signalling through TRAIL-R2 preferentially occurs when the receptor is presented with a higher-order oligomeric form of TRAIL. TRAIL is most likely to be oligomerised when membrane-bound on the surface of a cell. Thus, TRAIL-R2 signalling is thought to occur mostly in a cell-to-cell dependent manner. This is in contrast to TRAIL-R1, where ligation by soluble TRAIL alone is sufficient to drive DISC formation and downstream apoptosis.

Leucine zipper (LZ) motifs occur naturally in DNA-binding proteins. They are characterised by their ability to form a coiled-coil tertiary structure that can interact with other LZ-containing proteins to form dimers (Harbury et al., 1993; O'Shea et al., 1989). LZ motifs have been used in recombinant proteins to allow for the formation of dimerised proteins (Kalandadze et al., 1996). The Walczak group had previously made LZ TRAIL (Walczak et al., 1999) to test whether it had potential as a therapeutic agent for the treatment of cancer. The leucine residues in the motif can be replaced by isoleucine, which allows for trimers, instead of dimers, of proteins to form (Harbury et al., 1993). It is known that for TRAIL signalling to occur, three TRAIL molecules are required to induce the trimerisation of TRAIL receptors and therefore subsequent downstream signalling (see Chapter 1). Thus, due to the aforementioned preference of TRAIL-R2 for an oligomerised form of ligand, TRAIL

containing an isoleucine zipper motif (ILZ TRAIL) could potentially be even more effective for signalling to apoptosis through TRAIL-R2 than LZ TRAIL.

Using the TRAIL receptor-specific agonistic antibodies, ETR1 and ETR2, it was possible to elucidate whether preferential TRAIL signalling *via* TRAIL-R1 or TRAIL-R2 occurred in BEAS-2B and Jurkat E6.1 cells. However, due to the limited availability of these agonistic antibodies and the requirement for an appropriate tool to dissect out TRAIL-R signalling preferences in future experiments, recombinant ILZ TRAIL was generated, and its activity and ability to isolate the TRAIL DISC verified.

## **3.2 Results**

### **3.2.1 Characterisation of the lung epithelial cell line, BEAS-2B and the leukemic T lymphocyte cell line, Jurkat E6.1**

The BEAS-2B cell line is a lung epithelial cell line derived from non-cancerous tissue during autopsy. The cells were transformed using an adenovirus 12-SV40 virus hybrid (Reddel et al., 1988). Normal cell, cell lines are documented to be less sensitive to apoptotic stimuli however the viral transformation process is known to sensitise cells to extrinsic apoptotic stimuli (Ashkenazi et al., 1999; Kelley et al., 2001; Walczak et al., 1999). The T cell line, Jurkat E6.1, was derived from the peripheral blood of a 13 year old male with leukaemia (Weiss et al., 1984).

#### **3.2.1.1 BEAS-2B and Jurkat E6.1 cells display concentration-dependent sensitivity to TRAIL-induced apoptosis**

Prior to treatment with TRAIL, BEAS-2B and Jurkat E6.1 cells were analysed for their surface expression of the death receptors, TRAIL-R1 and TRAIL-R2 (Figure 3.1a). As represented by the fluorescence mean intensity, TRAIL-R2 was expressed on the surface of BEAS-2B cells. However, TRAIL-R1 was not expressed on the cellular surface of these cells. Similarly, TRAIL-R2, but not TRAIL-R1, was expressed on the surface of Jurkat E6.1 cells.

In order to characterise the sensitivity of BEAS-2B and Jurkat E6.1 cells to TRAIL-induced apoptotic cell death, cells were treated with 0 – 2 µg/ml soluble recombinant TRAIL for 5 h at 37 °C and apoptosis then assessed using annexin V-FITC/PI staining and flow cytometry. Figure 3.1b shows that treatment of BEAS-2B cells with TRAIL (0 – 2 µg/ml) caused a small but significant amount of cell death over 5 h. A maximal 11 % cell death was reached with 2 µg/ml TRAIL. Concentration-dependent processing of the apical caspase, procaspase 8 (p55/53) to p43/41 and subsequently to p18 was clearly observed. Procaspase 9 (p46) processing to p35, but not p37, also occurred. This is indicative of caspase 9 autocatalytic cleavage mediated *via* the apoptosome and not by caspase 3, consistent with the observation that procaspase 3 (p32) was only processed to its p20 form and not the active

cleavage fragments, p19 and p17. There was also little evidence of PARP (p116) cleavage as shown by the lack of PARP processing to p89. Taken together, these immunoblot observations are consistent with the low level of apoptosis detected, as assessed by PS externalisation and flow cytometry.

Upon treatment with TRAIL (0.1 – 1 µg/ml), Jurkat E6.1 cells displayed a concentration-dependent increase in annexin V-FITC/PI positive stained cells (both early and late stage apoptotic cells) (Figure 3.1b). However, apoptosis was moderate, with a maximum of 29 % cell death detected with 1 µg/ml TRAIL. Consistent with these flow cytometry measurements was cleavage of the initiator caspases, procaspase 8 and procaspase 9. Procaspase 8 processing to p43/41 was evident at all TRAIL concentrations (0.1 – 1 µg/ml). Furthermore, processing of caspase 8 to its most active form, as evidenced by generation of the p18 cleavage fragment, was detected at all concentrations of TRAIL. In addition, the executioner caspase, procaspase 3 was processed to its proteolytically active p19 fragment with a small amount of the p17 cleavage fragment also evident. Consistent with this, the downstream caspase substrate, PARP was cleaved to p89.

Additionally, pre-treatment of BEAS-2B and Jurkat E6.1 cells with the pan caspase inhibitor carbobenzoxy-Val-Ala-Asp-(O-methyl)-fluoromethylketone (zVAD.fmk), prior to TRAIL treatment (Figure 3.1c, lanes 8 and 15) inhibited TRAIL-induced apoptosis. Taken together, these data show that TRAIL treatment of Jurkat E6.1 cells resulted in a moderate but concentration-dependent induction of apoptotic cell death over 5 h which was caspase-dependent. In contrast, in BEAS-2B cells, TRAIL induced very little apoptotic cell death but the cell death was again caspase-dependent.

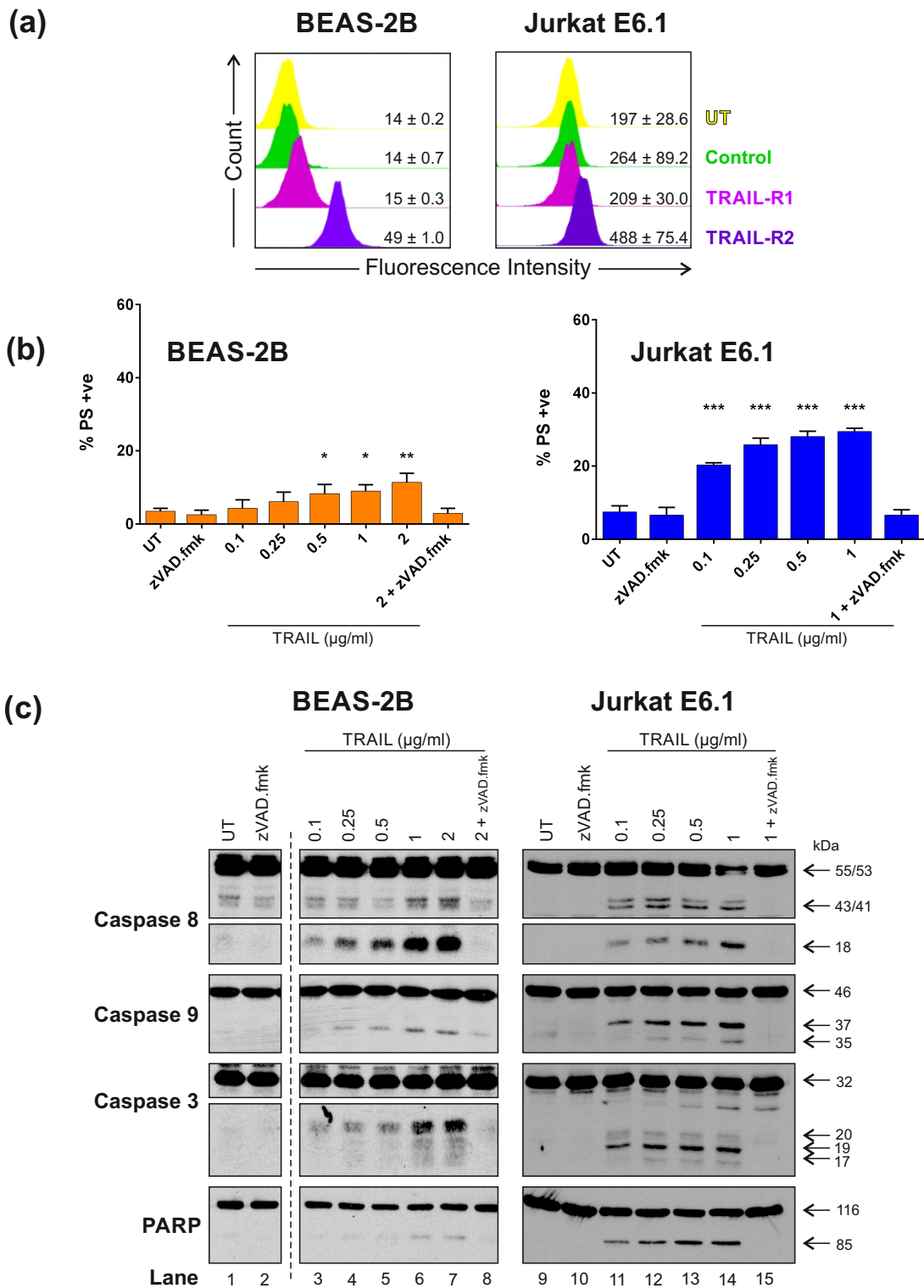


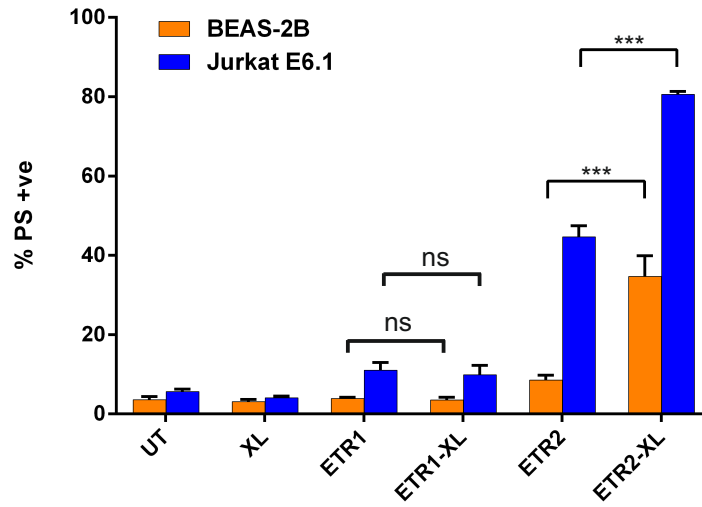
**Figure 3.1 BEAS-2B and Jurkat E6.1 cells display concentration-dependent sensitivity to TRAIL** (a) BEAS-2B and Jurkat E6.1 cells were analysed for cellular surface expression of TRAIL-R1 and -R2. Cells were incubated with either no antibody (control), isotype control antibody or PE-conjugated TRAIL-R1 or TRAIL-R2 antibodies. Following washing with PBS, cells were analysed by flow cytometry for changes in fluorescence intensity. Fluorescence intensity is represented by geometric mean with SEM (n=3). (b) BEAS-2B and Jurkat E6.1 cells were treated with 0 - 2 µg/ml soluble TRAIL for 5 h at 37 °C (+/- 10 µM zVAD.fmk) and analysed by flow cytometry for PS externalisation. Bar chart represents relative % cell death (annexin V-FITC/PI) (mean ± SEM, n=3). Significance asterisks are relative to UT, \* where p<0.05, \*\* where p<0.01 and \*\*\* where p<0.001. Cell pellets were analysed for caspase 8, caspase 9, caspase 3 and PARP cleavage by immunoblotting. Immunoblots are representative of three independent experiments. Dashed line indicates removal of irrelevant lanes.

### **3.2.1.2 Treatment of BEAS-2B and Jurkat E6.1 cells with cross-linked agonistic antibody to TRAIL-R2 results in increased cell death compared with TRAIL-R2 agonistic antibody alone**

Following the observation that both BEAS-2B and Jurkat E6.1 cells signal to TRAIL-induced apoptosis but express predominantly TRAIL-R2 rather than TRAIL-R1 on their cell surface, the response of these cells to TRAIL-R1/R2-specific agonistic antibodies was investigated. BEAS-2B and Jurkat E6.1 cells were incubated with the agonistic antibodies ETR1 or ETR2 (agonistic antibodies to TRAIL-R1 and TRAIL-R2, respectively), either in the presence or absence of a cross-linking antibody (XL) for 5 h at 37 °C. Flow cytometric analysis of annexin-V-FITC/PI stained cells showed that ETR1-XL treatment of either BEAS-2B or Jurkat E6.1 cells did not induce an increase in cell death compared to ETR1 alone (Figure 3.2a). In contrast, in both cell types, ETR2-XL induced a significant increase in apoptosis when compared with ETR2 alone. For the BEAS-2B cells, the increase in cell death was more than two-fold whereas in Jurkat E6.1 cells the increase in cell death was almost two-fold.

Immunoblots for caspases 8, 9 and 3 and the caspase substrate PARP further confirmed the increase in cell death with ETR2 treatment in the presence of XL (Figure 3.2b). Consistent with flow cytometric analysis of PS externalisation, ETR1-XL did not induce an increase in caspase-8, -9 and -3 cleavage in either BEAS-2B cells (lanes 3 and 4) or Jurkat E6.1 cells (lanes 9 and 10) when compared with ETR1 alone. In BEAS-2B cells (lanes 5 and 6) and Jurkat E6.1 cells (lanes 11 and 12) an increase in caspase-dependent cell death with ETR2-XL treatment compared to ETR2 alone was evidenced by the presence of caspase cleavage fragments and a corresponding loss of the equivalent caspase proform. Notably, in BEAS-2B cells, ETR2-XL did not induce caspase 3-mediated cleavage of caspase 9 to p35, rather only autocatalytic cleavage of caspase 9 to cleavage fragment p37 was observed. Most pronounced of all was the complete processing of PARP to p89 in Jurkat E6.1 cells, following ETR2-XL treatment (lane 12), consistent with the 80 % apoptotic cell death detected in these cells *via* PS externalisation (Figure 3.2a).

(a)



(b)

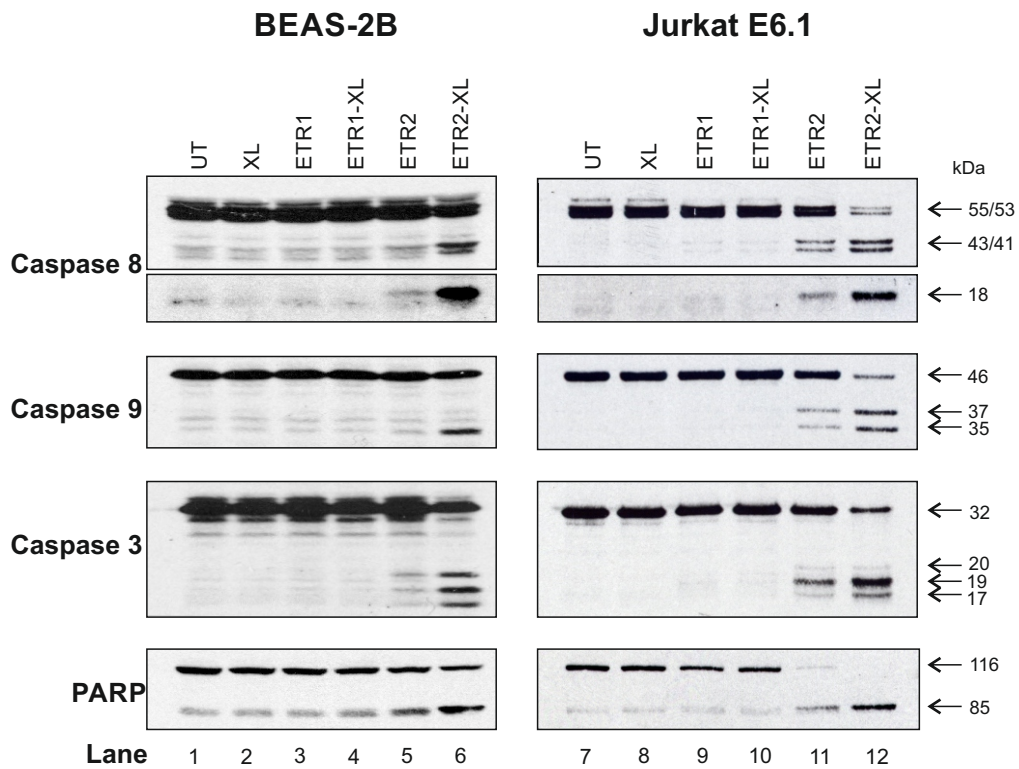


**Figure 3.2 Treatment of BEAS-2B and Jurkat E6.1 cells with cross-linked agonistic antibody to TRAIL-R2 results in increased cell death compared with TRAIL-R2 agonistic antibody alone**  
(a) BEAS-2B and Jurkat E6.1 cells were treated with either 0.5  $\mu$ g/ml ETR1 or ETR2 in the presence/absence of a crosslinking antibody for 5 h at 37  $^{\circ}$ C. Cells were analysed by flow cytometry for cell death. Bar chart represents relative % cell death (annexin V-FITC/PI) (mean  $\pm$  SEM, n=3). \* where p<0.05, \*\* where p<0.01 and \*\*\* where p<0.001 ns denotes not significant (b) Cell pellets were analysed for caspase 8, caspase 9, caspase 3 and PARP cleavage by immunoblotting. Immunoblots are representative of three independent experiments.

## 3.2.2 Generation and validation of ILZ TRAIL

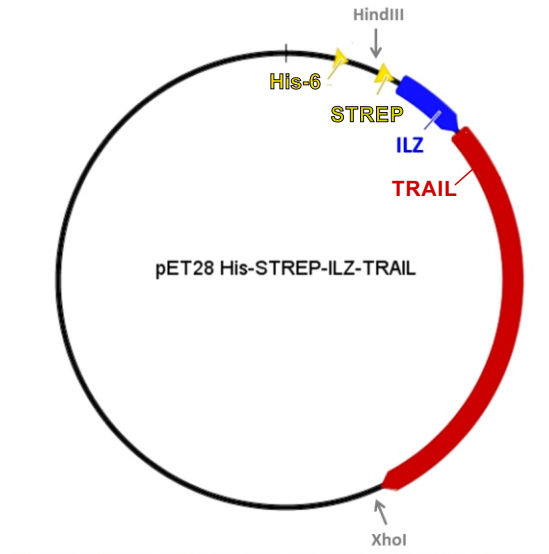
### 3.2.2.1 Synthesis and purification of ILZ TRAIL

As mentioned previously, ILZ motifs cause proteins to form trimers. Soluble recombinant TRAIL containing an ILZ motif was therefore synthesised, for future use as a tool to help elucidate TRAIL-R signalling in target cells. In order to do this, a strep-tag, the ILZ amino acid sequence and the extracellular domain of TRAIL were all cloned into the backbone vector, pET28a, which already contained a His<sub>6</sub> sequence, as schematically shown in Figure 3.3a. Hind III and Xho1 restriction sites are indicated using arrows to show the sites used to clone in the STREP-ILZ-TRAIL sequence.

The strep-tag was included in the construct for subsequent purification *via* this tag. A strep-tag consists of an eight amino acid sequence; tryptophan, serine, histidine, proline, glutamine, phenylalanine, glutamate and lysine. This relatively short, inert peptide was engineered based on the highly specific biotin-streptavidin interaction. Strep-tag has high affinity to another engineered protein, streptactin, a protein that is based on the structure of streptavidin (Schmidt and Skerra, 2007). The strep-tag is an attractive tool for protein purification due to the reversible nature of the specific interaction between strep-tag and streptactin.

Following successful generation of the His<sub>6</sub>-STREP-ILZ-TRAIL construct, protein expression and purification of ILZ TRAIL was carried out using the His<sub>6</sub>-tag as outlined in Materials and Methods (Chapter 2). To demonstrate successful purification of the protein, elutions of ILZ TRAIL were visualised by coomassie staining of SDS-PAGE gels (Figure 3.3b). Lanes 5 – 10 show the relative abundance of purified ILZ TRAIL (p32) present in each elution.

(a)



(b)

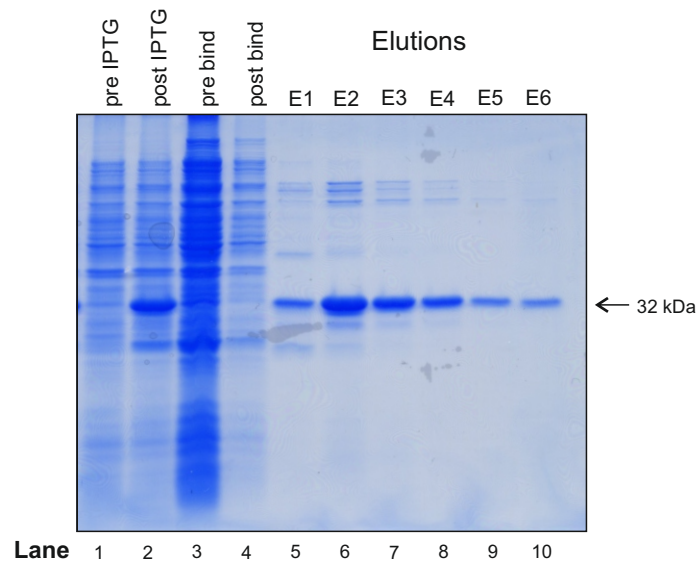


**Figure 3.3 Synthesis and purification of ILZ TRAIL** (a) The backbone vector, pET28, was digested at Hind III and Xho I restriction sites with subsequent insertion of STREP-ILZ-TRAIL to generate a final pET28 construct containing His<sub>6</sub>-STREP-ILZ-TRAIL (b) Purified elutions of ILZ TRAIL (5  $\mu$ l) were separated by SDS-PAGE. The gel was stained with coomassie to visualise proteins. E represents elution.

### 3.2.2.2 Validation of the oligomerised conformation of ILZ TRAIL

In order to ensure that purified recombinant ILZ TRAIL was in the correct trimerised/oligomerised conformation, size-exclusion chromatography was performed (Figure 3.4). The Superdex™ 200 gel filtration column, which separates proteins in the molecular weight range of 10 – 60 kDa, was selected for the separation of ILZ TRAIL and the buffer components initially chosen for protein separation were as follows; 20 mM HEPES-KOH, 150 mM NaCl, 5 % sucrose, 0.1 % CHAPS and 5 mM dithiothreitol, pH 7.0. However, using this buffer, ILZ TRAIL did not separate into any distinct fraction peaks (data not shown). Consequently, NaCl and pH concentrations were varied from the standard protocol to stabilise and retain the potential trimerised/oligomerised conformation of ILZ TRAIL.

Figure 3.4a displays the three variations of buffer components that were used to optimise the gel filtration conditions for size separation of ILZ TRAIL. For the first analysis, the NaCl concentration was doubled to 300 mM and for the two subsequent column experiments the pH was varied to either pH6 or pH8. Changing the NaCl concentration to 300 mM did improve the stability of ILZ TRAIL, allowing for a peak of ILZ TRAIL to be observed from fraction 12 to fraction 19. However, lowering the pH to 6 did not improve the stability of ILZ TRAIL, with the coomassie-stained SDS gel showing the wide molecular weight distribution of protein as previously observed with the use of the original standard buffer components. In contrast, changing the pH of the buffer to pH8 greatly improved the stability of ILZ TRAIL as shown by the distinct peak of protein observed in fractions 13 – 18. Based on the coomassie-stained SDS gels shown in Figure 3.4a, the standard buffer was adjusted to pH8, for subsequent analyses of ILZ TRAIL and TRAIL by size-exclusion chromatography.

Figure 3.4b shows the comparison of ILZ TRAIL and TRAIL when gel filtration fractions (6 – 30) were immunoblotted for His<sub>6</sub>. TRAIL eluted as two peaks, in fractions 20 – 22 and fractions 16 – 19, which according to the standards corresponds to between 158 and 43 kDa for the first peak and 13 and 43 kDa for the second peak. In contrast, ILZ TRAIL eluted as one peak, in fractions 16 – 18,

corresponding to between 158 and 43 kDa. These gel filtration experiments indicate that TRAIL is in a mixture of monomers, dimers, trimers and higher order oligomers. However, ILZ TRAIL is only present as trimers and higher order oligomers, confirming the reported functionality of the ILZ motif within the protein. In order to further confirm the oligomeric status of ILZ TRAIL, the cross-linker, BS<sup>3</sup> which allows for the stable linkage of amine groups between proteins, was used to covalently bind either TRAIL or ILZ TRAIL in their naturally forming conformations. Figure 3.4c shows that ILZ TRAIL exists in a mixture of dimers, trimers and oligomers, as indicated by the presence of bands at approx. 55, 100 and 200 kDa (lane 4). In contrast, TRAIL exists in a mixture of monomers, dimers and trimers, as specified by the bands at approx. 30, 55 and 100 kDa (lane 2). This finding is consistent with the previous gel filtration experiments, further confirming the higher oligomeric status of ILZ TRAIL compared to TRAIL.

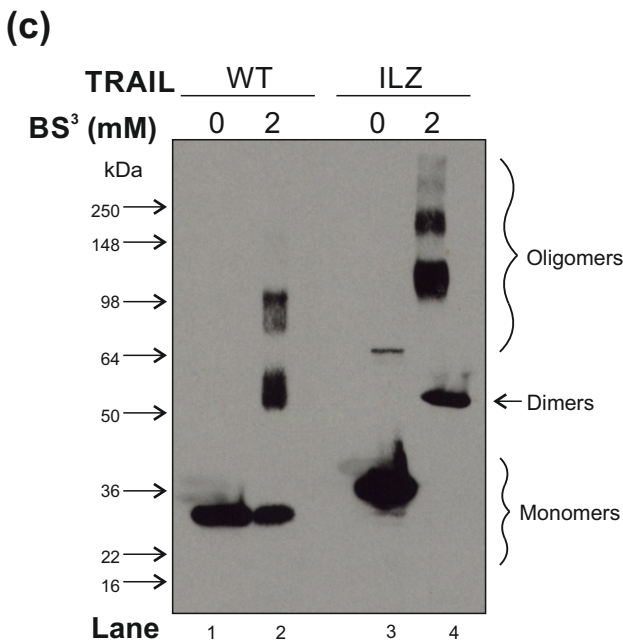
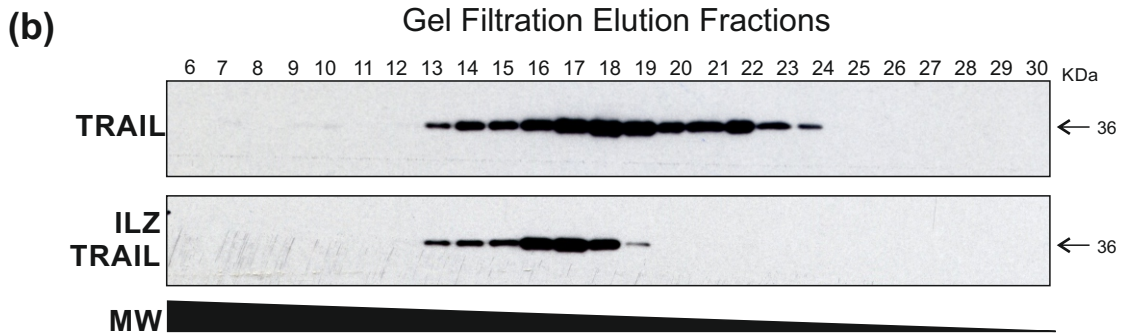
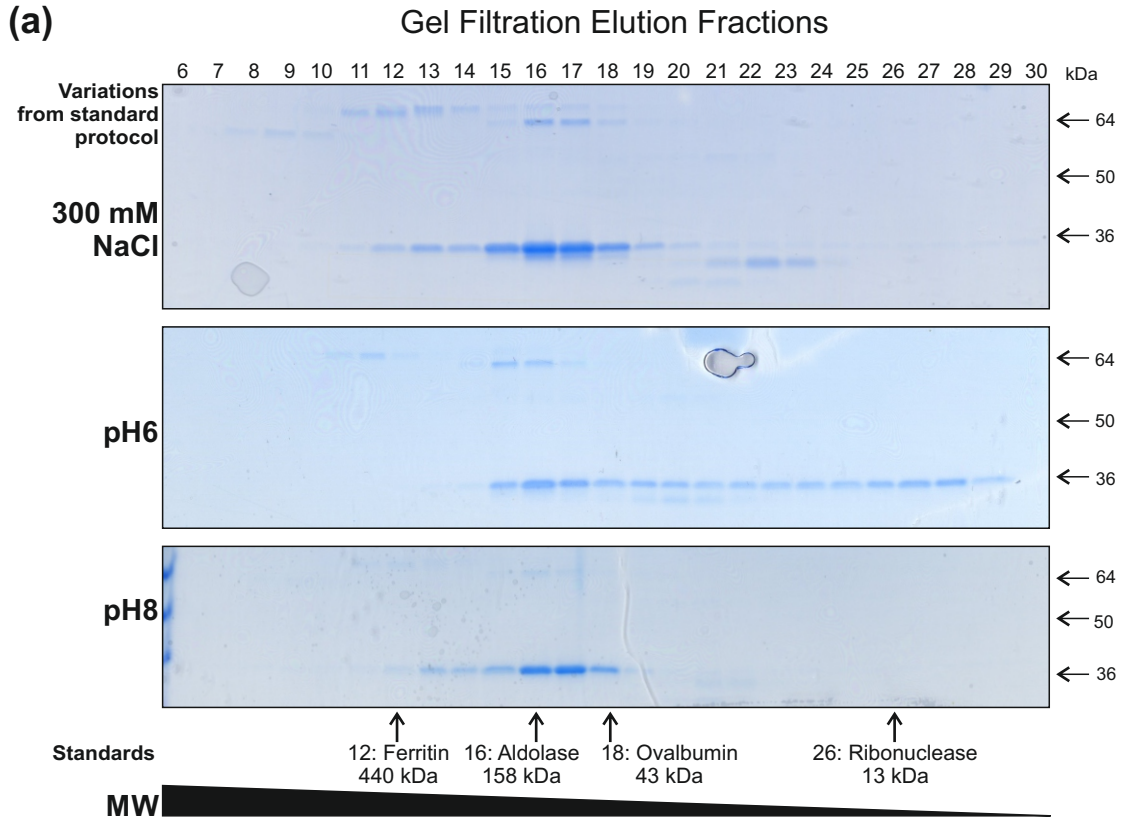


**Figure 3.4 Validation of the oligomerised conformation of ILZ TRAIL** (a) Purified ILZ TRAIL was run on a Superdex™ 200 size exclusion column three times as outlined in Chapter 2, each time with one variation in buffer components - either a change in NaCl concentration or pH. Elution fractions (6-30) were separated by size using SDS-PAGE and gels were stained with coomassie to visualise the presence of ILZ TRAIL in the different fractions. (b) Both recombinant proteins, TRAIL and ILZ TRAIL were eluted on the Superdex™ 200 column using the standard buffer at pH8. Elution fractions (6-30) were separated by SDS-PAGE and immunoblotted using anti-His<sub>6</sub> antibody. (c) Both TRAIL and ILZ TRAIL were treated with the BS<sup>3</sup> crosslinker (2 mM) for 30 min at RT. The ligands were separated by SDS-PAGE and immunoblotted for His<sub>6</sub>.

### **3.2.2.3 ILZ TRAIL induces increased cell death in BEAS-2B and Jurkat E6.1 cells compared to TRAIL**

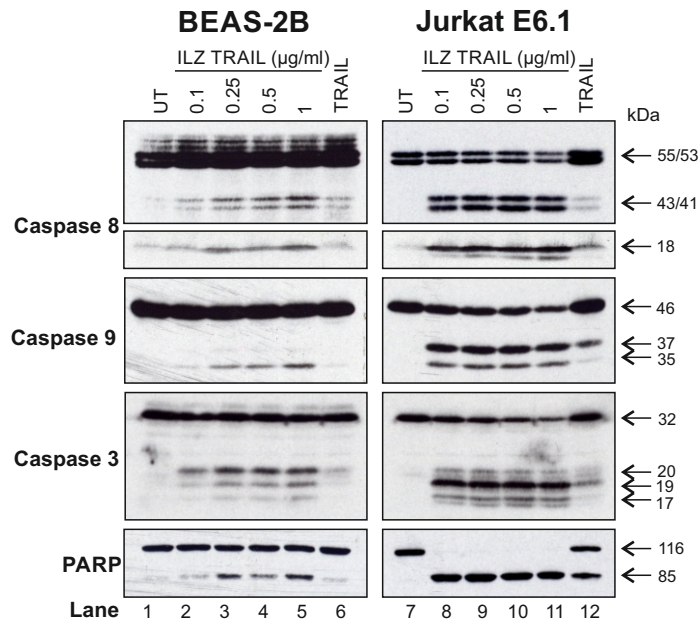
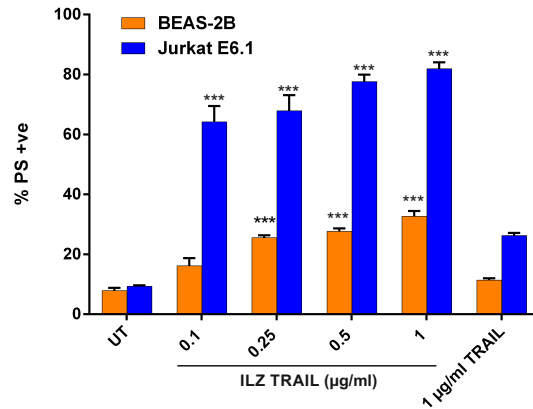
Following validation of the conformational status of ILZ TRAIL, BEAS-2B and Jurkat E6.1 cells were treated with ILZ TRAIL. The aim was to investigate the functionality of ILZ TRAIL by analysing whether ILZ TRAIL displayed increased apoptotic activity in comparison to TRAIL in TRAIL-R2 signalling cells (Figure 3.5).

BEAS-2B and Jurkat E6.1 cells were treated with 0 – 1 µg/ml ILZ TRAIL or 1 µg/ml TRAIL for 5 h and the results compared with the cell death data from Figure 3.2. BEAS-2B and Jurkat E6.1 cells both displayed a concentration-dependent increase in cell death as shown by annexin-V-FITC/PI staining (Figure 3.5a). BEAS-2B cells displayed a three-fold increase in cell death when treated with 1 µg/ml ILZ TRAIL (32 %) compared to 1 µg/ml TRAIL (11 %). Similarly, Jurkat E6.1 cells displayed a greater than three-fold increase in cell death when treated with 1 µg/ml ILZ TRAIL (82 %) compared to 1 µg/ml TRAIL (26 %).

Upon 0 – 1 µg/ml ILZ TRAIL treatment, dose-dependent processing of the apoptotic markers, caspase 8, 9, 3 and PARP was observed (Figure 3.5a) in BEAS-2B (lanes 1 – 5) and Jurkat E6.1 cells (lanes 7 – 11), consistent with the annexin-V-FITC/PI data. Pro-caspase 8 was processed to its p43/41 fragments and subsequently to the p18 fragment in BEAS-2B (lanes 2 – 5) and Jurkat E6.1 cells (lanes 7 – 11), indicating full activation of caspase 8. In BEAS-2B cells, pro-caspase 9 was processed to p35 but not to p37, whereas in Jurkat E6.1 cells pro-caspase 9 processing was observed to both p37 and p35 fragments. In both BEAS-2B and Jurkat E6.1 cells, pro-caspase 3 was processed to p20, p19 and p17. In BEAS-2B cells partial processing of PARP to p89 was also observed, consistent with the moderate cell death detected by flow cytometry. In Jurkat E6.1 cells, complete cleavage of PARP, as seen in lanes 7 – 11, was consistent with the high level of cell death observed as assessed by annexin-V-FITC/PI staining (82 %). TRAIL treatment (1 µg/ml) of BEAS-2B and Jurkat E6.1 cells (lanes 6 and 12, respectively) resulted in a similar cleavage of apoptotic markers as detected with ILZ TRAIL treatment, but to a lower extent, again consistent with the flow cytometry data.

The pan caspase inhibitor zVAD.fmk was used to determine whether the cell death induced by ILZ TRAIL treatment was indeed caspase-dependent and therefore apoptotic (Figure 3.5b). Incubation of BEAS-2B cells with zVAD.fmk, prior to 1 µg/ml ILZ TRAIL treatment, resulted in a reduction in cell death from 34 % to 9 % as measured by annexin-V-FITC/PI staining. Consistent with this, immunoblots of the apoptotic markers, caspase 8, 9, 3 and PARP showed inhibition of cleavage (lane 4). Pre-treatment of Jurkat E6.1 with zVAD.fmk also resulted in inhibition of cell death as assessed by flow cytometry (from 78 % to 10 % cell death) and corresponding immunoblots of caspase 8, 9, 3 and PARP (lane 8).

(a)



(b)

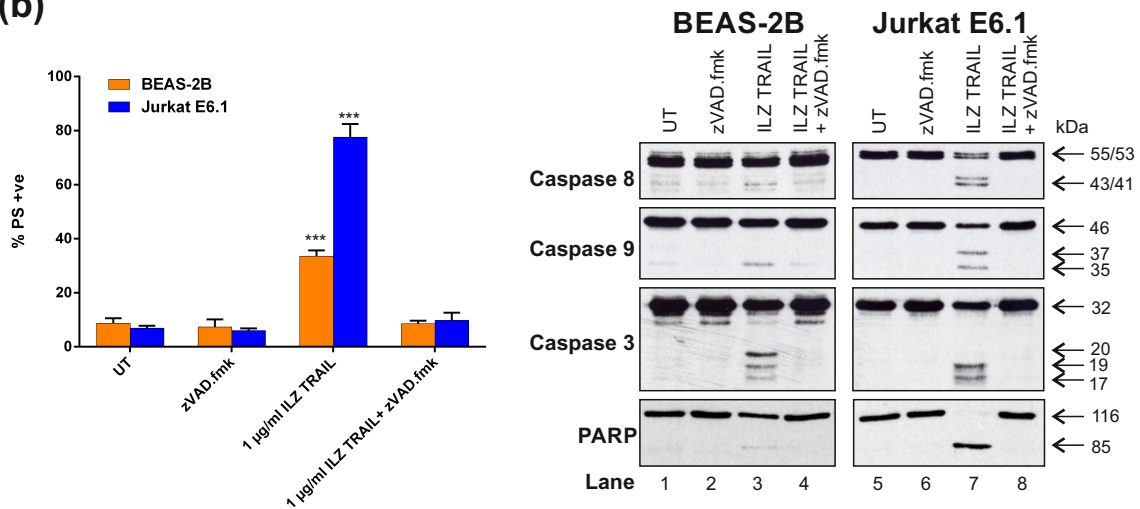


**Figure 3.5** ILZ TRAIL induces increased cell death in BEAS-2B and Jurkat E6.1 cells compared to TRAIL (a) BEAS-2B and Jurkat E6.1 cells were treated with 0 - 1 µg/ml ILZ TRAIL or TRAIL for 5 h at 37 °C following cell death analysis using flow cytometry. Bar chart represents relative % cell death (annexin V-FITC/PI) (mean ± SEM, n=3). Significance asterisks are relative to the corresponding TRAIL treatment. Cell pellets were analysed for caspase 8, caspase 9, caspase 3 and PARP cleavage by immunoblotting. (b) BEAS-2B and Jurkat E6.1 cells were treated with 1 µg/ml ILZ TRAIL for 5 h at 37 °C (+/- 10 µM zVAD.fmk) and analysed by flow cytometry for cell death. Bar chart represents relative % cell death (annexin V-FITC/PI) (mean ± SEM, n=3). Significance asterisks are relative to UT \* where p<0.05, \*\* where p<0.01 and \*\*\* where p<0.001. Cell pellets were analysed for caspase 8, caspase 9, caspase 3 and PARP cleavage by immunoblotting. All immunoblots are representative of three independent experiments.

### **3.2.3 Optimisation of ILZ TRAIL DISC isolations**

#### **3.2.3.1 Strep-tagged ILZ TRAIL DISC can be isolated in Jurkat E6.1 cells, but not without non-specific interactions**

Following successful demonstration of the apoptotic activity of ILZ TRAIL and its ability to signal efficiently to apoptosis through TRAIL-R2, isolation of the ILZ TRAIL DISC was attempted using the Strep-tag present in the recombinant protein (Figure 3.6). The Strep-tag was cloned into the ILZ TRAIL construct to enable isolation of the DISC. Since the interaction between biotin and streptavidin was the basis for initial generation of the Strep-tag (Schmidt and Skerra, 1993) magnetic or sepharose streptactin beads were employed to isolate the ILZ TRAIL DISC in Jurkat E6.1 cells. This was performed in order to find the optimal streptactin bead platform for subsequent pulldown experiments (Figure 3.6a). Known TRAIL DISC components were immunoblotted for; TRAIL-R1, TRAIL-R2, FADD and caspase 8. The magnetic beads (lane 3) successfully pulled down the ILZ TRAIL DISC as evidenced by the presence of the known DISC components. While the sepharose beads did pull down components of the DISC, as shown by the presence of caspase 8 (lane 4), indicating upstream TRAIL-R1 and –R2 recruitment into the DISC, the level of DISC pulled down was far less than observed with magnetic beads. Moreover, unstimulated TRAIL receptors (ILZ TRAIL added post lysis) pulled down components of the DISC (lane 1) indicating non-specific interaction of proteins with the magnetic beads.

Figure 3.6b shows an ILZ TRAIL DISC isolated using two different types of magnetic streptactin beads, from different companies, IBA (as used in Figure 3.6a) and Qiagen. Additionally, the elution conditions were altered to attempt to reduce the amount of unstimulated TRAIL receptor non-specific binding observed in Figure 3.6a. A lower temperature, 37 °C, and a longer incubation period of 1 h were employed to allow for more “gentle” removal of DISC complexes from the beads. Desthiobiotin, a modified form of biotin used to competitively bind to streptactin beads was also used to competitively elute off DISC complexes from both IBA and

Qiagen magnetic streptactin beads in a three step batch manner – to ensure complete elution of the DISC.

Upon treatment with ILZ TRAIL and subsequent elution at 37 °C for 1 h (lane 3), IBA beads pulled down significant amounts of known DISC components. However, the same DISC components (except FADD) were also observed in the unstimulated control sample (lane 1). Moreover, an even greater amount of caspase 8 was detected in the unstimulated control sample by elution with desthiobiotin (lane 5) compared with the unstimulated sample eluted at 37 °C for 1 h (lane 1). In unstimulated samples, Qiagen beads eluted either with desthiobiotin or at 37 °C for 1 h, did not pull down TRAIL-R1 or TRAIL-R2 (lanes 2, 6, 10, 14). Additionally, little or no TRAIL-R1 or TRAIL-R2 recruitment was observed in the matched DISC isolations (lanes 4, 8, 12, 16). However, using Qiagen beads, caspase 8 and FADD were detected in both unstimulated samples (lanes 2, 6, 10, 14) and the matched DISC complex isolations (lanes 4, 8, 12, 16).

Due to the inability of Qiagen magnetic beads to successfully isolate the DISC, these beads were no longer used for subsequent isolations. However, despite some non-specific interactions observed in unstimulated control samples, IBA magnetic beads appeared to successfully pull down the ILZ TRAIL DISC. To try and reduce the non-specific interactions observed, high capacity IBA magnetic streptactin beads were employed (Figure 3.6c), although in this case 30 µl beads were used rather than the 50 µl beads used for the earlier non-high capacity IBA magnetic bead experiments shown in Figure 3.6b.

Elution of the DISC was performed directly into sample buffer at either 37 °C for 1 h (lanes 1 and 2) or 70 °C for 10 min (lanes 3 and 4). Known components of the DISC, TRAIL-R2, FADD and caspase 8, but not TRAIL-R1 were detected by immunoblotting, using either elution method (lanes 2 and 4). Importantly, cleaved caspase 8 (p43/41 fragments) was present in the DISC isolations (lanes 2 and 4) but not in the matched unstimulated control samples (lanes 1 and 3). However, in the unstimulated control samples (lanes 1 and 3), the DISC components, TRAIL-R2,

FADD and caspase 8 were also pulled down albeit to a lesser extent than in the matching DISC isolations (lanes 2 and 4).



### **3.2.3.2 Biotinylation of ILZ TRAIL allows for specific isolation of the ILZ TRAIL DISC in Jurkat E6.1 cells**

Isolation of the ILZ TRAIL DISC using the Strep-tag resulted in non-specific interactions; therefore biotinylation of ILZ TRAIL was performed. Biotinylation of TRAIL has previously been successfully employed by our laboratory to isolate the TRAIL DISC (Harper and Macfarlane, 2008). Biotin is known to bind strongly to avidin or streptavidin and therefore can be used as a tag to isolate and purify proteins using insoluble supports such as agarose conjugated to streptavidin. In this chapter biotinylation of ILZ TRAIL was optimised so that the ILZ TRAIL DISC could be isolated without compromising the activity of the protein (Figure 3.7).

Biotinylation of TRAIL has previously been performed using either 5  $\mu$ l or 10  $\mu$ l of biotin (Harper and Macfarlane, 2008). Using these amounts of biotin, ILZ TRAIL was labelled and the resulting bILZ TRAIL analysed for activity in Jurkat E6.1 cells (Figure 3.7a). ILZ TRAIL (1) was the first batch to be labelled with either 5  $\mu$ l (sample A) or 10  $\mu$ l (sample B) of biotin. The coomassie stained SDS gel in Figure 3.7a shows that this batch of ILZ TRAIL (1) was pure and non-contaminated as indicated by the presence of the 32 kDa band known to be ILZ TRAIL in elutions 1 – 5 of samples A and B (lanes 5 – 10 and 15 – 20). To analyse the activity of bILZ TRAIL compared to ILZ TRAIL, Jurkat E6.1 cells were treated over 5 h using elution one of samples A and B from the first batch of ILZ TRAIL. The extent of apoptosis induced by bILZ TRAIL was analysed by staining the cells with annexin-V-FITC/PI (Figure 3.7a). The graph shows that elution one of samples A and B were less active (65 and 60 % cell death, respectively) than non-biotinylated ILZ TRAIL (77 % cell death).

Due to the loss of cell death-inducing activity when using either 5  $\mu$ l or 10  $\mu$ l of biotin to label ILZ TRAIL, the amount of biotin was reduced to identify whether this would help retain the activity of bILZ TRAIL in Jurkat E6.1 cells (Figure 3.7b). ILZ TRAIL (2) was labelled using either 1  $\mu$ l (sample A) or 3  $\mu$ l (sample B) biotin. Coomassie-stained SDS gels showed the relative abundance of purified bILZ TRAIL in each elution (lanes 5 – 9 for sample A and lanes 14 – 18 for sample B, respectively) at

32 kDa. Moreover, the immunoblot probed for streptavidin-HRP showed equal biotin labelling of elutions 1- 3 for sample A and B despite the reduction in biotin used for labelling.

The activity of both sample A and B of bILZ TRAIL (2) was confirmed to be comparable to non-biotinylated ILZ TRAIL (Figure 3.7c) and therefore a DISC pull-down was performed using either sample or A or B of bILZ TRAIL (2) (1 µg/ml). Aliquots of the samples from the cells treated with bILZ TRAIL were further incubated at 37 °C for 5 h to confirm activity of the labelled ligand. The extent of cell death as assessed by annexin-V-FITC/PI labelling was 84 % and 82 % for samples A and B as shown in lanes 2 and 4, respectively. Both batches of bILZ TRAIL allowed for TRAIL-R1, TRAIL-R2, FADD and caspase 8 to be pulled down in Jurkat E6.1 cells. Importantly, using bILZ TRAIL, no non-specific protein interactions were detected in the unstimulated samples (lanes 1 and 3).

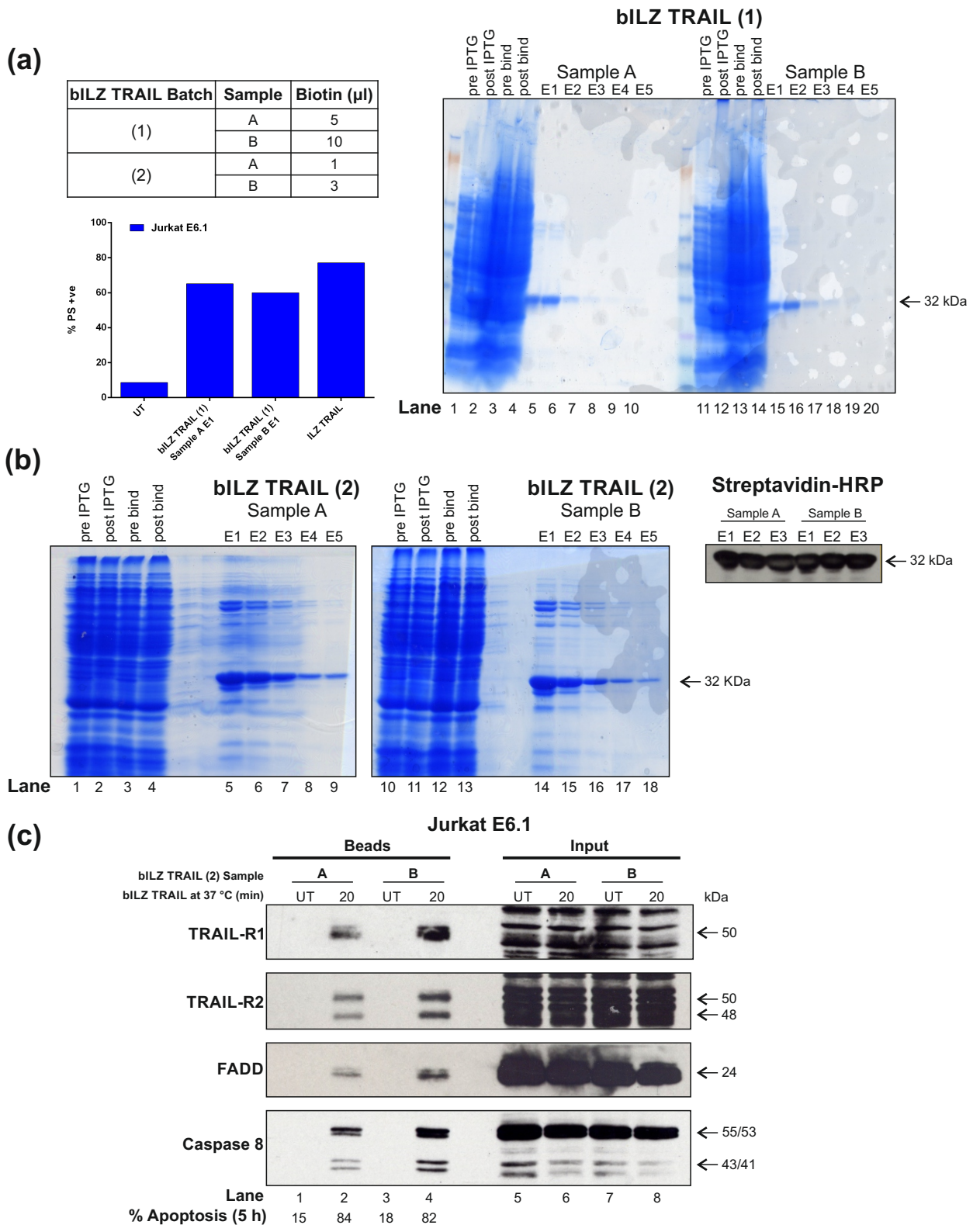


**Figure 3.7 Biotinylation of ILZ TRAIL allows for specific isolation of the ILZ TRAIL DISC in Jurkat E6.1 cells** (a) The first batch of bILZ TRAIL, (1), was aliquoted into two samples, A and B; each incubated with 5 and 10  $\mu$ l biotin respectively. Five elutions of each sample (5  $\mu$ l) was separated by SDS-PAGE and stained with coomassie to visualise proteins. Graph shows ability of 1  $\mu$ g/ml bILZ TRAIL (1) to cause cell death in Jurkat E6.1 cells compared to 1  $\mu$ g/ml non-biotinylated ILZ TRAIL for each sample. (b) Batch two of bILZ TRAIL, (2) was aliquoted into two samples, A and B; each incubated with 1 and 3  $\mu$ l biotin respectively. Five elutions of each sample (5  $\mu$ l) was separated by SDS-PAGE and stained with coomassie to visualise proteins. Elutions (E) 1 - 3 (5  $\mu$ g) of samples A and B of bILZ TRAIL (2) were separated by SDS-PAGE and immunoblotted for ILZ TRAIL using streptavidin-HRP. (c) bILZ TRAIL (2) samples A and B were used to isolate bILZ TRAIL DISC complexes. 20  $\mu$ l bead sample and 10  $\mu$ l of input were separated by SDS-PAGE and immunoblotted for known components of the DISC.

### 3.3 Discussion

The aim of this work was to elucidate the TRAIL-R surface expression of BEAS-2B and Jurkat E6.1 cells and the TRAIL-R1/R2 signalling preference of these cells. The data from Figures 3.1 and 3.2 revealed that both cell types predominantly expressed and signalled to apoptosis through TRAIL-R2. Due to this preference for TRAIL-R2, a higher ordered oligomeric form of TRAIL, ILZ TRAIL, was synthesised and purified for use as a tool to further dissect the TRAIL signalling pathways in BEAS-2B and Jurkat E6.1 cells, as well as for future work in this project. The data in Figures 3.1 and 3.2 show that caspase 9, a marker of intrinsic apoptosis, is cleaved suggesting that both BEAS-2B and Jurkat E6.1 cells may be type II cells with respect to TRAIL signalling, that is to say they rely on activation of the mitochondrial amplification loop to fully signal to apoptosis or there is some contribution of mitochondrial signalling to apoptosis in response to TRAIL (Rudner et al., 2005). Additionally, the presence of the caspase 9 cleavage fragment p35 in TRAIL-treated BEAS-2B cells (Figure 3.1) is indicative of apoptosome-mediated autocatalytic cleavage of procaspase 9, further highlighting the contribution of the intrinsic apoptotic pathway in these cells.

The lack of cell death following exposure of BEAS-2B and Jurkat E6.1 to the TRAIL-R1-specific agonistic antibody, ETR1 could be explained by the presence of little or no cell surface TRAIL-R1 in both cell types (Figure 3.2). Nonetheless, the lack of ETR1-induced cell death but a significant increase in ETR2-XL-induced cell death in BEAS-2B and Jurkat E6.1 cells shows that TRAIL-induced apoptotic signalling is reliant on the presence of TRAIL-R2 in these cells (Figure 3.2). Indeed, the TRAIL-R2 signalling characteristics of Jurkat E6.1 cells are well documented and have been reported previously by our laboratory and others (Macfarlane et al., 2005a; MacFarlane et al., 2005b; Natoni et al., 2007). However, characterisation of BEAS-2B cells with respect to TRAIL-R1/R2 apoptotic signalling has not been dissected to date and therefore the observations described in this chapter provide the first insight into how these lung epithelial cells respond to an extrinsic apoptotic stimulus.

Characterisation of the conformational status of both TRAIL and ILZ TRAIL (Figure 3.3) helped explain the differential cell death induced by TRAIL and ILZ TRAIL in BEAS-2B and Jurkat E6.1 cells. For example, in the gel filtration and BS<sup>3</sup> cross-linking experiments, TRAIL was shown to be in a mixture of monomeric, dimeric and trimeric conformations (Figure 3.3). Thus, the small but significant cell death induced by TRAIL in both cell types (Figure 3.1) can be attributed to the trimeric TRAIL present in the mixture of soluble protein, which allows for sufficient signalling through TRAIL-R2. In contrast, ILZ TRAIL was shown to comprise of predominantly dimeric, trimeric and higher order oligomeric conformations, thus explaining the increased cell death observed following treatment of both BEAS-2B and Jurkat E6.1 cells with ILZ TRAIL compared to treatment with TRAIL (Figure 3.5). These findings, together with the observation that ETR1 (which *specifically* engages TRAIL-R1) did not induce cell death in these cells (Figure 3.2), confirms that BEAS-2B and Jurkat E6.1 cells signal to TRAIL-induced apoptosis through TRAIL-R2. Moreover, the data obtained with ILZ TRAIL are consistent with the previously documented observation that signalling *via* TRAIL-R2 occurs more efficiently following presentation of a higher-ordered oligomeric of TRAIL (Natoni et al., 2007).

Efficient assembly of the DISC is essential for triggering downstream signalling to apoptosis. Therefore isolation of the DISC enables analysis of the relative amount of known DISC components in target cells. Isolation of ILZ TRAIL-induced DISC complexes in Jurkat E6.1 cells was initially performed using the Strep-tag and both magnetic and sepharose streptactin bead platforms were tested. Despite the presence of some non-specific interactions, magnetic streptactin beads from IBA were found to be the optimal streptactin bead platform tested for ILZ TRAIL DISC isolations and thus were used for subsequent optimisation experiments.

IBA high-capacity magnetic streptactin beads that have a higher capacity for binding Strep-tagged proteins were used to isolate ILZ TRAIL DISC complexes in Jurkat E6.1. However when purification conditions were further optimised, the non-specific interactions remained, as indicated by the presence of caspase 8 and FADD in unstimulated control samples. Therefore, it was decided that using the Strep-tag

for isolation and purification of the ILZ TRAIL DISC would make future results difficult to interpret and an alternative approach for ILZ DISC isolation was sought.

Purification through biotinylation of TRAIL has previously been shown to be a specific and robust method for isolation of DISC complexes (Harper and Macfarlane, 2008). Therefore, ILZ TRAIL was purified and subsequently biotinylated in a similar manner to TRAIL (see Chapter 2). However, the amount of biotin (5 or 10  $\mu$ l) routinely used caused a significant reduction in ligand activity as shown by a reduction in bILZ TRAIL-induced cell death in Jurkat E6.1 cells. Hence the amount of biotin was reduced (1 or 3  $\mu$ l) so as not to compromise the apoptosis-inducing activity of bILZ TRAIL (Figure 3.7a & b). Subsequently, a bILZ TRAIL DISC isolated from Jurkat E6.1 cells using ILZ TRAIL biotinylated using 3  $\mu$ l biotin was found to be most effective at isolating the DISC as shown by immunoblotting for known DISC components. These findings confirm that biotinylation of ILZ TRAIL enables specific purification of the ILZ TRAIL DISC.

Taken together the data presented in this Chapter show that both a lung epithelial cell line and a T cell line signal similarly in terms of TRAIL-induced apoptosis – with both cell types signalling predominantly in a TRAIL-R2-dependent manner. Moreover, for the first time, TRAIL containing an isoleucine zipper motif has been synthesised, purified and shown to be functional both in terms of apoptosis-inducing activity as well as isolation of the TRAIL DISC in TRAIL-R2 expressing cells.

## **4 Characterisation of TRAIL/TRAIL-R Signalling in Lung Epithelial Cells**

## 4.1 Introduction

As discussed in Chapter 1, the ultimate aim of this project was to uncover the signalling effects of TRAIL and ILZ TRAIL on a co-culture of lung epithelial and T cells. However, in order to identify changes that might occur in this co-culture model, basal levels of TRAIL and ILZ TRAIL signalling in lung epithelial and T cells alone must first be ascertained. Thus, the overall aim of this Chapter was to characterise a panel of epithelial cell lines for their TRAIL signalling and consider this to be 'basal levels' in comparison to when lung epithelial cells and T cells were co-cultured together.

The lung carcinoma epithelial cell line, A549, has previously been characterised in our laboratory in terms of TRAIL-induced apoptosis (MacFarlane et al., 2000). A549 cells were therefore used as positive control when assessing TRAIL sensitivity in the more relevant normal transformed lung epithelial cell lines, BEAS-2B and 16HBE and the immortalised bronchial epithelial cell line, iHBEC.

It is essential to note that both the BEAS-2B cell line and the 16HBE cell line, although not derived from cancerous lung tissue, have been retrovirally transformed (Cozens et al., 1994; Reddel et al., 1988). Notably, both cell lines can be grown to confluency to form monolayers that contain tight junctions. *In vivo*, lung epithelial cells exist as a monolayer with tight junctions to ensure crosstalk and tissue homeostasis (Anderson and Van Itallie, 1995). This feature is therefore important for this project where the aim is to mimic the *in vivo* setting as much as possible.

The iHBEC cell line was established from bronchial biopsies of non-cancerous tissue, without retroviral transformation; instead, telomerase (hTERT) and Cdk4 were overexpressed (Ramirez et al., 2004). Ramirez et al also reported that the iHBEC cell line clustered closely to non-immortalised primary lung epithelial cells following microarray analysis, suggesting iHBEC cells mimic the physiological setting much more than previously established lung epithelial cell lines such as BEAS-2B and 16HBE. Also reported was the ability of these cells to form monolayers.

Along with the aforementioned cell lines, donor-specific primary Normal Human Bronchial Epithelial cells (NHBE) were characterised for their basal TRAIL/TRAIL-R signalling profile to elucidate whether any of the previously established cell lines signalled in a comparable manner to these primary cells.

## **4.2 Results**

### **4.2.1 Characterisation of TRAIL/TRAIL-R signalling in lung epithelial cell lines, A549, BEAS-2B, 16HBE and iHBEC**

#### **4.2.1.1 TRAIL, TRAIL-R and CD95 surface expression profile of A549, BEAS-2B, 16HBE and iHBEC cells**

As previously discussed in Chapter 1, TRAIL-induced apoptosis requires the presence of either or both TRAIL death receptors, TRAIL-R1 and TRAIL-R2. Profiling for expression of these receptors can therefore provide an insight into the TRAIL-induced signalling potential of a particular cell. Hence, A549, BEAS-2B, 16HBE and iHBEC cells were profiled for basal cell surface expression of TRAIL-R1 and TRAIL-R2 using antibodies specific to these death receptors and flow cytometry. In addition, these lung epithelial cell lines were profiled for their cell surface expression of TRAIL and the additional death receptor, CD95 by detection of fluorescently labelled antibodies to these proteins (Figure 4.1). As assessed by the fluorescence intensity, TRAIL-R1 was only expressed on the surface of A549 and iHBEC cells. In contrast, TRAIL-R2 was found to be expressed on A549, BEAS-2B and iHBEC cells. However, neither TRAIL-R1 nor TRAIL-R2 was expressed on 16HBE cells. The related death receptor, CD95 was found to be expressed on BEAS-2B and iHBEC cells but not A549 or 16HBE cells. Flow cytometry also revealed that only BEAS-2B and 16HBE cells expressed the ligand TRAIL on their surface.

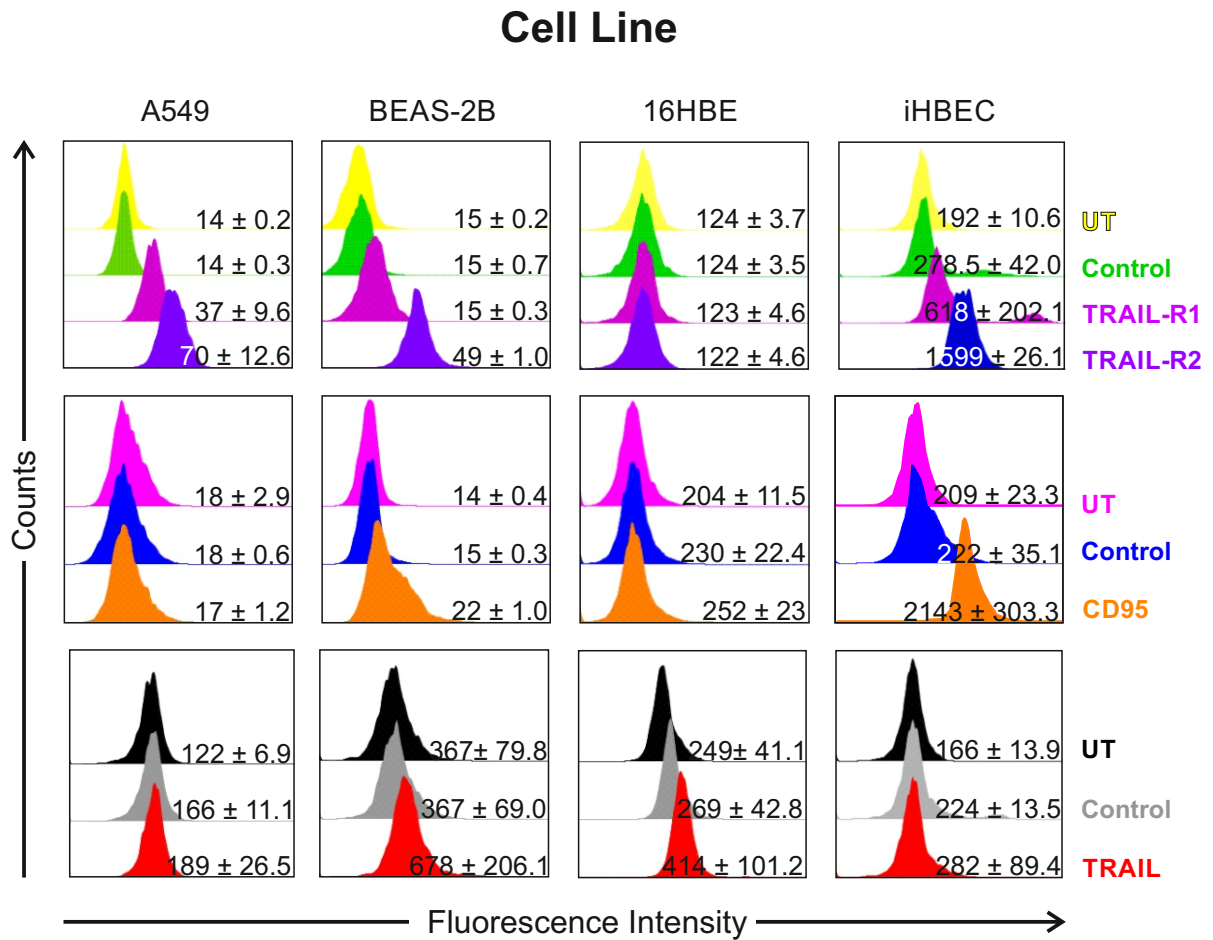


**Figure 4.1 TRAIL, TRAIL-R and CD95 surface expression profile of A549, BEAS-2B, 16HBE and iHBEC cells** (a) A549, BEAS-2B, 16HBE and iHBEC cells were analysed for cellular surface expression of TRAIL-R1, TRAIL-R2, CD95 and TRAIL. Cells were incubated with either no antibody (UT), isotype control antibody (control), PE-conjugated TRAIL-R1, TRAIL-R2, FITC-conjugated TRAIL or CH11 with FITC-conjugated secondary antibodies. Following washing with PBS, cells were analysed by flow cytometry for changes in fluorescence intensity. Mean fluorescence intensity is represented by the geometric mean  $\pm$  SEM (n=3).

#### **4.2.1.2 A549 and BEAS-2B but not 16HBE or iHBEC cells display a concentration-dependent sensitivity to TRAIL**

In order to characterise the sensitivity of A549, BEAS-2B, 16HBE and iHBEC cells to TRAIL-induced apoptosis, cells were treated with 0 – 1 µg/ml TRAIL at 37 °C for 5 h and analysed for PS externalisation by flow cytometry (Figure 4.2b). Both A549 and BEAS-2B cells displayed a small but significant concentration-dependent increase in annexin-V/FITC staining, peaking at 24 % and 10 % apoptosis, respectively. In contrast, TRAIL-treated 16HBE and iHBEC cells did not undergo apoptosis as evidenced by the absence of PS externalisation.

In order to further characterise the sensitivity of A549, BEAS-2B, 16HBE and iHBEC cells to TRAIL-induced apoptosis and their sensitivity to other intrinsic and extrinsic apoptotic stimuli, cells were treated with either 500 ng/ml anti-CD95, 0 – 2 µg/ml TRAIL, 100 µM etoposide or 1 µM staurosporine, either in the presence or absence of 25 µM zVAD.fmk and analysed for cleavage of markers of apoptosis by immunoblotting (Figure 4.2b).

Upon 0 – 2 µg/ml TRAIL treatment, A549 and BEAS-2B cells both showed a concentration-dependent cleavage of the apical caspase, procaspase 8 to p43/41 and its active p18 fragment (Figure 4.2b, lanes 5 – 9). The initiator caspase, procaspase 9 was cleaved to p35 but not to p37 in both cell lines. In addition, procaspase 3 was cleaved to p20 and a small amount also cleaved to p19 but there was no evidence of cleavage to the active cleavage fragment, p17. Minimal, but concentration-dependent, PARP cleavage was observed in both TRAIL-treated A549 and BEAS-2B cells, consistent with the corresponding PS externalisation data described above.

Similarly, TRAIL-treated iHBEC cells displayed a concentration-dependent cleavage of procaspase 8 to p43/41 (Figure 4.2b, lanes 5 – 9). However, further processing to p18 was not observed. Procaspase 9 was not cleaved following TRAIL treatment. In contrast, TRAIL induced cleavage of procaspase 3 to p20 in a concentration-dependent manner. In TRAIL-treated iHBEC cells, cleavage of the

caspase substrate, PARP cleavage was also not observed, consistent with the annexin-V/FITC data shown in Figure 4.2a.

In contrast to the other epithelial cell lines tested, 16HBE cells treated with TRAIL did not show cleavage of either the initiator caspases, procaspase 8 or procaspase 9, or processing of caspase 3 or PARP (Figure 4.2b, lanes 5 – 9). This observation is consistent with the flow cytometry data shown in Figure 4.2a, which indicated that these cells are resistant to TRAIL-induced apoptosis.

Pre-treatment of with the pan-caspase inhibitor zVAD.fmk, prior to TRAIL treatment, inhibited the processing of procaspases 8, 9 and 3 in A549, BEAS-2B and iHBEC cells. Cleavage of PARP was inhibited in A549 and BEAS-2B cells, consistent with marked inhibition of TRAIL-induced apoptosis (Figure 4.2b, lane 10).

Anti-CD95 treatment of A549 and BEAS-2B cells induced only minimal cleavage of procaspase 8 to p43/41 and p18 and processing of procaspase 9 to p35. Moreover neither procaspase 3 nor PARP were cleaved (Figure 4.2b lane 3). Anti-CD95 treatment of iHBEC cells did cause some cleavage of procaspase 8 to p43/41 but not p18. Furthermore, caspase 9 was not cleaved, although a small amount of procaspase 3 processing to p20 was observed. Similar to that seen in A549 and BEAS-2B cells, anti-CD95 did not induce PARP cleavage in iHBEC cells. In contrast, 16HBE cells were completely resistant to anti-CD95 treatment as evidenced by the lack of processing of all apoptotic markers tested.

Of the four cell lines tested, only BEAS-2B cells responded to etoposide treatment (100  $\mu$ M) as evidenced by cleavage of procaspase 8 to p43/41 and further processing to p18 (Figure 4.2b, lane 11). In addition, procaspase 9 was cleaved to p35 and procaspase 3 cleaved to p19, inducing the presence of a small amount of the PARP cleavage fragment, p85. Pre-treatment with zVAD.fmk partially inhibited the cleavage of caspases and prevented PARP cleavage. Thus, in the presence of zVAD.fmk, procaspase 8 was not processed, however, procaspase 3 was cleaved to p20, albeit not to the active cleavage fragments p19 and p17 (Figure 4.2b, lane 12).

Both 16HBE and iHBEC cells were treated with staurosporine (STS) to deduce whether a different intrinsic stimulus would induce apoptosis in these cells (Figure 4.2b, lane 13). None of the apoptotic markers tested displayed processing upon STS treatment, therefore suggesting that these cells are resistant to inducers of intrinsic apoptosis such as etoposide and STS.

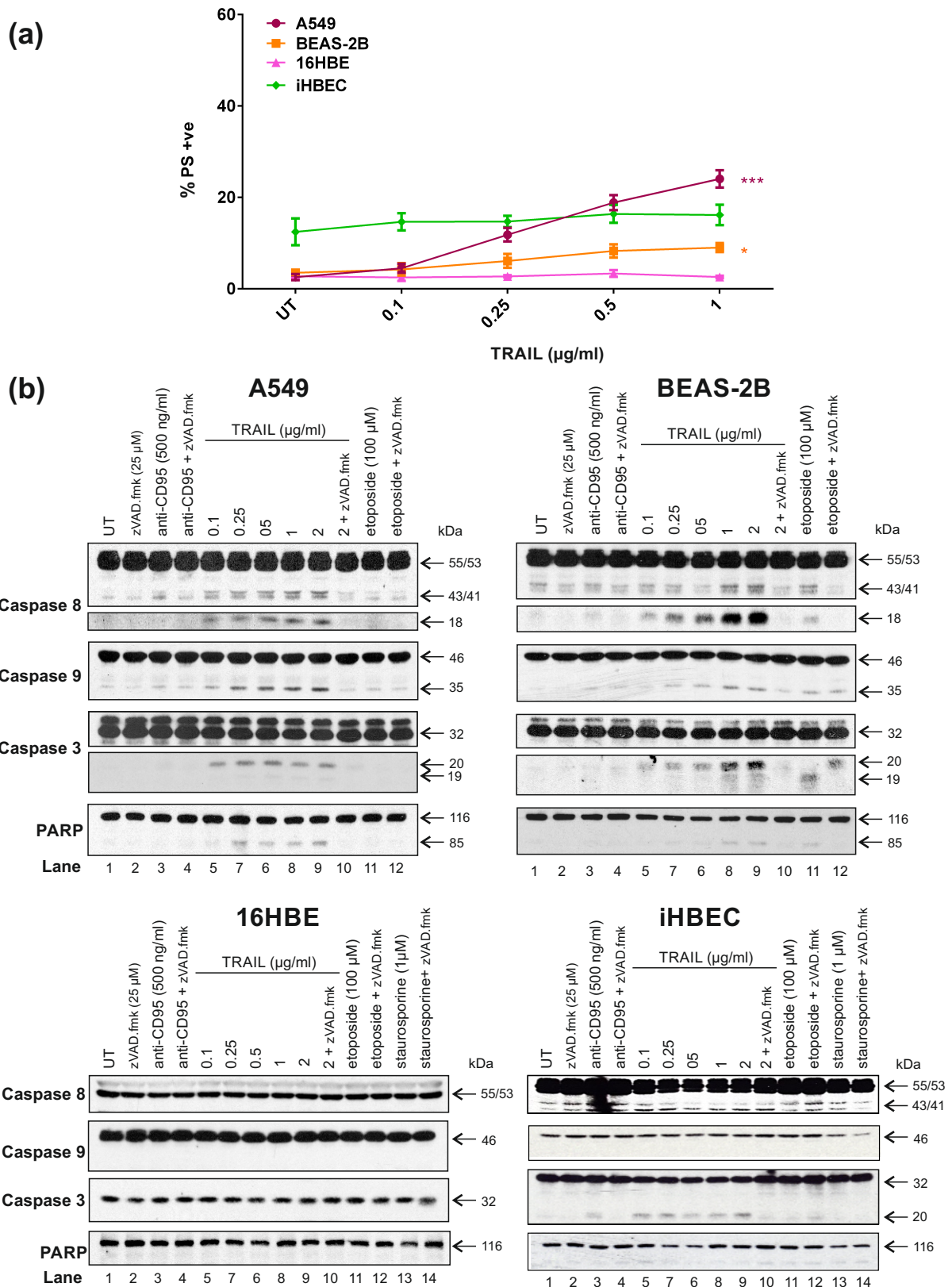


**Figure 4.2** A549 and BEAS-2B but not 16HBE and iHBEC cells display a concentration-dependent sensitivity to TRAIL (a) A549, BEAS-2B, 16HBE and iHBEC cells were treated with 0 - 1 µg/ml TRAIL and analysed by flow cytometry for PS externalisation. Graph represents % cell death (annexin V-FITC/PI) (mean ± SEM, n=3). Significance asterisks are relative to untreated cells (UT). (b) Cell pellets of A549, BEAS-2B, 16HBE and iHBEC treated with various apoptotic stimuli including 0 - 2 µg/ml TRAIL, in the presence or absence of zVAD.fmk, were analysed for caspase 8, caspase 9, caspase 3 and PARP cleavage by immunoblotting. Immunoblots are representative of three independent experiments.

#### **4.2.1.3 bTRAIL induces TRAIL DISC formation in A549, BEAS-2B and iHBEC but not 16HBE cells**

To further characterise the TRAIL-induced apoptosis observed in A549, BEAS-2B and iHBEC cells, and to identify whether 16HBE cells have the potential to induce apoptosis through ligation of TRAIL-R1/-R2, activation and affinity purification of the TRAIL DISC was performed in each cell line (Figure 4.3).

Firstly, the TRAIL DISC was isolated in A549 cells (Figure 4.3a). To find the optimal bTRAIL incubation time for maximal DISC isolation, A549 cells treated with 1 µg/ml bTRAIL were incubated with or without a pre-chill step (pre-incubation with TRAIL for 1 h at 4 °C) prior to incubating the cells at 37 °C for either 20 or 30 min. The pre-chill step was included to enable maximal interaction between bTRAIL and TRAIL-Rs, by minimising internalisation of the complex (Algeciras-Schimnich et al., 2002; Kohlhaas et al., 2007). Levels of the DISC were analysed by immunoblotting for the known components of the DISC; TRAIL-R1, TRAIL-R2, FADD and procaspase 8. Figure 4.3a shows that pre-incubation of A549 cells with bTRAIL for 1 h at 4 °C significantly increased the amount of DISC isolated compared to incubation at 37 °C alone. This is evidenced by the increase in TRAIL-R1, TRAIL-R2, FADD and procaspase 8 detected (compare lanes 4 and 6 with lanes 3 and 5). In this case, it is important to note that the bTRAIL DISC isolated was catalytically active, as evidenced by the processing of procaspase 8 to p43/41. Further analysis revealed that, following a pre-chill step, the optimal period of bTRAIL incubation at 37 °C was 20 min as shown by the increased amount of procaspase 8 detected compared to incubation with bTRAIL for 30 min (compare lane 4 to lane 6).

BEAS-2B cells were similarly incubated with 1 µg/ml bTRAIL, with or without a pre-chill step, followed by incubation at 37 °C for either 20 or 30 min and analysed for DISC formation by immunoblotting (Figure 4.3b). Inclusion of the pre-chill step, prior to incubation at 37 °C, resulted in increased formation of the active DISC as shown by increased recruitment of FADD and procaspase 8 (lanes 4 & 6). Additionally, in BEAS-2B cells, the optimal incubation period for bTRAIL at 37 °C (following a pre-

chill step) was chosen as 20 min, again based on maximal recruitment of both FADD and procaspase 8.

Flow cytometric analysis had shown that 16HBE cells do not express either TRAIL-R1 or TRAIL-R2 on their cell surface (Figure 4.1). Therefore, to determine whether these cells have the potential to signal to TRAIL-induced apoptosis, total cellular expression of TRAIL-R1 and TRAIL-R2 was investigated (Figure 4.3c). 16HBE and HeLa cells were incubated with 1 µg/ml bTRAIL post-lysis, thus allowing for precipitation and analysis for the presence of TRAIL-R1 and TRAIL-R2 by immunoblotting. In parallel, HeLa cells (which express both TRAIL-R1 and -R2), were used as a positive control. However, although HeLa cells showed detectable levels of both death receptors. 16HBE cells did not express TRAIL-R1 or TRAIL-R2. This finding is consistent with the lack of cell surface expression of TRAIL-R1/-R2 as detected by flow cytometry (Figure 4.1) and the resistance of these cells to TRAIL-induced apoptosis as evidenced by PS externalisation and immunoblotting (Figure 4.2a & b).

Finally, iHBEC cells were incubated with 1 µg/ml bTRAIL with a pre-chill step followed by incubation at 37 °C for 0 – 30 min and similarly analysed for DISC formation by immunoblotting (Figure 4.3d). In these cells, the optimal incubation period at 37 °C (following a pre-chill step) for detection of the active DISC and this maximal recruitment of both FADD and procaspase-8 was identified as 10 min.

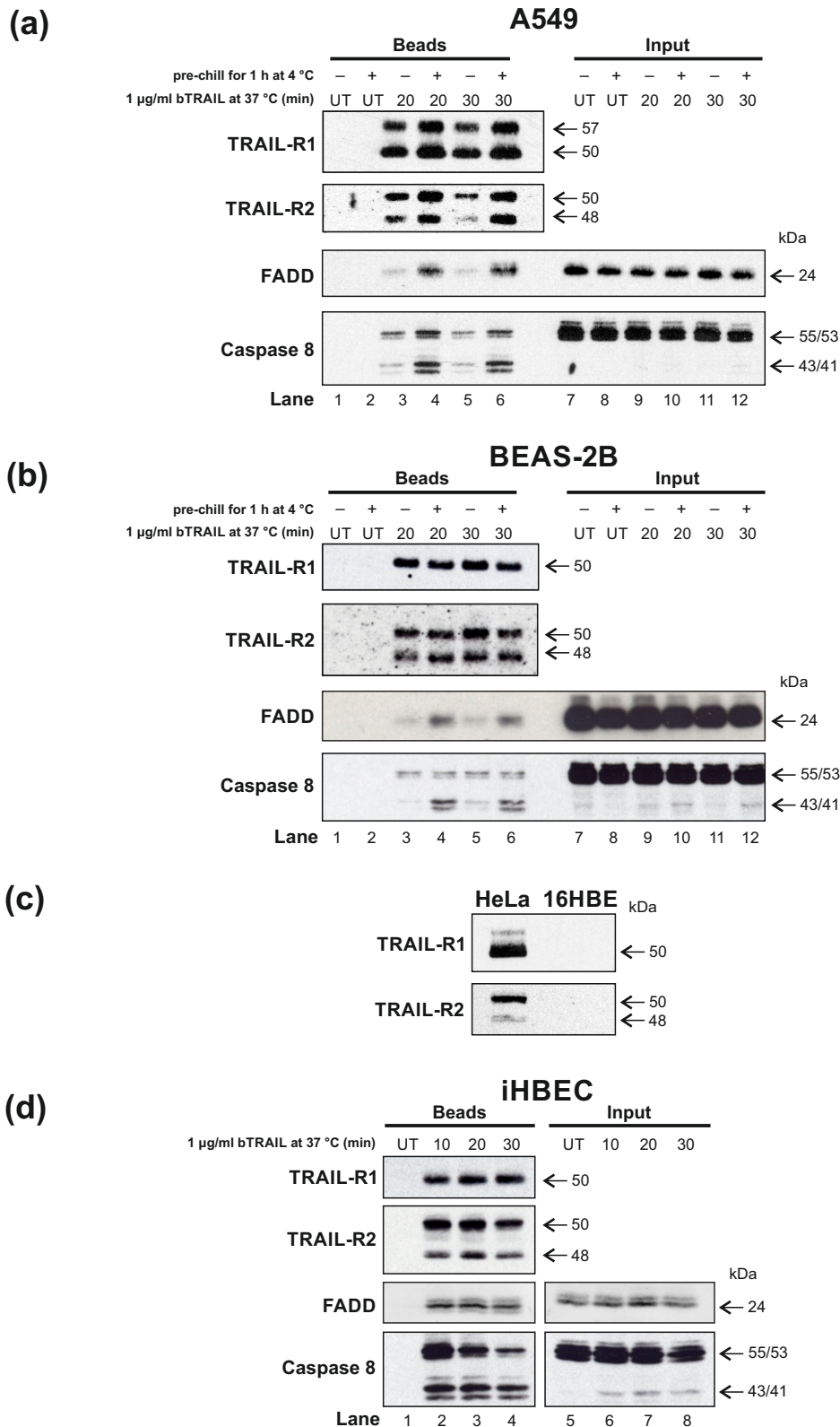


**Figure 4.3 bTRAIL induces TRAIL DISC formation in A549, BEAS-2B and iHBEC but not 16HBE cells** (a) A549 cells were analysed for DISC formation at 0-30 min at 37 °C, +/- pre-chill for 1 h at 4 °C as outlined in Chapter 2. (b) BEAS-2B cells were analysed for DISC formation at 0-30 min 37 °C, +/- pre-chill for 1 h at 4 °C. (c) 16HBE cells were analysed for the presence of TRAIL-R1 or -R2 with 1 µg/ml bTRAIL added post-lysis. HeLa cells were analysed in the same manner as a positive control. (d) iHBEC cells were analysed for the formation of the DISC from 0-30 min at 37 °C, with a pre-chill step for 1 h at 4 °C. For all immunoblots, 20 µl of Bead sample and 10 µl Sample Input were loaded onto SDS gels. Immunoblots are representative of two independent experiments. UT refers to untreated.

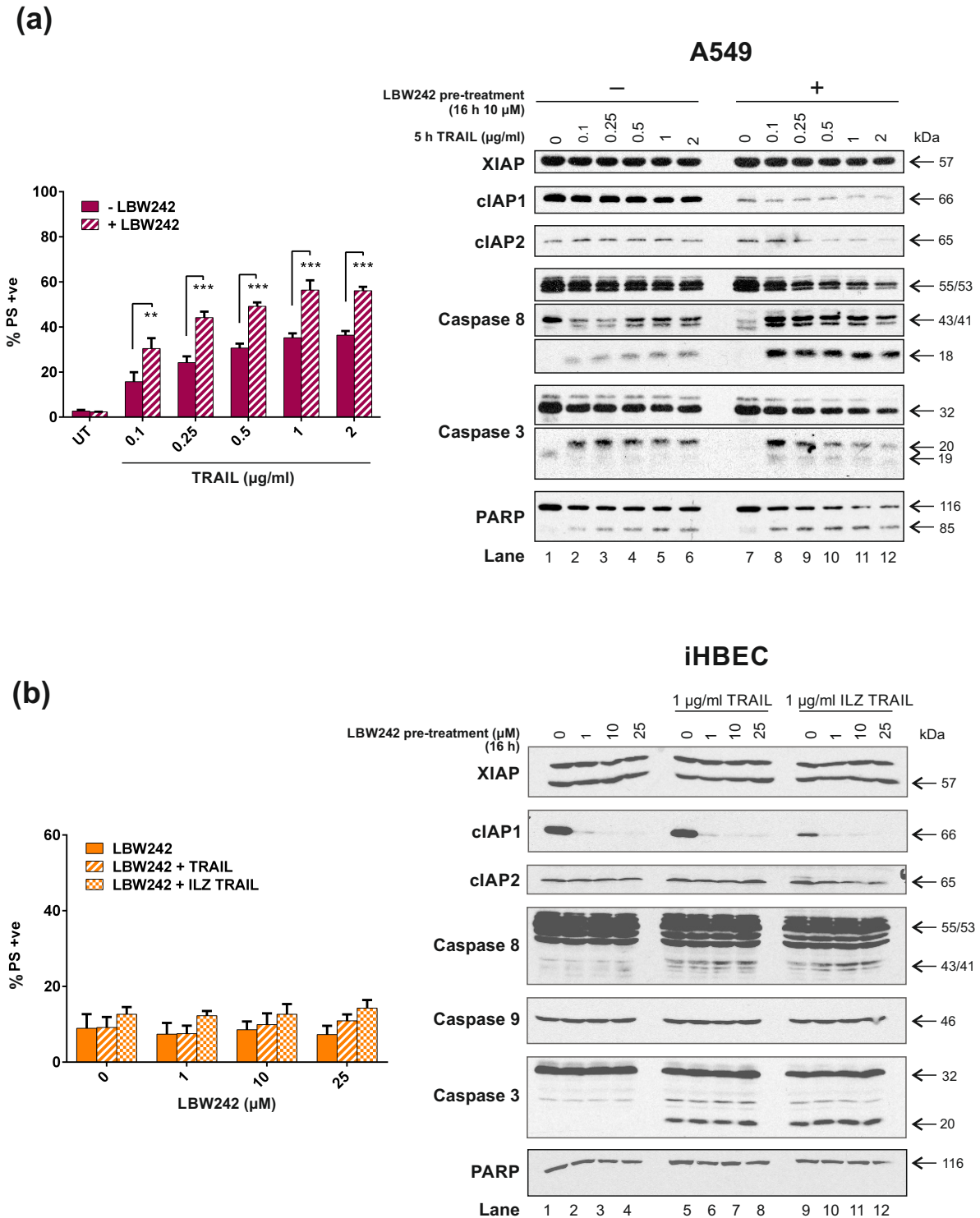
#### 4.2.1.4 The SMAC mimetic LBW242 sensitises A549, but not iHBEC cells to TRAIL-induced apoptosis

Figure 4.2 showed that A549 and BEAS-2B cells treated with TRAIL resulted in cleavage of procaspase 3 to p20 but not to its most catalytically active cleavage fragment, p19 and p17. A halt in processing of procaspase 3 at p20 is indicative of inhibition by XIAP (Bratton et al., 2002). This inhibition can be relieved by SMAC *in vivo*, as discussed in Chapter 1 (Du et al., 2000; Verhagen et al., 2000). However, SMAC mimetics (SM) can also be used *in vitro* to release inhibition of caspase 3 processing, resulting in full maturation of p20 to p19/p17 (L. Li et al., 2004). LBW242 is one of many SM used both *in vivo* and *in vitro* to release the inhibition of caspases by XIAP (Ziegler et al., 2008).

To elucidate whether XIAP was causing the inhibition of caspase 3 processing to p19 and p17, A549 cells were pre-treated with 10  $\mu$ M LBW242, followed by 0 – 2  $\mu$ g/ml TRAIL treatment (Figure 4.4a). Treated cells were stained with annexin-V-FITC/PI and analysed by flow cytometry to evaluate the amount of apoptosis. Pre-treatment with LBW242 followed by TRAIL treatment caused a significant increase in apoptosis, which was TRAIL concentration-dependent. Cell pellets were immunoblotted for presence of the IAPs; XIAP, cIAP1 and cIAP2, as well as for the apoptotic markers; procaspase 8, procaspase 9, procaspase 3 and PARP. XIAP levels remained constant under all conditions (lanes 1 – 12), whereas in the presence of LBW242 cIAP1 and cIAP2 levels decreased in a TRAIL concentration-dependent manner (lanes 7 – 12). In LBW242 pre-treated cells (lanes 7 – 12), procaspase 8 was processed to p43/41 and subsequently to p18 in a TRAIL concentration-dependent manner, and this was enhanced when compared to cells treated with TRAIL alone (lanes 1 – 6). This effect was further emphasised by the corresponding loss of procaspase 8 seen in lanes 7 – 12. Importantly, processing of procaspase 3 to p19 was only observed in the presence of both LBW242 and TRAIL with a corresponding loss of proform also observed in a TRAIL concentration-dependent manner (lanes 7 – 12). Consistent with this, increased PARP cleavage was seen in cells pre-treated with LBW242 when compared to cells treated with TRAIL alone (compare lanes 1 – 6 with lanes 7 -12). Taken together, these data

show that pre-treatment of A549 cells with the SM LBW242 results in increased sensitivity of these cells to TRAIL-induced apoptosis.

iHBEC cells pre-treated with LBW242 (0 – 25  $\mu$ M) followed by treatment with 1  $\mu$ g/ml TRAIL or ILZ TRAIL were stained with annexin-V-FITC/PI and analysed by flow cytometry for PS externalisation (Figure 4.4b). However, LBW242 pre-treated iHBEC cells did not show a significant increase in cell death when compared to cells treated with TRAIL alone. In a similar manner to A549 cells, iHBEC cell pellets were immunoblotted for IAPs and apoptotic markers. XIAP and cIAP2 levels remained the same with all treatments; however cIAP1 levels were depleted following LBW242 pre-treatment (lanes 2 – 4, 6 – 8 and 10 – 12). In iHBEC cells pre-treated with LBW242 (followed by TRAIL or ILZ TRAIL treatment), an increase in the p43/41 fragment of caspase 8 was observed (lanes 6 – 8 and 10 – 12). However, the initiator procaspase, caspase 9 was not cleaved under any treatment condition, and in cells pre-treated with LBW242 (followed by TRAIL or ILZ TRAIL treatment), procaspase 3 cleavage remained halted at p20. Consistent with this, there was no evidence of PARP in any of the treated cells (lanes 1 – 12). In support of these findings, analysis of PS externalisation by flow cytometry revealed that pre-treatment with the SM LBW242 did not sensitise iHBEC cells to TRAIL-induced apoptosis (Figure 4.4b).



**Figure 4.4 The SMAC mimetic LBW242 sensitises A549, but not iHBEC cells to TRAIL-induced apoptosis** (a) A549 cells pre-treated with 10 µM LBW242 for 16h at 37 °C followed by incubation with 0-2 µg/ml TRAIL for 5 h at 37 °C, were analysed for PS externalisation by flow cytometry. Cell pellets were analysed for XIAP, cIAP1, cIAP2, caspase 8, caspase 9, caspase 3 and PARP presence and/or cleavage by immunoblot. (b) iHBEC cells pre-treated with 0-25 µM LBW242 for 16h at 37 °C followed by incubation with 1 µg/ml TRAIL or 1 µg/ml ILZ TRAIL for 5 h at 37 °C, were analysed for PS externalisation by flow cytometry. Cell pellets were analysed for XIAP, cIAP1, cIAP2, caspase 8, caspase 9, caspase 3 and PARP presence and/or cleavage by immunoblot. All bar charts represent % cell death (annexin V-FITC/PI) (mean ± SEM, n=3). All immunoblots are representative of three independent experiments.

#### **4.2.1.5 iHBEC cells treated with TRAIL or ILZ TRAIL do not undergo apoptosis but do display a time- and concentration-dependent cleavage of caspase 8 and caspase 3 and phosphorylation of I $\kappa$ B $\alpha$**

Figure 4.2 showed that iHBEC cells did not die by apoptosis upon treatment with TRAIL over a 5 h time period; however at this time caspase 8 processing was observed, albeit only to p43/41 cleavage fragments. Subsequently, iHBEC cells displayed significant TRAIL DISC formation (with Figure 4.3d), following a pre-chill step and only a short incubation period of 10 min with bTRAIL at 37 °C. These two pieces of data indicated that TRAIL (or ILZ TRAIL) treatment of iHBEC cells caused rapid assembly of the DISC. Thus, in order to analyse whether, downstream of the DISC, the time-frame in which processing of the apoptotic markers, procaspase 8, procaspase 9, procaspase 3 and PARP occurred considerably quicker than 5 h, iHBEC cells were treated with either 1  $\mu$ g/ml TRAIL or ILZ TRAIL for 0 – 5 h.

As described in Chapter 1, ligation of TRAIL to its cognate death receptors can also result in signalling to pathways other than apoptosis, such as activation of NF $\kappa$ B. Therefore, to determine whether this signalling pathway was activated by TRAIL in iHBEC cells, samples were also immunoblotted for phosphorylated I $\kappa$ B $\alpha$  (pI $\kappa$ B $\alpha$ ) and I $\kappa$ B $\alpha$ , which are both involved in NF $\kappa$ B activation (as outlined in Chapter 1) (Figure 4.5a).

iHBEC cells treated with 1  $\mu$ g/ml TRAIL or ILZ TRAIL over 0 – 5 h did not result in a significant increase in cell death as measured by PS externalisation (Figure 4.5a). Immunoblotting revealed that procaspase 8 processing was very rapid, with processing to p43/41 and to the most active cleavage fragment, p18 observed as early as 30 min (lanes 2 and 9). TRAIL-treated iHBEC cells showed prolonged processing of caspase 8 to p18 over 5 h (lanes 2 – 7), whereas ILZ TRAIL-treated iHBEC cells showed a peak of caspase 8 processing to p18 at 0.5 – 2 h (lanes 19 – 11). Additionally, ILZ TRAIL treatment of iHBEC cells appeared to more efficiently induce assembly of the DISC (lanes 9 – 14), compared to iHBEC cells treated with TRAIL (lanes 2 – 7), as evidenced by the loss of procaspase (p55/53). Neither procaspase 9 nor PARP were cleaved following treatment with either TRAIL or ILZ

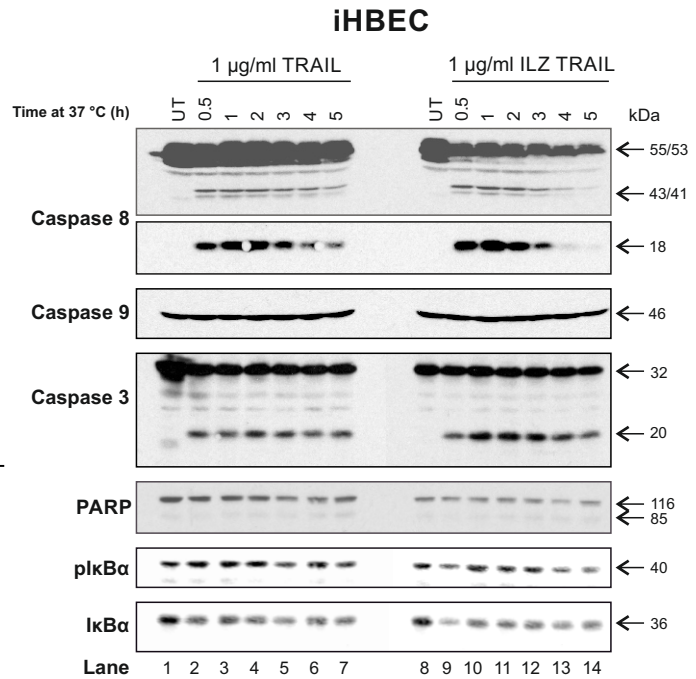
TRAIL, consistent with the lack of PS externalisation and the TRAIL treatment of iHBEC cells shown previously in Figure 4.2. Also consistent was the observation that, following treatment with either TRAIL or ILZ TRAIL, procaspase 3 cleavage was halted at p20 (lanes 1 – 14). The presence of more of the cleavage fragment, p20, following ILZ TRAIL treatment (lanes 9 – 14) compared to TRAIL treatment (lanes 2 – 7), provides further evidence of more rapid and efficient DISC assembly in iHBEC cells treated with ILZ TRAIL. Treatment of iHBEC cells with TRAIL induced the phosphorylation of I $\kappa$ B $\alpha$  (lanes 2 – 7), with a peak evident at 2 h (lane 4). This observation correlates with the loss of total I $\kappa$ B $\alpha$ , when comparing TRAIL-treated cells in lanes 2 – 7 with untreated control cells in lane 1. In a similar manner, iHBEC cells treated with ILZ TRAIL displayed induction of pI $\kappa$ B $\alpha$  and corresponding loss of I $\kappa$ B $\alpha$  over 5 h (lanes 8 – 14) indicating activation of the NF $\kappa$ B pathway. Taken together, these data showed that in iHBEC cells exposed to either TRAIL or ILZ TRAIL, the peak of DISC assembly and thus downstream signalling for either caspase-8 cleavage or NF $\kappa$ B activation was approximately 2 h. In addition, the significantly increased processing of caspases -8 and -3 induced by ILZ TRAIL compared to TRAIL suggests that iHBEC cells predominantly signal through TRAIL-R2. It was therefore decided to explore whether TRAIL and ILZ TRAIL signalling at this time point of 2 h was also concentration-dependent.

iHBEC cells were treated with either 0 – 1  $\mu$ g/ml TRAIL or ILZ TRAIL for 2 h and analysed for annexin-V-FITC/PI staining and immunoblotted for downstream signalling markers (Figure 4.5b). iHBEC cells treated with either TRAIL or ILZ TRAIL did not show significant cell death over this 2 h period as measured by PS externalisation. TRAIL or ILZ TRAIL -treated iHBEC cells analysed by immunoblotting showed concentration-dependent processing of procaspase 8 to p43/41, predominantly at 0.25 – 1  $\mu$ g/ml TRAIL treatment and 0.1 – 1  $\mu$ g/ml ILZ TRAIL treatment. Consistent with the data shown in Figure 4.5a, ILZ TRAIL treatment of iHBEC cells induced significantly more caspase 8 cleavage than TRAIL treatment, as shown by the enhanced loss of caspase 8 proform (compare lanes 7 – 10 to lanes 2 – 5). Once again, neither caspase 9 nor PARP were cleaved following treatment of iHBEC cells with either TRAIL or ILZ TRAIL. In contrast,

following treatment with 0.25 – 1 µg/ml TRAIL or ILZ TRAIL concentration-dependent cleavage of procaspase 3 to p20 was observed. Furthermore, in both TRAIL (lanes 2 – 5) and ILZ TRAIL (lanes 7 – 10) treated iHBEC cells; IκBα was phosphorylated in a concentration-dependent manner which corresponded with the parallel loss of total IκBα.

Collectively, the data from Figure 4.5a and b show that TRAIL or ILZ TRAIL treated iHBEC cells do not die by apoptosis but do form a functional DISC, with caspase 8 cleavage and processing of caspase 3 to p20 fragment occurring in a both a time- and concentration-dependent manner. In the same time-frame (2 h), both TRAIL and ILZ TRAIL induce NFκB signalling in iHBEC cells, as demonstrated by phosphorylation of IκBα.

(a)



(b)

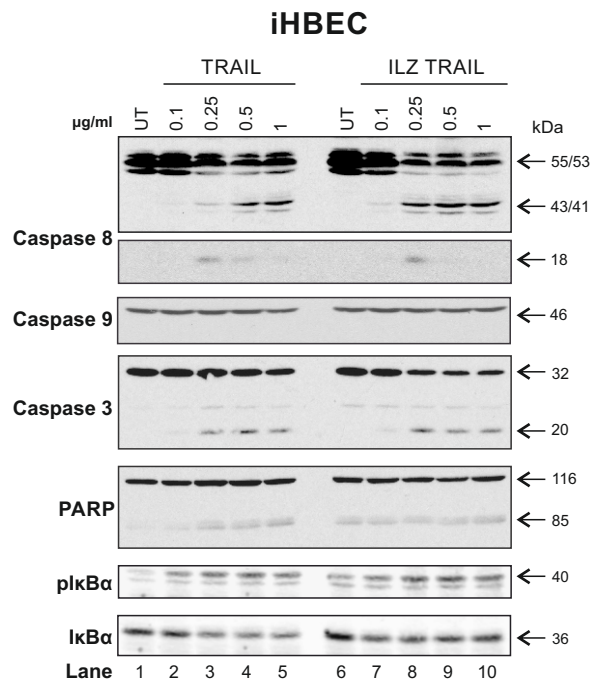
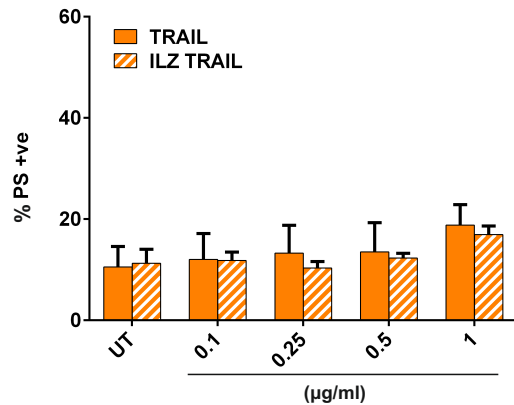


**Figure 4.5** iHBEc cells treated with TRAIL or ILZ TRAIL do not undergo apoptosis but do display a time- and concentration-dependent cleavage of caspase 8 and caspase 3 and phosphorylation of I $\kappa$ B (a) iHBEc cells treated with 1 µg/ml TRAIL or ILZ TRAIL for 0-5 h at 37 °C were analysed for PS externalisation by flow cytometry. Cell pellets were analysed for the presence and/or cleavage of caspase 8, caspase 9, caspase 3, PARP, plkB and I $\kappa$ B by immunoblotting. (b) iHBEc cells treated with 0-1 µg/ml TRAIL or ILZ TRAIL 2 h at 37 °C were analysed for PS externalisation by flow cytometry. Cell pellets were analysed for the presence and/or cleavage of caspase 8, caspase 9, caspase 3, PARP, plkB and I $\kappa$ B by immunoblotting. All bar charts represent relative % cell death (annexin V-FITC/PI) (Mean  $\pm$  SEM, n=3). All immunoblots are representative of three independent experiments.

#### **4.2.1.6 TRAIL or ILZ TRAIL treatment of iHBEC cells induces p65 translocation to the nucleus in a time-dependent manner**

In order to confirm the activation of the NF $\kappa$ B pathway in TRAIL and ILZ TRAIL - treated iHBEC cells, p65, a subunit of NF $\kappa$ B was stained for and visualised by confocal microscopy (Figure 4.6). As discussed in Chapter 1, upon activation of the NF $\kappa$ B pathway, p65 is known to translocate to the nucleus to modulate gene transcription.

iHBEC cells were treated with either 1  $\mu$ g/ml TRAIL for 0 – 5 h and stained for; nuclei (blue), to determine the nuclear space, actin (red), to display the outline of individual cells and p65 (green) (Figure 4.6a). When compared to untreated cells, TRAIL treatment of iHBEC cells caused translocation of p65 to the nucleus very rapidly at 30 min which was then evident to a lesser extent at time-points up to 4 h. In contrast, iHBEC cells treated with 1  $\mu$ g/ml ILZ TRAIL for 0 – 5 h showed nuclear translocation of p65 but this occurred more slowly, gradually increasing from 1 – 5 h with the peak occurring between 2 – 3 h (Figure 4.6b). Taken together, these findings are consistent with the time-course of I $\kappa$ B $\alpha$  phosphorylation observed previously in iHBEC cells treated with either 1  $\mu$ g/ml TRAIL or ILZ TRAIL (Figure 4.5a).

As discussed in Chapter 1, once in the nucleus, p65 acts as a transcription factor to modulate the expression of many genes, including interleukins. The canonical interleukins released following NF $\kappa$ B activation in inflammation of the lung epithelium include IL-6 and IL-8 (Han et al., 1999; Hoffmann and Dittrich-Breiholz, 2002). Thus iHBEC cells treated with either TRAIL or ILZ TRAIL were analysed for time-dependent release of both IL-6 and IL-8 and were shown to release neither (data not shown).

(a)

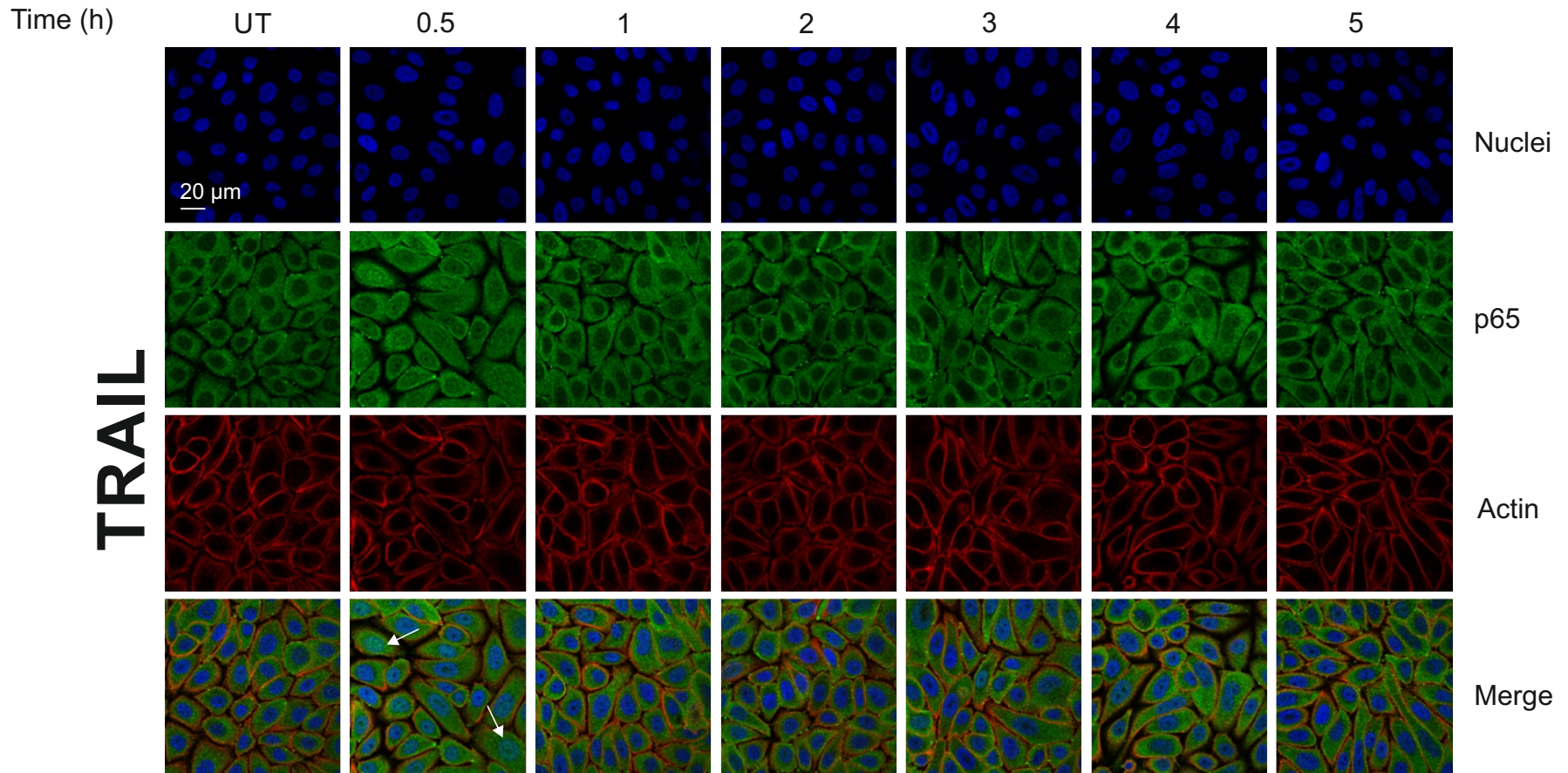


**Figure 4.6 TRAIL or ILZ TRAIL treatment of iHBEC cells induces p65 translocation to the nucleus in a time- dependent manner** (a) iHBEC cells were treated with 1  $\mu$ g/ml TRAIL for 0-5 h at 37  $^{\circ}$ C and subsequently fixed, permeabilised and stained for p65, nuclei and actin as outlined in Chapter 2. Data are representative of two independent experiments and images are representative of several images. White arrows indicate examples of translocation of p65 to the nucleus.

(b)

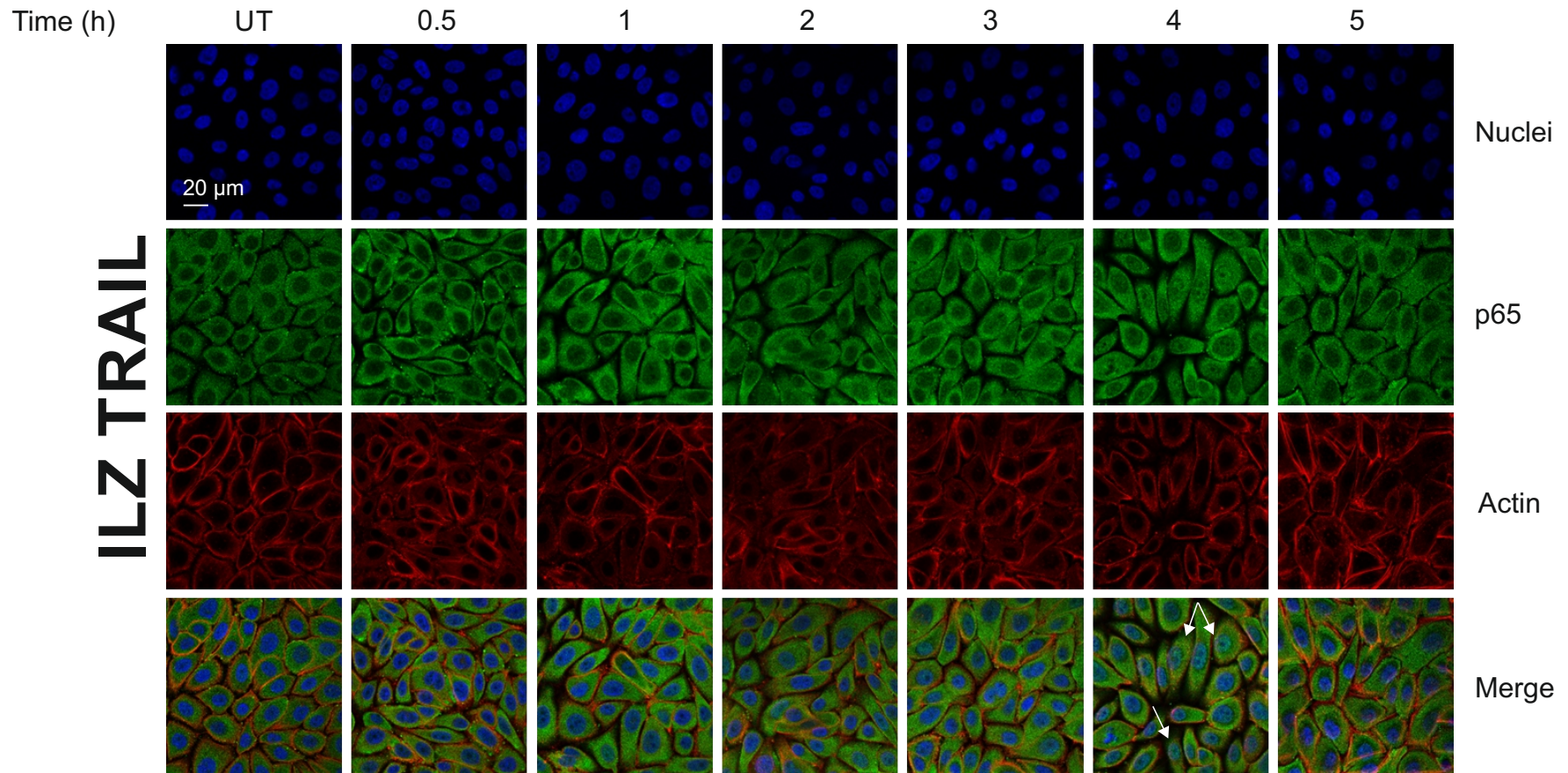


**Figure 4.6 TRAIL or ILZ TRAIL treatment of iHBEC cells induces p65 translocation to the nucleus in a time-dependent manner** (b) iHBEC cells were treated with 1  $\mu$ g/ml ILZ TRAIL for 0-5 h at 37  $^{\circ}$ C and subsequently fixed, permeabilised and stained for p65, nuclei and actin as outlined in Chapter 2. Data are representative of two independent experiments and images are representative of several images. White arrows indicate examples of translocation of p65 to the nucleus.

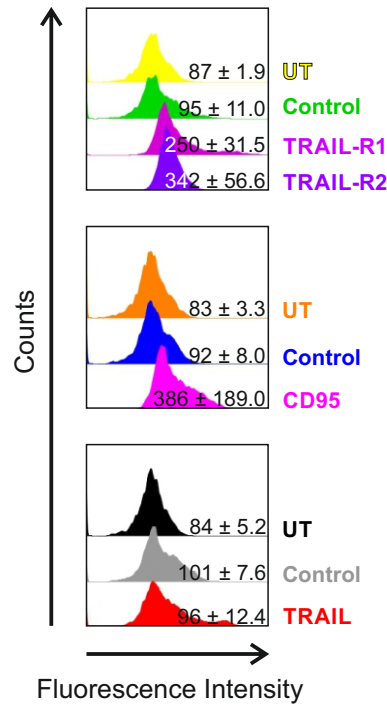
## 4.2.2 Characterisation of NHBE cells

### 4.2.2.1 NHBE cells treated with TRAIL do not undergo apoptosis but do display a concentration-dependent cleavage of caspase 8 and caspase 3

In order to profile the TRAIL/TRAIL-R signalling axis in primary lung epithelial cells, normal human bronchial epithelial (NHBE) cells were characterised for their cell surface expression of TRAIL, TRAIL-R1, TRAIL-R2 and CD95 (Figure 4.7a). In a similar manner to the immortalized lung epithelial cell line iHBEC, NHBE cells were found to express both TRAIL death receptors, TRAIL-R1 and TRAIL-R2, along with expression of CD95 but the ligand TRAIL was not expressed.

To investigate the sensitivity of these primary cells to TRAIL-induced apoptosis, NHBE cells were treated with 0 – 1 µg/ml TRAIL for 5 h and analysed for PS externalisation (Figure 4.7b). TRAIL-treated NHBE cells were annexin-V-FITC/PI negative indicating resistance to TRAIL-induced apoptosis. To explore the sensitivity of NHBE cells to other apoptotic stimuli, NHBE cells were treated with anti-CD95, TRAIL, etoposide or STS, both in the presence and absence of zVAD.fmk, and immunoblotted for the following apoptotic markers; procaspase 8, 9 and 3 (Figure 4.7b). NHBE cells treated with 500 ng/ml anti-CD95 did not show cleavage of procaspase 8 or 9 or the downstream effector procaspase 3 (lanes 3 and 4). In contrast, NHBE cells treated with 0 – 2 µg/ml TRAIL displayed cleavage of procaspase 8 to p43/41 and cleavage of procaspase 3 to p20, but no cleavage of procaspase 9, consistent with the lack of PS externalisation observed under the same conditions. Limited processing of procaspase 3 to its p20 fragment is reminiscent of that seen previously in iHBEC cells treated with TRAIL (Figure 4.2b). Neither etoposide (100 µM) nor STS (1 µM) -treated NHBE cells showed cleavage of procaspase 8, 9 or 3. Taken together, these data show that NHBE cells do have the capacity to form a TRAIL DISC, as evidenced by cell surface expression of TRAIL-R1 and TRAIL-R2 and TRAIL-induced cleavage of procaspase 8. However, procaspase 3 cleavage is halted at p20 and PS externalisation is not detected, demonstrating that TRAIL-treated NHBE cells do not die by apoptosis.

(a)



(b)

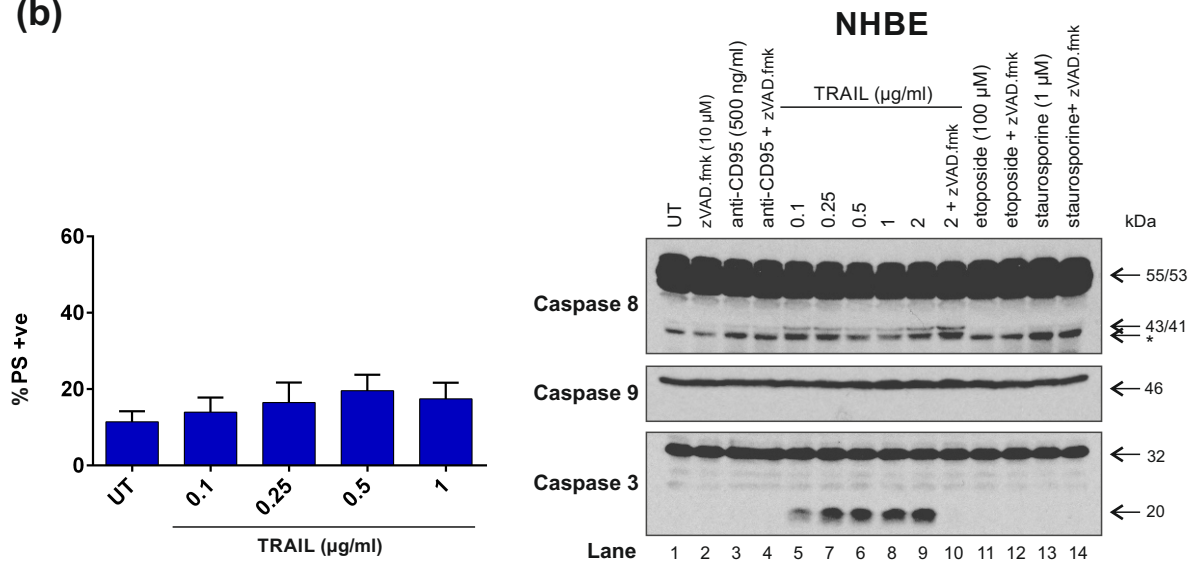


**Figure 4.7 NHBE cells treated with TRAIL do not undergo apoptosis but do display a concentration-dependent cleavage of caspase 8 and caspase 3** (a) NHBE cells were analysed for their cellular surface expression of TRAIL-R1, -R2, CD95 and TRAIL. Cells were incubated with either no antibody (control), isotype control antibody, PE-conjugated TRAIL-R1, TRAIL-R2, FITC-conjugated TRAIL or CH11 with FITC-conjugated secondary antibodies. Following washing with PBS, cells were analysed by flow cytometry for changes in fluorescence intensity. Fluorescence intensity is represented by geometric mean  $\pm$  SEM (n=3). (b) NHBE cells treated with 0-1  $\mu$ g/ml TRAIL were analysed for PS externalisation by flow cytometry. Bar chart represents relative % cell death (annexin V-FITC/PI) (mean  $\pm$  SEM, n=3). Cell pellets treated with various apoptotic stimuli including 0-2  $\mu$ g/ml TRAIL, +/- zVAD.fmk were analysed for cleavage of caspase 8, caspase 9 and caspase 3 by immunoblotting. Immunoblots are representative of three independent experiments.\* indicates the presence of an unknown non-specific band.

#### **4.2.2.2 iHBEC and NHBE cells express E-cadherin on their cell surface when cultured to confluency**

As described in Figure 4.7, the pattern of TRAIL-induced cleavage of caspases 8 and 3 observed in NHBE cells was very similar to that seen previously in TRAIL-treated iHBEC cells (Figure 4.5). Thus to explore whether iHBEC cells retained indeed key features of primary lung epithelial cells, iHBEC and NHBE cells were analysed for the formation of tight junctions between neighbouring cells – a characteristic of the lung epithelium. Tight junctions can be identified by the presence of E-cadherin localised to the cell membrane (Guillot and Lecuit, 2013; Vestweber and Kemler, 1985); therefore iHBEC and NHBE cells were immunoblotted and immunostained for E-cadherin 1 – 5 days post-seeding (Figure 4.8).

Figure 4.8a shows that expression of total E-cadherin increased from day 1 – day 5 post-seeding in both iHBEC and NHBE cells. Immunostaining and confocal analysis revealed that expression of E-cadherin was largely diffuse from day 1 – day 3 post-seeding in both iHBEC and NHBE cells (Figure 4.8b). However, at 4 – 5 days post-seeding, as the cells became more confluent and began to form a monolayer, re-localisation of E-cadherin to the cell membrane was evident. Taken together, these data show that both iHBEC and NHBE cells are capable of forming monolayers that contain tight junctions between neighbouring cells, and thus retain this important characteristic of the lung epithelium.

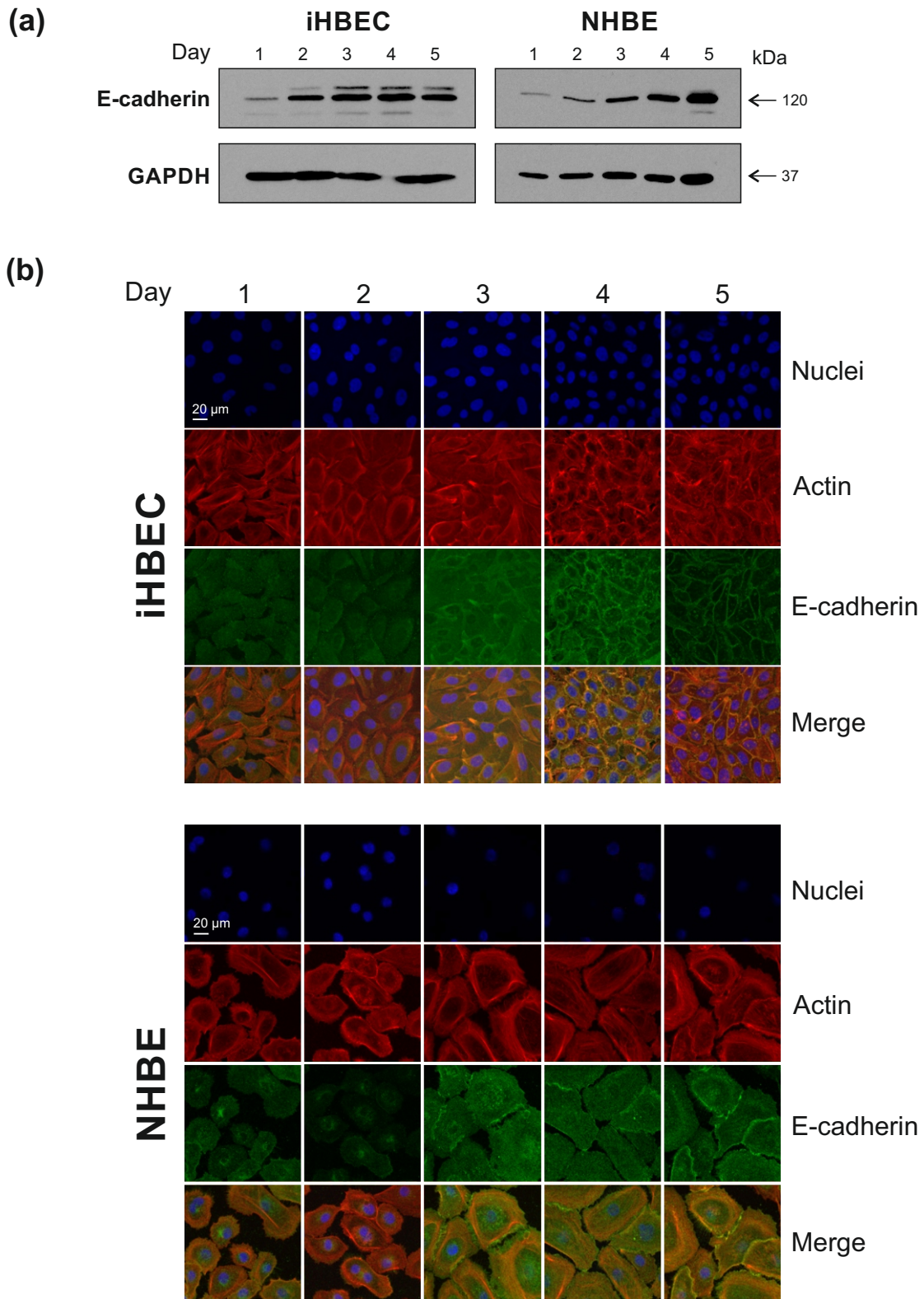


**Figure 4.8 iHBEC and NHBE cells express E-cadherin on their cell surface when cultured to confluency** (a) Cell pellets of iHBEC and NHBE cells were collected for five consecutive days after seeding to analyse for E-cadherin and GAPDH expression by immunoblotting. Immunoblots are representative of two independent experiments. (b) iHBEC and NHBE cells, 1-5 days post-seeding were fixed, permeabilised and stained for E-cadherin, nuclei and actin as outlined in Chapter 2. Data are representative of two independent experiments and images are representative of several images.

#### **4.2.2.3 NHBE cells form a DISC upon TRAIL treatment but are not sensitised to TRAIL-induced apoptosis when pre-treated with the SMAC mimetic, LBW242**

Figure 4.7b had shown that treatment of NHBE cells with TRAIL induced cleavage of procaspase 8, suggesting that exposure of these primary lung epithelial cells to TRAIL results in TRAIL DISC formation. To investigate TRAIL DISC assembly in NHBE cells, NHBE cells were incubated with 1 µg/ml bTRAIL (with a pre-chill step) at 37 °C for either 10 or 20 min and samples analysed by immunoblotting for the presence of the known components of the DISC; TRAIL-R1, TRAIL-R2, FADD and caspase 8 (Figure 4.9a). NHBE cells assembled an active DISC very rapidly as evidenced by the presence of core DISC components at both 10 and 20 min (lanes 2 and 3). Based on the greater amount of TRAIL DISC detected in lane 2 compared with lane 3, the optimal incubation period was chosen as 10 min at 37 °C. It should also be noted that these findings are reminiscent of the rapid TRAIL DISC assembly observed in iHBEC cells, under the same conditions (Figure 4.3d).

It was previously observed that caspase 3 processing was halted at p20 in NHBE cells treated with TRAIL (Figure 4.7b). Thus, to investigate whether this block in caspase 3 processing at p20 was due to inhibition of caspase-3 by XIAP, NHBE cells were pre-treated with the SM, LBW242 (0 – 25 µM, 16 h) prior to exposure to 1 µg/ml of either TRAIL or ILZ TRAIL for 5 h (Figure 4.9b). Cells were then analysed for PS externalisation by flow cytometry; this showed that pre-treatment of NHBE cells with LBW242 did not significantly increase the extent of apoptosis over that seen with TRAIL or ILZ TRAIL alone.

Matching cell pellets were further analysed by immunoblotting for IAPs and apoptotic markers (Figure 4.9b). Levels of both XIAP and cIAP2 remained constant across all samples (lanes 1 – 12). However, consistent with the ability of SM to target cIAP1 for degradation, pre-treatment of NHBE cells with LBW242 resulted in loss of cIAP1 (lanes 2 – 4; 6 – 8; 10 – 12). When NHBE cells were treated with either TRAIL (lanes 5 – 8) or ILZ TRAIL (lanes (9 – 12), procaspase 8 was processed to p43/41. In this case, ILZ TRAIL induced a greater amount of caspase 8

processing compared to TRAIL, as evidenced by the enhanced loss of procaspase 8. Neither caspase 9 nor PARP were processed under any treatment condition. In contrast, in NHBE cells treated with TRAIL or ILZ TRAIL, procaspase 3 was processed to p20 (Figure 4.9b lanes 5 and 9) consistent with that observed previously (Figure 4.7b). Treatment of NHBE cells with 0 – 25  $\mu$ M LBW242, prior to exposure to TRAIL or ILZ TRAIL, did not alter the extent of procaspase 8 processing (compare lanes 6 – 8 to lane 5, and lanes 10 – 12 to lane 9). Moreover, no further processing of caspase 3 was evident in NHBE cells pre-treated with LBW242 prior to TRAIL (compare lanes 6 – 8 to lane 5). In contrast, in NHBE cells treated with LBW242 prior to ILZ TRAIL, there was some evidence of concentration-dependent cleavage of caspase 3 to the active fragment p19 (lanes 9 – 12). However, it is important to note that there were only minimal levels of p19 fragment detected. Further processing to the fully active caspase 3 fragment p17 was not observed, which in turn may explain the lack of enhanced apoptosis detected by flow cytometry in NHBE cells treated with LBW242 and ILZ TRAIL.

Taken together these data show that TRAIL DISC formation in NHBE cells is rapid and thus exhibits similar kinetics to TRAIL DISC assembly in iHBEC cells (Figure 4.3d). Additionally, it has been deduced that SM-mediated inhibition of XIAP does not significantly enhance processing of caspase 3 p20 to the catalytically active fragment p17; thus SM do not sensitize NHBE cells to TRAIL or ILZ TRAIL-induced apoptosis.

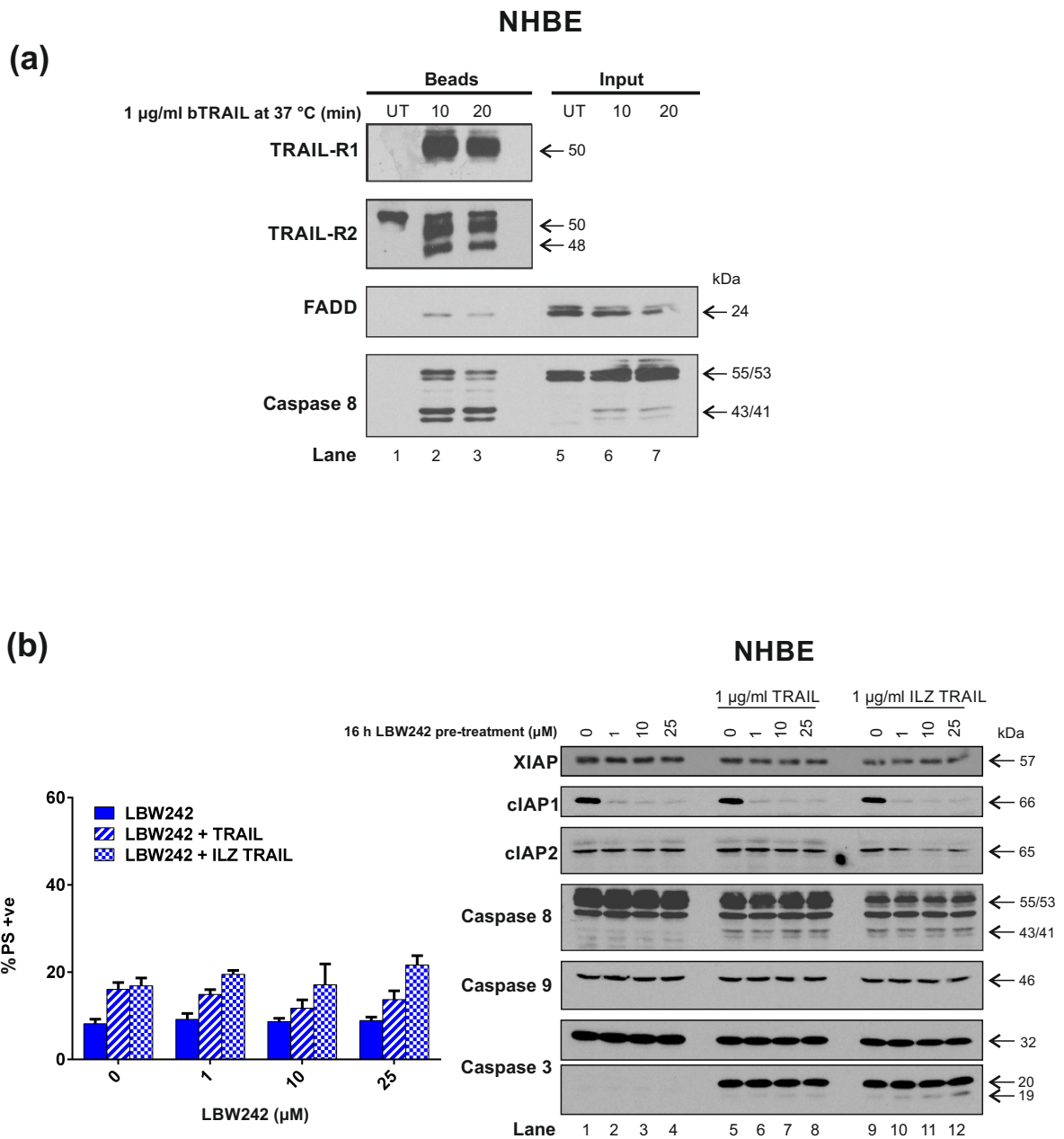


**Figure 4.9 NHBE cells form a DISC upon TRAIL treatment but are not sensitised to TRAIL-induced apoptosis when pre-treated with the SMAC mimetic, LBW242** (a) NHBE cells were analysed for DISC formation at 0-20 min at 37 °C, +/- pre-chill for 1 h at 4 °C as outlined in Chapter 2. For the immunoblots, 20  $\mu\text{l}$  of Bead sample and 10  $\mu\text{l}$  Sample Input were loaded onto SDS gels. Immunoblots are representative of two independent experiments. UT refers to untreated. (b) NHBE cells pre-treated with 0-25  $\mu\text{M}$  LBW242 16h at 37 °C followed by incubation with 1  $\mu\text{g/ml}$  TRAIL or 1  $\mu\text{g/ml}$  ILZ TRAIL for 5 h at 37 °C, were analysed for PS externalisation by flow cytometry. Cell pellets were analysed for XIAP, cIAP1, cIAP2, caspase 8, caspase 9, caspase 3 and PARP presence and/or cleavage by immunoblot. Bar chart represents relative % cell death (annexin V-FITC/PI) (mean  $\pm$  SEM,  $n=3$ ). Immunoblots are representative of three independent experiments and are loaded on cell number.

#### **4.2.2.4 NHBE cells treated with TRAIL or ILZ TRAIL do not undergo apoptosis but do display a time- and concentration-dependent cleavage of caspase 8 and caspase 3 and phosphorylation of I $\kappa$ B $\alpha$**

Following the observation that TRAIL DISC formation occurred rapidly in NHBE cells (Figure 4.9), it was decided to explore two aspects of TRAIL signalling in these cells. Firstly, the time-frame in which TRAIL or ILZ TRAIL induced caspase cleavage downstream of the DISC, and secondly, whether TRAIL/ILZ TRAIL treatment induced activation of the NF $\kappa$ B pathway (Figure 4.10).

Firstly, NHBE cells treated with either 1  $\mu$ g/ml TRAIL or ILZ TRAIL over 0 – 5 h were analysed for annexin-V-FITC/PI positive cells. Figure 4.10a shows that, consistent with previous experiments (Figures 4.7 and 4.9), exposure of NHBE cells to TRAIL or ILZ TRAIL did not result in any significant increase in apoptosis compared to untreated cells. In both TRAIL and ILZ TRAIL -treated NHBE cells, procaspase 8 was cleaved to p43/41 but also to the active cleavage fragment, p18 (Figure 4.10a). Procaspase 8 processing occurred very quickly, and as early as 30 min in both TRAIL and ILZ TRAIL-treated cells (lanes 2 and 9). Indeed this cleavage occurred in a concentration-dependent manner as evidenced by the loss of procaspase 8 (lanes 1 – 14). Again, consistent with previous findings, procaspase 9 was not cleaved. In contrast, procaspase 3 was cleaved to its p20 subunit in a time-dependent manner, in both TRAIL and ILZ TRAIL treated cells. The peak of TRAIL-induced caspase 3 cleavage was observed at 4 h (lane 6), whereas ILZ TRAIL induced a peak of caspase 3 cleavage in NHBE cells at the earlier time-point of 3 h (lane 12). This is consistent with a more rapid loss of procaspase 8 proform following ILZ TRAIL treatment compared to TRAIL treatment of NHBE cells (Figure 4.10a). This enhanced response to ILZ TRAIL (which more efficiently ligates TRAIL-R2) suggests that NHBE cells signal predominantly through ligation of TRAIL-R2.

To determine whether DISC formation occurs in a concentration-dependent manner, NHBE cells were treated with either 0 – 1  $\mu$ g/ml TRAIL or ILZ TRAIL for 2 h and analysed for PS externalisation and cleavage of apoptotic markers (Figure 4.10b). Following treatment with either TRAIL or ILZ TRAIL, there was no significant

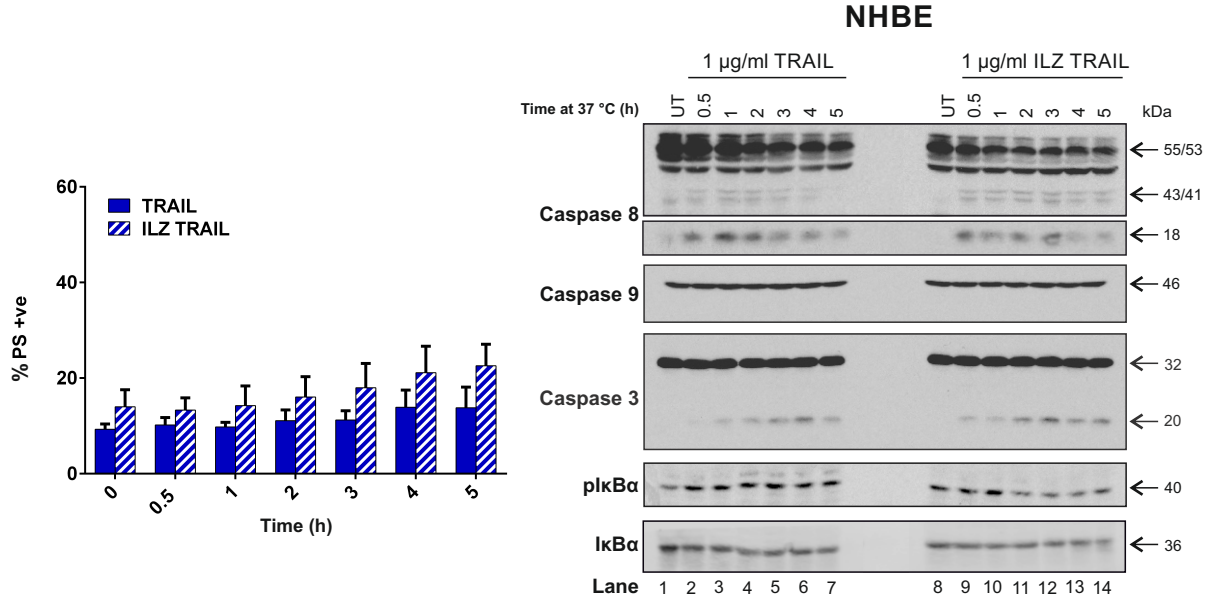
increase in annexin-V-FITC/PI stained cells. In line with this, procaspase 9 and PARP immunoblots showed that neither protein was cleaved. In contrast, on exposure to either TRAIL (lanes 1 – 5) or ILZ TRAIL (lanes 6 – 10), procaspase 8 and procaspase 3 were processed to their respective cleavage fragment(s) in a concentration-dependent manner, consistent with findings in Figure 4.10a. Once again, ILZ TRAIL treatment was more effective at inducing caspase 8 processing and thus formation of an active DISC than TRAIL, as evidenced by both procaspase 8 and partial procaspase 3 processing. In all treated cells, p17, the most active cleavage fragment of caspase 3, was not detected thus providing an explanation for the lack of both PARP cleavage and PS externalisation observed in these cells.

Cell pellets from the same pool of treated cells in Figures 4.10a and b were analysed by immunoblotting for apoptotic markers, as well as pI $\kappa$ B $\alpha$  and I $\kappa$ B $\alpha$ . NHBE cells treated with TRAIL showed a sustained phosphorylation of I $\kappa$ B $\alpha$  from 0 – 5 h as well as a corresponding loss of I $\kappa$ B $\alpha$  (lanes 1 – 7). In contrast, NHBE cells treated with ILZ TRAIL showed a peak of I $\kappa$ B $\alpha$  phosphorylation after only 1 h (lane 10). This observation shows that activation of the NF $\kappa$ B pathway may occur in NHBE cells treated with either TRAIL or ILZ TRAIL. Taken together, these data show that NHBE cells exhibit a time-dependent response to TRAIL or ILZ TRAIL, which results in both formation of the DISC and potential activation of NF $\kappa$ B. Like iHBEC cells exposed to TRAIL/ILZ TRAIL (Figure 4.5), NHBE cells rapidly activate downstream pathways following ligation of TRAIL-Rs with TRAIL/ILZ TRAIL.

At this 2 h time point, potential activation of the NF $\kappa$ B pathway was also observed in both TRAIL and ILZ TRAIL treated NHBE cells. Thus, I $\kappa$ B $\alpha$  was phosphorylated in a concentration-dependent manner in both TRAIL and ILZ TRAIL treated cells resulting in a corresponding loss of I $\kappa$ B $\alpha$  (lanes 1 – 5 and 6 – 10).

Taken together these data show that NHBE cells exposed to either TRAIL or ILZ TRAIL signal to apoptosis in a concentration-dependent manner very rapidly, and within 2 h, but caspase 3 cleavage is then halted at p20. In parallel, the NF $\kappa$ B pathway is activated by TRAIL or ILZ TRAIL in a time and concentration -dependent manner as assessed by phosphorylation of I $\kappa$ B $\alpha$ .

(a)



(b)

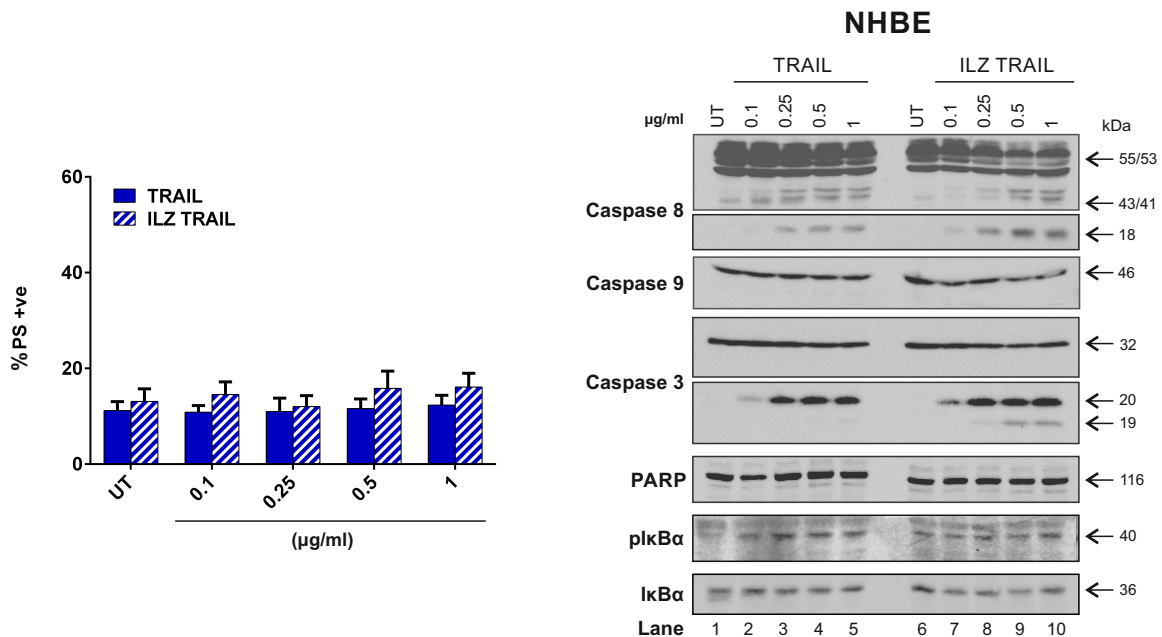


**Figure 4.10 NHBE cells treated with TRAIL or ILZ TRAIL do not undergo apoptosis but do display a time- and concentration-dependent cleavage of caspase 8 and caspase 3 and phosphorylation of I $\kappa$ B** (a) NHBE cells treated with 1  $\mu$ g/ml TRAIL or ILZ TRAIL for 0-5 h at 37  $^{\circ}$ C were analysed for PS externalisation by flow cytometry. Cell pellets were analysed for the presence and/or cleavage of caspase 8, caspase 9, caspase 3, PARP, plkB and I $\kappa$ B by immunoblotting. (b) NHBE cells treated with 0-1  $\mu$ g/ml TRAIL or ILZ TRAIL for 2 h at 37  $^{\circ}$ C were analysed for PS externalisation by flow cytometry. Cell pellets were analysed for the presence and/or cleavage of caspase 8, caspase 9, caspase 3, PARP, plkB and I $\kappa$ B by immunoblotting. All bar charts represent relative % cell death (annexin V-FITC/PI) (mean  $\pm$  SEM, n=3). All immunoblots are representative of three independent experiments.

#### **4.2.2.5 TRAIL or ILZ TRAIL treatment of NHBE cells induces p65 translocation to the nucleus in a time-dependent manner**

To verify the possible NF $\kappa$ B activation observed in Figure 4.10, NHBE cells treated with TRAIL or ILZ TRAIL were analysed for translocation of the NF $\kappa$ B subunit, p65, to the nucleus (Figure 4.11).

NHBE cells treated with 1  $\mu$ g/ml TRAIL or ILZ TRAIL for 0 – 5 h were immunostained for nuclei (blue), actin (red) and p65 (green) and analysed by confocal microscopy. TRAIL treatment caused p65 nuclear translocation in a gradual manner, with distinct nuclear staining evident from 2 – 5 h. In contrast, ILZ TRAIL treatment resulted in a more rapid translocation of p65, observed as early as 0.5 – 2 h. The immunoblot data in Figure 4.10a showed that TRAIL treatment induced phosphorylation of I $\kappa$ B $\alpha$  in a sustained manner over 5 h, consistent with the above p65 translocation data. In contrast, ILZ TRAIL treatment showed phosphorylation of I $\kappa$ B $\alpha$  to peak at 2 h, coupled with a continued loss of total I $\kappa$ B $\alpha$  over 5 h, indicating a possible time lag between induction of pI $\kappa$ B $\alpha$  and p65 translocation. Thus, collectively these data provide more evidence for TRAIL and ILZ TRAIL inducing NF $\kappa$ B activation in NHBE cells.

In addition, conditioned media from NHBE cells treated with TRAIL or ILZ TRAIL over 0 – 5 h were profiled for IL-6 and IL-8 release by measurement by ELISA and these cytokines were not found to be secreted (data not shown).

(a)

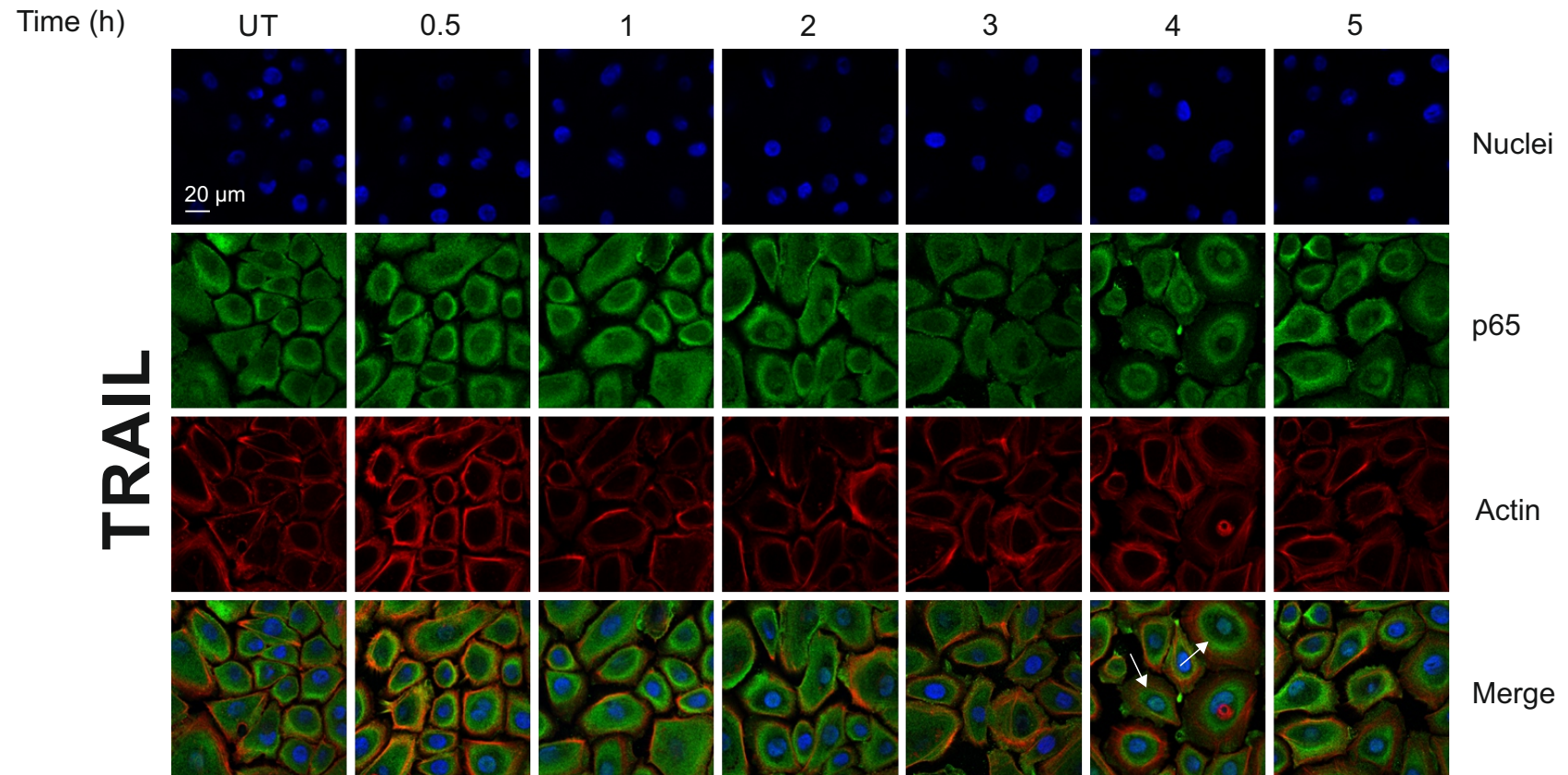


**Figure 4.11 TRAIL or ILZ TRAIL treatment of NHBE cells induces p65 translocation to the nucleus in a time- dependent manner** (a) NHBE cells were treated with 1 μg/ml TRAIL for 0-5 h at 37 °C and subsequently fixed, permeabilised and stained for p65, nuclei and actin as outlined in Chapter 2. Data are representative of two independent experiments and images are representative of several images. White arrows indicate examples of translocation of p65 to the nucleus.

(b)

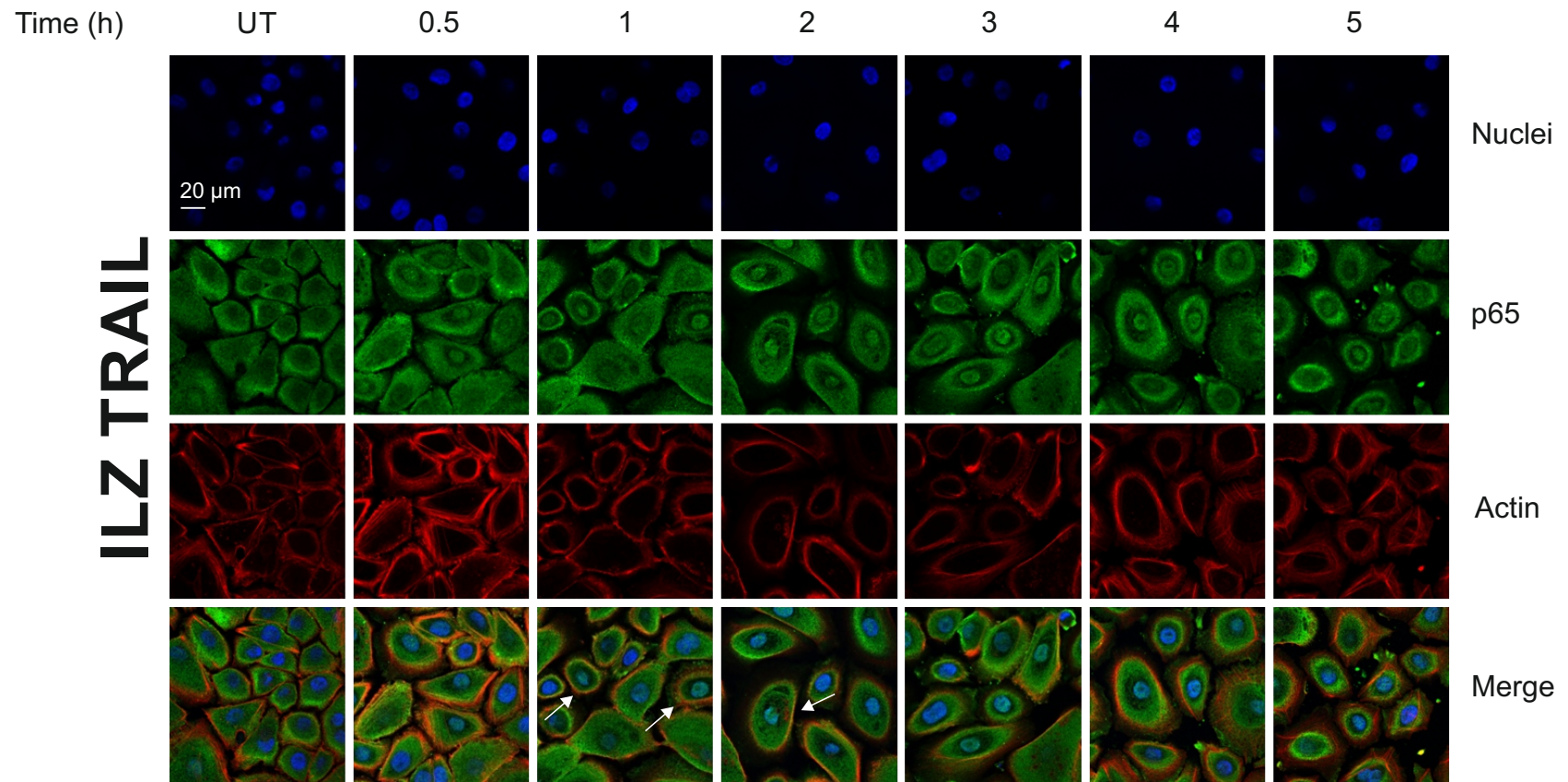


**Figure 4.11 TRAIL or ILZ TRAIL treatment of NHBE cells induces p65 translocation to the nucleus in a time- dependent manner** (b) NHBE cells were treated with 1  $\mu$ g/ml ILZ TRAIL for 0-5 h at 37  $^{\circ}$ C and subsequently fixed, permeabilised and stained for p65, nuclei and actin as outlined in Chapter 2. Data are representative of two independent experiments and images are representative of several images. White arrows indicate examples of translocation of p65 to the nucleus.

#### **4.2.2.6 Profile of the key pro- and anti-apoptotic proteins involved in regulating the mitochondrial amplification loop**

Pre-treatment of both iHBEC and NHBE cells with the SM, LBW242, did not promote cleavage of caspase 3 p20 fragment to its catalytically active subunit p17 or sensitise these normal lung epithelial cells to TRAIL or ILZ TRAIL -induced apoptosis (Figures 4.4 and 4.9). Therefore other proteins, such as members of the Bcl-2 family could have contributed to the block in apoptosis by inhibiting caspase 8-dependent engagement of the mitochondrial amplification loop. To explore this possibility, the epithelial cell lines, (A549, BEAS-2B and iHBEC) and the two primary NHBE donor cells (NHBE-D1 and NHBE-D2) were profiled for basal levels of key Bcl-2 family proteins by immunoblotting (Figure 4.12). Thus, levels of the pro-apoptotic Bcl-2 family proteins, Bax, Bak and Bid, in addition to the anti-apoptotic proteins, Bcl-XL and Mcl-1, were determined.

In both A549 and BEAS-2B cells, the pro-apoptotic proteins Bim, Bax and Bid, but not BAK were expressed. In terms of anti-apoptotic proteins, A549 cells expressed more Bcl-XL than BEAS-2B cells, whereas BEAS-2B cells expressed a greater amount of Mcl-1 compared with A549 cells. In contrast, the immortalized normal bronchial epithelial cell line, iHBEC, expressed the pro-apoptotic protein Bid, but expressed only minor levels of Bax or Bak. In terms of anti-apoptotic proteins tested, iHBEC cells expressed Mcl-1 but only low levels of Bcl-XL. In contrast, the two primary normal bronchial epithelial cell donors, NHBE-D1 and NHBE-D2, were found to express all of the pro-apoptotic proteins tested (Bax, Bak, Bid) as well as the anti-apoptotic proteins (Mcl-1, Bcl-XL).

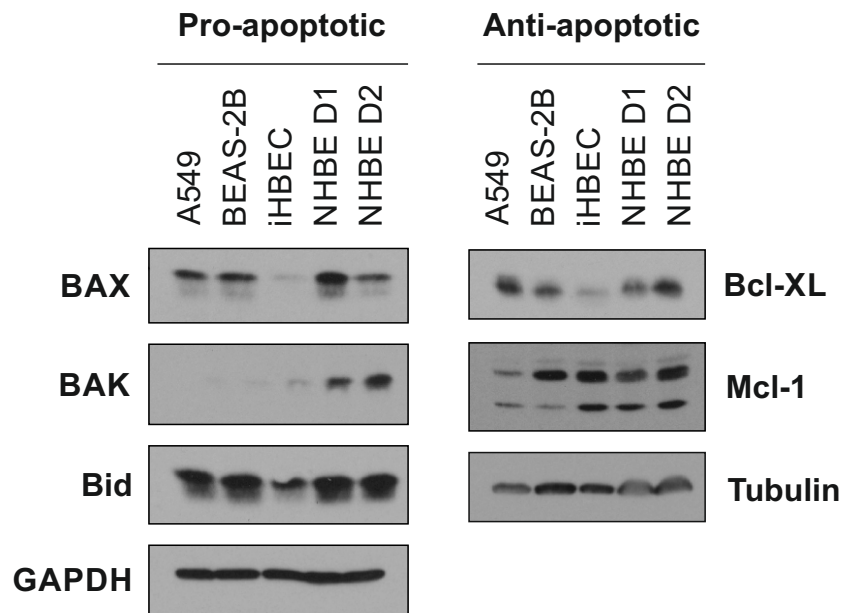


**Figure 4.12 Profile of the key pro- and anti-apoptotic proteins involved in regulating the mitochondrial amplification loop** (a) A549, BEAS-2B, 16HBE, iHBEC, NHBE-D1 and NHBE-D2 were analysed for their basal expression of the Bcl-2 family members, BAX, BAK, Bid, Bcl-XL and Mcl-1 by immunoblotting. Immunoblots are representative of two independent experiments.

### 4.3 Discussion

As lung epithelial cells are required for subsequent establishment of a co-culture of lung epithelial cells and T cells, it was important to first obtain information on basal TRAIL/TRAIL-R signalling in these cells. Therefore, the aim of this Chapter was to characterise both lung epithelial cell lines and primary lung epithelial cells in terms of their basal response to TRAIL and ILZ TRAIL.

It was quickly acknowledged that following treatment with TRAIL, the retrovirally transformed lung epithelial cell line, BEAS-2B, behaved in a similar manner to the lung carcinoma cell line, A549. Both cell lines showed PS externalisation in a concentration-dependent manner, a similar pattern of caspase processing and a similar rate of TRAIL DISC formation (Figures 4.1, 4.2 and 4.3). As outlined in Section 4.1, the BEAS-2B cell line was immortalised using a transformation process, which is documented in the literature to cause tumour-cell like behaviour (Reddel et al., 1988). The influence of cell transformation status has especially been documented when investigating responses to TRAIL treatment (MacFarlane et al., 2005a; Macfarlane et al., 2005b). In contrast, the retrovirally transformed lung epithelial cell line, 16HBE, was found to not express the TRAIL death receptors, TRAIL-R1 or TRAIL-R2, either on the cell surface (Figure 4.1) or intracellularly (Figure 4.3), thus explaining the lack of caspase cleavage or apoptosis observed in these cells (Figure 4.2). As a result, the 16HBE cell line was not further investigated for TRAIL signalling.

The immortalized normal bronchial epithelial cell line, iHBEC and donor-specific primary NHBE cells responded in a similar way to TRAIL or ILZ TRAIL, but very differently when compared with the cell lines, A549 and BEAS-2B. Thus, in iHBEC and NHBE cells, TRAIL DISC assembly occurred within 10 min of bTRAIL treatment (following a pre-chill step), activation of caspase 8 to p18 occurred as early as 30 min with subsequent and sustained caspase 3 cleavage to p20 fragment evident up to 5 h (Figures 4.2, 4.3, 4.5, 4.7, 4.9 and 4.10). However, in one aspect the cells behaved somewhat differently. To a small degree, primary NHBE cells pre-treated with the SM, LBW242, showed release of the halt in caspase 3 processing at p20

(Figure 4.9), whereas in iHBEC cells, LBW242 did not have any effect on caspase 3 processing (Figure 4.4). This suggested that, in NHBE cells, XIAP was to a small extent responsible for inhibition of processing of the caspase 3 p20 fragment to its catalytically active subunit, p17. It is also important to note that ILZ TRAIL proved to be a valuable tool for dissecting differential TRAIL-R signalling in both iHBEC and NHBE cells. Using ILZ TRAIL, a preference for these cells to signal predominantly *via* TRAIL-R2 was revealed as evidenced by the greater induction and accelerated processing of procaspase 8 and procaspase 3 induced by ILZ TRAIL compared to TRAIL. Another important characteristic shared by iHBEC and NHBE cells was the presence of tight junctions, as shown by membrane localisation of E-cadherin when cells were cultured in a confluent monolayer (Figure 4.8). Following these observations, the immortalized cell line, iHBEC, but not the retrovirally transformed cell line BEAS-2B, was selected for future experiments due to its better commonality with primary epithelial cells in terms of TRAIL signalling.

In addition to activation of the apoptotic pathway, TRAIL or ILZ TRAIL ligation of TRAIL-R1/R2 in iHBEC and NHBE cells resulted in the possible activation of the NF $\kappa$ B pathway as shown by increased phosphorylation of I $\kappa$ B $\alpha$  and downstream nuclear translocation of p65 (Figures 4.5, 4.6, 4.10 and 4.11). As described in Chapter 1, although not the predominant arm of TRAIL signalling, NF $\kappa$ B activation can occur downstream of ligation of either TRAIL-R1 or TRAIL-R2 NF $\kappa$ B activation is known to signal to survival of cells and p65 has been reported to upregulate a wide variety of genes to protect against the induction of apoptosis, including IAPs, Bcl-2 proteins and cFLIP (Braeuer et al., 2006; Harper et al., 2001; Hu et al., 1999; Schneider et al., 1997; Wang et al., 1998; Zong et al., 1999). More recently, although in a lung cancer setting, microRNAs also have been implicated in the inhibition of TRAIL-induced apoptosis following NF $\kappa$ B activation. Jeon et al., (2015) have shown that microRNA 21 can downregulate caspase 8 activation, induced by TRAIL, leading to the downregulation of RIP-1 cleavage and therefore allowing activation of NF $\kappa$ B. This demonstrates how multi-dimensional NF $\kappa$ B gene regulation can be.

The data presented in this Chapter, showing functional TRAIL DISC formation in both iHBEC and NHBE bronchial cells, would argue against cFLIP upregulation contributing to inhibition of TRAIL-induced apoptosis in these cells. In this context, it has also been recently noted by (Arish et al., 2015) that overexpression of h-TERT in epithelial cells causes cFLIP upregulation which in turn protects cells from CD95-mediated cell death. Although the idea of high levels of cFLIP resulting in inhibition of death receptor-mediated apoptosis is well documented, it is unlikely that cFLIP inhibition of TRAIL-induced apoptosis is occurring in iHBEC cells (immortalised by overexpression of h-TERT and Cdk4 as described in Section 4.1). Since cFLIP functions as an inhibitor of apoptosis at the level of the DISC, cleavage of procaspase 8 and subsequently procaspase 3 in iHBEC cells treated with anti-CD95, TRAIL or ILZ TRAIL provides evidence against inhibition of apoptosis in iHBEC cells being mediated by cFLIP.

The block of apoptosis that occurred at the level of caspase 3 processing in iHBEC and NHBE cells treated with TRAIL or ILZ TRAIL could not be released with LBW242 pre-treatment. Therefore it was proposed that along with XIAP, other mechanisms of inhibition could be involved. Due to the observation that neither iHBEC nor NHBE cells treated with TRAIL or ILZ TRAIL exhibited caspase 9 cleavage and thus lacked engagement of the mitochondrial amplification loop (as described in Chapter 1), it was theorised that the Bcl-2 family of proteins may have contributed to this block. Hence, in A549, BEAS-2B, iHBEC and NHBE cells, the expression of members of the Bcl-2 family known to be involved in regulation of the mitochondrial amplification loop was examined. This revealed that both A549 and BEAS-2B cells displayed high levels of pro-apoptotic Bcl-2 proteins, namely the effector Bax, suggesting that both cell lines have the potential to undergo Bax-driven apoptosis. This may provide an explanation for the cleavage of procaspase 9 and PS externalisation observed following exposure of these cells to TRAIL or ILZ TRAIL (Czabotar et al., 2013; Gavathiotis et al., 2008; Sarosiek et al., 2013). In contrast, iHBEC and NHBE cells had differential profiles of the Bcl-2 proteins. It appeared that NHBE cells possessed high levels of the pro-apoptotic proteins, Bak, Bax and Bid and high levels of the anti-apoptotic Bcl-2 proteins, Bcl-XL and Mcl-1. In contrast, iHBEC cells expressed low levels of pro-apoptotic proteins, except Bid,

and similarly low levels of the anti-apoptotic Bcl-2 proteins (Figure 4.12). Interestingly, particularly low levels of Bak and Bax in iHBEC cells may explain the observed lack of apoptosis induced by cytotoxic drugs such as etoposide and STS – lack of these pore forming Bcl-2 proteins allows for limited activation of apoptosis. These observations demonstrate how complex and multifaceted the regulation of apoptosis can be in any given cell. Although, iHBEC and NHBE cells appear to signal to TRAIL-induced apoptosis and NFκB activation by very similar mechanisms and in very similar time frames, upon closer inspection, the signal to block apoptosis at the level of caspase 3 processing may be different between these cells.

In summary, in this Chapter, TRAIL/TRAIL-R signalling has been characterised for the first time in normal bronchial epithelial cells and this has shown that both iHBEC and NHBE cells respond similarly to TRAIL or ILZ TRAIL. With all of the data taken together, it can be deduced that, in terms of TRAIL signalling, iHBEC cells provide a good model for primary lung epithelial cells as their response is more analogous to donor NHBE cells than any of the other established epithelial cell lines characterised.

**5 Characterisation of TRAIL/TRAIL-R Signalling in Primary T Cells and Development of a Co-culture of Lung Epithelial Cells and Activated T cells**

## 5.1 Introduction

As described in Chapter 1, the aim of this project was to implement a co-culture of lung epithelial cells with primary activated T cells as a model of lung inflammation. Following the establishment of basal levels of TRAIL/TRAIL-R signalling in a panel of epithelial cell lines and primary epithelial cells, the aim of this chapter was to characterise the TRAIL/TRAIL-R signalling of both naïve and activated primary T cells. Following characterisation of basal TRAIL signalling, the aim was to investigate the role of both TRAIL/TRAIL-R signalling both in terms of apoptosis and activation of NFκB. Thus, endpoints investigated were cellular surface expression of relevant receptors and ligands, exposure of PS and cytokine release into conditioned medium.

Both CD4<sup>+</sup> and CD8<sup>+</sup> T cells have been implicated in the progression and promotion of lung inflammation for conditions such as COPD (Bagdonas et al., 2015; Cosio et al., 2002). However, there has been a lack of research into the role of TRAIL /TRAIL-R signalling of T cells in the context of lung inflammation. Thus, CD4<sup>+</sup> and CD8<sup>+</sup> T cells subtypes, along with lung epithelial cells, were selected for investigation in this project.

*In vivo*, the activation of naïve T cells is vital for the immuno-protective role these cells play in disease and infection. The activation signal requires engagement of the T cell receptor (TCR) by antigen-presenting cells and signals for T cells to proliferate and produce pro-inflammatory cytokines. *In vitro*, a well-documented method of activating T cells is stimulation by CD28 and CD3 antibodies (Kay et al., 1991). Accordingly, this was the experimental approach of T cell activation adopted for this project.

T cells are documented to become sensitive to the death ligand, CD95L, following activation (Klaus et al., 1993; Nagata and Golstein, 1995). Thus, it was decided to investigate the TRAIL/TRAIL-R signalling of both naïve and activated CD4<sup>+</sup> and CD8<sup>+</sup> T cells to explore whether a similar effect occurs with TRAIL. In addition, this would also provide the basal levels of TRAIL/TRAIL-R signalling in T cells for subsequent implementation of a lung epithelial cell and T cell co-culture model.

Co-culture experimental approaches are widely used and documented to mimic the *in vivo* scenario much more closely than mono-cultures (Cruickshank et al., 2004; Miki et al., 2012). In the context of this project, the approach was selected for two reasons, firstly to be able to mimic the *in vivo* situation as much as possible and secondly, to be able to elucidate the effects of direct cell-to-cell interactions versus indirect cell-to-cell signalling (e.g. *via* the addition of conditioned media).

As previously described, TRAIL can ligate its cognate receptors both as a soluble factor and as a membrane-bound ligand. The downstream signalling effects of different forms of TRAIL (soluble versus membrane-bound) are potentially different. This phenomenon was explored in Chapter 3 where ILZ TRAIL was generated based on previous research showing the conformation of TRAIL to be important when transducing an apoptotic signal *via* either TRAIL-R1 or TRAIL-R2. Further highlighting this point, the exposure of iHBEC or NHBE cells to TRAIL or ILZ TRAIL was shown to cause differential signalling, both in terms of time frame and intensity. Thus, one of the aims of the co-culture experiments was to explore whether there was a differential signalling effect caused by treatment with either TRAIL or ILZ TRAIL.

As described in Chapter 4, in terms of TRAIL/TRAIL-R signalling, iHBEC cells were found to be much more similar to NHBE cells than previously established lung epithelial cell lines. Thus, it was decided to take both iHBEC and NHBE cells forward for implementation of co-cultures with activated primary CD4<sup>+</sup> and CD8<sup>+</sup> T cells to assess whether the cells were also similar in terms of their response under co-culture conditions to be the two cell types.

Although the primary aim of the co-culture model was to see what effects TRAIL and ILZ TRAIL have on the interplay between epithelial cells and T cells, it would also provide the opportunity to evaluate the effect of activated CD4<sup>+</sup> and CD8<sup>+</sup>T cells on TRAIL/TRAIL-R and CD95/CD95L expression in lung epithelial cells.

## **5.2 Results**

### **5.2.1 Characterisation of TRAIL/TRAIL-R Signalling in Primary T cells**

#### **5.2.1.1 Isolation of T cells by positive selection**

Figure 5.1 shows the work flow for the isolation of both CD4<sup>+</sup> and CD8<sup>+</sup> T cells for this project. Fresh healthy volunteer blood (drawn no more than 3 h prior to isolation) was used to isolate peripheral blood mononuclear cells (PBMC) using histopaque (see Chapter 2). From these PBMC, CD4<sup>+</sup> T cells were isolated by a positive selection method (Figure 5.1a). The flow through from the CD4<sup>+</sup> T cell isolation was used for the subsequent isolation of CD8<sup>+</sup> T cells.

Figure 5.1b shows the purity and efficiency of the positive selection method employed for T cell isolation by CD4<sup>+</sup> and CD8<sup>+</sup> staining measured by flow cytometry. The final CD8<sup>+</sup> flow through dot blot shows the absence of CD4<sup>+</sup> and CD8<sup>+</sup> populations, highlighting the efficiency of this method. Both CD4<sup>+</sup> and CD8<sup>+</sup> T cells used for this project were isolated to 95 % purity or above.

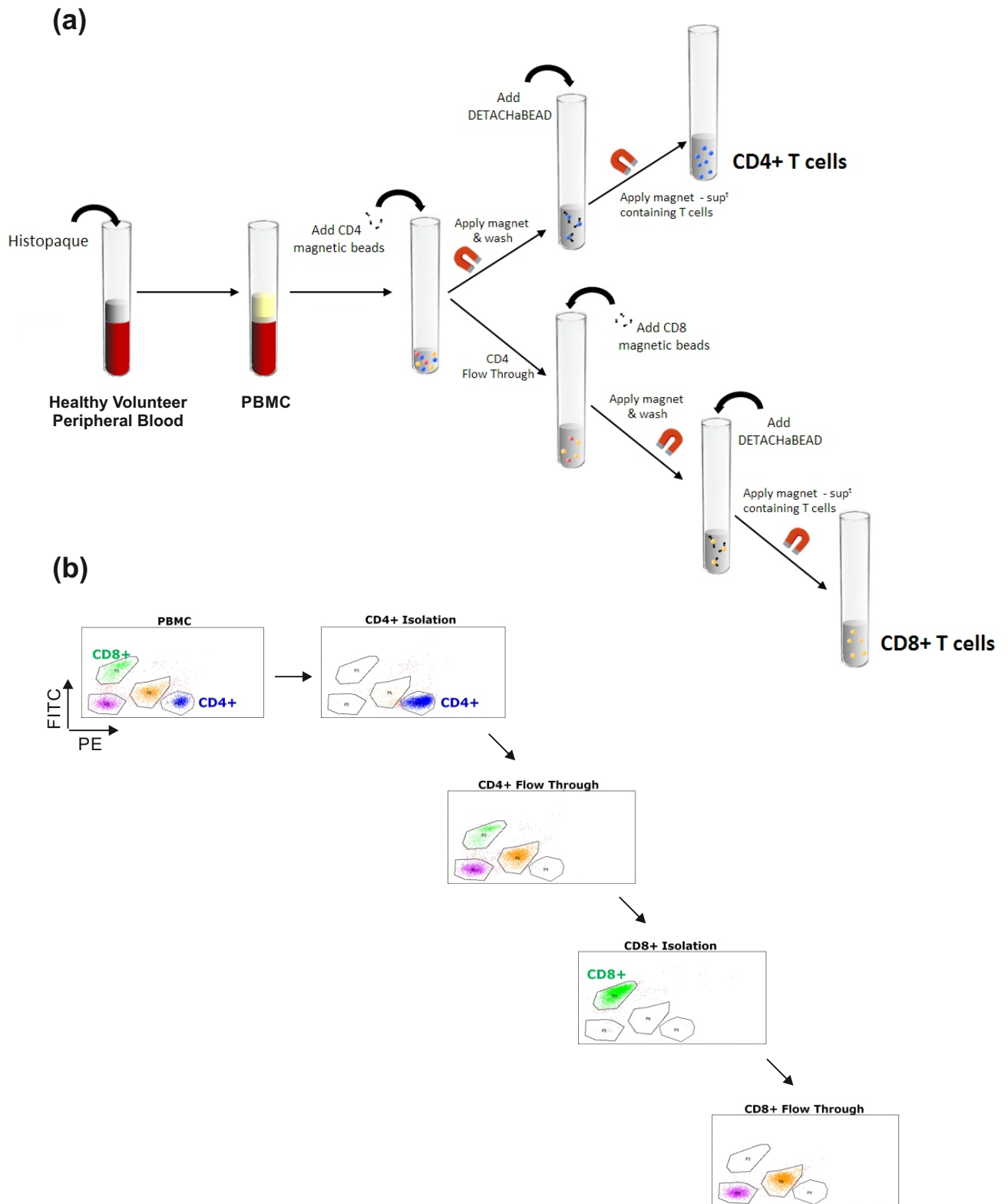


**Figure 5.1 T cell isolation method by positive selection** (a) Schematic representation of the flow of work to isolate CD4<sup>+</sup> and CD8<sup>+</sup> T cells from fresh human peripheral blood. PBMC - peripheral blood mononuclear cells and sup<sup>1</sup> for supernatant (b) A representative example of the relative CD4<sup>+</sup> and CD8<sup>+</sup> T cell populations measured by flow cytometry, in the steps of T cell isolation. Blue represents CD4<sup>+</sup>, green for CD8<sup>+</sup>, purple for CD4<sup>+</sup>CD8<sup>+</sup> and yellow for CD4<sup>+</sup>CD8<sup>+</sup>

### **5.2.1.2 Surface expression profile of naïve and 19 h activated CD4<sup>+</sup> and CD8<sup>+</sup> T cells**

Once isolated, CD4<sup>+</sup> and CD8<sup>+</sup> T cells were referred to as naïve and following incubation with CD3 and CD28 antibodies (as outlined in Chapter 2) they were referred to as activated. CD4<sup>+</sup> and CD8<sup>+</sup> T cells, both naïve and 19 h activated were profiled for their surface expression of TRAIL-Rs, TRAIL, CD95 and CD95L (Figure 5.2).

Naïve CD4<sup>+</sup> T cells expressed a small amount of TRAIL-R1 and whereas activated CD4<sup>+</sup> T cells did not express TRAIL-R1 on their surface. Neither cell type expressed TRAIL-R2. CD95 levels appeared to increase upon activation of CD4<sup>+</sup> T cells, whereas TRAIL and CD95L levels decreased upon activation.

Naïve CD8<sup>+</sup> T cells did not express TRAIL-R1, TRAIL-R2 or CD95L but following 19 h activation they appear to express some TRAIL-R1. Conversely, TRAIL was expressed on naïve CD8<sup>+</sup> T cells but not on activated CD8<sup>+</sup> T cells. As with CD4<sup>+</sup> T cells, CD8<sup>+</sup> T cells showed an increased expression of CD95 on their surface following activation for 19 h.

Taken together these data demonstrate that both CD4<sup>+</sup> and CD8<sup>+</sup> T cells exhibit different basal surface death expression receptor/ligand profiles but also that these profiles change following activation for 19 h.

## Naïve and 19 h Activated CD4<sup>+</sup> & CD8<sup>+</sup> T Cells

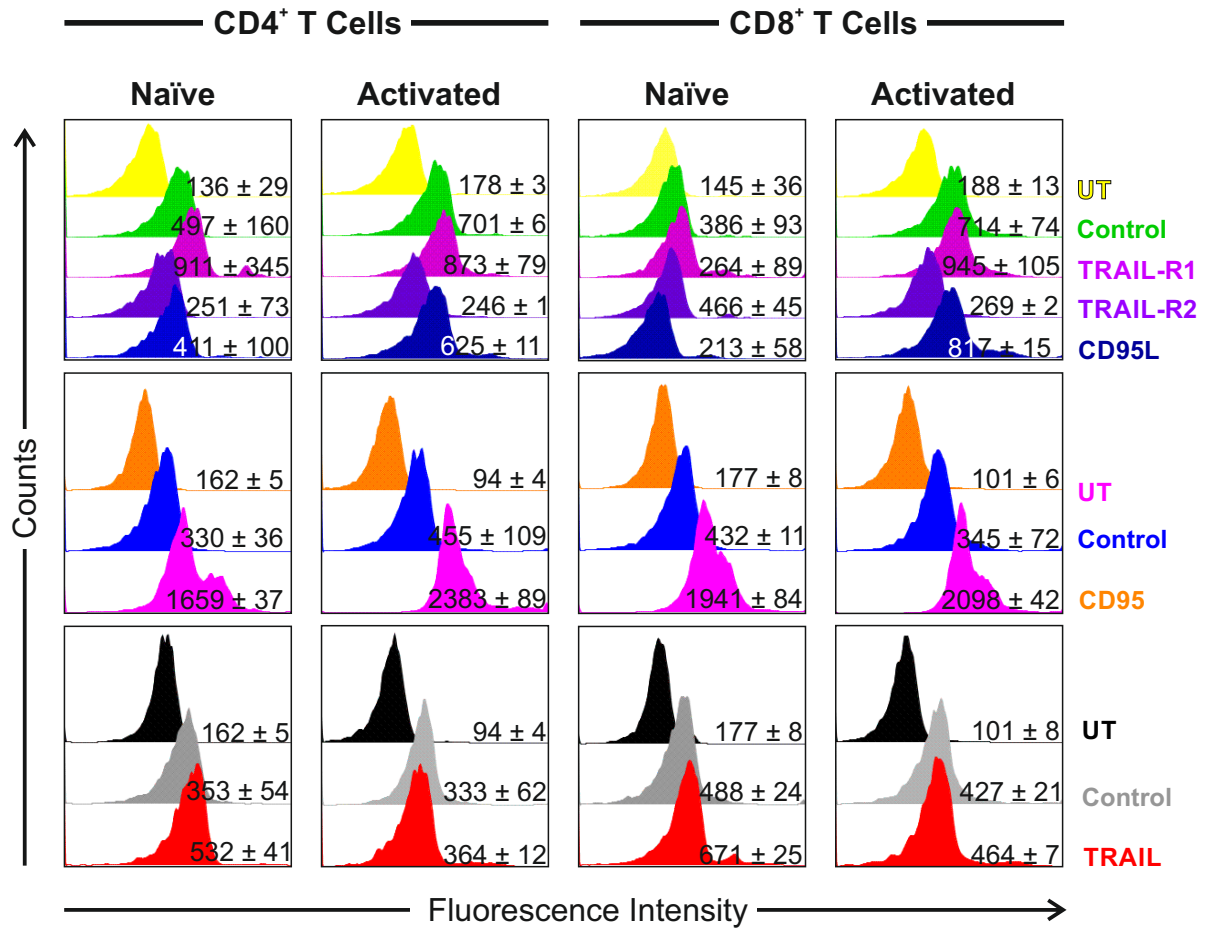


**Figure 5.2 Surface expression profile of naïve and 19 h activated CD4<sup>+</sup> and CD8<sup>+</sup> T cells** Naïve and 19 h activated CD4<sup>+</sup> and CD8<sup>+</sup> T cells were analysed for the cell surface expression of TRAIL-R1, TRAIL-R2, CD95, CD95L and TRAIL. Cells were incubated with either no antibody (UT), isotype control antibody (control), PE-conjugated TRAIL-R1, TRAIL-R2, FITC-conjugated TRAIL, PE-conjugated CD95L or CH11 with FITC-conjugated secondary antibodies. Following washing with PBS, cells were analysed by flow cytometry for changes in fluorescence intensity. Mean fluorescence intensity is represented by geometric mean ± SEM (n=3).

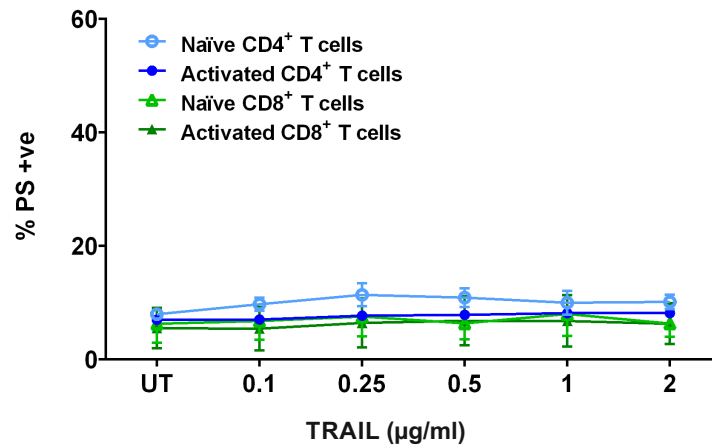
### **5.2.1.3 Naïve and 19 h activated CD4<sup>+</sup> T cells are not sensitive to TRAIL or ILZ TRAIL treatment**

The naïve and 19 h activated T cells shown in Figure 5.2 were treated with 0 – 2 µg/ml TRAIL for 5 h to establish whether the TRAIL apoptotic pathway was active in these cells (Figure 5.3a). Neither naïve nor activated CD4<sup>+</sup> or CD8<sup>+</sup> T cells were found to show PS externalisation following exposure to TRAIL.

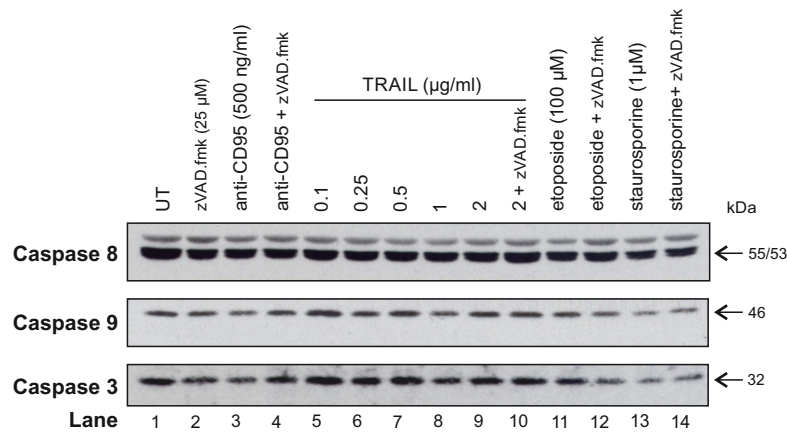
Cell pellets from 19 h activated CD4<sup>+</sup> T cells treated with anti-CD95, TRAIL, etoposide or STS +/- zVAD.fmk, were immunoblotted for cleavage of the following markers of apoptosis; caspase 8, caspase 9 and caspase 3 (Figure 5.3b). Activated CD4<sup>+</sup> T cells did not show cleavage of any of the apoptotic markers following treatment any of the above intrinsic or extrinsic apoptotic stimuli.

Activated CD4<sup>+</sup> T cells were similarly treated with ILZ TRAIL +/- zVAD.fmk and were once again found to not display processing of the aforementioned apoptotic markers. These data suggest a lack of TRAIL-induced DISC formation in both 19 h activated and naïve CD4<sup>+</sup> and CD8<sup>+</sup> T cells.

(a) **19 h Naïve & Activated CD4<sup>+</sup> T cells**



(b) **19 h Activated CD4<sup>+</sup> T cells**



(c)

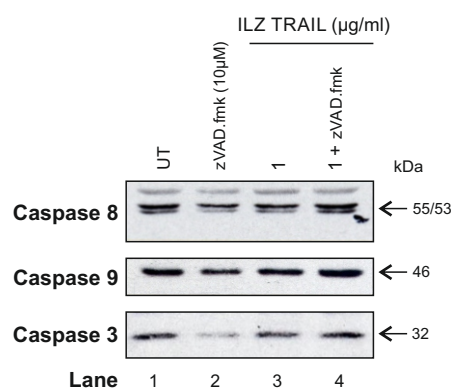


**Figure 5.3 Naïve and 19 h activated CD4<sup>+</sup> T cells are not sensitive to TRAIL or ILZ TRAIL treatment** (a) Activated (19 h) CD4<sup>+</sup> T cells were treated with 0 - 1 µg/ml TRAIL and analysed by flow cytometry for PS externalisation. Graph represents % cell death (annexin V-FITC/PI) (mean ± SEM, n=3) (b) Cell pellets of activated (19 h) CD4<sup>+</sup> T cells treated with various apoptotic stimuli including 0 - 2 µg/ml TRAIL, in the presence or absence of zVAD.fmk, were analysed for caspase 8, caspase 9, caspase 3 and PARP cleavage by immunoblotting. (c) Cell pellets of activated (19 h) CD4<sup>+</sup> T cells treated with 1 µg/ml ILZ TRAIL, in the presence or absence of zVAD.fmk, were analysed for caspase 8, caspase 9, caspase 3 and PARP cleavage by immunoblotting. Immunoblots are representative of three independent experiments.

#### **5.2.1.4 Cell surface expression profile of 6 day activated CD4<sup>+</sup> and CD8<sup>+</sup> T cells**

It has been widely documented that CD4<sup>+</sup> and CD8<sup>+</sup> T cells activated for prolonged periods of time undergo a phenomenon called activation-induced cell death (AICD). AICD is mediated by the CD95L:CD95 interaction which requires the upregulation of CD95 and CD95L on the surface of T cells and is characterised by autocrine signalling to regulate the population of activated cells and therefore the intensity of the immune response (Caricchio et al., 1998; Dhein et al., 1995; Klaus et al., 1993; Nagata and Golstein, 1995). It has been well documented that AICD requires prolonged activation, in the range of days (Maksimow et al., 2003; Sagi et al., 2011); therefore it was decided to investigate the surface expression of TRAIL-Rs and TRAIL on prolonged activated T cells to explore whether a similar phenomenon occurs for TRAIL/TRAIL-R signalling (Figure 5.4).

As expected, CD95 was expressed highly in both CD4<sup>+</sup> and CD8<sup>+</sup> activated for 6 days. In CD8<sup>+</sup> T cells, cell surface levels of TRAIL-R1 remained the same compared to 19 h activated CD8<sup>+</sup> T cells. Neither CD4<sup>+</sup> nor CD8<sup>+</sup> T cells expressed TRAIL-R2 on their surface following activation over 6 days. These data indicate the potential for TRAIL-mediated signalling to occur in 6 d activated CD8<sup>+</sup> T cells.

## 6 Day Activated CD4<sup>+</sup> & CD8<sup>+</sup> T Cells

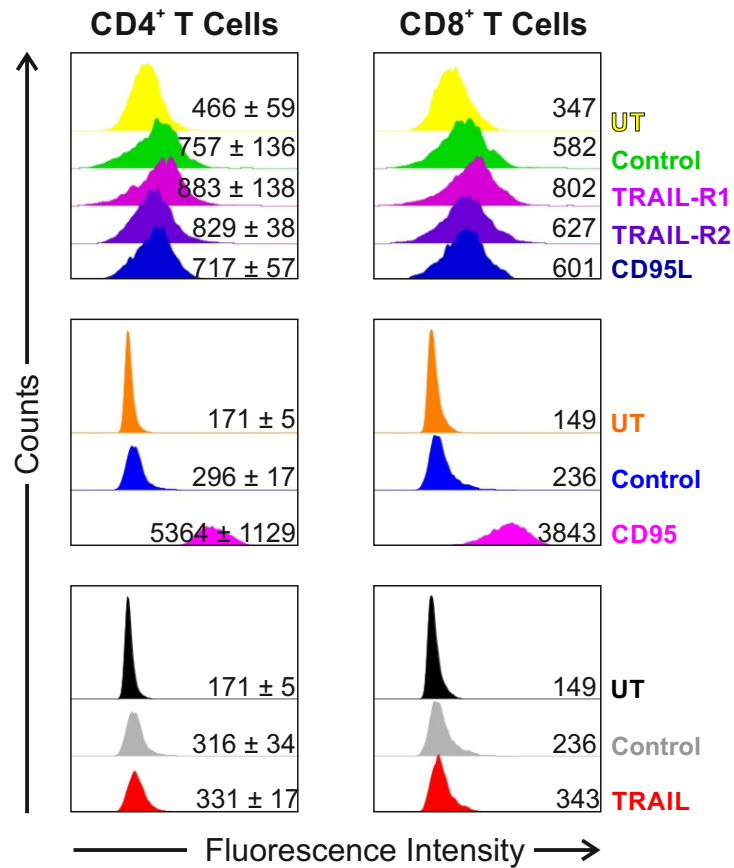


**Figure 5.4 Cell surface expression profile of 6 day activated CD4<sup>+</sup> and CD8<sup>+</sup> T cells** Activated (6 day) CD4<sup>+</sup> and CD8<sup>+</sup> T cells were analysed for the cell surface expression of TRAIL-R1, TRAIL-R2, CD95, CD95L and TRAIL. Cells were incubated with either no antibody (UT), isotype control antibody (control), PE-conjugated TRAIL-R1, TRAIL-R2, FITC-conjugated TRAIL, PE-conjugated CD95L or CH11 with FITC-conjugated secondary antibodies. Following washing with PBS, cells were analysed by flow cytometry for changes in fluorescence intensity. Mean fluorescence intensity is represented by geometric mean ± SEM (n=3) for CD4<sup>+</sup> T cells and the fluorescence intensity average for CD8<sup>+</sup> T cells (n=2).

### **5.2.1.5 CD4<sup>+</sup> and CD8<sup>+</sup> T cells activated for 6 days are not sensitive to TRAIL or ILZ TRAIL treatment**

Following the observation of the presence of low levels of TRAIL-R1 (Figure 5.4), CD4<sup>+</sup> and CD8<sup>+</sup> T cells activated for 6 days were investigated for their ability to signal to TRAIL-induced apoptosis (Figure 5.5).

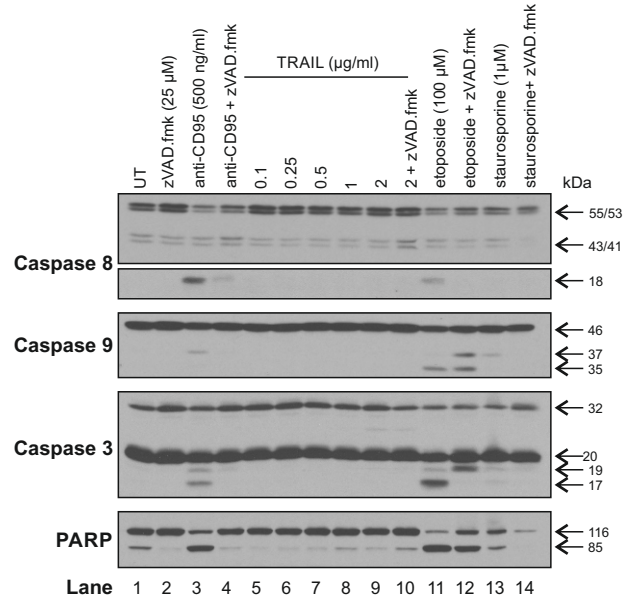
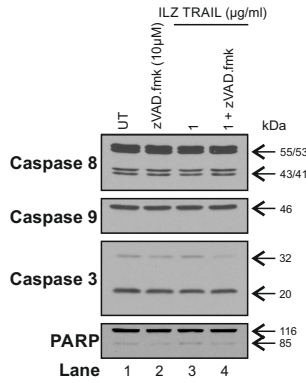
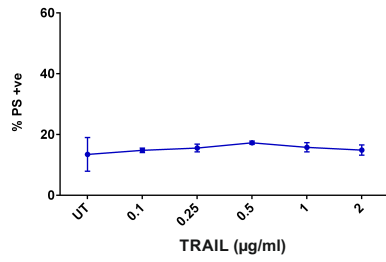
Activated (6 days) CD4<sup>+</sup> T cells treated with 0 – 2 µg/ml TRAIL for 5 h did not exhibit PS externalisation (Figure 5.5a). Cell pellets from CD4<sup>+</sup> T cells treated with anti-CD95, TRAIL, etoposide or STS +/- zVAD.fmk were immunoblotted for the following markers of apoptosis; caspase 8, caspase 9, caspase 3 and PARP. A background level of caspase 8 activation was observed across all treatments and control cells as indicated by the presence of caspase 8 p43/41 fragments (lanes 1 – 14). Downstream of caspase 8, procaspase 3 was processed to the p20 cleavage fragment across all treatments. This can most likely be attributed to the Activation-induced cell death (AICD) phenomenon described above. In addition to the background cell death seen, anti-CD95 treatment induced further cell death as shown by the presence of the most active cleavage fragment of procaspase 8, p18 (lane 3). Consistent with this, procaspase 3 was observed to be cleaved to its active p19 and p17 fragments, which in turn resulted in partial cleavage of the caspase substrate, PARP. The presence of zVAD.fmk inhibited the processing of caspase 8 and therefore the subsequent cleavage of downstream proteins in the pathway (lane 4). Treatment of CD4<sup>+</sup> T cells with the intrinsic pathway stimulus, etoposide, also caused further cleavage of procaspase 8 to p18 (lane 11). Procaspase 9 processing was also observed indicating engagement of the intrinsic pathway in these cells. Downstream cleavage of procaspase 3 to p19 and p17 was seen followed by significant processing of PARP. Pre-treatment with zVAD.fmk inhibited the processing of caspases, although not fully (lane 12). Treatment of these cells with TRAIL or STS did not appear to cause any significant increase in the processing of apoptotic markers (lanes 4 – 10 & 13 – 14) therefore confirming the PS externalisation data shown in Figure 5.5a.

CD8<sup>+</sup> T cells activated for 6 days were similarly treated with various apoptotic stimuli to characterise their response (Figure 5.5b). TRAIL treatment (0 – 2 µg/ml) did not induce positive staining for annexin-V-FITC/PI indicating little cell death. CD8<sup>+</sup> T cells were also treated with anti-CD95, TRAIL, etoposide or STS +/- zVAD.fmk and immunoblotted for caspase 8, caspase 9, caspase 3 and PARP. Similar to CD4<sup>+</sup> T cells, a portion of CD8<sup>+</sup> T cells were found to be apoptotic, across all treatments and control cells as indicated by the presence of cleavage fragments of caspase 8 (to p43/41) and caspase 3 (to p20) and PARP. However, in contrast to CD4<sup>+</sup> T cells, in CD8<sup>+</sup> T cells, caspase 9 was also found to be cleaved to the p37 fragment across all treatments, signifying cleavage to p37 by active caspase 3 rather than apoptosome mediated autocatalytic cleavage. Furthermore, anti-CD95 induced processing of procaspase 8 and 3 to their respective active cleavage fragments therefore resulting in almost complete processing of PARP. Pre-treatment of these cells with zVAD.fmk inhibited caspase processing and also inhibited PARP cleavage. Etoposide treatment of CD8<sup>+</sup> T cells induced processing of caspase 8 to p18 and processing of caspase 9 to p37 and p35 cleavage fragments, indicative of apoptosome formation (lane 11). Downstream of this, procaspase 3 was processed to all three cleavage fragments, p20, p19 and p17, which resulted in complete cleavage of PARP. Pre-treatment of etoposide treated CD8<sup>+</sup> T cells with zVAD.fmk rescued the cell death observed by etoposide alone (lane 12). Treatment with TRAIL or STS did not result in any increase in apoptosis (lanes 4 – 10 & 13 – 14) consistent with the lack of annexin-V-FITC/PI staining observed.

Pre-treatment of 6 day activated CD8<sup>+</sup> T cells with zVAD.fmk prior to 1 µg/ml ILZ TRAIL did not result in cleavage of any apoptotic markers above UT (lane 1) due to constant levels of AICD in these long-term activated T cells.

These results confirm previous reports of T cells exhibiting increased sensitivity to CD95-mediated apoptosis following prolonged activation. In contrast, the sensitivity of either CD4<sup>+</sup> or CD8<sup>+</sup> T cells to TRAIL or ILZ TRAIL was not altered following activation for 6 days.

**(a) 6 Day Activated CD4<sup>+</sup> T cells**



**(b) 6 Day Activated CD8<sup>+</sup> T cells**

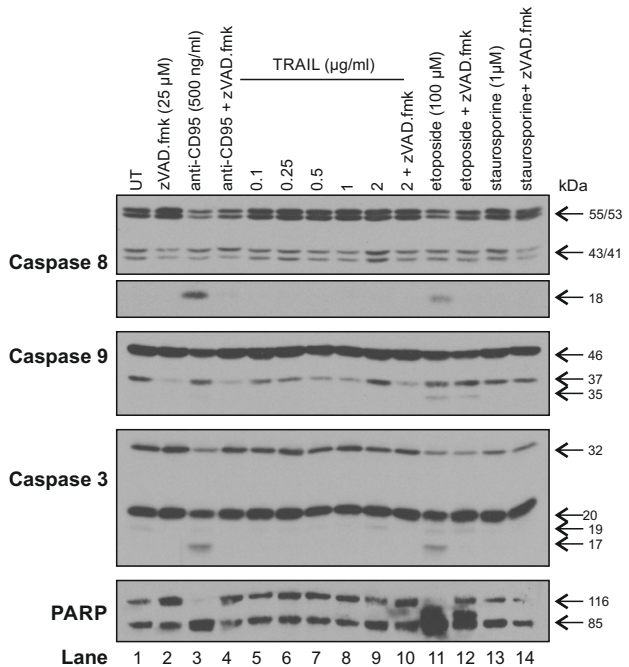
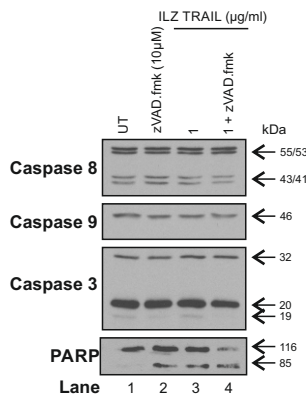
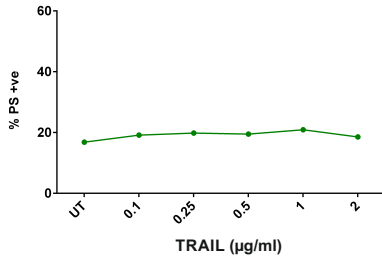


**Figure 5.5 CD4<sup>+</sup> and CD8<sup>+</sup> T cells activated for 6 day are not sensitive to TRAIL or ILZ TRAIL treatment** (a) CD4<sup>+</sup> T cells and (b) CD8<sup>+</sup> T cells activated for 6 days treated with 0 - 2 µg/ml TRAIL were analysed by flow cytometry for PS externalisation. Graph represents % cell death (annexin V-FITC/PI) (mean ± SEM, n=3 for CD4<sup>+</sup> T cells and average (n=2) for CD8<sup>+</sup> T cells). Pellets of cells treated with various apoptotic stimuli including 0 - 2 µg/ml TRAIL and 1 µg/ml ILZ TRAIL, in the presence and absence of zVAD.fmk were analysed by immunoblotting for caspase 8, caspase 9, caspase 3 and PARP cleavage.

## **5.2.2 Implementation of a co-culture of lung epithelial cells and primary T cells**

### **5.2.2.1 Work flow for the establishment of the conditioned media and cell-to-cell co-culture models of lung epithelial cells and primary T cells**

Following the characterisation of TRAIL/TRAIL-R signalling in epithelial cells (Chapter 4) and the characterisation of primary T cells (in this Chapter), the aim was to implement a co-culture of epithelial cells and primary T cells (Figure 5.6) to explore the interplay of these cells in terms of TRAIL induced apoptosis and/or inflammation.

Both iHBEC and NHBE cells were used to implement the co-culture, with the aim of investigating potential differences between an established lung epithelial cell line versus primary cells cultured with T cells. This interest arose from the similarities in TRAIL/TRAIL-R signalling seen between iHBEC and NHBE cells (Chapter 4).

Due to the lack of change in TRAIL signalling in CD4<sup>+</sup> and CD8<sup>+</sup> T cells following activation for 6 days and the increase in the AICD observed, it was decided that for the implementation of the co-culture model, CD4<sup>+</sup> and CD8<sup>+</sup> T cells would be activated for 19 h prior to incubation with lung epithelial cells (Figure 5.6).

Figure 5.6 shows subsequent incubation of the co-culture for 18 h; this time frame was selected due to the observation that cytokine release can take up to 18 h, due to *de novo* synthesis of proteins (Mascher et al., 1999). In fact, *de novo* synthesis can take longer than this but due to potential drop in viability of the two cell types once in co-culture, 18 h was chosen as the optimal incubation period.

Importantly, isolated CD4<sup>+</sup> and CD8<sup>+</sup> T cells were activated in the culture medium of the lung epithelial targets they were subsequently to be co-cultured with, with the addition of IL-2 (see Chapter 2). Therefore the conditioned media subsequently added from activated T cells to iHBEC or NHBE cells was optimal for epithelial cells. This was decided due to the high sensitivity of epithelial cells to different types of culture medium and to FCS (contained in T cell medium). With these experimental

conditions, once in co-culture iHBEC and NHBE cells were then in the most optimal conditions to retain their viability.

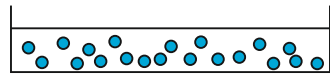
The aim of the co-culture was to investigate both inflammatory and apoptotic signalling. Therefore conditioned medium was collected for analysis of cytokine release. In addition, epithelial cells were collected for the profiling of cell surface expression of TRAIL-R1, -R2, CD95, CD95L and TRAIL. Epithelial cells were analysed for PS externalisation and assessed for cleavage of apoptotic markers by immunoblotting.

As outlined in Chapter 1, TRAIL can ligate to its cognate receptors in one of two forms; either as a soluble factor or membrane bound ligand. This difference is important since TRAIL-R2 signalling has been shown to occur more efficiently when presented with a membrane-bound form of TRAIL ligand.

Therefore, the decision was made to set up the co-culture in two orientations, the first being the addition of conditioned media (CM) from activated T cells to lung epithelial cells and the second being the addition of activated T cells in their conditioned media (C2C) to lung epithelial cells. This was deemed to be important to investigate the differences that may occur between cell-to-cell interactions versus soluble factor interactions, especially in the context of TRAIL/TRAIL-R signalling.

In order to dissect the role of TRAIL in the co-culture model, TRAIL and ILZ TRAIL were added exogenously in both orientations of the co-culture using both iHBEC and NHBE cells as the target lung epithelial cells.

### Conditioned Media Model



19 h Activated  
CD4<sup>+</sup> or CD8<sup>+</sup> T Cells

Addition of  
Filtered Conditioned  
Media from T Cells

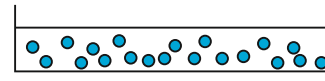


iHBEC or NHBE Cells  
Grown to Confluency



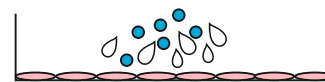
18 h at 37 °C

### Cell-to-Cell Model



19 h Activated  
CD4<sup>+</sup> or CD8<sup>+</sup> T Cells

Addition of  
T Cells in  
Conditioned Media



iHBEC or NHBE Cells  
Grown to Confluency



18 h at 37 °C

- Epithelial cells collected for PS externalisation analysis, immunoblotting analysis & surface expression profiling
- Conditioned media filtered & collected for cytokine analysis

**Figure 5.6** Work flow for the establishment of the conditioned media and cell-to-cell co-culture models of lung epithelial cells and primary T cells

### **5.2.2.2 Cell surface expression profile of iHBEC cells co-cultured with activated CD4<sup>+</sup> T cells**

iHBEC cells co-cultured with 19 h activated CD4<sup>+</sup> T cells in both CM and C2C orientations, either with or without 1 µg/ml TRAIL or ILZ TRAIL were profiled for their surface expression of TRAIL-R1, -R2, CD95, CD95L and TRAIL (Figure 5.7).

In the case of the CM co-culture model, iHBEC cells appeared to significantly upregulate their surface expression of TRAIL-R2 and CD95 compared to iHBEC cells not co-cultured (Figure 5.7a). The addition of either TRAIL or ILZ TRAIL to the CM co-culture model pointedly resulted in downregulated cell surface levels of TRAIL-R2 indicating either engagement of the TRAIL DISC and therefore internalisation of the receptor or indirect downregulation of the receptor. The levels of CD95 also appeared to be downregulated in the presence of TRAIL or ILZ TRAIL compared to the CM alone. In addition, TRAIL expression was upregulated in the CM co-culture compared to iHBEC cells cultured alone but downregulated following TRAIL treatment with TRAIL, indicating a change induced by the co-culture. TRAIL-R1 and CD95L levels did not change a great deal following incubation with CM +/- TRAIL or ILZ TRAIL.

iHBEC cells in the CD4<sup>+</sup> T cell C2C co-culture model were also analysed for their cell surface expression of the aforementioned death receptors and ligands (Figure 5.7b). iHBEC cells displayed the same pattern of TRAIL-R2 and CD95 up and downregulation. However, the level to which CD95 cell surface expression was upregulated in CD4<sup>+</sup> C2C alone was much greater when compared to CD4<sup>+</sup> CM alone. TRAIL levels were not apparently changed compared to iHBEC cells cultured alone.

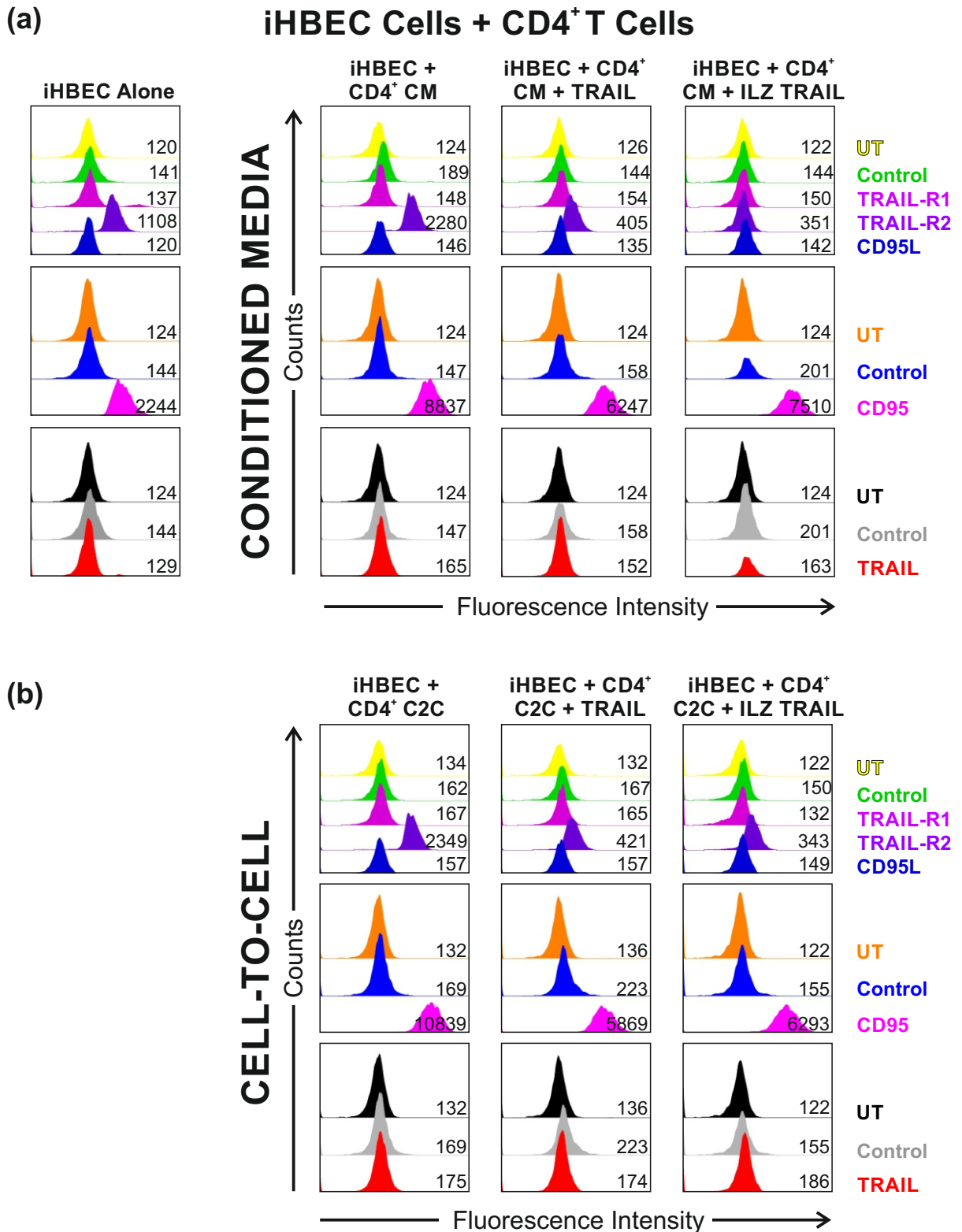


**Figure 5.7 Cell surface expression profile of iHBEC cells co-cultured with activated CD4<sup>+</sup> T cells** (a) iHBEC cells co-cultured with activated conditioned media from CD4<sup>+</sup> T cells +/- TRAIL/ILZ TRAIL and (b) iHBEC cells co-cultured with activated CD4<sup>+</sup> T cells (cell-to-cell) +/- ILZ TRAIL, were analysed for the cell surface expression of TRAIL-R1, TRAIL-R2, CD95, CD95L and TRAIL. Cells were incubated with either no antibody (UT), isotype control antibody (control), PE-conjugated TRAIL-R1, TRAIL-R2, FITC-conjugated TRAIL, PE-conjugated CD95L or CH11 with FITC-conjugated secondary antibodies. Following washing with PBS, cells were analysed by flow cytometry for changes in fluorescence intensity. Fluorescence intensity is represented by geometric mean (n=1). C2C represents cell-to-cell and CM represents conditioned media. Results shown are of a single experiment and therefore statistical analysis could not be performed.

### **5.2.2.3 Cell surface expression profile of iHBEC cells co-cultured with activated CD8<sup>+</sup> T cells**

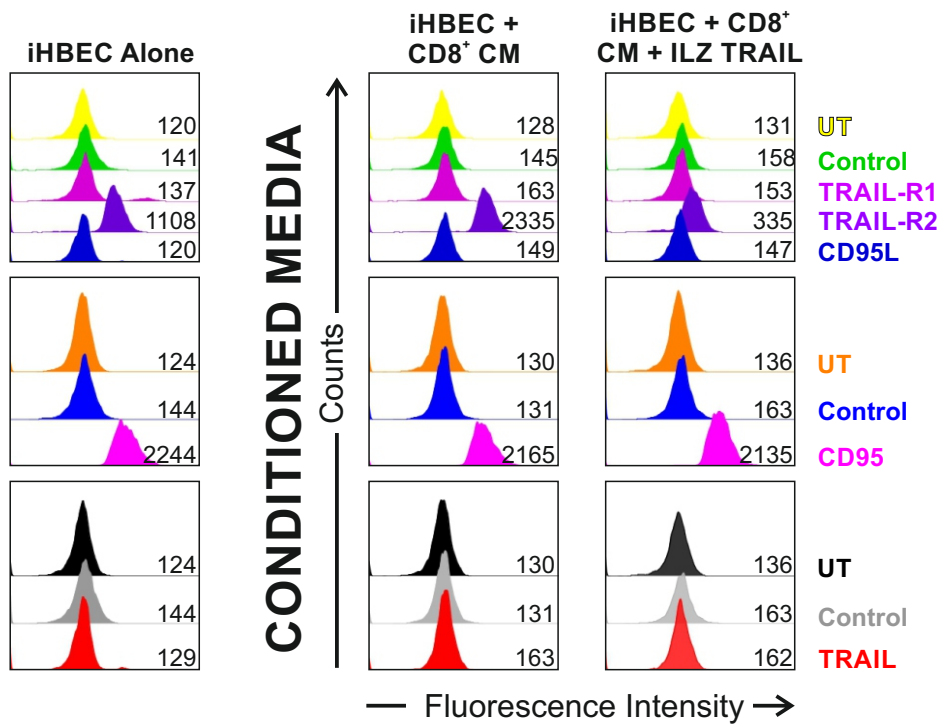
The cell surface expression of iHBEC cells co-cultured with activated CD8<sup>+</sup> T cell CM or using C2C, was measured following incubation at 37 °C for 18 h (Figure 5.8).

In the first instance, iHBEC cells co-cultured with CD8<sup>+</sup> CM, +/- ILZ TRAIL, were measured for their cell surface levels of TRAIL-R1, TRAIL-R2, CD95, CD95L and TRAIL (Figure 5.8a). Neither TRAIL-R1 nor CD95L were expressed on the surface of iHBEC cells and remained absent on iHBEC cells in CM co-culture, with or without ILZ TRAIL. However, cell surface expression of TRAIL-R2 increased in iHBEC cells in CM co-culture. The addition of ILZ TRAIL caused a decrease in the cell surface expression of TRAIL-R2 observed in the presence of CM alone and this may be due to the formation of the TRAIL DISC and subsequent internalisation of the receptor. TRAIL expression was also increased in CM alone but not CM treated with ILZ TRAIL compared to iHBEC cells cultured alone. Surface CD95 levels remained unchanged across all treatments.

iHBEC cells co-cultured with CD8<sup>+</sup> C2C +/- ILZ TRAIL were also analysed for their surface expression of receptors and ligands (Figure 5.8b). These cells displayed the same pattern of surface expression as iHBEC cells co-cultured with CD8<sup>+</sup> CM.

(a)

### iHBEC Cells + CD8<sup>+</sup> T Cells



(b)

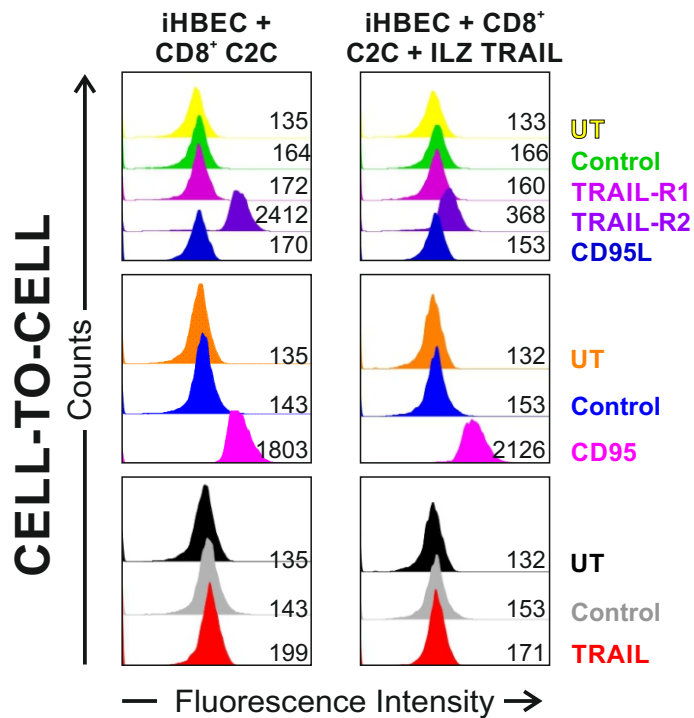


**Figure 5.8 Cell surface expression profile of iHBEC cells co-cultured with activated CD8<sup>+</sup> T cells** (a) iHBEC cells co-cultured with activated conditioned media from CD8<sup>+</sup> T cells +/- TRAIL/ILZ TRAIL and (b) iHBEC cells co-cultured with activated CD8<sup>+</sup> T cells (cell-to-cell) +/- ILZ TRAIL, were analysed for the cell surface expression of TRAIL-R1, TRAIL-R2, CD95, CD95L and TRAIL. Cells were incubated with either no antibody (UT), isotype control antibody (control), PE-conjugated TRAIL-R1, TRAIL-R2, FITC-conjugated TRAIL, PE-conjugated CD95L or CH11 with FITC-conjugated secondary antibodies. Following washing with PBS, cells were analysed by flow cytometry for changes in fluorescence intensity. Fluorescence intensity is represented by geometric mean (n=1). C2C represents cell-to-cell and CM represents conditioned media.

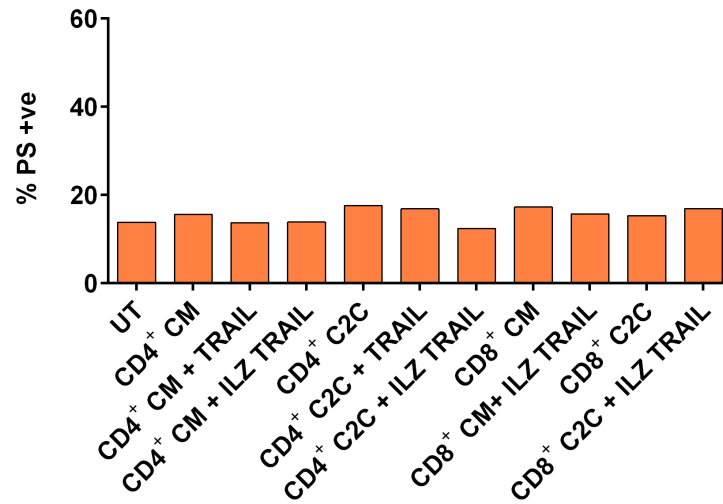
#### **5.2.2.4 iHBEC cells co-cultured with activated CD4<sup>+</sup> or CD8<sup>+</sup> T cells do not die by apoptosis but do display cleavage of caspase 8 and caspase 3**

iHBEC cells co-cultured in both CM and C2C orientations, with either activated CD4<sup>+</sup> or CD8<sup>+</sup> T cells, were analysed for their levels of apoptosis (Figure 5.9).

Firstly, co-cultured iHBEC cells were analysed for PS externalisation which showed negative staining for annexin-V-FITC/PI across all treatments compared to untreated iHBEC cells (Figure 5.9a).

Secondly, cell pellets of co-cultured iHBEC cells were immunoblotted for the following apoptotic markers; caspase 8, caspase 9, caspase 3 and PARP. In the absence of TRAIL and ILZ TRAIL, iHBEC cells co-cultured with either CM from CD4<sup>+</sup> or CD8<sup>+</sup> T cells or C2C exhibited no cleavage of caspase 8 and therefore downstream cleaved caspase 9, caspase 3 or PARP was not observed. In contrast, cleavage of procaspase 8 was evident in the presence of either TRAIL or ILZ TRAIL, regardless of the orientation of the co-culture (lanes 3, 4, 6, 7, 9 and 11). Caspase 3, but not caspase 9, was processed to p20. Consistent with this and the PS externalisation data in Figure 5.9a, PARP was not cleaved. In iHBEC cells from CD4<sup>+</sup> CM or C2C co-cultures, ILZ TRAIL caused increased processing of caspase 8 and caspase 3 compared to TRAIL. These data are consistent with the TRAIL/TRAIL-R signalling characteristics of the untreated iHBEC cells previously documented in Chapter 4.

(a) **iHBEC Cells + CD4<sup>+</sup> or CD8<sup>+</sup> T Cells**



(b)

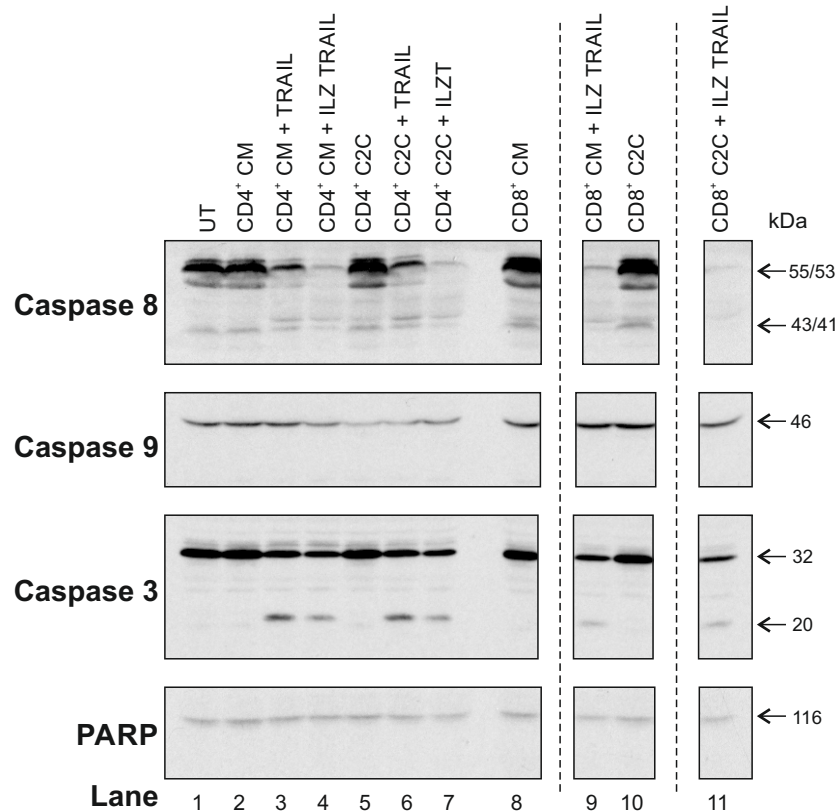


**Figure 5.9 iHBEC cells co-cultured with activated CD4<sup>+</sup> or CD8<sup>+</sup> T cells do not die by apoptosis but do display cleavage of caspase 8 and caspase 3** (a) iHBEC cells co-cultured with conditioned media from CD4<sup>+</sup> or CD8<sup>+</sup> T cells or co-cultured with CD4<sup>+</sup> or CD8<sup>+</sup> T cells (cell-to-cell) +/- 1 µg/ml TRAIL/ILZ TRAIL were analysed for PS externalisation by flow cytometry. (n=1) (b) Cell pellets were analysed for the cleavage of caspase 8, caspase 9, caspase 3 and PARP by immunoblotting (n=1). The dashed line indicates removal of unnecessary lanes.

### **5.2.2.5 Profiling of cytokines released from CD4<sup>+</sup>, CD8<sup>+</sup> T cells and iHBEC cells cultured alone or following ILZ TRAIL treatment**

In order to identify whether any changes in cytokines in the co-culture models were due to the cells alone releasing cytokines or due to the effect of co-culturing two cell types together; iHBEC cells, activated CD4<sup>+</sup> and CD8<sup>+</sup> T cells, in the absence or presence of ILZ TRAIL were analysed for cytokines released following 18 h incubation at 37 °C (Figure 5.10).

Measurement of cytokines was carried out by addition of conditioned media to protein profiler arrays (see Chapter 2). These arrays detect cytokines *via* antibody-based interactions, thus the results obtained are not quantitative, and only provide an indication of the presence or absence and/or a general increase or decrease of a particular cytokine. The arrays are supplied spotted with high and low reference antibodies along with the antibodies for each cytokine. The quantification of the spots was carried out on membranes where the exposure gave rise to a full but not overexposed high reference intensity. Of the 102 cytokines analysed, the ones included in the graphs shown in Figure 5.10 were cytokines whose intensity was no lower intensity than the low reference spots (600 arbitrary units of luminescence).

iHBEC cells incubated with or without ILZ TRAIL displayed a very similar pattern of cytokines. Angiogenin, insulin-like growth factor binding protein 2 (IGFBP-2), macrophage migration inhibitory factor (MIF), platelet-derived growth factor AA (PDGF-AA) and serpin E1 were all present in CM from these cells.

Both activated CD4<sup>+</sup> and CD8<sup>+</sup> T cells treated with or without ILZ TRAIL displayed a similar pattern of cytokines. The arrays showed the presence of EGF and IL-2, both of which were used to supplement the media (see Chapter 2) and were therefore not cytokines released by the T cells. Granulocyte macrophage colony-stimulating factor (GM-CSF) and MIF were also present in both T cell types. In contrast, osteopontin was present in CD8<sup>+</sup>, but not CD4<sup>+</sup> T cells and fibroblast growth factor 19 (FGF-19) was present in CD4<sup>+</sup>, but not CD8<sup>+</sup> T cells. Interestingly, osteopontin was the only cytokine that appeared to be significantly changed

following ILZ TRAIL in which case it appeared to be downregulated in CD8<sup>+</sup> T cells treated with ILZ TRAIL.

Overall, these findings demonstrate that only a few cytokines are released when iHBEC or T cells are cultured under basal conditions either alone or in the presence of ILZ TRAIL.

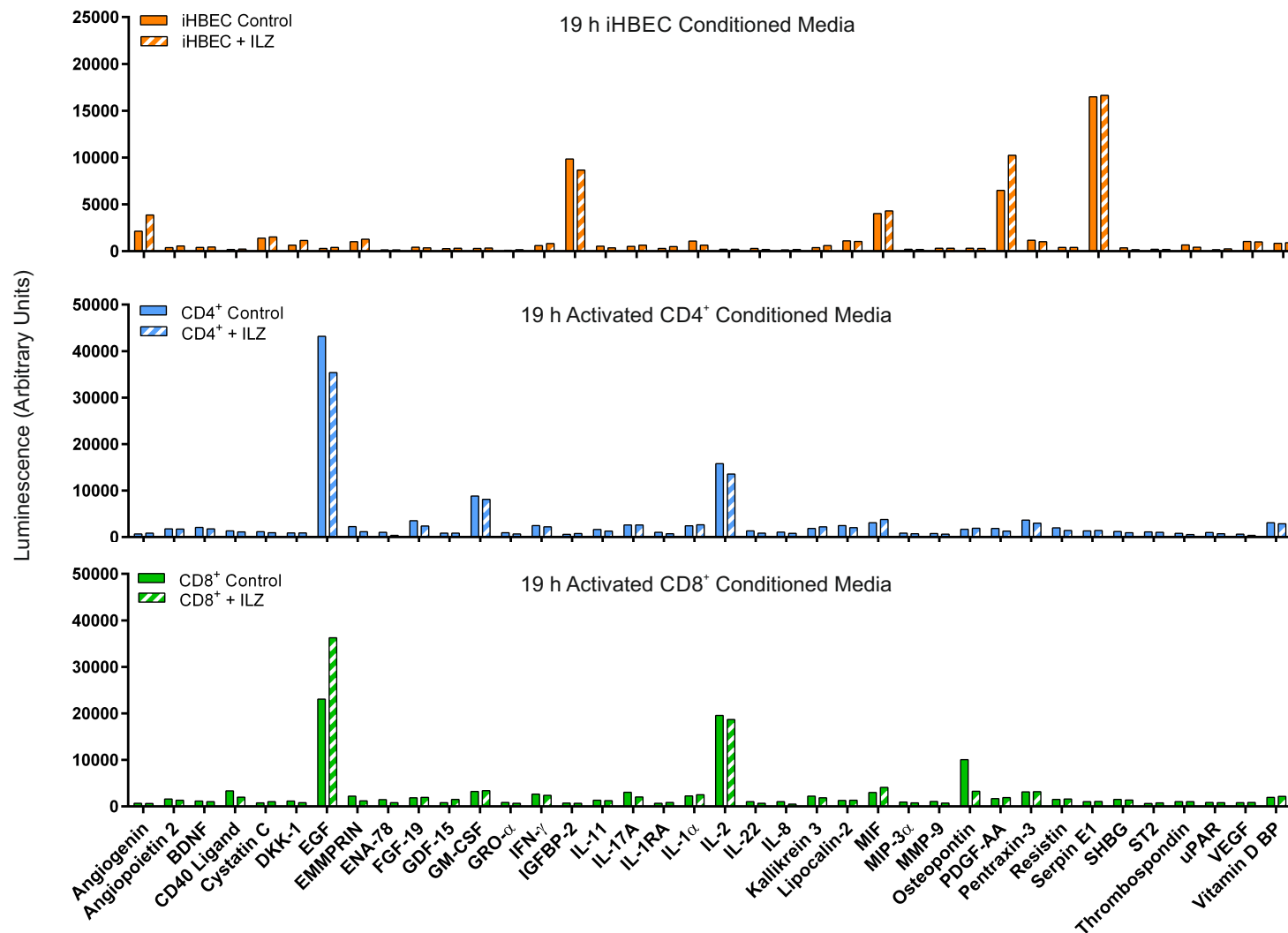


**Figure 5.10 Profiling cytokines released by CD4<sup>+</sup>, CD8<sup>+</sup> T cells and iHBEC cells cultured alone or following ILZ TRAIL treatment** Conditioned media from CD4<sup>+</sup> and CD8<sup>+</sup> T cells activated for 19 h and iHBEC cells +/- 1  $\mu$ g/ml ILZ TRAIL were analysed for the presence of various cytokines by protein profiler arrays as outlined in Chapter 2 (n=1).

### **5.2.2.6 Profiling the cytokines released by iHBEC cells co-cultured with conditioned media from CD4<sup>+</sup> or CD8<sup>+</sup> T cells or iHBEC cells co-cultured cell-to-cell with CD4<sup>+</sup> or CD8<sup>+</sup> T cells, both in the absence or presence of ILZ TRAIL**

Following the characterisation of cytokines released under control conditions, conditioned media from iHBEC cells co-cultured with either activated CD4<sup>+</sup> or CD8<sup>+</sup> T cells was profiled to determine the cytokines released (Figure 5.11).

Figure 5.11a shows the cytokine profile obtained when iHBEC cells were co-cultured either with activated CD4<sup>+</sup> CM or CD4<sup>+</sup> C2C. When compared to iHBEC cells not co-cultured, the pattern of cytokine release between the two co-culture orientations were very similar with both showing the presence of angiogenin, cystatin C, extracellular matrix metalloproteinase inducer (EMMPRIN), FGF-19, IGFBP-2, interleukin-1 receptor antagonist (IL-1RA), IL-2, MIF, matrix metalloproteinase 9 (MMP9), PDGF-AA and serpin E1.

Reminiscent of the data shown in Figure 5.10, IL-2 detection was due to the addition of this interleukin to the culture media as a supplement for T cell proliferation. Interestingly, EMMPRIN, IL-1RA and MMP-9 were the only cytokines to display a marked increase when ILZ TRAIL was added to either CM or C2C co-cultures. In addition, PDGF-AA was the only cytokine to show a decrease level in the co-culture (with or without TRAIL or ILZ TRAIL) compared to iHBEC cells not co-cultured.

Conditioned media from iHBEC cells co-cultured with CD8<sup>+</sup> CM or C2C co-cultures, +/- ILZ TRAIL were analysed for the presence of cytokines (Figure 5.11b). Conditioned media from CD8<sup>+</sup> co-cultures generally appeared to contain fewer cytokines than CD4<sup>+</sup> co-cultures (Figure 5.11a). However, a similar pattern of cytokines was observed for the two orientations of co-culture, which again was analogous to the CD4<sup>+</sup> co-cultures in Figure 5.11a. The cytokines that were detected more highly in the co-culture compared to iHBEC cells not co-cultured were; cystatin C, IGFBP-2, IL-2, MIF, PDGF-AA and serpin E1. Once again, PDGF-AA was the only cytokine to display an obvious decrease in co-culture when compared with iHBEC cells not co-cultured.

In terms of cytokine release, taken together these data indicate very little difference between co-cultures of CD4<sup>+</sup> and CD8<sup>+</sup> T cell with iHBEC cells. Moreover, the addition of TRAIL or ILZ TRAIL to these co-cultures did not induce a significant change in the profile of cytokines released into the media but did show an increase in those cytokines already secreted during the co-culture itself, namely EMMPRIN, IL-1RA, MIF and MMP-9.

(a)

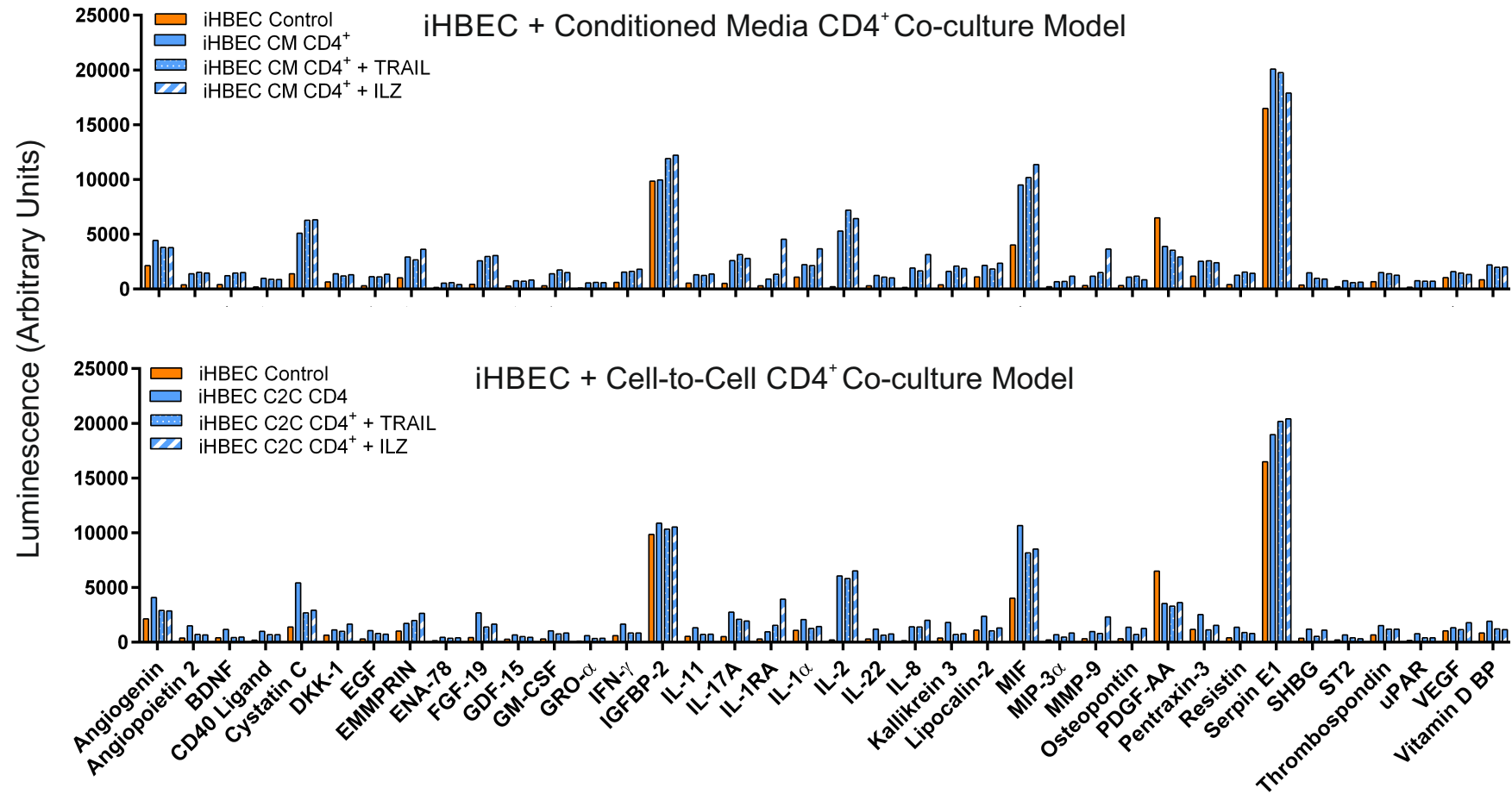


**Figure 5.11 Profiling of cytokines released by iHBEC cells co-cultured with conditioned media from CD4<sup>+</sup> or CD8<sup>+</sup> T cells or iHBEC cells co-cultured cell-to-cell with CD4<sup>+</sup> or CD8<sup>+</sup> T cells both in the absence or presence of ILZ TRAIL** (a) Conditioned media from CD4<sup>+</sup> T cells activated for 19 h, +/- 1  $\mu$ g/ml ILZ TRAIL incubated with iHBEC cells for 18 h at 37  $^{\circ}$ C was analysed for the presence of various cytokines by protein profiler arrays as outlined in Chapter 2 (n=1).

(b)

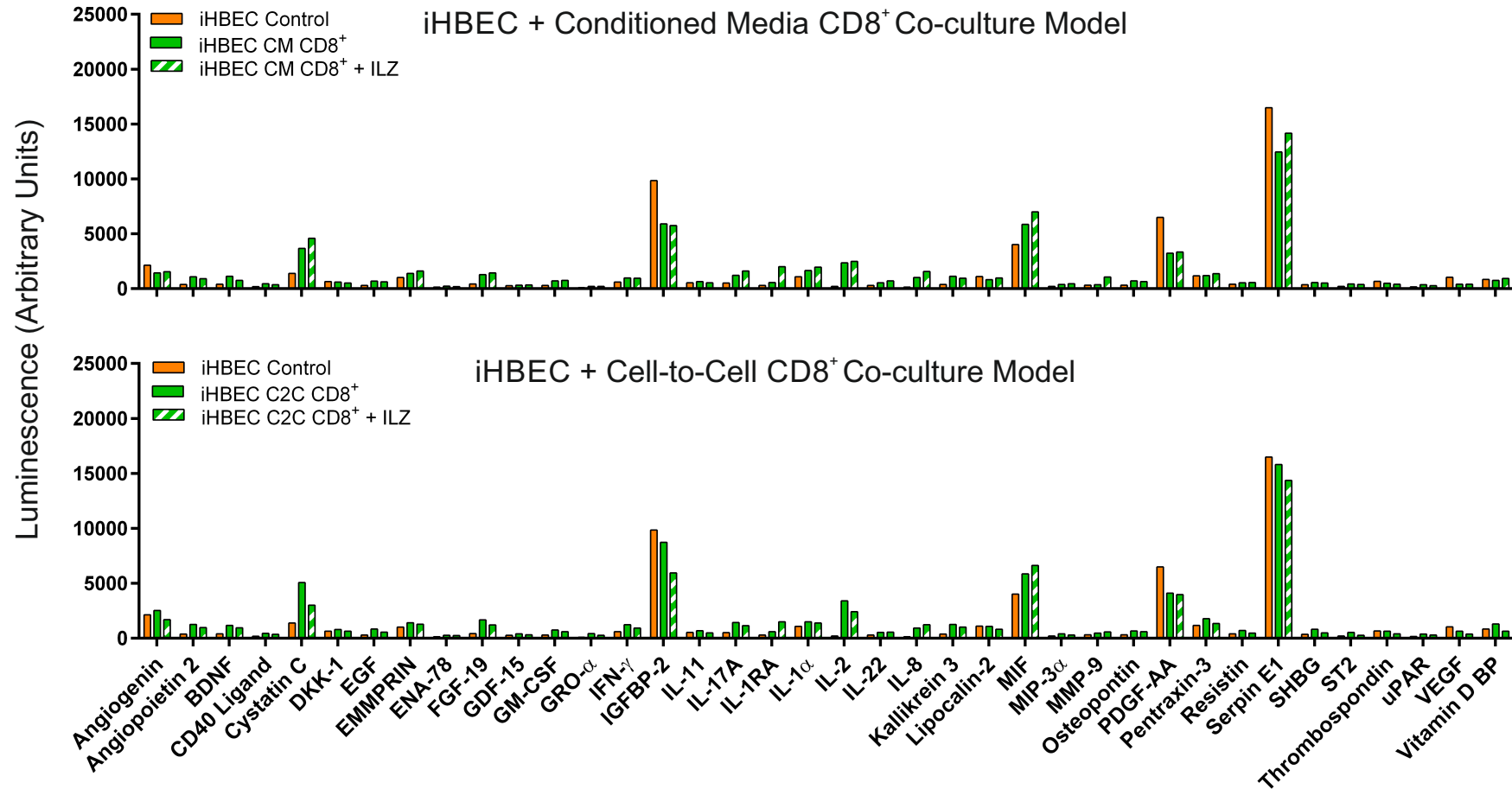


**Figure 5.11 Profiling of cytokines released by iHBEC cells co-cultured with conditioned media from CD4<sup>+</sup> or CD8<sup>+</sup> T cells or iHBEC cells co-cultured cell-to-cell with CD4<sup>+</sup> or CD8<sup>+</sup> T cells both in the absence or presence of ILZ TRAIL (b) Conditioned media from CD8<sup>+</sup> T cells activated for 19 h, +/- 1  $\mu$ g/ml ILZ TRAIL incubated with iHBEC cells for 18 h at 37 °C was analysed for the presence of various cytokines by protein profiler arrays as outlined in Chapter 2 (n=1).**

### **5.2.2.7 Cell surface expression profile of NHBE cells co-cultured with activated CD4<sup>+</sup> T cells**

Having shown the results of co-culturing activated CD4<sup>+</sup> and CD8<sup>+</sup> T cells individually on iHBEC cells, experiments were repeated with NHBE cells instead of iHBEC cells. NHBE cells co-cultured with 19 h activated CD4<sup>+</sup> T cells in both CM and C2C orientations with or without 1 µg/ml TRAIL or ILZ TRAIL were profiled for their surface expression of TRAIL-R1, -R2, CD95, CD95L and TRAIL (Figure 5.12).

NHBE cells co-cultured with CD4<sup>+</sup> CM displayed a decrease in their cell surface expression of TRAIL-R1 but an increase in the expression of CD95 when compared to untreated NHBE cells (Figure 5.12a). TRAIL-R2, CD95L and TRAIL levels remained unchanged. The inclusion of TRAIL in the co-culture resulted in a slight decrease in cell surface expression of TRAIL-R1 but a greater decrease in cell surface expression of TRAIL-R2. The presence of ILZ TRAIL caused the same decrease in TRAIL-R1/-R2 as TRAIL but to a greater extent.

NHBE cells co-cultured with CD4<sup>+</sup> T cells C2C were also profiled for their cell surface receptor and ligand expression (Figure 5.12b). The same pattern of changes induced by the co-culture itself and then in the presence of either TRAIL or ILZ TRAIL as seen with CD4<sup>+</sup> CM co-cultured cells (Figure 5.12a) was observed with CD4<sup>+</sup> C2C co-cultured NHBE cells (Figure 5.12b).

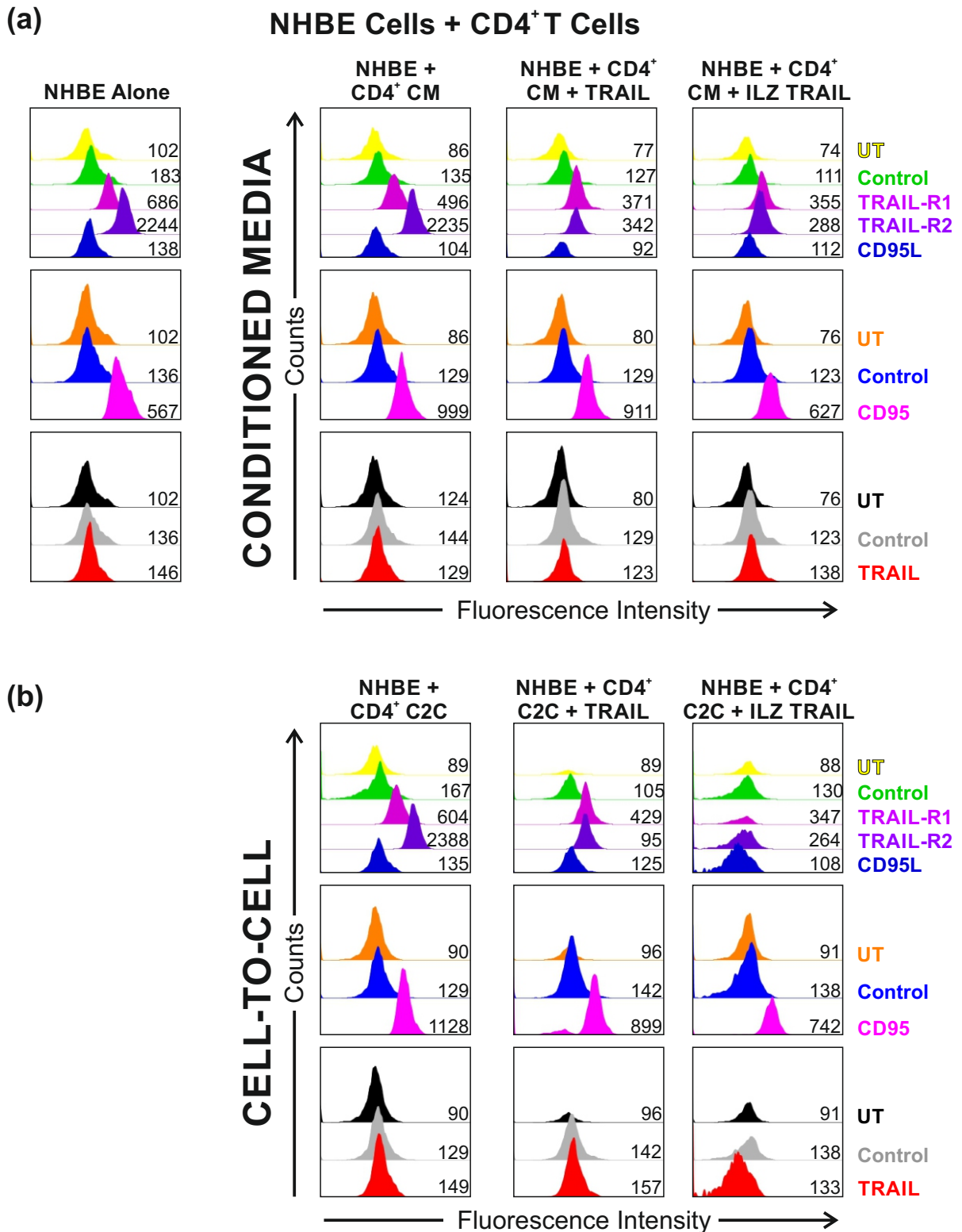


**Figure 5.12 Cell surface expression profile of NHBE cells co-cultured with activated CD4<sup>+</sup> T cells** (a) NHBE cells co-cultured with activated conditioned media from CD4<sup>+</sup> T cells +/- TRAIL/ILZ TRAIL and (b) NHBE cells co-cultured with activated CD4<sup>+</sup> T cells (cell-to-cell) +/- ILZ TRAIL, were analysed for the cell surface expression of TRAIL-R1, TRAIL-R2, CD95, CD95L and TRAIL. Cells were incubated with either no antibody (UT), isotype control antibody (control), PE-conjugated TRAIL-R1, TRAIL-R2, FITC-conjugated TRAIL, PE-conjugated CD95L or CH11 with FITC-conjugated secondary antibodies. Following washing with PBS, cells were analysed by flow cytometry for changes in fluorescence intensity. Fluorescence intensity is represented by geometric mean (n=1). C2C represents cell-to-cell and CM represents conditioned media.

#### **5.2.2.8 The addition of TRAIL or ILZ TRAIL to NHBE cells co-cultured with activated CD4<sup>+</sup> T cells resulted in apoptosis of NHBE cells**

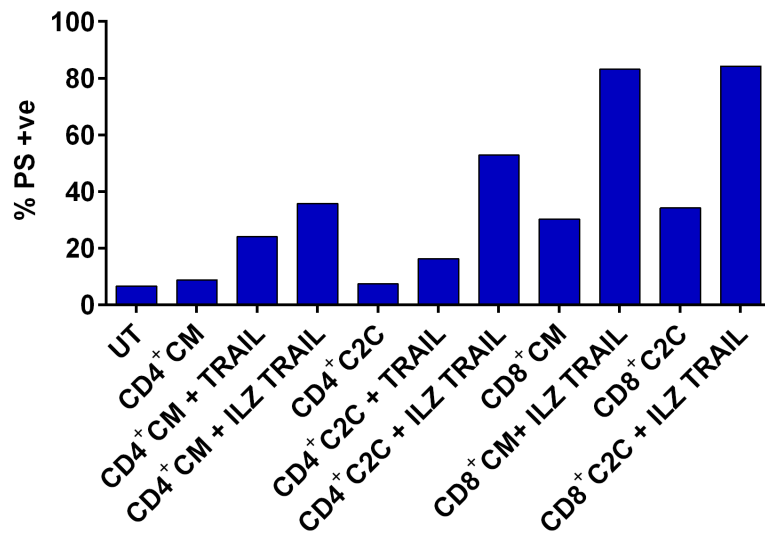
The NHBE cells from both activated CD4<sup>+</sup> and CD8<sup>+</sup> T cell co-cultures, in both orientations, were analysed for their levels of apoptosis (Figure 5.13).

Firstly, the NHBE cells from each of the co-culture conditions were analysed for PS externalisation (Figure 5.13a). NHBE cells co-cultured with either activated CD4<sup>+</sup> T cell CM or activated CD4<sup>+</sup> T cell C2C did not display increases levels of apoptosis compared with untreated NHBE cells. However, the addition of TRAIL in either of these co-cultures caused an increase in annexin-V-FITC/PI staining with the addition of ILZ TRAIL resulting in an even greater increase in PS externalisation.

NHBE cells co-cultured with activated CD8<sup>+</sup> T cell CM or C2C again showed an increase in PS externalisation compared with untreated NHBE cells. The addition of ILZ TRAIL caused a sharp increase in the proportion of positive annexin-V-FITC/PI cells observed, to around 80 % apoptosis. Therefore the surface expression data from Figure 5.13a and b should be interpreted with caution since only a small portion of NHBE cells were viable for the measurement of death receptors and ligands. Thus, cellular surface expression data is not shown and was not interpreted.

(a)

### NHBE Cells + CD4<sup>+</sup> or CD8<sup>+</sup> T Cells



(b)

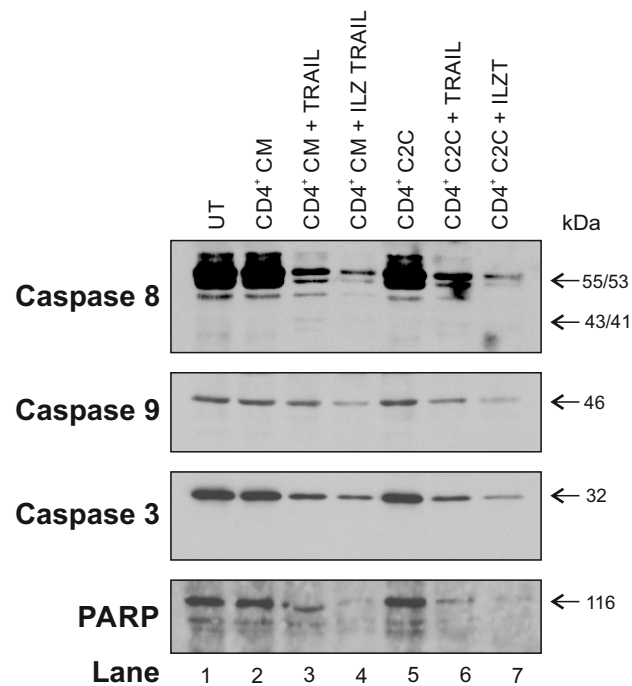


**Figure 5.13** The addition of TRAIL or ILZ TRAIL to NHBE cells co-cultured with activated CD4<sup>+</sup> T cells results in apoptosis of NHBE cells (a) NHBE cells co-cultured with conditioned media from CD4<sup>+</sup> or CD8<sup>+</sup> T cells or co-cultured with CD4<sup>+</sup> or CD8<sup>+</sup> T cells (cell-to-cell) +/- 1 µg/ml TRAIL/ILZ TRAIL were analysed for PS externalisation by flow cytometry (n=1). (b) Cell pellets were analysed for the cleavage of caspase 8, caspase 9, caspase 3 and PARP by immunoblotting. (n=1)

### **5.2.2.9 Profiling cytokines released by CD4<sup>+</sup>, CD8<sup>+</sup> T cells and NHBE cells cultured alone or following ILZ TRAIL treatment**

In order to identify whether any changes in the cytokines released in the co-culture models were due to the cells alone or due to the effect of the co-culture, NHBE cells were analysed for those cytokines released following 18 h incubation at 37 °C (Figure 5.14).

Untreated NHBE cells released the following cytokines; extracellular matrix metalloproteinase inducer (EMMPRIN), melanoma growth stimulating activity alpha (GRO- $\alpha$ ), interleukin-1 receptor antagonist (IL-1RA), IL-1 $\alpha$ , IL-8, lipocalin-2, MIF, macrophage inflammatory protein-3 alpha (MIP-3 $\alpha$ ) and serpin E1. The addition of ILZ TRAIL to NHBE cells caused a decrease in all but the following cytokines, EMMPRIN, IL-1RA and IL-1 $\alpha$ , all of which increased. EGF was added as a supplement to the media and is therefore the reason this was detected in the media of the NHBE cells. These results suggest that ILZ TRAIL treatment of NHBE did not induce many changes in terms of those cytokines that were released.

The CM of activated CD4<sup>+</sup> and CD8<sup>+</sup> T cells incubated with or without ILZ TRAIL had already been analysed for their cytokine profile in Figure 5.10 and these results were included in this figure to serve as a comparison and to identify any the changes in those cytokine released by NHBE cells. The only similarity between the T cell and NHBE cell cytokine profile was the release of MIF, which was also detected in iHBEC cells, in both untreated and in cells in co-culture with activated T cells.

Overall there were not very many changes induced by the addition of ILZ TRAIL to either NHBE or activated T cells and the profile of cytokines that were released were very different between the two cell types.

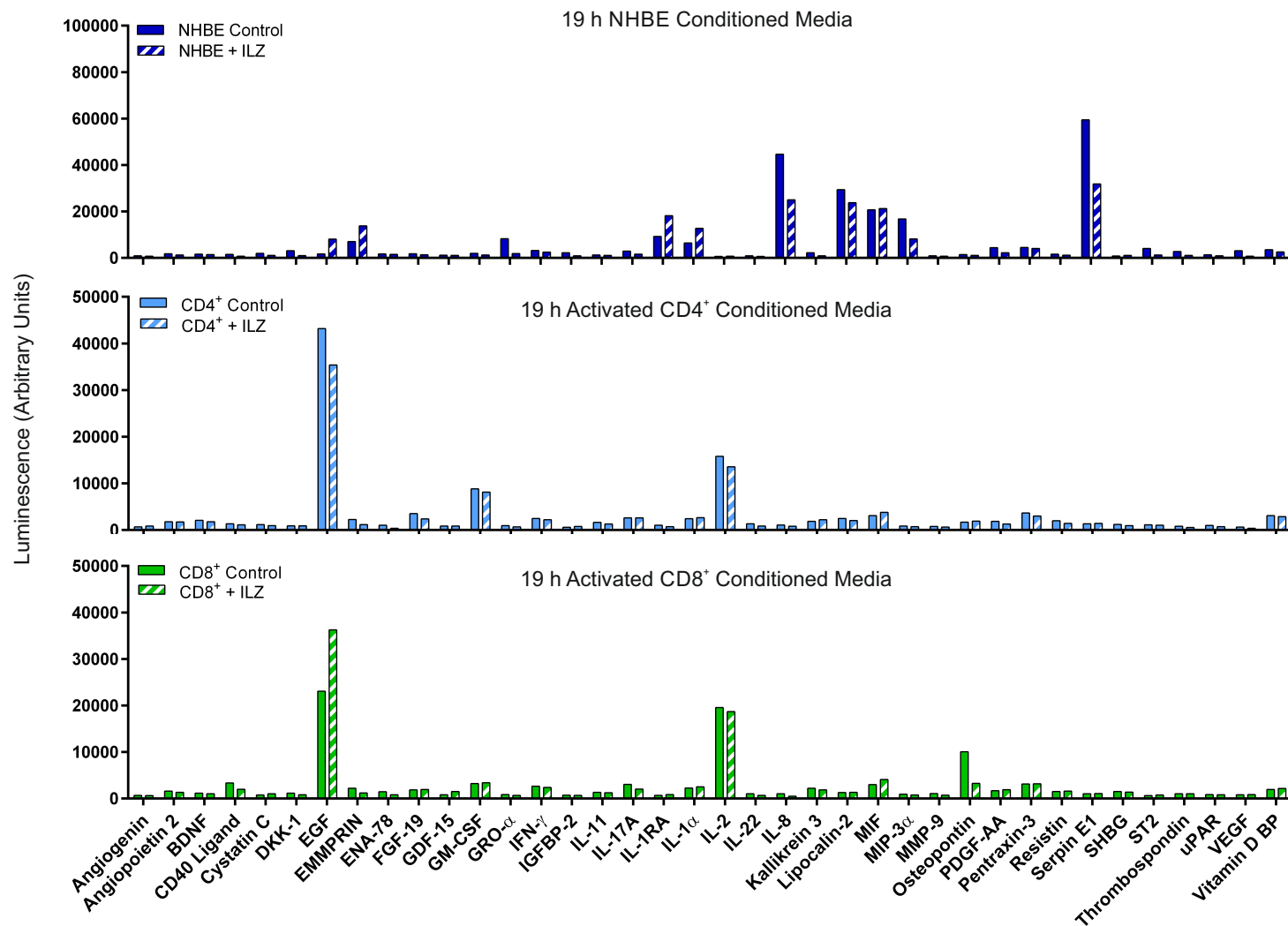


**Figure 5.14 Profiling cytokines released by CD4<sup>+</sup>, CD8<sup>+</sup> T cells and NHBE cells cultured alone or following ILZ TRAIL treatment** Conditioned media from CD4<sup>+</sup> and CD8<sup>+</sup> T cells activated for 19 h and NHBE cells +/- 1  $\mu$ g/ml ILZ TRAIL were analysed for the presence of various cytokines by protein profiler arrays as outlined in Chapter 2 (n=1).

#### **5.2.2.10 Profiling cytokines released by NHBE cells co-cultured with conditioned media from CD4<sup>+</sup> or CD8<sup>+</sup> T cells of NHBE cells co-cultured cell-to-cell with CD4<sup>+</sup> or CD8<sup>+</sup> T cells, both in the absence or presence of ILZ TRAIL**

Following characterisation of the cytokines released under control conditions, conditioned media from NHBE cells co-cultured with either activated CD4<sup>+</sup> or CD8<sup>+</sup> T cells were profiled to determine the cytokines released (Figure 5.15).

Media from NHBE cells co-cultured with activated CD4<sup>+</sup> T cells either with CM or C2C were analysed for cytokine content (Figure 5.15a). The CD4<sup>+</sup> CM and C2C co-culture orientations induced a very similar pattern of detected cytokines. Compared to untreated NHBE cells, the two orientations of co-culture induced or increased the release of a number of cytokines; angiogenin, cystatin C, dickkopf WNT signalling pathway inhibitor 1 (DKK-1), EMMPRIN, FGF-19, GDF-15, GRO- $\alpha$ , IGFBP-2, IL-1RA, IL-8, lipocalin-2, MIF, PDGF-AA, serpin E1, suppression of tumourigenicity 2 (ST2), thrombospondin and urokinase receptor (uPAR). The addition of TRAIL or ILZ TRAIL to either co-culture induced an increase in the above stated cytokines, except for the following cytokines; IGFBP-2, serpin E1, ST2 and VEGF, all of which decreased compared to the CM or C2C co-cultures. However, a reduction in DKK-1, GRO- $\alpha$ , IL-8 and lipocalin-2 was observed following the addition of TRAIL or ILZ TRAIL in the C2C, but not CM, co-culture model.

Furthermore, media from NHBE cells co-cultured with activated CD8<sup>+</sup> T cells either as CM or C2C were analysed for cytokine content (Figure 5.15b). Once again, a similar pattern was observed between CD8<sup>+</sup> CM and C2C co-cultures although to a lower degree in C2C co-cultures – see luminescence scale. All of the cytokines that displayed an increase, compared to NHBE cells alone, also increased in co-cultures containing CD4<sup>+</sup> T cells (Figure 5.15a). These cytokines were, DKK-1, EMMPRIN, ENA-78, FGF-19, GDF-15, GRO- $\alpha$ , IL-17A, IL-1RA, IL-1 $\alpha$ , IL-8, lipocalin-2, MIF, MMP-3 $\alpha$ , PDGF-AA and serpin E1. Of the cytokines that increased following the co-culture itself, only IL-1RA, IL-1 $\alpha$ , IL-8, MIF, MIP-3 $\alpha$  and serpin E1 increased following either TRAIL or ILZ TRAIL treatment. The remaining cytokines that

increased in the co-culture showed a decrease upon treatment with TRAIL or ILZ TRAIL.

Overall, it is important to acknowledge the similarities in the cytokine profiles between CM and C2C co-cultures, for either activated CD4<sup>+</sup> or CD8<sup>+</sup> T cells. In addition, the general trend for NHBE cells co-cultured with CD4<sup>+</sup> CM or C2C showed that the addition of TRAIL or ILZ TRAIL caused an increase in the same cytokines already present due to the co-culture alone. In contrast, the media from NHBE cells co-cultured with activated CD8<sup>+</sup> CM or C2C showed that addition of TRAIL or ILZ TRAIL caused a decrease in the same cytokines observed due to the co-culture alone. This could be attributed to the loss in cell number due to the apoptosis observed in the co-culture (Figure 5.13) or as a direct result of exposure to TRAIL or ILZ TRAIL.

(a)

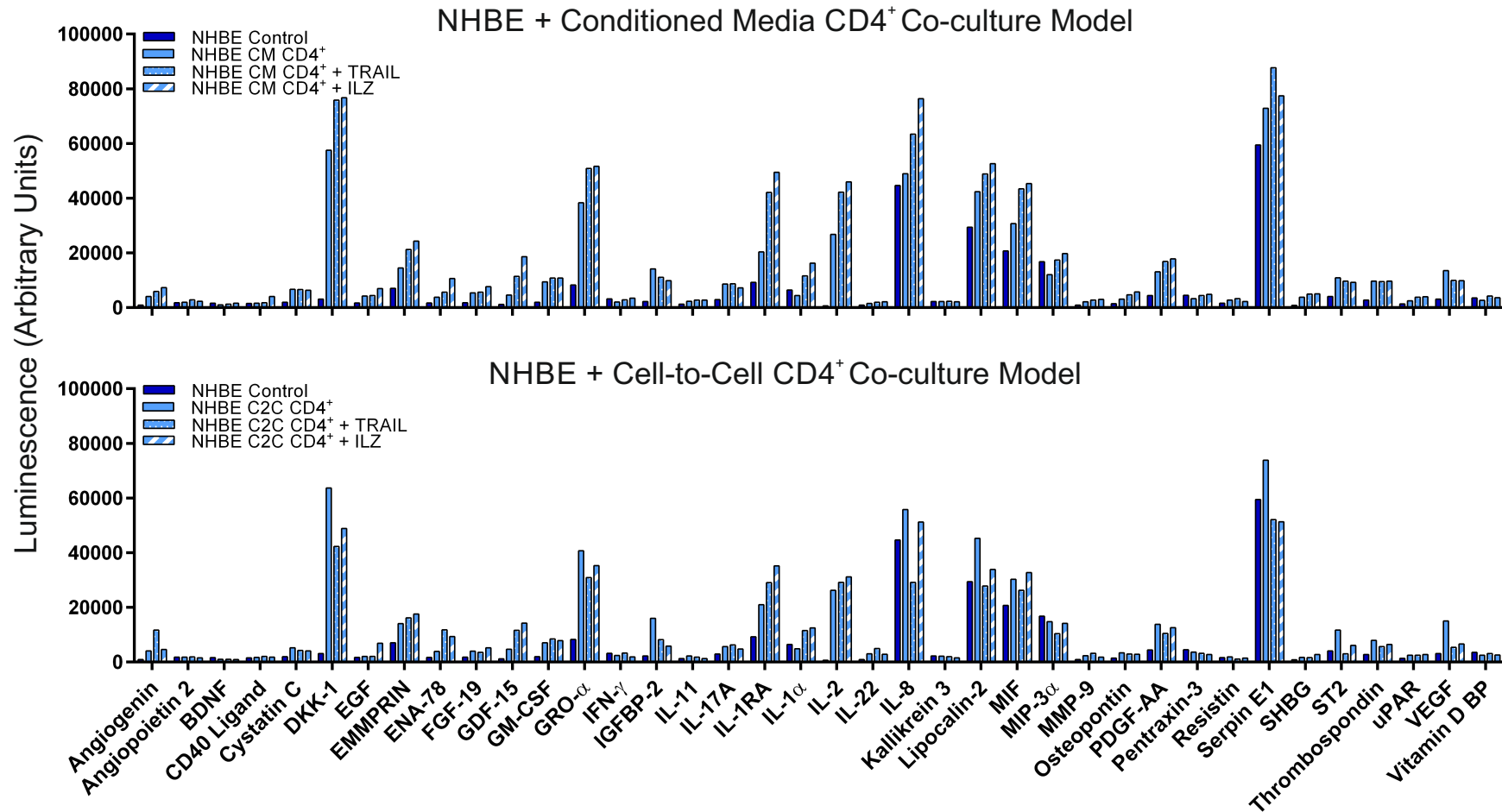


**Figure 5.15 Profiling the cytokine release of NHBE cells co-cultured with conditioned media from CD4<sup>+</sup> or CD8<sup>+</sup> T cells or NHBE cells co-cultured cell-to-cell with CD4<sup>+</sup> or CD8<sup>+</sup> T cells both in the presence and absence of ILZ TRAIL** (a) Conditioned media from CD4<sup>+</sup> T cells activated for 19 h, +/- 1  $\mu$ g/ml ILZ TRAIL incubated with NHBE cells for 18 h at 37  $^{\circ}$ C was analysed for the presence of various cytokines by protein profiler arrays as outlined in Chapter 2 (n=1).

(b)

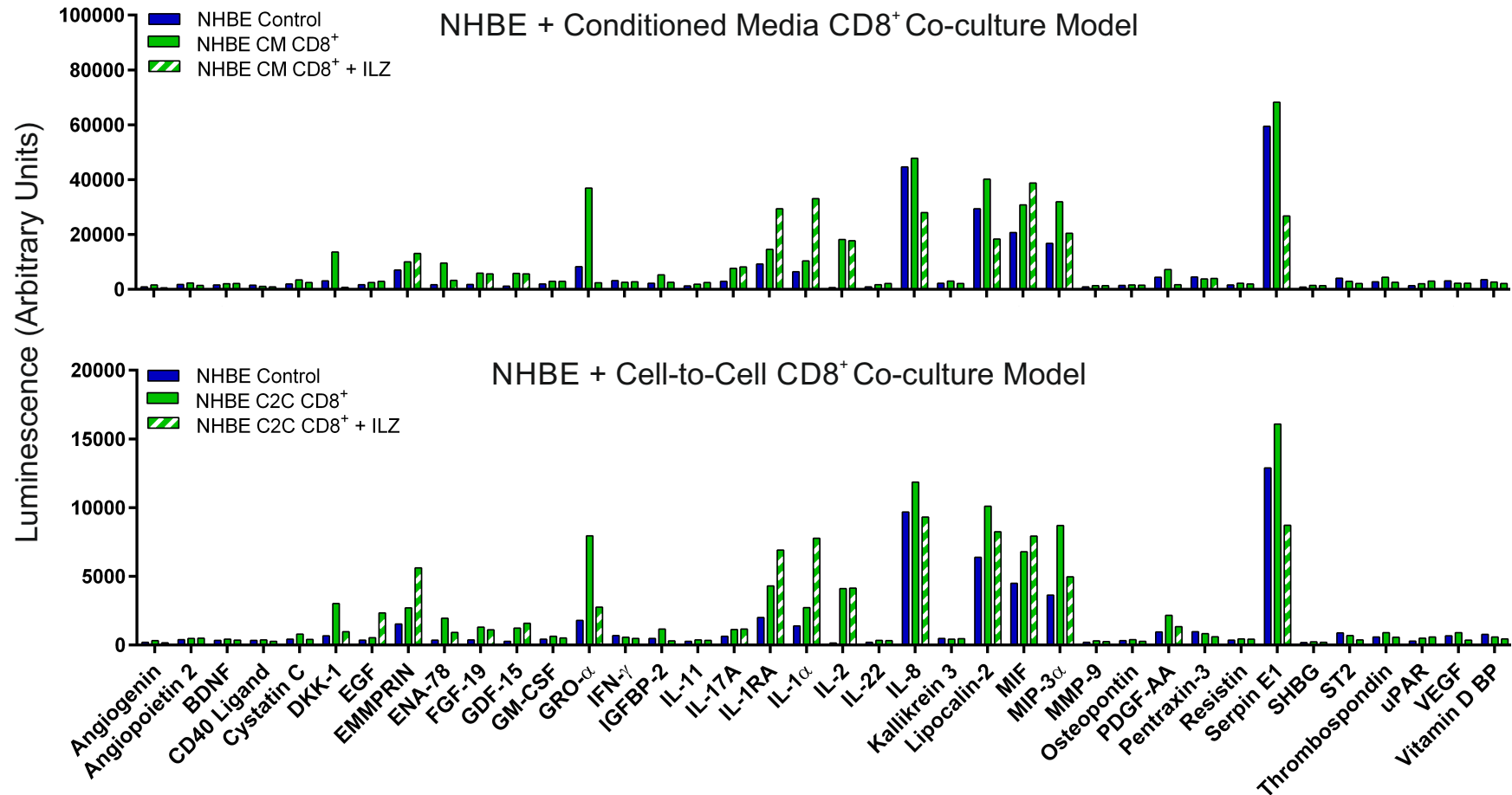


**Figure 5.15 Profiling the cytokine release of NHBE cells co-cultured with conditioned media from CD4<sup>+</sup> or CD8<sup>+</sup> T cells or NHBE cells co-cultured cell-to-cell with CD4<sup>+</sup> or CD8<sup>+</sup> T cells both in the presence and absence of ILZ TRAIL** (b) Conditioned media from CD8<sup>+</sup> T cells activated for 19 h, +/- 1  $\mu$ g/ml ILZ TRAIL incubated with NHBE cells for 18 h at 37 °C was analysed for the presence of various cytokines by protein profiler arrays as outlined in Chapter 2 (n=1).

### 5.2.2.11 Cell surface expression profile of differentiated NHBE cells

As described in Chapter 1, the lung epithelium *in vivo* consists of three main cell types, basal cells, ciliated cells and goblet cells. The tissue is a monolayer but appears to consist of many layers and therefore is referred to as being pseudostratified-like. Although time consuming, it is possible, by an adopting air liquid interface (ALI) culturing method *in vitro*, to differentiate NHBE cells into a pseudostratified-like monolayer containing ciliated and basal cells.

The co-culture in this project would ideally have been implemented between primary activated T cells and differentiated NHBE cells. Due to the time consuming nature of differentiating these cells (see Chapter 2) and their low yield this was not possible. However, differentiated NHBE cells produced by ALI culture were profiled for their cell surface expression of TRAIL-R1, -R2, CD95, CD95L and TRAIL in order to compare this to cell surface levels observed in undifferentiated NHBE cells (Figure 5.16).

Firstly, confirmation of the differentiation of the NHBE cells was sought. Figure 5.16a shows a phase contrast image showing the even monolayer of differentiated cells. In addition, cross-sectional slices of the monolayer were stained by Haematoxylin and eosin to show the presence of basal and ciliated cells (Figure 5.16b).

Following confirmation of the differentiation process, the cells were measured by flow cytometry for the presence of the aforementioned receptors and ligands (Figure 5.16c). The immunostaining showed the presence of CD95 and potentially TRAIL-R1, one of the death receptors required to signalling downstream of TRAIL or ILZ TRAIL ligation. These data were only performed once and thus have to be interpreted with caution due to the lack of experimental repeats. NHBE cells have been shown to possess both TRAIL death receptors, TRAIL-R1 and TRAIL-R2 and CD95, suggesting a potential difference between these primary cells and differentiated NHBE cells (Chapter 4).

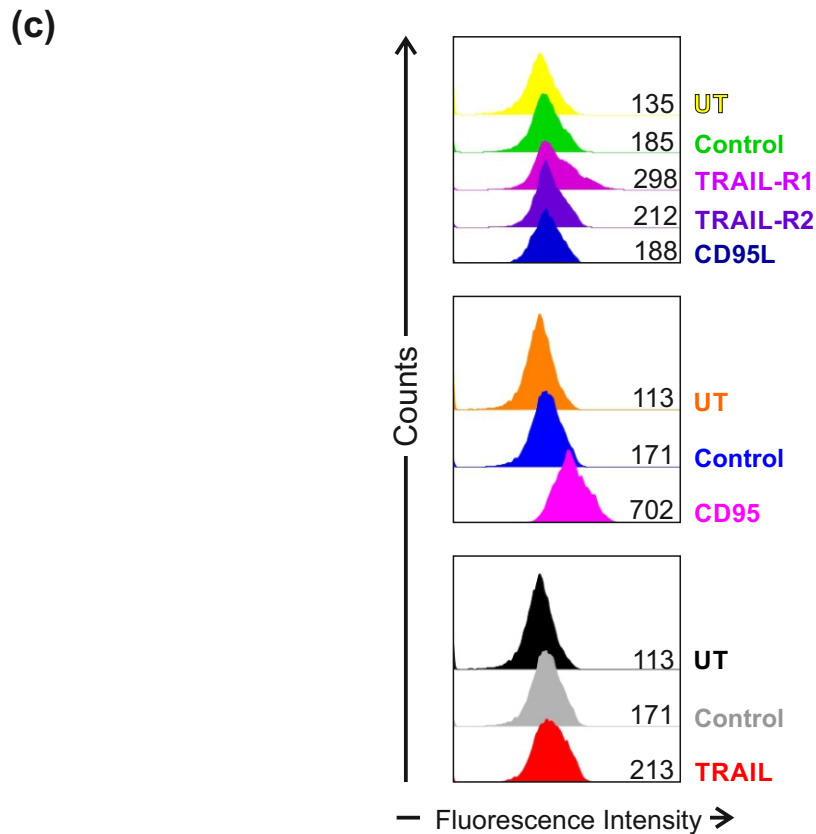
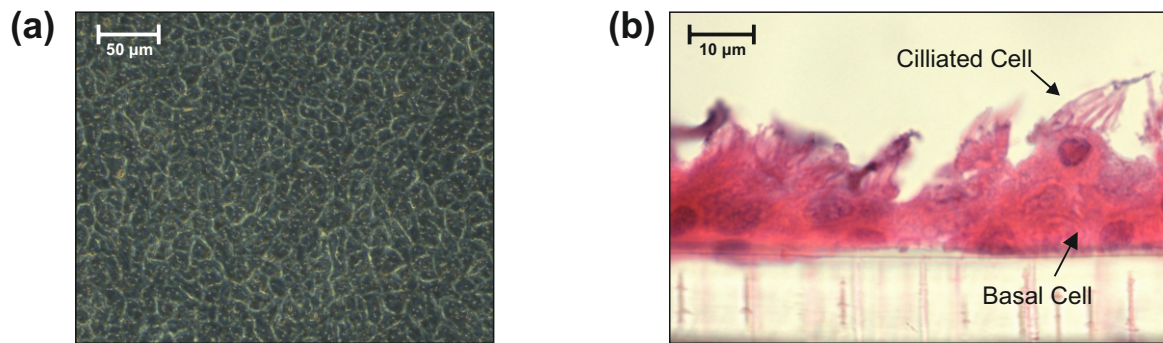


**Figure 5.16 Cell surface expression profile of differentiated NHBE cells** (a) Phase contrast image (40X) of a monolayer of differentiated NHBE cells (b) Digital image contrast image (100X) of H&E stained differentiated NHBE cells from a cross-sectional view. (c) NHBE cells were analysed for the cell surface expression of TRAIL-R1, TRAIL-R2, CD95, CD95L and TRAIL. Cells were incubated with either no antibody (UT), isotype control antibody (control), PE-conjugated TRAIL-R1, TRAIL-R2, FITC-conjugated TRAIL, PE-conjugated CD95L or CH11 with FITC-conjugated secondary antibodies. Following washing with PBS, cells were analysed by flow cytometry for changes in fluorescence intensity. Fluorescence intensity is represented by geometric mean (n=1).

### 5.3 Discussion

The aim of the work in this Chapter was to characterise the TRAIL/TRAIL-R signalling of activated primary CD4<sup>+</sup> and CD8<sup>+</sup> T cells, with the subsequent implementation of a co-culture to explore TRAIL/TRAIL-R signalling between these T cells with the previously characterised iHBEC and NHBE cells.

It has been documented that T cells become sensitive to CD95-mediated cell death over prolonged periods of activation. Indeed, the data shown here corroborates this, as evidenced by the significant increase in surface expression of CD95 and by the apoptosis observed for 6 day activated CD4<sup>+</sup> and CD8<sup>+</sup> T cells treated with anti-CD95.

T cells were characterised for their TRAIL/TRAIL-R signalling over a 6 day activation period. It was shown in Figures 5.2 and 5.3 that although both CD4<sup>+</sup> and CD8<sup>+</sup> T cells activated for 19 h expressed low levels of TRAIL-R1, they did not form a DISC and therefore did not induce any downstream signalling in these cells. Figure 5.4 showed 6 day activated CD4<sup>+</sup> and CD8<sup>+</sup> T cells to express some TRAIL-R1 on their surface again indicating a potential sensitivity to TRAIL-induced apoptosis. However, treatment of these cells with either TRAIL or ILZ TRAIL did not result in apoptosis above the levels induced by AICD (Figure 5.5). Thus, illustrating that surface expression of TRAIL death receptors does not necessarily equate to sensitivity to TRAIL. The lack of apoptosis could have been due to the presence of cellular FLICE (FADD-like IL-1 $\beta$ -converting enzyme)-inhibitory protein short (cFLIP<sub>short</sub>) at the DISC which would result in inhibition of caspase 8 processing. It is widely documented that the sensitivity of activated T cells to CD95 occurs due to a drop in levels of cFLIP<sub>short</sub> (Schmitz et al., 2004). Therefore the insensitivity of short term activated T cells to TRAIL-induced apoptosis could have been attributed to high levels of cFLIP<sub>short</sub> but 6 day activated T cells were sensitive to CD95-mediated cell death suggesting a decrease in cFLIP<sub>short</sub> levels and therefore suggesting that high cFLIP<sub>short</sub> levels are not responsible for the resistance to TRAIL or ILZ TRAIL. Another possible explanation for the lack of DISC formation could have been the potential presence and/or upregulation of the decoy TRAIL receptors,

TRAIL-R3 and TRAIL-R4. TRAIL-R3 and TRAIL-R4 can ligate TRAIL or ILZ TRAIL but cannot induce downstream signalling due to the lack of functional intracellular death domains (as discussed in Chapter 1).

Characterisation of TRAIL/TRAIL-R signalling in CD4<sup>+</sup> and CD8<sup>+</sup> T cells provided additional information required for basal TRAIL/TRAIL-R signalling in both T cells and epithelial cells under co-culture conditions. Thus the implementation of the co-culture was sought. Figure 5.6 outlines the details of the co-culture experimental set up. Particular focus was given to the viability and response of the epithelial cells as reflected in the collection of epithelial cells for surface expression, PS externalisation and apoptotic marker measurements. The overarching aim of the co-culture was to assess if and what effect the addition of TRAIL and/or ILZ TRAIL had on the two cell types cultured together in terms of cytokine release and therefore inflammation. Another focus of the co-culture was to evaluate the differences in cytokine release caused by each CD4<sup>+</sup> and CD8<sup>+</sup> T cells in the co-culture. The third aim was to see if iHBEC cells behaved in a similar way to NHBE cells in a co-culture model with T cells.

Profiling of cell surface expression of death receptors and ligands in iHBEC or NHBE cells following incubation in the co-culture model, revealed upregulation of CD95 for both co-culture orientations whether co-cultured with activated CD4<sup>+</sup> or CD8<sup>+</sup> T cells. The only difference between iHBEC cells co-cultured with CM or C2C was the small upregulation of TRAIL in the CM co-culture model. Indicating little effects caused by direct cell-to-cell contact in these cells. In the same vein, the NHBE cells did not display any significant differences in cell surface expression of death receptors or ligands between the two co-culture orientations. The only significant difference in the surface profile of iHBEC or NHBE cells caused by co-culturing with either CD4<sup>+</sup> or CD8<sup>+</sup> activated T cells was the substantial increase in CD95 cell surface expression in CD4<sup>+</sup> co-cultures, which was not observed in CD8<sup>+</sup> co-culture models.

In terms of apoptosis, TRAIL or ILZ TRAIL addition to the iHBEC co-cultures resulted in the engagement of the DISC in iHBEC cells, but did not result in cell

death (Figures 4.9 and 4.10). This was further evidenced by the decrease in surface expression of TRAIL-R2 shown in Figures 5.7 and 5.8. This suggested signalling downstream of the DISC occurring, not involving caspases. The increase in the number of cytokines released following TRAIL or ILZ TRAIL addition iHBEC co-cultures with CD4<sup>+</sup> T cells (CM and C2C) confirmed activation of other pathways, most likely NFκB activation. There were a limited number of cytokines that displayed an increase following the addition of TRAIL or ILZ TRAIL in the iHBEC co-cultures with either CD8<sup>+</sup> or CD4<sup>+</sup> (CM or C2C), these were; EMMPRIN, IL-1RA, MIF and MMP-9. Of these increased cytokines, IL-1RA and MMP-9 have previously been shown to be NFκB response genes (Smith et al, 1994; He, 1996)

EMMPRIN, also known as CD147 or basigin is considered to be a pro-inflammatory cyclophilin receptor that induces the production of MMPs, such as MMP-9. It has been documented to be released by all leukocytes and platelets but also activated T cells and shown to contribute to the promotion of inflammation in conditions such as asthma (Gwinn et al., 2006; R. Schmidt et al., 2008). EMMPRIN has been documented to be under the regulation of NFκB but also shown to regulate the activation of NFκB (Huang et al., 2000; R. Schmidt et al., 2008). In the context of the co-culture experiments here, it appears to be plausible that TRAIL or ILZ TRAIL-induced NFκB activation caused the upregulation of EMMPRIN levels observed in conditioned media of CD4<sup>+</sup> T cell co-cultures with iHBEC cells.

IL-1RA is a cytokine that regulates the inflammatory signal caused by IL-1 by binding to the IL-1 receptor as an antagonist. IL-1RA was first discovered to be expressed and released by monocytes and macrophages following interaction with stimulated T cells (Rosenstreich et al., 1988; Vey et al., 1997) but has also been found to be expressed by epithelial cells as a variant that resides intracellularly and is not secreted (Bigler et al., 1991). Therefore, the IL-1RA that had been detected in these experiments was either a result of contamination of T cells by macrophages or due to epithelial cells that had died and thus released their intracellular content. Interestingly, IL-1RA has been implicated in regulating IL-1 levels in asthmatic tissue (Hagaman et al., 2001; Sousa et al., 1996) and could be upregulated by

iHBEC cells in this context in an attempt to dampen the potential inflammatory signal induced by TRAIL or ILZ TRAIL.

The pro-inflammatory cytokine, MIF, is a known glucocorticoid antagonist. Glucocorticoids are a widespread treatment option for lung inflammatory conditions such as asthma, thus making MIF an attractive therapeutic target (Flaster et al., 2007). It has been associated with airway remodelling which occurs in asthmatic patients and documented to be released by a wide variety of cells including T cells and lung epithelium (Chen et al., 2010). In the context of these experiments, the addition of TRAIL or ILZ TRAIL to either CD4<sup>+</sup> or CD8<sup>+</sup> co-cultures with iHBEC cells caused an increase in MIF levels. This could have been due to TRAIL or ILZ TRAIL mediated NFκB activation since MIF has been reported to be a downstream target of NFκB (Hagemann et al., 2005).

MMP-9 is a metalloproteinase widely regarded as being pro-inflammatory and has been reported to be increased in lung inflammatory conditions such as asthma and idiopathic pulmonary fibrosis, and has been shown to be involved in causing lung epithelium damage (Dahlen et al., 1999; Hayashi et al., 1996; Warner et al., 2004). Importantly, MMP-9 has been shown to be regulated by NFκB in lung epithelium (Hozumi et al., 2001; Shin et al., 2007) consistent with the upregulated expression of EMMPRIN seen in Figure 5.11. This could be a result of TRAIL or ILZ TRAIL - induced NFκB activation in iHBEC cells.

In the iHBEC co-cultures with CD4<sup>+</sup> CM or C2C, the addition of TRAIL or ILZ TRAIL caused a decrease in one cytokine, cystatin C that was already present in the CM or C2C co-culture. Cystatin C is a cysteine protease inhibitor used a marker of kidney function (Stevens et al., 2009). Cysteine proteases cause damage to connective tissue in the lung and therefore cystatin C inhibits this from occurring (Burnett et al., 1995). It has been shown to be released by bronchial epithelium and is elevated in patients with community-acquired pneumonia (Burnett et al., 1995; Lee et al., 2012). Cystatin C decreased release following treatment with TRAIL or ILZ TRAIL was only observed when either CD4<sup>+</sup> or CD8<sup>+</sup> T cells were co-cultured C2C and but not with CM. This suggests a C2C interaction to be a prerequisite for

TRAIL or ILZ TRAIL to induce the downregulation of cystatin C release into the media.

Compared to the co-culture alone, TRAIL or ILZ TRAIL treatment of NHBE co-cultures were shown to cause a decline in TRAIL-R2 levels correlating with the increase in cell death observed by PS externalisation. This was especially evident for CD8<sup>+</sup> T cell co-cultures where the majority of NHBE cells post-treatment were apoptotic. This was reflected in the low levels of cytokines detected with ILZ TRAIL treatment making the data difficult to interpret and providing the reason for the decision to disregard the cytokine secretion data for the CD8<sup>+</sup> T cell co-cultures with the primary cells. Despite this, it was evident that NHBE cells co-cultured with CD4<sup>+</sup> T cells (CM or C2C) generally caused a secretion of a greater number of cytokines than with the previously described iHBEC co-cultures. A number of cytokines were increased following TRAIL or ILZ TRAIL treatment of the CD4<sup>+</sup> T cell co-cultures (CM and/or C2C) and these were; DKK1, EMMPRIN, GDF-15, GRO- $\alpha$ , IL-8, IL-1RA, MIF and serpin E1.

Similar to iHBEC co-cultures, EMMPRIN, DKK1 and MIF levels were shown to be elevated in with the addition of TRAIL or ILZ TRAIL to NHBE co-cultures with either CD4<sup>+</sup> or CD8<sup>+</sup> T cells. This further emphasises the possible upregulation of this secreted protein due to TRAIL or ILZ TRAIL -mediated NF $\kappa$ B activation. Similar to the results from the iHBEC co-cultures, IL1-RA was shown to be upregulated in all of the TRAIL or ILZ TRAIL treated NHBE co-cultures, compared to the co-cultures alone. This is most likely the variant of IL-1RA that is found intracellularly in epithelial cells, detected due to the NHBE cell death observed in the co-cultures treated with TRAIL or ILZ TRAIL.

DKK1 is an inhibitor of Wnt signalling and has been shown to be involved in the progression non-small cell lung cancer (Salim et al., 2015). However, DKK1 had not been shown to be involved in lung inflammation until very recently Guo et al., (2015) showed increased DKK1 levels in a model of acute lung inflammation and suggested DKK1 to be responsible for the suppression of the Wnt signalling pathway seen to be active in lung inflammatory conditions. DKK1 levels were

increased with the addition of TRAIL or ILZ TRAIL in the NHBE co-culture with CM from CD4<sup>+</sup> T cells. On the other hand, in CD8<sup>+</sup> co-cultures, ILZ TRAIL caused an increase in DKK1 levels with the C2C orientation rather than with CM.

GDF-15 is known to play a role in the balance between apoptosis and inflammation and has been shown to be expressed in a variety of tissues including the brain and lung. It has been implicated in causing increased mucin production in COPD by (Q. Wu et al., 2012) and more recently (Freeman et al., 2015) have shown increased levels of GDF-15 to correlate with decreased levels of CD4<sup>+</sup> and CD8<sup>+</sup> T cells in acute episodes of COPD.

GRO- $\alpha$  and IL-8 are both known to be produced downstream of NF $\kappa$ B activation induced by IL-17 in human bronchial epithelial cells (Jones and Chan, 2002). IL-17 is released by a subset of CD4<sup>+</sup> T cells known as T helper-17 (Th17) cells (Weaver et al., 2006). The release of these cytokines are thought to stimulate neutrophil infiltration. TRAIL or ILZ TRAIL addition to CM CD4<sup>+</sup> co-culture of NHBE cells caused an increase in both GRO- $\alpha$  and IL-8, suggesting a pro-inflammatory effect, whereas in the C2C CD4<sup>+</sup> co-culture the addition of TRAIL or ILZ TRAIL resulted in a decrease of these cytokines suggesting a potential anti-inflammatory effect.

Serpin E1 or plasminogen activation inhibitor-1 is another pro-inflammatory protein released by lung epithelium and known to be involved in lung inflammatory conditions such as COPD and asthma. This protein functions to promote airway remodelling (Bhandary et al., 2015). Untreated iHBEC cells released this cytokine and it was also detected in the iHBEC cell co-culture models. TRAIL and ILZ TRAIL induced differential changes in the levels of serpin E1 in the different co-cultures, suggesting the change in levels, compared to a co-culture alone, is dependent on whether cells are interacting directly or *via* soluble mediators.

In addition to cytokines that were detected at higher levels following the addition of TRAIL or ILZ TRAIL, there were a small number of cytokines that appeared to decline compared to the co-cultures alone, these were; IGFBP2 and lipocalin-2.

IGFBP2 has been implicated in cancer as both a tumour suppressor gene and an oncogene (reviewed in Pickard and McCance, 2015). IGFBP2 levels are increased in cancer and therefore it has the potential as a biomarker. In contrast, this protein has not been studied in the setting of lung inflammation in great detail. It has been reported that activated PBMC express higher levels of IGFBP2 mRNA, suggesting a role for promoting proliferation of T cells and other PBMCs (Hettmer et al., 2004). In this context, CD4<sup>+</sup> and CD8<sup>+</sup> T cells alone did not release this protein (Figure 5.10) but iHBEC cells +/- ILZ TRAIL did release IGFBP2 into the media. In terms of the iHBEC co-cultures, CD8<sup>+</sup> and not CD4<sup>+</sup> T cells (CM or C2C) saw a decrease in the levels of secreted IGFBP2 when ILZ TRAIL was added. The significance of this observation is unclear and would be interesting to explore further.

Lipocalin-2 is involved in the innate immune system, known to assist the combatting of bacterial infections (Goetz et al., 2002). However, it has also been shown to function as a growth factor under certain conditions, such as in the kidney (Schmidt-Ott et al., 2007). It is expressed in a variety of tissues including the stomach, pancreas and the lung and has been shown to be upregulated in lung adenocarcinoma (Friedl et al., 1999). With this taken into consideration it is unclear but possible that the increase of lipocalin-2 observed in TRAIL and ILZ TRAIL treated NHBE co-cultures with CD4<sup>+</sup> T cells, was due to secretion by NHBE cells as a pro-inflammatory factor.

Having summarised the roles of the cytokines whose levels were shown to change following treatment with TRAIL or ILZ TRAIL and having speculated why these cytokines changed in this experimental setting, it is clear that the general trend is of increase in pro-inflammatory cytokines for both iHBEC and NHBE co-cultures. It is interesting to note the overlap of cytokine changes such as increases in EMMPRIN, MIF and IL-1RA in both iHBEC and NHBE co-cultures. This overlap does indicate a similarity between the two cell types in this context. However, it is important to acknowledge the limitations of the co-culture experiments carried out for this part of the project. Although the changes seen between the different orientations of co-culture and between cell types used in the co-cultures yielded similar effects and

therefore appear to be promising results, the co-culture experiments were designed to be exploratory. Thus, there is a definite requirement to validate any potential changes in cytokine secretion seen in these experiments.

In addition to the co-culture experiments, NHBE cells were differentiated into basal and ciliated cells to demonstrate the potential for a more physiologically relevant model than NHBE cells for mimicking lung epithelium. These cells were shown to possess CD95 but without the relevant experimental repeats it was difficult to determine whether the indication of TRAIL-R1 presence was a definite result or not. Thus, in terms of TRAIL, is difficult to predict whether differentiated NHBE cells signal similarly to NHBE cells.

Taken together these results indicate that in the co-cultures of T cells with either iHBEC or NHBE cells, treatment with TRAIL and ILZ TRAIL caused ligation of the cognate death receptors, TRAIL-R1 and/or TRAIL-R2, which induced downstream NF $\kappa$ B activation as evidenced by the increases in pro-inflammatory cytokines observed. In NHBE co-cultures, in parallel to this activation, a degree of apoptosis was also detected.

## **6 Final Discussion**

## 6.1 Overview

TRAIL is a cytokine that can be present in either a soluble or membrane-bound form (Walczak and Haas, 2008). The form of TRAIL that is presented to TRAIL death receptors can be critical in dictating which receptor is engaged more efficiently (TRAIL-R1 or TRAIL-R2) and therefore the potency of the downstream signal to either apoptosis or NF $\kappa$ B activation (Natoni et al., 2007; Wajant et al., 2001). Based on this knowledge, the first aim of this project was to generate an appropriate tool to mimic the membrane-bound form of TRAIL ligand. Recombinant ILZ TRAIL was generated to use in conjunction with the existing in-house recombinant TRAIL for investigating TRAIL/TRAIL-R signalling in lung epithelial cells and activated T cells cultured either alone or under co-culture conditions. ILZ TRAIL was synthesised with a His<sub>6</sub>-tag to allow for effective purification and to enable specific isolation of the TRAIL DISC. Synthesised ILZ TRAIL was confirmed to be in a highly oligomerised conformation by size exclusion chromatography. As TRAIL-R2 is more efficiently engaged when presented with an oligomerized form of TRAIL, ILZ TRAIL was tested in two predominantly TRAIL-R2 signalling cell lines – the Jurkat T cell line, E6.1 and the bronchial epithelial cell line, BEAS-2B. Importantly, ILZ TRAIL was found to be just as effective at inducing apoptosis as a cross-linked TRAIL-R2 specific agonistic antibody. Also, ILZ TRAIL was more active than soluble TRAIL in terms of inducing apoptosis, thus confirming its ability to facilitate TRAIL-R2-targeted ligation. In addition, the ILZ TRAIL DISC was successfully isolated in Jurkat E6.1 cells and analysed for the known components of the TRAIL DISC thus proving ILZ TRAIL specificity and its use as a tool for the investigation of TRAIL-R2 signalling in this project. Based on the results of this project, there is a strong rationale for using ILZ TRAIL in tandem with soluble TRAIL as a tool for investigating the dependency of any cell on TRAIL-R1 or TRAIL-R2 death receptors and furthermore dissecting the mechanisms that regulate cellular sensitivity to TRAIL-R1/R2-mediated apoptosis.

Many lung epithelial cell lines exist and in order to create the most accurate model of lung inflammation, profiling of several different cell lines was carried out. This profiling also provided a baseline to subsequently interpret potential changes in

TRAIL/TRAIL-R signalling induced in the co-culture of lung epithelial cells and activated T cells. Initially, a panel of non-cancerous lung epithelial cell lines, 16HBE, BEAS-2B and iHBEC and the cancerous cell line A549 (as a control) were profiled for their basal TRAIL/TRAIL-R signalling. The aim was to understand whether they signalled similarly and to analyse whether any particular cell line would provide a suitable model to recapitulate the basal levels of TRAIL/TRAIL-R signalling of primary cells, NHBE.

Notably, all of the lung epithelial cell lines tested, except 16HBE, were found to signal predominantly through TRAIL-R2. This was established using cell surface TRAIL-R2 expression profiling and treatment of cells with ILZ TRAIL compared with treatment with TRAIL. Thus, it can be concluded that 16HBE cells do not represent an appropriate cell line for studying TRAIL-induced apoptosis in the lung epithelium. Although this cell line has been widely used in industry for the investigation of lung inflammation, it is important to recognise the limitations of its use in terms of apoptosis research (Pace et al., 2012; West et al., 2002). Moreover, this data brings into question the general use of 16HBE cells as a representative model of the lung epithelium.

The retrovirally transformed cell line BEAS-2B, treated with TRAIL or ILZ TRAIL, died by apoptosis in a similar way to the carcinoma cell line, A549. This result is consistent with previous reports, where a retrovirally-transformed cell line was found to behave like a tumour cell line, causing tumours when injected in nude mice (Reddel et al., 1993). In contrast, very little apoptosis was observed in iHBEC or NHBE cells and therefore in this respect iHBEC cells appeared the most similar cell line to primary NHBE cells. Not only were their cell surface death receptor and ligand profiles the same but they also both responded to TRAIL or ILZ TRAIL treatment in a concentration-dependent manner. Importantly, the use of ILZ TRAIL revealed a dependence of both cell types on signalling *via* TRAIL-R2, once again emphasising the usefulness of this tool for investigating TRAIL/TRAIL-R signalling preference in a particular cell type. Although similar signalling occurs at the level of the DISC in both cell types, downstream of the DISC, caspase 3 processing was apparently halted at cleavage fragment p20. Pre-treatment with SM did not significantly relieve

this caspase 3 processing halt in either cell type and therefore it was speculated that other apoptosis resistance mechanisms were at play. To explore this, iHBEC and NHBE cells were profiled for a subset of Bcl-2 family proteins involved in regulation of the mitochondrial amplification loop which revealed a potential role for Bcl-XL as an anti-apoptotic protein in both of these cell types (Czabotar et al., 2013).

Both iHBEC and NHBE cells treated with TRAIL or ILZ TRAIL were found to signal to NF $\kappa$ B activation as shown by phosphorylation of I $\kappa$ B $\alpha$  and translocation of p65 to the nucleus. It is possible that this was due to the formation of complex II (outlined in Chapter 1). Alternatively, it has also been reported that cFLIP recruitment to the DISC can not only inhibit the activation of caspase 8 at the DISC but also directly induce formation of the IKK complex thereby inducing activation of NF $\kappa$ B (Kataoka et al., 2000). However, it should be noted that cFLIP-mediated IKK complex formation was observed in a cancer cell setting. Due to the lack of IL-6 or IL-8 secreted in both iHBEC and NHBE cells following treatment with TRAIL or ILZ TRAIL, it can be hypothesised that activation of NF $\kappa$ B in these cells serves solely an apoptosis rescue signal rather than a pro-inflammatory signal.

From profiling the above panel of lung epithelial cell lines alongside primary NHBE cells, it was evident that 16HBE cells were the anomaly cell line. Although profiling in this case was specifically focussed on apoptosis, these observations demonstrate the importance of identifying the most appropriate cell line to model an *in vivo* situation. Thus, future work with the 16HBE cell line in industry should be carefully considered. Moreover, in terms of TRAIL-induced apoptosis, the retrovirally transformed cell line, BEAS-2B was also not considered an appropriate cell line for taking forward to the co-culture experiments due to its tumour cell-like behaviour. In contrast, the iHBEC cell line, investigated here for the first time with respect to TRAIL/TRAIL-R signalling, was shown to closely mimic TRAIL/TRAIL-R signalling in primary NHBE cells. Even the timing of TRAIL DISC formation was found to be similar, further highlighting their signalling similarities (evaluated in Figure 6.1). A potential explanation for iHBEC cells being more representative of NHBE cells, in this context, is the way in which these cells were immortalised. Overexpression of Cdk4 and hTERT, rather than transformation, gave rise to the establishment of the

iHBEC cell line (Ramirez et al., 2004). This suggests that the transformation process may be detrimental to maintaining the basal cell apoptotic signalling profile found in primary lung epithelial cells. Overall, it can be concluded that the iHBEC cell line is a good model for primary lung epithelial cells and should be considered for future projects instead of the 16HBE or BEAS-2B cell lines. Moreover, the ease of culturing and the cost-effectiveness of using iHBEC cells over NHBE cells provides added reason for using this cell line as a suitable model of primary lung epithelial cells for investigating TRAIL-induced signalling.

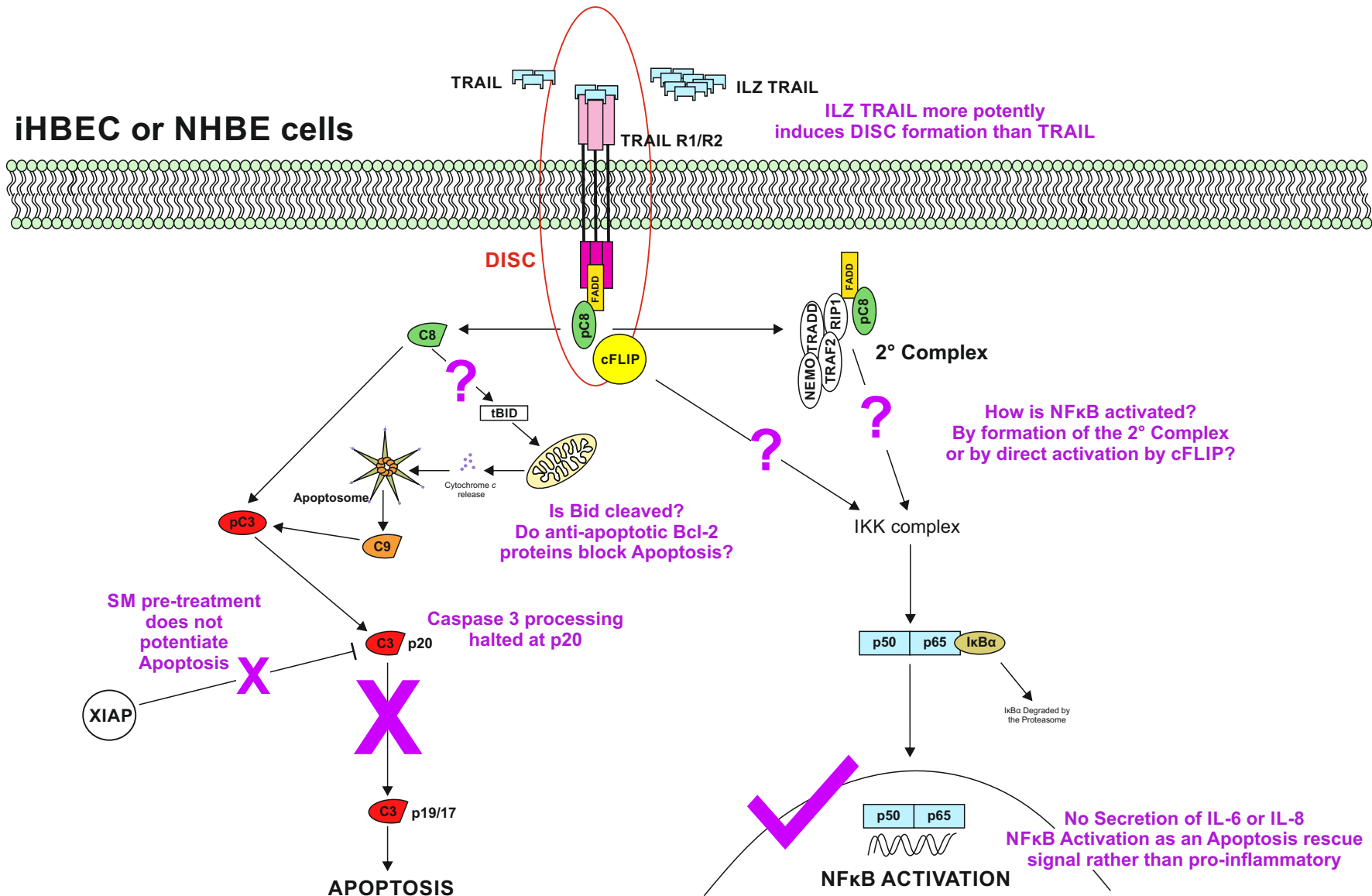


**Figure 6.1 Dissecting basal levels of TRAIL/TRAIL-R signalling in iHBEC and NHBE cells** Schematic to show what has been elucidated and to show what remains to be investigated about TRAIL/TRAIL-R signalling in the immortalised lung epithelial cell line, iHBEC and in primary lung epithelial cells, NHBE in this project.

CD4<sup>+</sup> and CD8<sup>+</sup> T cells were selected for investigation in this project due to their importance in driving inflammatory responses in asthma and COPD, respectively. Although CD95 signalling in T cells has been researched widely with vast knowledge of AICD to be found in the literature, little is known about TRAIL/TRAIL-R signalling in primary T cells. Thus, it was interesting to observe the changes in cell surface expression of TRAIL death receptors and ligand in naïve and 19 h or 6 d activation of CD4<sup>+</sup> and CD8<sup>+</sup> T cells (summarised in Figure 6.2). The data in this project show cell surface expression of TRAIL-R1 to decrease in CD4<sup>+</sup> T cells over 19 h and remain low over 6 d activation, whereas in CD8<sup>+</sup> T cells surface TRAIL-R1 levels increased and were maintained over 6 d activation. In contrast, TRAIL-R2 levels were negligible in both naïve and activated CD4<sup>+</sup> and CD8<sup>+</sup> T cells. Despite the presence of TRAIL-R1 in 6 d activated CD8<sup>+</sup> T cells, treatment with TRAIL or ILZ TRAIL did not result in DISC formation or apoptosis. It is unlikely that this is due to cFLIP<sub>short</sub> inhibiting activation of caspase 8 at the level of the DISC. It has been well documented that decreasing cFLIP<sub>short</sub> levels correlate with activated T cells becoming more sensitive to CD95-mediated apoptosis (Schmitz et al, 2004). Hence, adding weight to the argument that cFLIP<sub>short</sub> does not inhibit TRAIL-induced apoptosis in 6 d activated CD8<sup>+</sup> T cells. However, (Janssen et al., 2005) have reported a specific situation in which activated CD8<sup>+</sup> T cells have been observed to become sensitive to TRAIL-mediated apoptosis. In this study by the Doug Green laboratory, memory CD8<sup>+</sup> T cells not primed by CD4<sup>+</sup> T cells, which encounter a secondary stimulation, are shown to undergo TRAIL-mediated AICD. CD8<sup>+</sup> T cells in this project were not stimulated twice, providing an explanation for the lack of TRAIL-mediated cell death observed here. However, the increase in TRAIL-R1 in activated CD8<sup>+</sup> T cells suggests a possible priming of these cells to TRAIL-mediated cell death once encountering a secondary stimulating signal. Due to the lack of any change in TRAIL/TRAIL-R signalling over 6 d activation and because of the increase in AICD levels observed in 19 h activated T cells, 19 h activation was deemed to be optimal for the subsequent use of CD4<sup>+</sup> and CD8<sup>+</sup> T cells in the co-culture experiments.

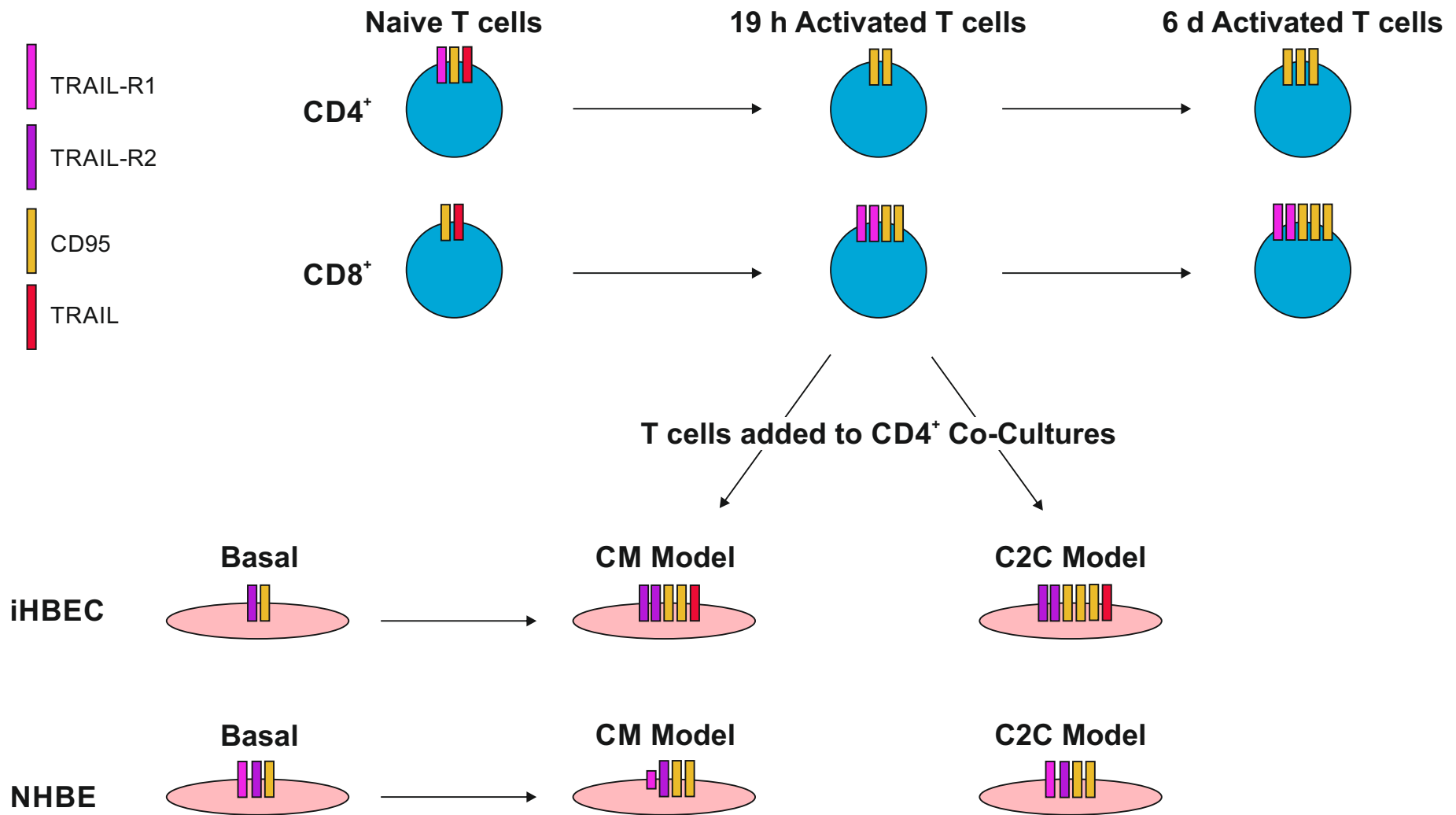


**Figure 6.2 Key changes in cell surface expression of death receptors and ligands in naive and activated T cells and in iHBEC and NHBE cells co-cultured** Schematic showing changes in cell surface expression of TRAIL-R2 and CD95 in T cells and the lung epithelial cells, iHBEC and NHBE

Two orientations of co-culturing iHBEC or NHBE cells with activated CD4<sup>+</sup> or CD8<sup>+</sup> T cells were chosen to investigate effects caused by soluble factors (the addition of CM) compared with direct contact between target cells (C2C). Compared to basal levels, iHBEC cells co-cultured with CD4<sup>+</sup> T cells exhibited upregulated TRAIL-R2 and CD95 under both CM and C2C orientations. In all NHBE co-cultures, TRAIL-R2 levels remained consistent and CD95 levels were upregulated, whereas in the CD4<sup>+</sup> T cell CM co-culture TRAIL-R1 was downregulated and in the CD4<sup>+</sup> T cell C2C co-culture TRAIL-R1 levels remained the same as basal levels. The few changes in cell surface expression between the two co-culture orientations for both iHBEC and NHBE shows how little effect direct cell to cell contact has on death receptor cell surface expression (summarised in Figure 6.2). However, the upregulation of CD95 induced by all co-culture orientations compared to basal levels of CD95 observed in iHBEC and NHBE cells is noteworthy, indicating a potential increase in susceptibility to CD95-mediated apoptosis in co-culture.

The addition of TRAIL or ILZ TRAIL in the co-cultures caused the downregulation of TRAIL-R2 in both iHBEC and NHBE cells and TRAIL-R1 in NHBE cells. Rather than being an effect of the co-culture, these data indicate that direct ligation of TRAIL or ILZ TRAIL to TRAIL-R1 and/or TRAIL-R2 induces DISC formation and internalisation of these receptors thus resulting in their downregulation at the cell surface. Further adding to this conclusion is the observation that ILZ TRAIL in general caused a greater downregulation of TRAIL-R1 or TRAIL-R2 compared to TRAIL which correlates with the findings from Chapter 4 where both iHBEC and NHBE cells were found to be predominately reliant on TRAIL-R2. Interestingly, CD95 is also observed to be downregulated in both iHBEC and NHBE co-cultures following treatment with TRAIL or ILZ TRAIL. A possible explanation for the downregulation of CD95 by iHBEC and NHBE cells could be due to the formation of the TRAIL DISC serving as a death priming signal and the cells then responding by preventing any further encounter of death signals.

Treatment of iHBEC or NHBE cells with TRAIL or ILZ TRAIL did not result in the secretion of any cytokines above basal levels. These findings emphasise the argument for NFκB activation downstream of TRAIL death receptor ligation in these

cells to be an apoptosis rescue signal rather than a pro-inflammatory signal. However, under both CM and C2C orientations, both iHBEC and NHBE co-cultures resulted in the secretion of multiple cytokines, thus demonstrating that the addition of activated T cells induced an inflammatory response in both cell types, and emphasising the establishment of a lung inflammatory scenario.

The addition of TRAIL or ILZ TRAIL to iHBEC or NHBE co-cultures resulted in the up and down regulation of multiple cytokines. However, three cytokines in particular, EMMPRIN, MIF and IL-1RA were changed in a similar manner in both iHBEC and NHBE co-cultures. Both EMMPRIN and MIF are pro-inflammatory cytokines implicated in asthma and their increase in the co-cultures treated with TRAIL or ILZ TRAIL confirm the potentiation of the existing inflammatory milieu between lung epithelial and activated T cells (Chen et al., 2010; Gwinn et al., 2006; R. Schmidt et al., 2008). Interestingly IL-1RA is an anti-inflammatory cytokine potentially indicating that iHBEC and NHBE cells under co-culture conditions are attempting to regulate the inflammatory response (Hagaman et al., 2001; Sousa et al., 1996).

Taken together, these data indicate TRAIL/ILZ TRAIL to be an apoptosis rescue signal in lung epithelial cells cultured alone, whereas in co-cultures with activated T cells, the addition of TRAIL or ILZ TRAIL potentiates an existing inflammatory signal. Thus the data from this project, albeit *in vitro*, agrees with Weckmann et al., (2007) who reported TRAIL to be pro-inflammatory in a mouse model in an asthma setting.

It is important to note that investigation of TRAIL/TRAIL-R signalling in lung inflammatory conditions should be carried out using models consisting of human cells. Mouse models can be valuable for researching many diseases and conditions, however mice have only one TRAIL death receptor (Wu et al., 1999) and as observed in this project, differences between TRAIL-R1 and TRAIL-R2 signalling are important to evaluate and this would not have been possible in a mouse model of inflammation. Thus it can be concluded that using primary human cells (NHBE), in which case differentiated NHBE cells are probably the most representative of the *in vivo* scenario of the lung epithelium, or suitably characterised human cell lines (iHBEC) are appropriate for modelling the lung epithelium. It is also important to

note the limitations of the amount of primary human cells available in this project. For example, blood from healthy volunteers was taken locally and therefore the amount of blood that could be drawn from each individual was limited to 45 ml. This limited the number of peripheral T cells that could be isolated and used for subsequent experiments. In addition, the NHBE cells, although capable of being passaged, grew slowly in culture and were limited in number. Due to these constraints, experimental plans were adjusted, thus resulting in a number of experiments that should be followed up in the future.

## 6.2 Conclusions

The key findings from this project are as follows:

1. ILZ TRAIL is a valuable tool for investigating the dependence of TRAIL-mediated signalling on TRAIL-R2 in and should be used in conjunction with soluble TRAIL to fully investigate TRAIL/TRAIL-R1/2 signalling
2. For the first time, primary lung epithelial cells have been profiled in terms of their basal TRAIL/TRAIL-R signalling and have been shown to signal predominantly via TRAIL-R2 (like the majority of lung epithelial cell lines profiled); although an active DISC is formed this does not induce apoptosis but results in activation of NFκB.
3. The iHBEC cell line provides a good model of primary lung epithelium in the context of TRAIL signalling and should be considered instead of other cell lines for future research into apoptosis in the lung epithelium.
4. An *in vitro* model of lung inflammation has successfully been established. This model consists of a co-culture of activated T cells and appropriate lung epithelial cells; either primary NHBE cells or the immortalised cell line, iHBEC
5. TRAIL/ILZ TRAIL function differently depending on the cellular context. In lung epithelial cells cultured alone, it appears that TRAIL-mediated NFκB

activation serves as an apoptosis rescue signal, whereas in a co-culture model of lung inflammation TRAIL-mediated NF $\kappa$ B activation potentiates existing inflammation and thus in this context TRAIL can be considered to be pro-inflammatory.

### 6.3 Future Work

With all of the findings taken into consideration, there are further experiments that could be performed in order to confirm and/or validate these conclusions.

Firstly, I propose the detailed investigation of the contribution of the anti-apoptotic Bcl-2 family of proteins and cFLIP in causing the block in apoptosis observed in iHBEC and NHBE cells treated with TRAIL or ILZ TRAIL. Further characterisation of the mechanism whereby TRAIL-induced apoptosis is inhibited in these cells could lead to the identification of potential therapeutic targets.

The substantial increase in cell death observed in NHBE cells in co-culture with activated T cells following TRAIL or ILZ TRAIL treatment requires confirmation with further experiments to elucidate whether this is a genuine difference between iHBEC and NHBE cells in co-culture.

The cytokines observed to be increased on the addition of TRAIL or ILZ TRAIL to iHBEC or NHBE co-cultures, namely EMMPRIN, IL-1RA and MIF, require further validation by ELISA and if confirmed could be subsequently investigated to elucidate their potential role in the lung inflammatory model.

Since CD95 cell surface levels increased following the establishment of the co-culture model for both lung epithelial cell types and decreased when co-cultures were treated with TRAIL or ILZ TRAIL, it would be interesting to also include anti-CD95 or CD95L as a treatment in the co-culture model. Addition of anti-CD95/CD95L would allow for elucidation of whether the CD95-mediated apoptosis pathway is active in lung epithelial cells that are co-cultured with activated T cells.

Finally, further characterisation of differentiated lung epithelial cells and their subsequent comparison to bronchial brushings taken from normal and asthmatic human donors could provide new insight into how representative differentiated NHBE cells, as well as NHBE and iHBEC cells as characterised here are of biopsied tissue.

## 7 References

- World Health Organisation, 2012:  
<http://www.who.int/mediacentre/factsheets/fs307/en/> Date of access: 01/08/15
- Acehan, D., Jiang, X., Morgan, D.G., Heuser, J.E., Wang, X., Akey, C.W., 2002. Three-dimensional structure of the apoptosome: implications for assembly, procaspase-9 binding, and activation. *Mol. Cell* 9, 423–432.
- Adams, J.M., Cory, S., 2007. Bcl-2-regulated apoptosis: mechanism and therapeutic potential. *Curr. Opin. Immunol.* 19, 488–496.  
doi:10.1016/j.coi.2007.05.004
- Aggarwal, B.B., 2003. Signalling pathways of the TNF superfamily: a double-edged sword. *Nat. Rev. Immunol.* 3, 745–756. doi:10.1038/nri1184
- Algeciras-Schimmich, A., Shen, L., Barnhart, B.C., Murmann, A.E., Burkhardt, J.K., Peter, M.E., 2002. Molecular ordering of the initial signaling events of CD95. *Mol. Cell. Biol.* 22, 207–220.
- Allen, M., Heinzmann, A., Noguchi, E., Abecasis, G., Broxholme, J., Ponting, C.P., Bhattacharyya, S., Tinsley, J., Zhang, Y., Holt, R., Jones, E.Y., Lench, N., Carey, A., Jones, H., Dickens, N.J., Dimon, C., Nicholls, R., Baker, C., Xue, L., Townsend, E., Kabesch, M., Weiland, S.K., Carr, D., Mutius, von, E., Adcock, I.M., Barnes, P.J., Lathrop, G.M., Edwards, M., Moffatt, M.F., Cookson, W.O.C.M., 2003. Positional cloning of a novel gene influencing asthma from chromosome 2q14. *Nat. Genet.* 35, 258–263. doi:10.1038/ng1256
- Alnemri, E.S., Livingston, D.J., Nicholson, D.W., Salvesen, G., Thornberry, N.A., Wong, W.W., Yuan, J., 1996. Human ICE/CED-3 protease nomenclature. *Cell* 87, 171.
- Anderson, J.M., Van Itallie, C.M., 1995. Tight junctions and the molecular basis for regulation of paracellular permeability. *Am. J. Physiol.* 269, G467–75.
- Arish, N., Cohen, P.Y., Golan-Gerstl, R., Fridlender, Z., Dayan, M.R., Zisman, P., Breuer, R., Wallach-Dayana, S.B., 2015. Overexpression of Telomerase Protects Human and Murine Lung Epithelial Cells from Fas- and Bleomycin-Induced Apoptosis via FLIP Upregulation. *PLoS ONE* 10, e0126730.  
doi:10.1371/journal.pone.0126730
- Ashkenazi, A., 2002. Targeting death and decoy receptors of the tumour-necrosis factor superfamily. *Nat. Rev. Cancer.* 2, 420–430. doi:10.1038/nrc821
- Ashkenazi, A., Pai, R.C., Fong, S., Leung, S., Lawrence, D.A., Marsters, S.A., Blackie, C., Chang, L., McMurtrey, A.E., Hebert, A., DeForge, L., Koumenis, I.L., Lewis, D., Harris, L., Bussiere, J., Koeppen, H., Shahrokh, Z., Schwall, R.H., 1999. Safety and antitumor activity of recombinant soluble Apo2 ligand. *J. Clin. Invest.* 104, 155–162. doi:10.1172/JCI6926
- Bagdonas, E., Raudoniute, J., Bruzauskaite, I., Aldonyte, R., 2015. Novel aspects of pathogenesis and regeneration mechanisms in COPD. *Int J Chron Obstruct Pulmon Dis* 10, 995–1013. doi:10.2147/COPD.S82518
- Barnes, P.J., 2009. Intrinsic asthma: not so different from allergic asthma but driven by superantigens? *Clin. Exp. Allergy* 39, 1145–1151.  
doi:10.1111/j.1365-2222.2009.03298.x
- Barnes, P.J., 2006. New therapies for asthma. *Trends Mol Med* 12, 515–520.  
doi:10.1016/j.molmed.2006.09.006
- Barnes, P.J., Adcock, I.M., 2003. How do corticosteroids work in asthma? *Ann. Intern. Med.* 139, 359–370.
- Barnes, P.J., Chung, K.F., Page, C.P., 1998. Inflammatory mediators of asthma:

- an update. *Pharmacol. Rev.* 50, 515–596.
- Barnes, P.J., Karin, M., 1997. Nuclear factor-kappaB: a pivotal transcription factor in chronic inflammatory diseases. *N. Engl. J. Med.* 336, 1066–1071. doi:10.1056/NEJM199704103361506
- Benayoun, L., Druilhe, A., Dombret, M.-C., Aubier, M., Pretolani, M., 2003. Airway structural alterations selectively associated with severe asthma. *Am. J. Respir. Crit. Care Med.* 167, 1360–1368. doi:10.1164/rccm.200209-1030OC
- Bergeron, C., Tulic, M.K., Hamid, Q., 2010. Airway remodelling in asthma: from benchside to clinical practice. *Can. Respir. J.* 17, e85–93.
- Berry, M., Brightling, C., Pavord, I., Wardlaw, A., 2007. TNF-alpha in asthma. *Curr Opin Pharmacol* 7, 279–282. doi:10.1016/j.coph.2007.03.001
- Berry, M.A., Hargadon, B., Shelley, M., Parker, D., Shaw, D.E., Green, R.H., Bradding, P., Brightling, C.E., Wardlaw, A.J., Pavord, I.D., 2006. Evidence of a role of tumor necrosis factor alpha in refractory asthma. *N. Engl. J. Med.* 354, 697–708. doi:10.1056/NEJMoa050580
- Bhakta, N.R., Woodruff, P.G., 2011. Human asthma phenotypes: from the clinic, to cytokines, and back again. *Immunol. Rev.* 242, 220–232. doi:10.1111/j.1600-065X.2011.01032.x
- Bhandary, Y.P., Shetty, S.K., Marudamuthu, A.S., Midde, K.K., Ji, H.-L., Shams, H., Subramaniam, R., Fu, J., Idell, S., Shetty, S., 2015. Plasminogen activator inhibitor-1 in cigarette smoke exposure and influenza A virus infection-induced lung injury. *PLoS ONE* 10, e0123187. doi:10.1371/journal.pone.0123187
- Bigler, R.D., Crilley, P., Micaily, B., Brady, L.W., Topolsky, D., Bulova, S., Vonderheid, E.C., Brodsky, I., 1991. Autologous bone marrow transplantation for advanced stage mycosis fungoides. *Bone Marrow Transplant.* 7, 133–137.
- Boatright, K.M., Renatus, M., Scott, F.L., Sperandio, S., Shin, H., Pedersen, I.M., Ricci, J.E., Edris, W.A., Sutherlin, D.P., Green, D.R., Salvesen, G.S., 2003. A unified model for apical caspase activation. *Mol. Cell* 11, 529–541.
- Boatright, K.M., Salvesen, G.S., 2003. Mechanisms of caspase activation. *Curr. Opin. Cell Biol.* 15, 725–731.
- Bongartz, T., Sutton, A.J., Sweeting, M.J., Buchan, I., Matteson, E.L., Montori, V., 2006. Anti-TNF antibody therapy in rheumatoid arthritis and the risk of serious infections and malignancies: systematic review and meta-analysis of rare harmful effects in randomized controlled trials. *JAMA* 295, 2275–2285. doi:10.1001/jama.295.19.2275
- Bousquet, J., Wenzel, S., Holgate, S., Lumry, W., Freeman, P., Fox, H., 2004. Predicting response to omalizumab, an anti-IgE antibody, in patients with allergic asthma. *Chest* 125, 1378–1386.
- Bradding, P., Roberts, J.A., Britten, K.M., Montefort, S., Djukanovic, R., Mueller, R., Heusser, C.H., Howarth, P.H., Holgate, S.T., 1994. Interleukin-4, -5, and -6 and tumor necrosis factor-alpha in normal and asthmatic airways: evidence for the human mast cell as a source of these cytokines. *Am. J. Respir. Cell Mol. Biol.* 10, 471–480. doi:10.1165/ajrcmb.10.5.8179909
- Bradford, M.M., 1976. A rapid and sensitive method for the quantitation of microgram quantities of protein utilizing the principle of protein-dye binding. *Anal. Biochem.* 72, 248–254.
- Brauer, S.J., Büneker, C., Mohr, A., Zwacka, R.M., 2006. Constitutively activated nuclear factor-kappaB, but not induced NF-kappaB, leads to TRAIL resistance

- by up-regulation of X-linked inhibitor of apoptosis protein in human cancer cells. *Mol. Cancer Res.* 4, 715–728. doi:10.1158/1541-7786.MCR-05-0231
- Bratton, S.B., Lewis, J., Butterworth, M., Duckett, C.S., Cohen, G.M., 2002. XIAP inhibition of caspase-3 preserves its association with the Apaf-1 apoptosome and prevents CD95- and Bax-induced apoptosis. *Cell Death Differ.* 9, 881–892. doi:10.1038/sj.cdd.4401069
- Burnett, D., Abrahamson, M., Devalia, J.L., Sapsford, R.J., Davies, R.J., Buttle, D.J., 1995. Synthesis and secretion of procathepsin B and cystatin C by human bronchial epithelial cells in vitro: modulation of cathepsin B activity by neutrophil elastase. *Arch. Biochem. Biophys.* 317, 305–310. doi:10.1006/abbi.1995.1167
- Cain, K., Bratton, S.B., Cohen, G.M., 2002. The Apaf-1 apoptosome: a large caspase-activating complex. *Biochimie* 84, 203–214.
- Caricchio, R., Reap, E.A., Cohen, P.L., 1998. Fas/Fas ligand interactions are involved in ultraviolet-B-induced human lymphocyte apoptosis. *J. Immunol.* 161, 241–251.
- Celedón, J.C., Lange, C., Raby, B.A., Litonjua, A.A., Palmer, L.J., DeMeo, D.L., Reilly, J.J., Kwiatkowski, D.J., Chapman, H.A., Laird, N., Sylvia, J.S., Hernandez, M., Speizer, F.E., Weiss, S.T., Silverman, E.K., 2004. The transforming growth factor-beta1 (TGFB1) gene is associated with chronic obstructive pulmonary disease (COPD). *Hum. Mol. Genet.* 13, 1649–1656. doi:10.1093/hmg/ddh171
- Chang, D.W., Xing, Z., Pan, Y., Algeciras-Schimmich, A., Barnhart, B.C., Yaish-Ohad, S., Peter, M.E., Yang, X., 2002. c-FLIP(L) is a dual function regulator for caspase-8 activation and CD95-mediated apoptosis. *EMBO J.* 21, 3704–3714. doi:10.1093/emboj/cdf356
- Chao, D.T., Korsmeyer, S.J., 1998. BCL-2 family: regulators of cell death. *Annu. Rev. Immunol.* 16, 395–419. doi:10.1146/annurev.immunol.16.1.395
- Chen, P.-F., Luo, Y.-L., Wang, W., Wang, J.-X., Lai, W.-Y., Hu, S.-M., Cheng, K.F., Al-Abed, Y., 2010. ISO-1, a macrophage migration inhibitory factor antagonist, inhibits airway remodeling in a murine model of chronic asthma. *Mol. Med.* 16, 400–408. doi:10.2119/molmed.2009.00128
- Cheng, S.L., Yu, C.J., Chen, C.J., Yang, P.C., 2004. Genetic polymorphism of epoxide hydrolase and glutathione S-transferase in COPD. *Eur. Respir. J.* 23, 818–824.
- Chinnaiyan, A.M., O'Rourke, K., Tewari, M., Dixit, V.M., 1995. FADD, a novel death domain-containing protein, interacts with the death domain of Fas and initiates apoptosis. *Cell* 81, 505–512.
- Chipuk, J.E., Bouchier-Hayes, L., Green, D.R., 2006. Mitochondrial outer membrane permeabilization during apoptosis: the innocent bystander scenario. *Cell Death Differ.* 13, 1396–1402. doi:10.1038/sj.cdd.4401963
- Clancy, L., Mruk, K., Archer, K., Woelfel, M., Mongkolsapaya, J., Screaton, G., Lenardo, M.J., Chan, F.K.-M., 2005. Pre-ligand assembly domain-mediated ligand-independent association between TRAIL receptor 4 (TR4) and TR2 regulates TRAIL-induced apoptosis. *Proc. Natl. Acad. Sci. U.S.A.* 102, 18099–18104. doi:10.1073/pnas.0507329102
- Cohen, G.M., 1997. Caspases: the executioners of apoptosis. *Biochem. J.* 326 ( Pt 1), 1–16.

- Cookson, W., 2004. The immunogenetics of asthma and eczema: a new focus on the epithelium. *Nat. Rev. Immunol.*
- Cosio, M.G., Majo, J., Cosio, M.G., 2002. Inflammation of the airways and lung parenchyma in COPD: role of T cells. *Chest* 121, 160S–165S.
- Cotter, T.G., Lennon, S.V., Glynn, J.M., Green, D.R., 1992. Microfilament-disrupting agents prevent the formation of apoptotic bodies in tumor cells undergoing apoptosis. *Cancer Res.* 52, 997–1005.
- Cozens, A.L., Yezzi, M.J., Kunzelmann, K., Ohru, T., Chin, L., Eng, K., Finkbeiner, W.E., Widdicombe, J.H., Gruenert, D.C., 1994. CFTR expression and chloride secretion in polarized immortal human bronchial epithelial cells. *Am. J. Respir. Cell Mol. Biol.* 10, 38–47. doi:10.1165/ajrcmb.10.1.7507342
- Cruickshank, S.M., McVay, L.D., Baumgart, D.C., Felsburg, P.J., Carding, S.R., 2004. Colonic epithelial cell mediated suppression of CD4 T cell activation. *Gut* 53, 678–684.
- Czabotar, P.E., Westphal, D., Dewson, G., Ma, S., Hockings, C., Fairlie, W.D., Lee, E.F., Yao, S., Robin, A.Y., Smith, B.J., Huang, D.C.S., Kluck, R.M., Adams, J.M., Colman, P.M., 2013. Bax crystal structures reveal how BH3 domains activate Bax and nucleate its oligomerization to induce apoptosis. *Cell* 152, 519–531. doi:10.1016/j.cell.2012.12.031
- Dahlen, B., Shute, J., Howarth, P., 1999. Immunohistochemical localisation of the matrix metalloproteinases MMP-3 and MMP-9 within the airways in asthma. *Thorax* 54, 590–596.
- Darding, M., Feltham, R., Tenev, T., Bianchi, K., Benetatos, C., Silke, J., Meier, P., 2011. Molecular determinants of Smac mimetic induced degradation of cIAP1 and cIAP2. *Cell Death Differ.* 18, 1376–1386. doi:10.1038/cdd.2011.10
- Dhein, J., Walczak, H., Westendorp, M.O., Bäuml, C., Stricker, K., Frank, R., Debatin, K.M., Krammer, P.H., 1995. Molecular mechanisms of APO-1/Fas(CD95)-mediated apoptosis in tolerance and AIDS. *Behring Inst. Mitt.* 13–20.
- Dickens, L.S., Boyd, R.S., Jukes-Jones, R., Hughes, M.A., Robinson, G.L., Fairall, L., Schwabe, J.W.R., Cain, K., Macfarlane, M., 2012. A Death Effector Domain Chain DISC Model Reveals a Crucial Role for Caspase-8 Chain Assembly in Mediating Apoptotic Cell Death. *Mol. Cell* 47, 291–305. doi:10.1016/j.molcel.2012.05.004
- Du, C., Fang, M., Li, Y., Li, L., Wang, X., 2000. Smac, a mitochondrial protein that promotes cytochrome c-dependent caspase activation by eliminating IAP inhibition. *Cell* 102, 33–42.
- Fadok, V.A., Voelker, D.R., Campbell, P.A., Cohen, J.J., Bratton, D.L., Henson, P.M., 1992. Exposure of phosphatidylserine on the surface of apoptotic lymphocytes triggers specific recognition and removal by macrophages. *J. Immunol.* 148, 2207–2216.
- Fang, Y., Sharp, G.C., Yagita, H., Braley-Mullen, H., 2008. A critical role for TRAIL in resolution of granulomatous experimental autoimmune thyroiditis. *J. Pathol.* 216, 505–513. doi:10.1002/path.2428
- Faustman, D., Davis, M., 2010. TNF receptor 2 pathway: drug target for autoimmune diseases. *Nat Rev Drug Discov* 9, 482–493. doi:10.1038/nrd3030
- Fischer, U., Jänicke, R.U., Schulze-Osthoff, K., 2003. Many cuts to ruin: a comprehensive update of caspase substrates. *Cell Death Differ.* 10, 76–100.

doi:10.1038/sj.cdd.4401160

- Flaster, H., Bernhagen, J., Calandra, T., Bucala, R., 2007. The macrophage migration inhibitory factor-glucocorticoid dyad: regulation of inflammation and immunity. *Mol. Endocrinol.* 21, 1267–1280. doi:10.1210/me.2007-0065
- Franciosi, L.G., Diamant, Z., Banner, K.H., Zuiker, R., Morelli, N., Kamberling, I.M.C., de Kam, M.L., Burggraaf, J., Cohen, A.F., Cazzola, M., Calzetta, L., Singh, D., Spina, D., Walker, M.J.A., Page, C.P., 2013. Efficacy and safety of RPL554, a dual PDE3 and PDE4 inhibitor, in healthy volunteers and in patients with asthma or chronic obstructive pulmonary disease: findings from four clinical trials. *Lancet Respir Med* 1, 714–727. doi:10.1016/S2213-2600(13)70187-5
- Freeman, C.M., Martinez, C.H., Todt, J.C., Martinez, F.J., Han, M.K., Thompson, D.L., McCloskey, L., Curtis, J.L., 2015. Acute exacerbations of chronic obstructive pulmonary disease are associated with decreased CD4+ & CD8+ T cells and increased growth & differentiation factor-15 (GDF-15) in peripheral blood. *Respir Res* 16, 94. doi:10.1186/s12931-015-0251-1
- Fricker, N., Beaudouin, J., Richter, P., Eils, R., Krammer, P.H., Lavrik, I.N., 2010. Model-based dissection of CD95 signaling dynamics reveals both a pro- and antiapoptotic role of c-FLIPL. *J. Cell Biol.* 190, 377–389. doi:10.1083/jcb.201002060
- Friedl, A., Stoesz, S.P., Buckley, P., Gould, M.N., 1999. Neutrophil gelatinase-associated lipocalin in normal and neoplastic human tissues. Cell type-specific pattern of expression. *Histochem. J.* 31, 433–441.
- Fuentes-Prior, P., Salvesen, G.S., 2004. The protein structures that shape caspase activity, specificity, activation and inhibition. *Biochem. J.* 384, 201–232. doi:10.1042/BJ20041142
- Gavathiotis, E., Suzuki, M., Davis, M.L., Pitter, K., Bird, G.H., Katz, S.G., Tu, H.-C., Kim, H., Cheng, E.H.-Y., Tjandra, N., Walensky, L.D., 2008. BAX activation is initiated at a novel interaction site. *Nature* 455, 1076–1081. doi:10.1038/nature07396
- Goetz, D.H., Holmes, M.A., Borregaard, N., Bluhm, M.E., Raymond, K.N., Strong, R.K., 2002. The neutrophil lipocalin NGAL is a bacteriostatic agent that interferes with siderophore-mediated iron acquisition. *Mol. Cell* 10, 1033–1043.
- Golks, A., Brenner, D., Fritsch, C., Krammer, P.H., Lavrik, I.N., 2005. c-FLIPR, a new regulator of death receptor-induced apoptosis. *J. Biol. Chem.* 280, 14507–14513. doi:10.1074/jbc.M414425200
- Gonzalvez, F., Ashkenazi, A., 2010. New insights into apoptosis signaling by Apo2L/TRAIL. *Oncogene* 29, 4752–4765. doi:10.1038/onc.2010.221
- Green, Brightling, C.E., Woltmann, G., Parker, D., Wardlaw, A.J., Pavord, I.D., 2002. Analysis of induced sputum in adults with asthma: identification of subgroup with isolated sputum neutrophilia and poor response to inhaled corticosteroids. *Thorax* 57, 875–879.
- Grunert, M., Gottschalk, K., Kapahnke, J., Gündisch, S., Kieser, A., Jeremias, I., 2012. The adaptor protein FADD and the initiator caspase-8 mediate activation of NF- $\kappa$ B by TRAIL. *Cell Death Dis* 3, e414. doi:10.1038/cddis.2012.154
- Guillot, C., Lecuit, T., 2013. Mechanics of epithelial tissue homeostasis and morphogenesis. *Science* 340, 1185–1189. doi:10.1126/science.1235249
- Guo, Y., Mishra, A., Howland, E., Zhao, C., Shukla, D., Weng, T., Liu, L., 2015.

- Platelet-derived Wnt antagonist Dickkopf-1 is implicated in ICAM-1/VCAM-1-mediated neutrophilic acute lung inflammation. *Blood*. doi:10.1182/blood-2015-02-622233
- Gwinn, W.M., Damsker, J.M., Falahati, R., Okwumabua, I., Kelly-Welch, A., Keegan, A.D., Vanpouille, C., Lee, J.J., Dent, L.A., Leitenberg, D., Bukrinsky, M.I., Constant, S.L., 2006. Novel approach to inhibit asthma-mediated lung inflammation using anti-CD147 intervention. *J. Immunol.* 177, 4870–4879.
- Hagaman, D.D., Okayama, Y., D'Ambrosio, C., Prussin, C., Gilfillan, A.M., Metcalfe, D.D., 2001. Secretion of interleukin-1 receptor antagonist from human mast cells after immunoglobulin E-mediated activation and after segmental antigen challenge. *Am. J. Respir. Cell Mol. Biol.* 25, 685–691. doi:10.1165/ajrcmb.25.6.4541
- Hagemann, T., Wilson, J., Kulbe, H., Li, N.F., Leinster, D.A., Charles, K., Klemm, F., Pukrop, T., Binder, C., Balkwill, F.R., 2005. Macrophages induce invasiveness of epithelial cancer cells via NF-kappa B and JNK. *J. Immunol.* 175, 1197–1205.
- Han, Y., Runge, M.S., Brasier, A.R., 1999. Angiotensin II induces interleukin-6 transcription in vascular smooth muscle cells through pleiotropic activation of nuclear factor-kappa B transcription factors. *Circ. Res.* 84, 695–703.
- Harbury, P.B., Zhang, T., Kim, P.S., Alber, T., 1993. A switch between two-, three-, and four-stranded coiled coils in GCN4 leucine zipper mutants. *Science* 262, 1401–1407.
- Harper, N., Farrow, S.N., Kaptein, A., Cohen, G.M., MacFarlane, M., 2001. Modulation of tumor necrosis factor apoptosis-inducing ligand-induced NF-kappa B activation by inhibition of apical caspases. *J. Biol. Chem.* 276, 34743–34752. doi:10.1074/jbc.M105693200
- Harper, N., Macfarlane, M., 2008. Recombinant TRAIL and TRAIL receptor analysis. *Meth. Enzymol.* 446, 293–313. doi:10.1016/S0076-6879(08)01618-2
- Hart, S.R., Davidson, A.C., 1999. Acute adult asthma--assessment of severity and management and comparison with British Thoracic Society Guidelines. *Respir Med* 93, 8–10.
- Hayashi, T., Stetler-Stevenson, W.G., Fleming, M.V., Fishback, N., Koss, M.N., Liotta, L.A., Ferrans, V.J., Travis, W.D., 1996. Immunohistochemical study of metalloproteinases and their tissue inhibitors in the lungs of patients with diffuse alveolar damage and idiopathic pulmonary fibrosis. *Am. J. Pathol.* 149, 1241–1256.
- Hettmer, S., McCarter, R., Ladisch, S., Kaucic, K., 2004. Alterations in neuroblastoma ganglioside synthesis by induction of GD1b synthase by retinoic acid. *Br. J. Cancer* 91, 389–397. doi:10.1038/sj.bjc.6601914
- Hoffmann, E., Dittrich-Breiholz, O., 2002. Multiple control of interleukin-8 gene expression. *Journal of leukocyte ...*
- Hogg, J.C., McDonough, J.E., Suzuki, M., 2013. Small airway obstruction in COPD: new insights based on micro-CT imaging and MRI imaging. *Chest* 143, 1436–1443. doi:10.1378/chest.12-1766
- Holgate, S.T., Noonan, M., Chanez, P., Busse, W., Dupont, L., Pavord, I., Hakulinen, A., Paolozzi, L., Wajdula, J., Zang, C., Nelson, H., Raible, D., 2011. Efficacy and safety of etanercept in moderate-to-severe asthma: a randomised, controlled trial. *Eur. Respir. J.* 37, 1352–1359.

doi:10.1183/09031936.00063510

- Holgate, S.T., Polosa, R., 2008. Treatment strategies for allergy and asthma. *Nat. Rev. Immunol.* 8, 218–230. doi:10.1038/nri2262
- Howarth, P.H., Babu, K.S., Arshad, H.S., Lau, L., Buckley, M., McConnell, W., Beckett, P., Ali, A.I., Chauhan, A., Wilson, S.J., Reynolds, A., Davies, D.E., Holgate, S.T., 2005. Tumour necrosis factor (TNF $\alpha$ ) as a novel therapeutic target in symptomatic corticosteroid dependent asthma. *Thorax* 60, 1012–1018. doi:10.1136/thx.2005.045260
- Hozumi, A., Nishimura, Y., Nishiuma, T., Kotani, Y., Yokoyama, M., 2001. Induction of MMP-9 in normal human bronchial epithelial cells by TNF- $\alpha$  via NF- $\kappa$ B-mediated pathway. *Am. J. Physiol. Lung Cell Mol. Physiol.* 281, L1444–52.
- Hsu, H., Shu, H.B., Pan, M.G., Goeddel, D.V., 1996. TRADD-TRAF2 and TRADD-FADD interactions define two distinct TNF receptor 1 signal transduction pathways. *Cell* 84, 299–308.
- Hu, W.H., Johnson, H., Shu, H.B., 1999. Tumor necrosis factor-related apoptosis-inducing ligand receptors signal NF- $\kappa$ B and JNK activation and apoptosis through distinct pathways. *J. Biol. Chem.* 274, 30603–30610.
- Huang, L., Smit, J.W., Meijer, D.K., Vore, M., 2000. Mrp2 is essential for estradiol-17 $\beta$ ( $\beta$ -D -glucuronide)-induced cholestasis in rats. *Hepatology* 32, 66–72. doi:10.1053/jhep.2000.8263
- Hughes, M.A., Harper, N., Butterworth, M., Cain, K., Cohen, G.M., Macfarlane, M., 2009. Reconstitution of the death-inducing signaling complex reveals a substrate switch that determines CD95-mediated death or survival. *Mol. Cell* 35, 265–279. doi:10.1016/j.molcel.2009.06.012
- Janssen, E.M., Droin, N.M., Lemmens, E.E., Pinkoski, M.J., Bensinger, S.J., Ehst, B.D., Griffith, T.S., Green, D.R., Schoenberger, S.P., 2005. CD4+ T-cell help controls CD8+ T-cell memory via TRAIL-mediated activation-induced cell death. *Nature* 434, 88–93. doi:10.1038/nature03337
- Jeon, Y.-J., Middleton, J., Kim, T., Laganà, A., Piovan, C., Secchiero, P., Nuovo, G.J., Cui, R., Joshi, P., Romano, G., Di Leva, G., Lee, B.-K., Sun, H.-L., Kim, Y., Fadda, P., Alder, H., Garofalo, M., Croce, C.M., 2015. A set of NF- $\kappa$ B-regulated microRNAs induces acquired TRAIL resistance in lung cancer. *Proceedings of the National Academy of Sciences* 112, E3355–64. doi:10.1073/pnas.1504630112
- Jones, C.E., Chan, K., 2002. Interleukin-17 stimulates the expression of interleukin-8, growth-related oncogene- $\alpha$ , and granulocyte-colony-stimulating factor by human airway epithelial cells. *Am. J. Respir. Cell Mol. Biol.* 26, 748–753.
- Kalandadze, A., Galleno, M., Foncerrada, L., Strominger, J.L., Wucherpfennig, K.W., 1996. Expression of recombinant HLA-DR2 molecules. Replacement of the hydrophobic transmembrane region by a leucine zipper dimerization motif allows the assembly and secretion of soluble DR  $\alpha$   $\beta$  heterodimers. *J. Biol. Chem.* 271, 20156–20162.
- Kataoka, T., Budd, R.C., Holler, N., Thome, M., Martinon, F., Irmeler, M., Burns, K., Hahne, M., Kennedy, N., Kovacsovics, M., Tschopp, J., 2000. The caspase-8 inhibitor FLIP promotes activation of NF- $\kappa$ B and Erk signaling pathways. *Curr. Biol.* 10, 640–648.

- Kay, J.E., Kromwel, L., Doe, S.E., Denyer, M., 1991. Inhibition of T and B lymphocyte proliferation by rapamycin. *Immunology* 72, 544–549.
- Keatings, V.M., Cave, S.J., Henry, M.J., Morgan, K., O'Connor, C.M., FitzGerald, M.X., Kalsheker, N., 2000. A polymorphism in the tumor necrosis factor-alpha gene promoter region may predispose to a poor prognosis in COPD. *Chest* 118, 971–975.
- Keatings, V.M., Collins, P.D., Scott, D.M., Barnes, P.J., 1996. Differences in interleukin-8 and tumor necrosis factor-alpha in induced sputum from patients with chronic obstructive pulmonary disease or asthma. *Am. J. Respir. Crit. Care Med.* 153, 530–534. doi:10.1164/ajrccm.153.2.8564092
- Kelley, S.K., Harris, L.A., Xie, D., DeForge, L., Totpal, K., Bussiere, J., Fox, J.A., 2001. Preclinical studies to predict the disposition of Apo2L/tumor necrosis factor-related apoptosis-inducing ligand in humans: characterization of in vivo efficacy, pharmacokinetics, and safety. *J. Pharmacol. Exp. Ther.* 299, 31–38.
- Kerr, J.F., Wyllie, A.H., Currie, A.R., 1972. Apoptosis: a basic biological phenomenon with wide-ranging implications in tissue kinetics. *Br. J. Cancer* 26, 239–257.
- Kischkel, F.C., Lawrence, D.A., Chuntharapai, A., Schow, P., Kim, K.J., Ashkenazi, A., 2000. Apo2L/TRAIL-dependent recruitment of endogenous FADD and caspase-8 to death receptors 4 and 5. *Immunity* 12, 611–620.
- Klaus, S.J., Phillips, N.E., Parker, D.C., 1993. Effects of IL-4 and Fc gamma receptor II engagement on Egr-1 expression during stimulation of B lymphocytes by membrane immunoglobulin crosslinking. *Mol. Immunol.* 30, 1553–1558.
- Kohlhaas, S.L., Craxton, A., Sun, X.-M., Pinkoski, M.J., Cohen, G.M., 2007. Receptor-mediated endocytosis is not required for tumor necrosis factor-related apoptosis-inducing ligand (TRAIL)-induced apoptosis. *J. Biol. Chem.* 282, 12831–12841. doi:10.1074/jbc.M700438200
- Kong, Y.Y., Feige, U., Sarosi, I., Bolon, B., Tafuri, A., Morony, S., Capparelli, C., Li, J., Elliott, R., McCabe, S., Wong, T., Campagnuolo, G., Moran, E., Bogoch, E.R., Van, G., Nguyen, L.T., Ohashi, P.S., Lacey, D.L., Fish, E., Boyle, W.J., Penninger, J.M., 1999. Activated T cells regulate bone loss and joint destruction in adjuvant arthritis through osteoprotegerin ligand. *Nature* 402, 304–309. doi:10.1038/46303
- Kraft, M., 2006. Asthma and chronic obstructive pulmonary disease exhibit common origins in any country! *Am. J. Respir. Crit. Care Med.* 174, 238–40–discussion 243–4. doi:10.1164/rccm.2604007
- Krueger, A., Schmitz, I., Baumann, S., Krammer, P.H., Kirchhoff, S., 2001. Cellular FLICE-inhibitory protein splice variants inhibit different steps of caspase-8 activation at the CD95 death-inducing signaling complex. *J. Biol. Chem.* 276, 20633–20640. doi:10.1074/jbc.M101780200
- Laitinen, T., Polvi, A., Rydman, P., Vendelin, J., Pulkkinen, V., 2004. Characterization of a common susceptibility locus for asthma-related traits. *Science*.
- Larché, M., 2007. Regulatory T cells in allergy and asthma. *Chest* 132, 1007–1014. doi:10.1378/chest.06-2434
- Lawrence, D., Shahrokh, Z., Marsters, S., Achilles, K., Shih, D., Mounho, B., Hillan, K., Totpal, K., DeForge, L., Schow, P., Hooley, J., Sherwood, S., Pai,

- R., Leung, S., Khan, L., Gliniak, B., Bussiere, J., Smith, C.A., Strom, S.S., Kelley, S., Fox, J.A., Thomas, D., Ashkenazi, A., 2001. Differential hepatocyte toxicity of recombinant Apo2L/TRAIL versions. *Nat. Med.* 7, 383–385. doi:10.1038/86397
- Lee, Y.-T., Chen, S.-C., Shyu, L.-Y., Lee, M.-C., Wu, T.-C., Tsao, S.-M., Yang, S.-F., 2012. Significant elevation of plasma cathepsin B and cystatin C in patients with community-acquired pneumonia. *Clin. Chim. Acta* 413, 630–635. doi:10.1016/j.cca.2011.12.010
- Leopold, J.G., Gough, J., 1957. The centrilobular form of hypertrophic emphysema and its relation to chronic bronchitis. *Thorax* 12, 219–235.
- Letai, A., Bassik, M.C., Walensky, L.D., Sorcinelli, M.D., Weiler, S., Korsmeyer, S.J., 2002. Distinct BH3 domains either sensitize or activate mitochondrial apoptosis, serving as prototype cancer therapeutics. *Cancer Cell* 2, 183–192.
- Levy, M.L., Fletcher, M., Price, D.B., Hausen, T., Halbert, R.J., Yawn, B.P., 2006. International Primary Care Respiratory Group (IPCRG) Guidelines: diagnosis of respiratory diseases in primary care. *Prim Care Respir J.* doi:10.1016/j.pcrj.2005.10.004
- Li, H., Zhu, H., Xu, C.J., Yuan, J., 1998. Cleavage of BID by caspase 8 mediates the mitochondrial damage in the Fas pathway of apoptosis. *Cell* 94, 491–501.
- Li, L., Thomas, R.M., Suzuki, H., De Brabander, J.K., Wang, X., Harran, P.G., 2004. A small molecule Smac mimic potentiates TRAIL- and TNF $\alpha$ -mediated cell death. *Science* 305, 1471–1474. doi:10.1126/science.1098231
- Lin, Y., Devin, A., Cook, A., Keane, M.M., Kelliher, M., Lipkowitz, S., Liu, Z.G., 2000. The death domain kinase RIP is essential for TRAIL (Apo2L)-induced activation of IkappaB kinase and c-Jun N-terminal kinase. *Mol. Cell. Biol.* 20, 6638–6645.
- Locksley, R.M., Killeen, N., Lenardo, M.J., 2001. The TNF and TNF receptor superfamilies: integrating mammalian biology. *Cell* 104, 487–501.
- Lopez, A.D., Shibuya, K., Rao, C., Mathers, C.D., Hansell, A.L., Held, L.S., Schmid, V., Buist, S., 2006. Chronic obstructive pulmonary disease: current burden and future projections. *Eur. Respir. J.* 27, 397–412. doi:10.1183/09031936.06.00025805
- Löwhagen, O., 2012. Diagnosis of asthma - a new approach. *Allergy* 67, 713–717. doi:10.1111/j.1398-9995.2012.02821.x
- Lukacs, N.W., Strieter, R.M., Chensue, S.W., Widmer, M., Kunkel, S.L., 1995. TNF-alpha mediates recruitment of neutrophils and eosinophils during airway inflammation. *J. Immunol.* 154, 5411–5417.
- Luo, X., Budihardjo, I., Zou, H., Slaughter, C., Wang, X., 1998. Bid, a Bcl2 interacting protein, mediates cytochrome c release from mitochondria in response to activation of cell surface death receptors. *Cell* 94, 481–490.
- MacFarlane, M., Ahmad, M., Srinivasula, S.M., Fernandes-Alnemri, T., Cohen, G.M., Alnemri, E.S., 1997. Identification and molecular cloning of two novel receptors for the cytotoxic ligand TRAIL. *J. Biol. Chem.* 272, 25417–25420.
- Macfarlane, M., Harper, N., Snowden, R.T., Dyer, M.J.S., Barnett, G.A., Pringle, J.H., Cohen, G.M., 2002. Mechanisms of resistance to TRAIL-induced apoptosis in primary B cell chronic lymphocytic leukaemia. *Oncogene* 21, 6809–6818. doi:10.1038/sj.onc.1205853
- MacFarlane, M., Inoue, S., Kohlhaas, S.L., Majid, A., Harper, N., Kennedy, D.B.J.,

- Dyer, M.J.S., Cohen, G.M., 2005a. Chronic lymphocytic leukemic cells exhibit apoptotic signaling via TRAIL-R1. *Cell Death Differ.* 12, 773–782. doi:10.1038/sj.cdd.4401649
- Macfarlane, M., Kohlhaas, S.L., Sutcliffe, M.J., Dyer, M.J.S., Cohen, G.M., 2005b. TRAIL receptor-selective mutants signal to apoptosis via TRAIL-R1 in primary lymphoid malignancies. *Cancer Res.* 65, 11265–11270. doi:10.1158/0008-5472.CAN-05-2801
- MacFarlane, M., Merrison, W., Dinsdale, D., Cohen, G.M., 2000. Active caspases and cleaved cytokeratins are sequestered into cytoplasmic inclusions in TRAIL-induced apoptosis. *J. Cell Biol.* 148, 1239–1254.
- Maksimow, M., Santanen, M., Jalkanen, S., Hänninen, A., 2003. Responding naive T cells differ in their sensitivity to Fas engagement: early death of many T cells is compensated by costimulation of surviving T cells. *Blood* 101, 4022–4028. doi:10.1182/blood-2002-06-1904
- Mannino, D.M., Buist, A.S., 2007. Global burden of COPD: risk factors, prevalence, and future trends. *Lancet* 370, 765–773. doi:10.1016/S0140-6736(07)61380-4
- Marsters, S.A., Sheridan, J.P., Pitti, R.M., Huang, A., Skubatch, M., Baldwin, D., Yuan, J., Gurney, A., Goddard, A.D., Godowski, P., Ashkenazi, A., 1997. A novel receptor for Apo2L/TRAIL contains a truncated death domain. *Curr. Biol.* 7, 1003–1006.
- Mascher, B., Schlenke, P., Seyfarth, M., 1999. Expression and kinetics of cytokines determined by intracellular staining using flow cytometry. *J. Immunol. Methods* 223, 115–121.
- McDonough, J.E., Yuan, R., Suzuki, M., Seyednejad, N., Elliott, W.M., Sanchez, P.G., Wright, A.C., Geffer, W.B., Litzky, L., Coxson, H.O., Paré, P.D., Sin, D.D., Pierce, R.A., Woods, J.C., McWilliams, A.M., Mayo, J.R., Lam, S.C., Cooper, J.D., Hogg, J.C., 2011. Small-airway obstruction and emphysema in chronic obstructive pulmonary disease. *N. Engl. J. Med.* 365, 1567–1575. doi:10.1056/NEJMoa1106955
- McGrath, E.E., Lawrie, A., Marriott, H.M., Mercer, P., Cross, S.S., Arnold, N., Singleton, V., Thompson, A.A.R., Walmsley, S.R., Renshaw, S.A., Sabroe, I., Chambers, R.C., Dockrell, D.H., Whyte, M.K.B., 2012. Deficiency of tumour necrosis factor-related apoptosis-inducing ligand exacerbates lung injury and fibrosis. *Thorax* 67, 796–803. doi:10.1136/thoraxjnl-2011-200863
- McGrath, E.E., Marriott, H.M., Lawrie, A., Francis, S.E., Sabroe, I., Renshaw, S.A., Dockrell, D.H., Whyte, M.K.B., 2011. TNF-related apoptosis-inducing ligand (TRAIL) regulates inflammatory neutrophil apoptosis and enhances resolution of inflammation. *J. Leukoc. Biol.* 90, 855–865. doi:10.1189/jlb.0211062
- Mercurio, F., Zhu, H., Murray, B.W., Shevchenko, A., Bennett, B.L., Li, J., Young, D.B., Barbosa, M., Mann, M., Manning, A., Rao, A., 1997. IKK-1 and IKK-2: cytokine-activated I $\kappa$ B kinases essential for NF- $\kappa$ B activation. *Science* 278, 860–866.
- Meyer, E.H., DeKruyff, R.H., Umetsu, D.T., 2008. T cells and NKT cells in the pathogenesis of asthma. *Annu. Rev. Med.* 59, 281–292. doi:10.1146/annurev.med.59.061506.154139
- Mérino, D., Lalaoui, N., Morizot, A., Schneider, P., Solary, E., Micheau, O., 2006. Differential inhibition of TRAIL-mediated DR5-DISC formation by decoy

- receptors 1 and 2. *Mol. Cell. Biol.* 26, 7046–7055. doi:10.1128/MCB.00520-06
- Miki, Y., Ono, K., Hata, S., Suzuki, T., Kumamoto, H., Sasano, H., 2012. The advantages of co-culture over mono cell culture in simulating in vivo environment. *J. Steroid Biochem. Mol. Biol.* 131, 68–75. doi:10.1016/j.jsbmb.2011.12.004
- Muchmore, S.W., Sattler, M., Liang, H., Meadows, R.P., Harlan, J.E., Yoon, H.S., Nettesheim, D., Chang, B.S., Thompson, C.B., Wong, S.L., Ng, S.L., Fesik, S.W., 1996. X-ray and NMR structure of human Bcl-xL, an inhibitor of programmed cell death. *Nature* 381, 335–341. doi:10.1038/381335a0
- Nagata, S., Golstein, P., 1995. The Fas death factor. *Science* 267, 1449–1456.
- Nakano, K., Vousden, K.H., 2001. PUMA, a novel proapoptotic gene, is induced by p53. *Mol. Cell* 7, 683–694.
- Natoni, A., Macfarlane, M., Inoue, S., Walewska, R., Majid, A., Knee, D., Stover, D.R., Dyer, M.J.S., Cohen, G.M., 2007. TRAIL signals to apoptosis in chronic lymphocytic leukaemia cells primarily through TRAIL-R1 whereas cross-linked agonistic TRAIL-R2 antibodies facilitate signalling via TRAIL-R2. *Br. J. Haematol.* 139, 568–577. doi:10.1111/j.1365-2141.2007.06852.x
- O'Byrne, P.M., Inman, M.D., 2003. Airway hyperresponsiveness. *Chest* 123, 411S–6S.
- O'Shea, E.K., Rutkowski, R., Kim, P.S., 1989. Evidence that the leucine zipper is a coiled coil. *Science* 243, 538–542.
- Oda, E., Ohki, R., Murasawa, H., Nemoto, J., Shibue, T., Yamashita, T., Tokino, T., Taniguchi, T., Tanaka, N., 2000. Noxa, a BH3-only member of the Bcl-2 family and candidate mediator of p53-induced apoptosis. *Science* 288, 1053–1058.
- Oh, C.K., Leigh, R., McLaurin, K.K., Kim, K., Hultquist, M., Molino, N.A., 2013. A randomized, controlled trial to evaluate the effect of an anti-interleukin-9 monoclonal antibody in adults with uncontrolled asthma. *Respir Res* 14, 93. doi:10.1186/1465-9921-14-93
- Pace, E., Ferraro, M., Minervini, M.I., Vitulo, P., Pipitone, L., Chiappara, G., Siena, L., Montalbano, A.M., Johnson, M., Gjomarkaj, M., 2012. Beta defensin-2 is reduced in central but not in distal airways of smoker COPD patients. *PLoS ONE* 7, e33601. doi:10.1371/journal.pone.0033601
- Pahl, H.L., 1999. Activators and target genes of Rel/NF-kappaB transcription factors. *Oncogene* 18, 6853–6866. doi:10.1038/sj.onc.1203239
- Palmer, L.J., Burton, P.R., Faux, J.A., James, A.L., Musk, A.W., Cookson, W.O., 2000. Independent inheritance of serum immunoglobulin E concentrations and airway responsiveness. *Am. J. Respir. Crit. Care Med.* 161, 1836–1843. doi:10.1164/ajrccm.161.6.9805104
- Pan, G., O'Rourke, K., Chinnaiyan, A.M., Gentz, R., Ebner, R., Ni, J., Dixit, V.M., 1997. The receptor for the cytotoxic ligand TRAIL. *Science* 276, 111–113.
- Pardo, J., Aguilo, J.I., Anel, A., Martin, P., Joeckel, L., Borner, C., Wallich, R., Müllbacher, A., Froelich, C.J., Simon, M.M., 2009. The biology of cytotoxic cell granule exocytosis pathway: granzymes have evolved to induce cell death and inflammation. *Microbes Infect.* 11, 452–459. doi:10.1016/j.micinf.2009.02.004
- Park, K.-J., Lee, S.-H., Kim, T.-I., Lee, H.-W., Lee, C.-H., Kim, E.-H., Jang, J.-Y., Choi, K.S., Kwon, M.-H., Kim, Y.-S., 2007. A human scFv antibody against TRAIL receptor 2 induces autophagic cell death in both TRAIL-sensitive and

- TRAIL-resistant cancer cells. *Cancer Res.* 67, 7327–7334. doi:10.1158/0008-5472.CAN-06-4766
- Pickard, A., McCance, D.J., 2015. IGF-Binding Protein 2 - Oncogene or Tumor Suppressor? *Front Endocrinol (Lausanne)* 6, 25. doi:10.3389/fendo.2015.00025
- Rabe, K.F., Hurd, S., Anzueto, A., Barnes, P.J., Buist, S.A., Calverley, P., Fukuchi, Y., Jenkins, C., Rodriguez-Roisin, R., van Weel, C., Zielinski, J., Global Initiative for Chronic Obstructive Lung Disease, 2007. Global strategy for the diagnosis, management, and prevention of chronic obstructive pulmonary disease: GOLD executive summary. *Am. J. Respir. Crit. Care Med.* 176, 532–555. doi:10.1164/rccm.200703-456SO
- Ramirez, R.D., Sheridan, S., Girard, L., Sato, M., Kim, Y., Pollack, J., Peyton, M., Zou, Y., Kurie, J.M., Dimaio, J.M., Milchgrub, S., Smith, A.L., Souza, R.F., Gilbey, L., Zhang, X., Gandia, K., Vaughan, M.B., Wright, W.E., Gazdar, A.F., Shay, J.W., Minna, J.D., 2004. Immortalization of human bronchial epithelial cells in the absence of viral oncoproteins. *Cancer Res.* 64, 9027–9034. doi:10.1158/0008-5472.CAN-04-3703
- Ravi, R., Bedi, G.C., Engstrom, L.W., Zeng, Q., Mookerjee, B., Gélinas, C., Fuchs, E.J., Bedi, A., 2001. Regulation of death receptor expression and TRAIL/Apo2L-induced apoptosis by NF-kappaB. *Nat. Cell Biol.* 3, 409–416. doi:10.1038/35070096
- Reddel, R.R., Ke, Y., Gerwin, B.I., McMenamin, M.G., Lechner, J.F., Su, R.T., Brash, D.E., Park, J.B., Rhim, J.S., Harris, C.C., 1988. Transformation of human bronchial epithelial cells by infection with SV40 or adenovirus-12 SV40 hybrid virus, or transfection via strontium phosphate coprecipitation with a plasmid containing SV40 early region genes. *Cancer Res.* 48, 1904–1909.
- Reddel, R.R., Salghetti, S.E., Willey, J.C., Ohnuki, Y., Ke, Y., Gerwin, B.I., Lechner, J.F., Harris, C.C., 1993. Development of tumorigenicity in simian virus 40-immortalized human bronchial epithelial cell lines. *Cancer Res.* 53, 985–991.
- Ribe, E.M., Serrano-Saiz, E., Akpan, N., Troy, C.M., 2008. Mechanisms of neuronal death in disease: defining the models and the players. *Biochem. J.* 415, 165–182. doi:10.1042/BJ20081118
- Riedl, S.J., Salvesen, G.S., 2007. The apoptosome: signalling platform of cell death. *Nat Rev Mol Cell Biol* 8, 405–413. doi:10.1038/nrm2153
- Robertson, N.M., Zangrilli, J.G., Steplewski, A., Hastie, A., Lindemeyer, R.G., Planeta, M.A., Smith, M.K., Innocent, N., Musani, A., Pascual, R., Peters, S., Litwack, G., 2002. Differential expression of TRAIL and TRAIL receptors in allergic asthmatics following segmental antigen challenge: evidence for a role of TRAIL in eosinophil survival. *J. Immunol.* 169, 5986–5996.
- Rodrigo, G.J., Neffen, H., Castro-Rodriguez, J.A., 2011. Efficacy and safety of subcutaneous omalizumab vs placebo as add-on therapy to corticosteroids for children and adults with asthma: a systematic review. *Chest* 139, 28–35. doi:10.1378/chest.10-1194
- Roland, N.J., Bhalla, R.K., Earis, J., 2004. The local side effects of inhaled corticosteroids: current understanding and review of the literature. *Chest* 126, 213–219. doi:10.1378/chest.126.1.213
- Rosenstreich, D.L., Tu, J.H., Kinkade, P.R., Maurer-Fogy, I., Kahn, J., Barton,

- R.W., Farina, P.R., 1988. A human urine-derived interleukin 1 inhibitor. Homology with deoxyribonuclease I. *J. Exp. Med.* 168, 1767–1779.
- Rossin, A., Derouet, M., Abdel-Sater, F., Hueber, A.-O., 2009. Palmitoylation of the TRAIL receptor DR4 confers an efficient TRAIL-induced cell death signalling. *Biochem. J.* 419, 185–92– 2 p following 192. doi:10.1042/BJ20081212
- Rudner, J., Jendrossek, V., Lauber, K., Daniel, P.T., Wesselborg, S., Belka, C., 2005. Type I and type II reactions in TRAIL-induced apoptosis -- results from dose-response studies. *Oncogene* 24, 130–140. doi:10.1038/sj.onc.1208191
- Saetta, M., Di Stefano, A., Turato, G., Facchini, F.M., Corbino, L., Mapp, C.E., Maestrelli, P., Ciaccia, A., Fabbri, L.M., 1998. CD8+ T-lymphocytes in peripheral airways of smokers with chronic obstructive pulmonary disease. *Am. J. Respir. Crit. Care Med.* 157, 822–826. doi:10.1164/ajrccm.157.3.9709027
- Sagi, L., Baum, S., Agmon-Levin, N., Sherer, Y., Katz, B.S.P., Barzilai, O., Ram, M., Bizzaro, N., SanMarco, M., Trau, H., Shoenfeld, Y., 2011. Autoimmune bullous diseases the spectrum of infectious agent antibodies and review of the literature. *Autoimmun Rev* 10, 527–535. doi:10.1016/j.autrev.2011.04.003
- Salim, H., Zong, D., Hååg, P., Novak, M., Mörk, B., Lewensohn, R., Lundholm, L., Viktorsson, K., 2015. DKK1 is a potential novel mediator of cisplatin-refractoriness in non-small cell lung cancer cell lines. *BMC Cancer* 15, 628. doi:10.1186/s12885-015-1635-9
- Salvesen, G.S., Dixit, V.M., 1999. Caspase activation: the induced-proximity model. *Proc. Natl. Acad. Sci. U.S.A.* 96, 10964–10967.
- Sarosiek, K.A., Chi, X., Bachman, J.A., Sims, J.J., Montero, J., Patel, L., Flanagan, A., Andrews, D.W., Sorger, P., Letai, A., 2013. BID preferentially activates BAK while BIM preferentially activates BAX, affecting chemotherapy response. *Mol. Cell* 51, 751–765. doi:10.1016/j.molcel.2013.08.048
- Sattler, M., Liang, H., Nettlesheim, D., Meadows, R.P., Harlan, J.E., Eberstadt, M., Yoon, H.S., Shuker, S.B., Chang, B.S., Minn, A.J., Thompson, C.B., Fesik, S.W., 1997. Structure of Bcl-xL-Bak peptide complex: recognition between regulators of apoptosis. *Science* 275, 983–986.
- Savill, J., 1997. Apoptosis in resolution of inflammation. *J. Leukoc. Biol.* 61, 375–380.
- Scheurich, P., Thoma, B., Ucer, U., Pfizenmaier, K., 1987. Immunoregulatory activity of recombinant human tumor necrosis factor (TNF)-alpha: induction of TNF receptors on human T cells and TNF-alpha-mediated enhancement of T cell responses. *J. Immunol.* 138, 1786–1790.
- Schmidt, R., Staats, P., Groneberg, D.A., Wagner, U., 2008. Effect of montelukast on platelet activating factor- and tachykinin induced mucus secretion in the rat. *J Occup Med Toxicol* 3, 5. doi:10.1186/1745-6673-3-5
- Schmidt, T.G., Skerra, A., 1993. The random peptide library-assisted engineering of a C-terminal affinity peptide, useful for the detection and purification of a functional Ig Fv fragment. *Protein Eng.* 6, 109–122.
- Schmidt, T.G.M., Skerra, A., 2007. The Strep-tag system for one-step purification and high-affinity detection or capturing of proteins. *Nat Protoc* 2, 1528–1535. doi:10.1038/nprot.2007.209
- Schmidt-Ott, K.M., Mori, K., Li, J.Y., Kalandadze, A., Cohen, D.J., Devarajan, P.,

- Barasch, J., 2007. Dual action of neutrophil gelatinase-associated lipocalin. *J. Am. Soc. Nephrol.* 18, 407–413. doi:10.1681/ASN.2006080882
- Schmitz, I., Weyd, H., Krueger, A., Baumann, S., Fas, S.C., Krammer, P.H., Kirchhoff, S., 2004. Resistance of short term activated T cells to CD95-mediated apoptosis correlates with de novo protein synthesis of c-FLIPshort. *J. Immunol.* 172, 2194–2200.
- Schneider, P., Thome, M., Burns, K., Bodmer, J.L., Hofmann, K., Kataoka, T., Holler, N., Tschopp, J., 1997. TRAIL receptors 1 (DR4) and 2 (DR5) signal FADD-dependent apoptosis and activate NF-kappaB. *Immunity* 7, 831–836.
- Scott, F.L., Denault, J.-B., Riedl, S.J., Shin, H., Renatus, M., Salvesen, G.S., 2005. XIAP inhibits caspase-3 and -7 using two binding sites: evolutionarily conserved mechanism of IAPs. *EMBO J.* 24, 645–655. doi:10.1038/sj.emboj.7600544
- Sheridan, J.P., Marsters, S.A., Pitti, R.M., Gurney, A., Skubatch, M., Baldwin, D., Ramakrishnan, L., Gray, C.L., Baker, K., Wood, W.I., Goddard, A.D., Godowski, P., Ashkenazi, A., 1997. Control of TRAIL-induced apoptosis by a family of signaling and decoy receptors. *Science* 277, 818–821.
- Shi, Y., 2002. A conserved tetrapeptide motif: potentiating apoptosis through IAP-binding. *Cell Death Differ.* 9, 93–95. doi:10.1038/sj.cdd.4400957
- Shin, Y., Yoon, S.-H., Choe, E.-Y., Cho, S.-H., Woo, C.-H., Rho, J.-Y., Kim, J.-H., 2007. PMA-induced up-regulation of MMP-9 is regulated by a PKCalpha-NF-kappaB cascade in human lung epithelial cells. *Exp. Mol. Med.* 39, 97–105. doi:10.1038/emm.2007.11
- Shiozaki, E.N., Chai, J., Rigotti, D.J., Riedl, S.J., Li, P., Srinivasula, S.M., Alnemri, E.S., Fairman, R., Shi, Y., 2003. Mechanism of XIAP-mediated inhibition of caspase-9. *Mol. Cell* 11, 519–527.
- Siegel, R.M., Frederiksen, J.K., Zacharias, D.A., Chan, F.K., Johnson, M., Lynch, D., Tsien, R.Y., Lenardo, M.J., 2000. Fas preassociation required for apoptosis signaling and dominant inhibition by pathogenic mutations. *Science* 288, 2354–2357.
- Song, J.H., Tse, M.C.L., Bellail, A., Phuphanich, S., Khuri, F., Kneteman, N.M., Hao, C., 2007. Lipid rafts and nonrafts mediate tumor necrosis factor related apoptosis-inducing ligand induced apoptotic and nonapoptotic signals in non small cell lung carcinoma cells. *Cancer Res.* 67, 6946–6955. doi:10.1158/0008-5472.CAN-06-3896
- Sousa, A.R., Lane, S.J., Nakhosteen, J.A., Lee, T.H., Poston, R.N., 1996. Expression of interleukin-1 beta (IL-1beta) and interleukin-1 receptor antagonist (IL-1ra) on asthmatic bronchial epithelium. *Am. J. Respir. Crit. Care Med.* 154, 1061–1066. doi:10.1164/ajrccm.154.4.8887608
- Sprick, M.R., Weigand, M.A., Rieser, E., Rauch, C.T., Juo, P., Blenis, J., Krammer, P.H., Walczak, H., 2000. FADD/MORT1 and caspase-8 are recruited to TRAIL receptors 1 and 2 and are essential for apoptosis mediated by TRAIL receptor 2. *Immunity* 12, 599–609.
- Srinivasula, S.M., Hegde, R., Saleh, A., Datta, P., Shiozaki, E., Chai, J., Lee, R.A., Robbins, P.D., Fernandes-Alnemri, T., Shi, Y., Alnemri, E.S., 2001. A conserved XIAP-interaction motif in caspase-9 and Smac/DIABLO regulates caspase activity and apoptosis. *Nature* 410, 112–116. doi:10.1038/35065125
- Steinwede, K., Henken, S., Bohling, J., Maus, R., Ueberberg, B., Brumshagen, C.,

- Brincks, E.L., Griffith, T.S., Welte, T., Maus, U.A., 2012. TNF-related apoptosis-inducing ligand (TRAIL) exerts therapeutic efficacy for the treatment of pneumococcal pneumonia in mice. *J. Exp. Med.* 209, 1937–1952. doi:10.1084/jem.20120983
- Stennicke, H.R., Renatus, M., Meldal, M., Salvesen, G.S., 2000. Internally quenched fluorescent peptide substrates disclose the subsite preferences of human caspases 1, 3, 6, 7 and 8. *Biochem. J.* 350 Pt 2, 563–568.
- Stevens, L.A., Schmid, C.H., Greene, T., Li, L., Beck, G.J., Joffe, M.M., Froissart, M., Kusek, J.W., Zhang, Y.L., Coresh, J., Levey, A.S., 2009. Factors other than glomerular filtration rate affect serum cystatin C levels. *Kidney Int.* 75, 652–660. doi:10.1038/ki.2008.638
- Stokes, J.R., 2014. Promising future therapies for asthma. *Int. Immunopharmacol.* 23, 373–377. doi:10.1016/j.intimp.2014.05.032
- Stoller, J.K., Niewoehner, D.E., Fan, V.S., 2006. Disease management as an evolving role for respiratory therapists. *Respir Care* 51, 1400–1402.
- Sun, X.M., MacFarlane, M., Zhuang, J., Wolf, B.B., Green, D.R., Cohen, G.M., 1999. Distinct caspase cascades are initiated in receptor-mediated and chemical-induced apoptosis. *J. Biol. Chem.* 274, 5053–5060.
- Tait, S.W.G., Green, D.R., 2010. Mitochondria and cell death: outer membrane permeabilization and beyond. *Nat Rev Mol Cell Biol* 11, 621–632. doi:10.1038/nrm2952
- Thornberry, N.A., Rano, T.A., Peterson, E.P., Rasper, D.M., Timkey, T., Garcia-Calvo, M., Houtzager, V.M., Nordstrom, P.A., Roy, S., Vaillancourt, J.P., Chapman, K.T., Nicholson, D.W., 1997. A combinatorial approach defines specificities of members of the caspase family and granzyme B. Functional relationships established for key mediators of apoptosis. *J. Biol. Chem.* 272, 17907–17911.
- Truneh, A., Sharma, S., Silverman, C., Khandekar, S., Reddy, M.P., Deen, K.C., McLaughlin, M.M., Srinivasula, S.M., Livi, G.P., Marshall, L.A., Alnemri, E.S., Williams, W.V., Doyle, M.L., 2000. Temperature-sensitive differential affinity of TRAIL for its receptors. DR5 is the highest affinity receptor. *J. Biol. Chem.* 275, 23319–23325. doi:10.1074/jbc.M910438199
- Tschopp, J., Irmeler, M., Thome, M., 1998. Inhibition of fas death signals by FLIPs. *Curr. Opin. Immunol.* 10, 552–558.
- Van Cruchten, S., Van Den Broeck, W., 2002. Morphological and biochemical aspects of apoptosis, oncosis and necrosis. *Anat Histol Embryol* 31, 214–223.
- Varfolomeev, E., Maecker, H., Sharp, D., Lawrence, D., Renz, M., Vucic, D., Ashkenazi, A., 2005. Molecular determinants of kinase pathway activation by Apo2 ligand/tumor necrosis factor-related apoptosis-inducing ligand. *J. Biol. Chem.* 280, 40599–40608. doi:10.1074/jbc.M509560200
- Verhagen, A.M., Ekert, P.G., Pakusch, M., Silke, J., Connolly, L.M., Reid, G.E., Moritz, R.L., Simpson, R.J., Vaux, D.L., 2000. Identification of DIABLO, a mammalian protein that promotes apoptosis by binding to and antagonizing IAP proteins. *Cell* 102, 43–53.
- Vestweber, D., Kemler, R., 1985. Identification of a putative cell adhesion domain of uvomorulin. *EMBO J.* 4, 3393–3398.
- Vey, E., Dayer, J.M., Burger, D., 1997. Direct contact with stimulated T cells induces the expression of IL-1beta and IL-1 receptor antagonist in human

- monocytes. Involvement of serine/threonine phosphatases in differential regulation. *Cytokine* 9, 480–487. doi:10.1006/cyto.1997.0191
- Wachter, T., Sprick, M., Hausmann, D., Kerstan, A., McPherson, K., Stassi, G., Bröcker, E.-B., Walczak, H., Leverkus, M., 2004. cFLIPL inhibits tumor necrosis factor-related apoptosis-inducing ligand-mediated NF-kappaB activation at the death-inducing signaling complex in human keratinocytes. *J. Biol. Chem.* 279, 52824–52834. doi:10.1074/jbc.M409554200
- Wagner, K.W., Punnoose, E.A., Januario, T., Lawrence, D.A., Pitti, R.M., Lancaster, K., Lee, D., Goetz, von, M., Yee, S.F., Totpal, K., Huw, L., Katta, V., Cavet, G., Hymowitz, S.G., Amler, L., Ashkenazi, A., 2007. Death-receptor O-glycosylation controls tumor-cell sensitivity to the proapoptotic ligand Apo2L/TRAIL. *Nat. Med.* 13, 1070–1077. doi:10.1038/nm1627
- Wajant, H., Moosmayer, D., Wüest, T., Bartke, T., Gerlach, E., Schönherr, U., Peters, N., Scheurich, P., Pfizenmaier, K., 2001. Differential activation of TRAIL-R1 and -2 by soluble and membrane TRAIL allows selective surface antigen-directed activation of TRAIL-R2 by a soluble TRAIL derivative. *Oncogene* 20, 4101–4106. doi:10.1038/sj.onc.1204558
- Walczak, H., Haas, T.L., 2008. Biochemical analysis of the native TRAIL death-inducing signaling complex. *Methods Mol. Biol.* 414, 221–239.
- Walczak, H., Miller, R.E., Ariail, K., Gliniak, B., Griffith, T.S., Kubin, M., Chin, W., Jones, J., Woodward, A., Le, T., Smith, C., Smolak, P., Goodwin, R.G., Rauch, C.T., Schuh, J.C., Lynch, D.H., 1999. Tumoricidal activity of tumor necrosis factor-related apoptosis-inducing ligand in vivo. *Nat. Med.* 5, 157–163. doi:10.1038/5517
- Walley, A.J., Chavanas, S., Moffatt, M.F., Esnouf, R.M., Ubhi, B., Lawrence, R., Wong, K., Abecasis, G.R., Jones, E.Y., Harper, J.I., Hovnanian, A., Cookson, W.O., 2001. Gene polymorphism in Netherton and common atopic disease. *Nat. Genet.* 29, 175–178. doi:10.1038/ng728
- Wang, C.Y., Mayo, M.W., Korneluk, R.G., Goeddel, D.V., Baldwin, A.S., 1998. NF-kappaB antiapoptosis: induction of TRAF1 and TRAF2 and c-IAP1 and c-IAP2 to suppress caspase-8 activation. *Science* 281, 1680–1683.
- Warner, R.L., Bhagavathula, N., Nerusu, K.C., Lateef, H., Younkin, E., Johnson, K.J., Varani, J., 2004. Matrix metalloproteinases in acute inflammation: induction of MMP-3 and MMP-9 in fibroblasts and epithelial cells following exposure to pro-inflammatory mediators in vitro. *Exp. Mol. Pathol.* 76, 189–195. doi:10.1016/j.yexmp.2004.01.003
- Weaver, C.T., Harrington, L.E., Mangan, P.R., Gavrieli, M., Murphy, K.M., 2006. Th17: an effector CD4 T cell lineage with regulatory T cell ties. *Immunity* 24, 677–688. doi:10.1016/j.immuni.2006.06.002
- Weckmann, M., Collison, A., Simpson, J.L., Kopp, M.V., Wark, P.A.B., Smyth, M.J., Yagita, H., Matthaei, K.I., Hansbro, N., Whitehead, B., Gibson, P.G., Foster, P.S., Mattes, J., 2007. Critical link between TRAIL and CCL20 for the activation of TH2 cells and the expression of allergic airway disease. *Nat. Med.* 13, 1308–1315. doi:10.1038/nm1660
- Weiss, A., Wiskocil, R.L., Stobo, J.D., 1984. The role of T3 surface molecules in the activation of human T cells: a two-stimulus requirement for IL 2 production reflects events occurring at a pre-translational level. *J. Immunol.* 133, 123–128.

- West, M.R., Ferguson, D.J.P., Hart, V.J., Sanjar, S., Man, Y., 2002. Maintenance of the epithelial barrier in a bronchial epithelial cell line is dependent on functional E-cadherin local to the tight junctions. *Cell Commun. Adhes.* 9, 29–44.
- Wiley, S.R., Schooley, K., Smolak, P.J., Din, W.S., Huang, C.P., Nicholl, J.K., Sutherland, G.R., Smith, T.D., Rauch, C., Smith, C.A., 1995. Identification and characterization of a new member of the TNF family that induces apoptosis. *Immunity* 3, 673–682.
- Willis, S.N., Fletcher, J.I., Kaufmann, T., van Delft, M.F., Chen, L., Czabotar, P.E., Ierino, H., Lee, E.F., Fairlie, W.D., Bouillet, P., Strasser, A., Kluck, R.M., Adams, J.M., Huang, D.C.S., 2007. Apoptosis initiated when BH3 ligands engage multiple Bcl-2 homologs, not Bax or Bak. *Science* 315, 856–859. doi:10.1126/science.1133289
- Wu, G., Chai, J., Suber, T.L., Wu, J.W., Du, C., Wang, X., Shi, Y., 2000. Structural basis of IAP recognition by Smac/DIABLO. *Nature* 408, 1008–1012. doi:10.1038/35050012
- Wu, G.S., Burns, T.F., Zhan, Y., Alnemri, E.S., El-Deiry, W.S., 1999. Molecular cloning and functional analysis of the mouse homologue of the KILLER/DR5 tumor necrosis factor-related apoptosis-inducing ligand (TRAIL) death receptor. *Cancer Res.* 59, 2770–2775.
- Wu, Q., Jiang, D., Chu, H.W., 2012. Cigarette smoke induces growth differentiation factor 15 production in human lung epithelial cells: implication in mucin over-expression. *Innate Immun* 18, 617–626. doi:10.1177/1753425911429837
- Wu, W.G., Soria, J.C., Wang, L., Kemp, B.L., Mao, L., 2000. TRAIL-R2 is not correlated with p53 status and is rarely mutated in non-small cell lung cancer. *Anticancer Res.* 20, 4525–4529.
- Wyllie, A.H., Kerr, J.F., Currie, A.R., 1980. Cell death: the significance of apoptosis. *Int. Rev. Cytol.* 68, 251–306.
- Ying, S., Robinson, D.S., Varney, V., Meng, Q., Tsicopoulos, A., Moqbel, R., Durham, S.R., Kay, A.B., Hamid, Q., 1991. TNF alpha mRNA expression in allergic inflammation. *Clin. Exp. Allergy* 21, 745–750.
- Zandi, E., Rothwarf, D.M., Delhase, M., Hayakawa, M., Karin, M., 1997. The I $\kappa$ B kinase complex (IKK) contains two kinase subunits, IKK $\alpha$  and IKK $\beta$ , necessary for I $\kappa$ B phosphorylation and NF- $\kappa$ B activation. *Cell* 91, 243–252.
- Ziegler, D.S., Wright, R.D., Kesari, S., Lemieux, M.E., Tran, M.A., Jain, M., Zawal, L., Kung, A.L., 2008. Resistance of human glioblastoma multiforme cells to growth factor inhibitors is overcome by blockade of inhibitor of apoptosis proteins. *J. Clin. Invest.* 118, 3109–3122. doi:10.1172/JCI34120
- Zong, W.X., Edelstein, L.C., Chen, C., Bash, J., Gélinas, C., 1999. The prosurvival Bcl-2 homolog Bfl-1/A1 is a direct transcriptional target of NF- $\kappa$ B that blocks TNF $\alpha$ -induced apoptosis. *Genes Dev.* 13, 382–387.